African Journal of Biotechnology

Volume 13 Number 33, 13 August, 2014
ISSN 1684-5315

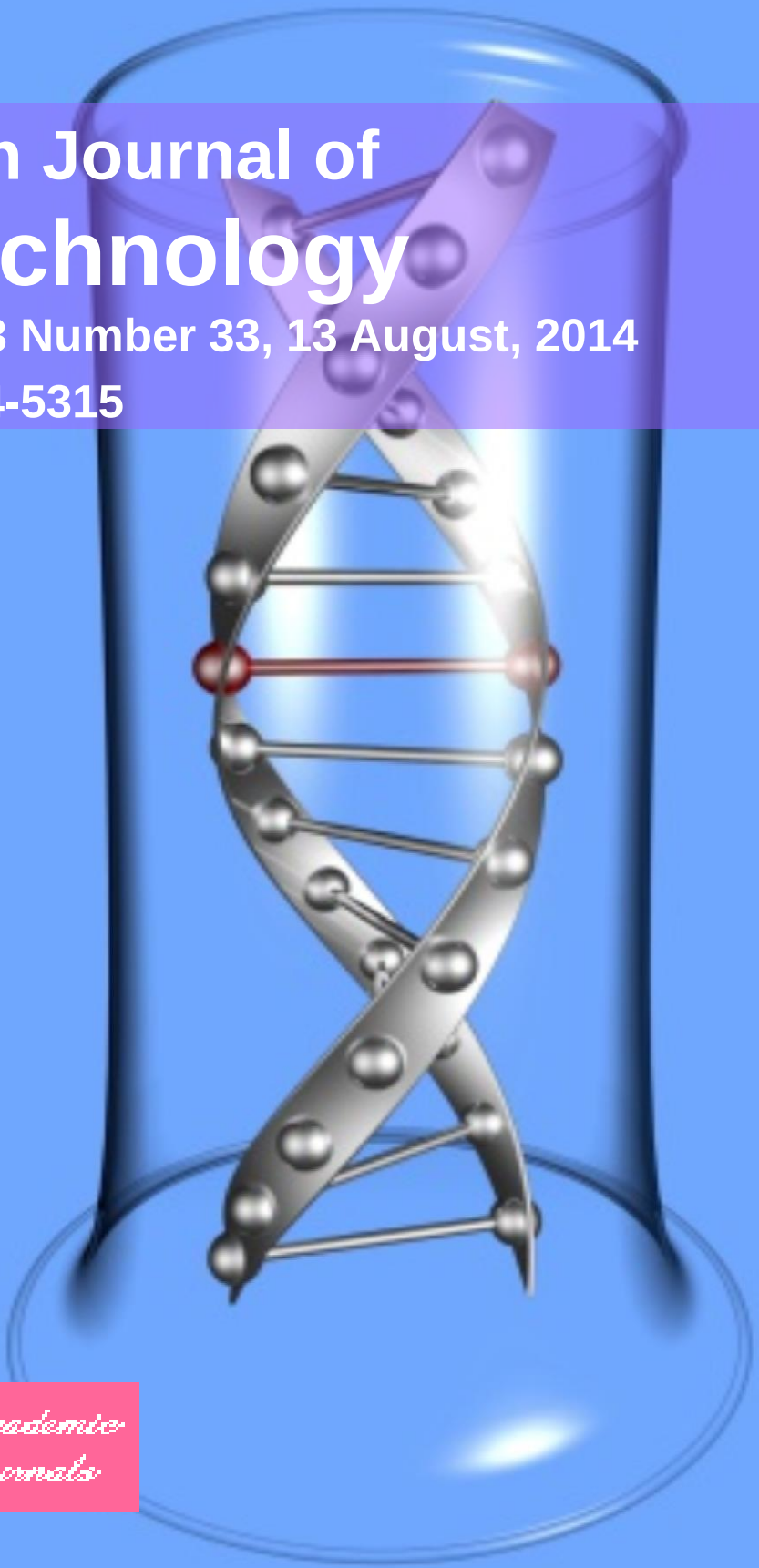

Academic Journals

ABOUT AJB

The **African Journal of Biotechnology (AJB)** (ISSN 1684-5315) is published weekly (one volume per year) by Academic Journals.

African Journal of Biotechnology (AJB), a new broad-based journal, is an open access journal that was founded on two key tenets: To publish the most exciting research in all areas of applied biochemistry, industrial microbiology, molecular biology, genomics and proteomics, food and agricultural technologies, and metabolic engineering. Secondly, to provide the most rapid turn-around time possible for reviewing and publishing, and to disseminate the articles freely for teaching and reference purposes. All articles published in AJB are peer-reviewed.

Submission of Manuscript

Please read the **Instructions for Authors** before submitting your manuscript. The manuscript files should be given the last name of the first author

Click here to Submit manuscripts online

If you have any difficulty using the online submission system, kindly submit via this email ajb@academicjournals.org.

With questions or concerns, please contact the Editorial Office at ajb@academicjournals.org.

Editorial Board

Instructions for Author

Electronic submission of manuscripts is strongly encouraged, provided that the text, tables, and figures are included in a single Microsoft Word file (preferably in Arial font).

The **cover letter** should include the corresponding author's full address and telephone/fax numbers and should be in an e-mail message sent to the Editor, with the file, whose name should begin with the first author's surname, as an attachment.

Article Types
Three types of manuscripts may be submitted:

Regular articles: These should describe new and carefully confirmed findings, and experimental procedures should be given in sufficient detail for others to verify the work. The length of a full paper should be the minimum required to describe and interpret the work clearly.
Short Communications: A Short Communication is suitable for recording the results of complete small investigations or giving details of new models or hypotheses, innovative methods, techniques or apparatus. The style of main sections need not conform to that of full-length papers. Short communications are 2 to 4 printed pages (about 6 to 12 manuscript pages) in length.

Reviews: Submissions of reviews and perspectives covering topics of current interest are welcome and encouraged. Reviews should be concise and no longer than 4-6 printed pages (about 12 to 18 manuscript pages). Reviews are also peer-reviewed.

Review Process

All manuscripts are reviewed by an editor and members of the Editorial Board or qualified outside reviewers. Authors cannot nominate reviewers. Only reviewers randomly selected from our database with specialization in the subject area will be contacted to evaluate the manuscripts. The process will be blind review.
Decisions will be made as rapidly as possible, and the journal strives to return reviewers' comments to authors as fast as possible. The editorial board will re-review manuscripts that are accepted pending revision. It is the goal of the AJFS to publish manuscripts within weeks after submission.

Regular articles

All portions of the manuscript must be typed double-spaced and all pages numbered starting from the title page.

The Title should be a brief phrase describing the contents of the paper. The Title Page should include the authors' full names and affiliations, the name of the corresponding author along with phone, fax and E-mail information. Present addresses of authors should appear as a footnote.

The Abstract should be informative and completely self-explanatory, briefly present the topic, state the scope of the experiments, indicate significant data, and point out major findings and conclusions. The Abstract should be 100 to 200 words in length.. Complete sentences, active verbs, and the third person should be used, and the abstract should be written in the past tense. Standard nomenclature should be used and abbreviations should be avoided. No literature should be cited.
Following the abstract, about 3 to 10 key words that will provide indexing references should be listed.

A list of non-standard **Abbreviations** should be added. In general, non-standard abbreviations should be used only when the full term is very long and used often. Each abbreviation should be spelled out and introduced in parentheses the first time it is used in the text. Only recommended SI units should be used. Authors should use the solidus presentation (mg/ml). Standard abbreviations (such as ATP and DNA) need not be defined.

The Introduction should provide a clear statement of the problem, the relevant literature on the subject, and the proposed approach or solution. It should be understandable to colleagues from a broad range of scientific disciplines.

Materials and methods should be complete enough to allow experiments to be reproduced. However, only truly new procedures should be described in detail; previously published procedures should be cited, and important modifications of published procedures should be mentioned briefly. Capitalize trade names and include the manufacturer's name and address. Subheadings should be used. Methods in general use need not be described in detail.

Results should be presented with clarity and precision. The results should be written in the past tense when describing findings in the authors' experiments. Previously published findings should be written in the present tense. Results should be explained, but largely without referring to the literature. Discussion, speculation and detailed interpretation of data should not be included in the Results but should be put into the Discussion section.

The Discussion should interpret the findings in view of the results obtained in this and in past studies on this topic. State the conclusions in a few sentences at the end of the paper. The Results and Discussion sections can include subheadings, and when appropriate, both sections can be combined.

The Acknowledgments of people, grants, funds, etc should be brief.

Tables should be kept to a minimum and be designed to be as simple as possible. Tables are to be typed double-spaced throughout, including headings and footnotes. Each table should be on a separate page, numbered consecutively in Arabic numerals and supplied with a heading and a legend. Tables should be self-explanatory without reference to the text. The details of the methods used in the experiments should preferably be described in the legend instead of in the text. The same data should not be presented in both table and graph form or repeated in the text.

Figure legends should be typed in numerical order on a separate sheet. Graphics should be prepared using applications capable of generating high resolution GIF, TIFF, JPEG or Powerpoint before pasting in the Microsoft Word manuscript file. Tables should be prepared in Microsoft Word. Use Arabic numerals to designate figures and upper case letters for their parts (Figure 1). Begin each legend with a title and include sufficient description so that the figure is understandable without reading the text of the manuscript. Information given in legends should not be repeated in the text.

References: In the text, a reference identified by means of an author‘s name should be followed by the date of the reference in parentheses. When there are more than two authors, only the first author‘s name should be mentioned, followed by ’et al‘. In the event that an author cited has had two or more works published during the same year, the reference, both in the text and in the reference list, should be identified by a lower case letter like ’a‘ and ’b‘ after the date to distinguish the works.

Examples:

Abayomi (2000), Agindotan et al. (2003), (Kelebeni, 1983), (Usman and Smith, 1992), (Chege, 1998; 1987a,b; Tijani, 1993,1995), (Kumasi et al., 2001)
References should be listed at the end of the paper in alphabetical order. Articles in preparation or articles submitted for publication, unpublished observations, personal communications, etc. should not be included in the reference list but should only be mentioned in the article text (e.g., A. Kingori, University of Nairobi, Kenya, personal communication). Journal names are abbreviated according to Chemical Abstracts. Authors are fully responsible for the accuracy of the references.

Examples:

Chikere CB, Omoni VT and Chikere BO (2008). Distribution of potential nosocomial pathogens in a hospital environment. Afr. J. Biotechnol. 7: 3535-3539.

Moran GJ, Amii RN, Abrahamian FM, Talan DA (2005). Methicillinresistant Staphylococcus aureus in community-acquired skin infections. Emerg. Infect. Dis. 11: 928-930.

Pitout JDD, Church DL, Gregson DB, Chow BL, McCracken M, Mulvey M, Laupland KB (2007). Molecular epidemiology of CTXM-producing Escherichia coli in the Calgary Health Region: emergence of CTX-M-15-producing isolates. Antimicrob. Agents Chemother. 51: 1281-1286.

Pelczar JR, Harley JP, Klein DA (1993). Microbiology: Concepts and Applications. McGraw-Hill Inc., New York, pp. 591-603.

Short Communications

Short Communications are limited to a maximum of two figures and one table. They should present a complete study that is more limited in scope than is found in full-length papers. The items of manuscript preparation listed above apply to Short Communications with the following differences: (1) Abstracts are limited to 100 words; (2) instead of a separate Materials and Methods section, experimental procedures may be incorporated into Figure Legends and Table footnotes; (3) Results and Discussion should be combined into a single section.
Proofs and Reprints: Electronic proofs will be sent (e-mail attachment) to the corresponding author as a PDF file. Page proofs are considered to be the final version of the manuscript. With the exception of typographical or minor clerical errors, no changes will be made in the manuscript at the proof stage.

Fees and Charges: Authors are required to pay a $650 handling fee. Publication of an article in the African Journal of Biotechnology is not contingent upon the author's ability to pay the charges. Neither is acceptance to pay the handling fee a guarantee that the paper will be accepted for publication. Authors may still request (in advance) that the editorial office waive some of the handling fee under special circumstances

Submission of a manuscript implies: that the work described has not been published before (except in the form of an abstract or as part of a published lecture, or thesis) that it is not under consideration for publication elsewhere; that if and when the manuscript is accepted for publication, the authors agree to automatic transfer of the copyright to the publisher.

African Journal of Biotechnology

Table of Contents: Volume 13 Number 33, 13 August, 2014

ARTICLES

Table of Contents: Volume 13 Number 33, 13 August, 2014

academicJournals

Vol. 13(33), pp. 3332-3343, 13 August, 2014
DOI: 10.5897/AJB2014.13911
Article Number: 222BAC446614
ISSN 1684-5315

http://www.academicjournals.org/AJB

African Journal of Biotechnology

Full Length Research Paper

Expressed sequence tags (EST) analysis of a normalized full-length cDNA library from the pinewood nematode (*Bursaphelenchus xylophilus*)

Ha Young Chung[1†], Man-Jung Kang[1†], Hye Rim Han[2], Joon-Soo Sim[1], Byung-Ju Oh[1], Inchan Choi[1], Chang-Muk Lee[1], Sang-Hong Yoon[1] and Bum-Soo Hahn[1]*

[1]National Academy of Agricultural Science, Suwon 441-857, Korea.
[2]Korea Forest Research Institute, Dongademun-gu, Seoul 130-712, Korea.
[†]Both authors contributed equally to this work.

Received 15 May, 2014; Accepted 21 July, 2014

The pinewood nematode (*Bursaphelenchus xylophilus*) infects pine trees and causes pine wilt disease. To clarify the functions and subcellular localization of *B. xylophilus* genes/proteins transcribed and predicted from mixed stages (egg, J1, J2, J3 J4 and adult), we prepared a normalized full-length *B. xylophilus* cDNA library and analyzed expressed sequence tags (ESTs) using the Pendant-Pro sequence analysis suite. Most cDNAs inserted into the library ranged from 0.9 to 1.8 kb (average 1.5 kb). The 1,902 ESTs from *B. xylophilus* consisted of 286 clusters and 1,273 singletons. EST sizes ranged from 9 to 743 bp with a mean of 336 bp. The predicted protein length from *B. xylophilus* ESTs revealed that most proteins ranged from 50 to 149 amino acids. Enzyme nomenclature (EC) numbers were classified into 133 (8.5%) of 1,559 contigs using UniProt database hits by the EC numbers method. Transmembrane regions of 1559 clusters were predicted using the TMpred algorithm. The 1,559 contigs with transmembrane regions were annotated; 481 (30.8%) contigs were assigned 'above one' domain and 1,078 (69.1%) were assigned 'none.' Additionally, taxonomy was classified for 672 (43.1%) of 1,559 contigs. Of the 1,559 contigs, 685 (43.9%) were assigned gene ontology terms using the gomerger method of contigs, including singletons. Thirty-one (31) contigs of predicted proteins grouped by BLASTP identity values had significant homology to genes expressed in subcellular structures (for example, mitochondrion, plasma membrane, endoplasmic reticulum, nucleus and golgi). *B. xylophilus* ESTs provide the foundation for research information on related plant parasite nematodes and contribute to finding an important novel parasite control strategy.

Key words: Pinewood nematode, *Bursaphelenchus xylophilus,* pine wilt disease, expressed sequence tag, Pendant-Pro Sequence Analysis Suite

INTRODUCTION

The pine wood nematode (PWN), *Bursaphelenchus xylophilus* (Steiner and Buhrer, 1934) Nickle, a plant parasitic nematode, was first described in 1934 in Louisiana, and thus originated in North America. From there

*Corresponding author. E-mail: bshahn@korea.kr. Tel: 82-31-299-1624. Fax: 82-31-299-1622.

it was introduced into Japan, then spread to neighboring East Asian countries, such as China and Korea in 1982 and 1988, respectively, and it was found in Portugal in 1999 (Mota et al., 1999; Mota and Vieira, 2008) and in Spain in 2008 (Abelleira et al., 2011). PWN is the causal agent of pine wilt disease (PWD) in pine trees (Linit, 1988; Yan et al., 2012). PWD typically occurs in mature pine trees 20 or more years old. Nematodes feed on the cells surrounding resin ducts, which causes resin to leak into tracheids, resulting in tracheid cavitation or air pockets in the water transport system. Next, transpiration of the tree cannot be sustained, which eventually leads to pine death (Myers, 1988; Donald et al., 2003). The beetle *Monochamus alternatus* (Hope) was immediately designed as a principal vector of the causal agent and spread nematodes from tree to tree (Shibata, 1987; Sakai and Yamasaki, 1990; Fan et al., 2007). Species of *Monochamus* from conifers are the principal vectors of *B. xylophilus*, and of these *M. alternatus* is the major vector in Japan, whereas *M. carolinensis* and *M. scutellatus* are the major vectors in North America and in Europe it is *Monochamus galloprovincialis*. The dispersal fourth-stage dauber larvae of the pinewood nematode cause primary transmission to occur during maturation feedings by the pine sawyer (Fielding and Evans, 1996). Also, nematode activity in pine trees is similar to natural infection by dispersal fourth-stage dauber larvae transmitted from pine sawyers when a pine tree is infected with nematodes isolated from fungal cultures (Linit 1988; Sriwati et al., 2007).

In recent years, the GenBank entries for *B. xylophilus* and *B. mucronatus* revealed 13,327 and 3,193 ESTs, respectively (Kikuchi et al., 2007). Additionally, the complete *B. xylophilus* genome (genome size of 74.5 Mb with a GC content of 40.4%) sequence was annotated by Kikuchi and colleagues (Kikuchi et al., 2011), as well as the complete mitochondrial genome of *B. xylophilus* (14,778 bp) (Sultana et al., 2013). Also, plant parasitic nematode ESTs have recently been generated for analyzing the function of genes from several plant-parasitic nematode species (Scholl et al., 2003; Dubreuil et al., 2007; Kikuchi et al., 2007; Nagaraj et al., 2008; Rosso et al., 2008; Sultana *et al*., 2013). However, since the majority of ESTs were generated from nematode total RNA without normalization of a cDNA library, these EST libraries may contain multiplicative ESTs of the nematode.

In this study, we report an analysis of 1,902 ESTs from a normalized full-length cDNA library of *B. xylophilus* mixed stages (egg, J1, J2, J3 J4, and adult). Firstly, the ESTs from the *B. xylophilus* library were grouped into clusters that were analyzed by the most conserved nematode genes between *B. xylophilus* and other nematodes, classification of EC number, transmembrane regions, taxonomy, gene ontology (GO), and the identification of gene-related subcellular localization were done. These results provide the foundation for information studies focusing on understanding the gene function of *B. xylophilus* nematode, as well as the development of a novel parasite control strategy.

MATERIALS AND METHODS

Nematode propagation

B. xylophilus (Bx90) used in this study were isolated from the Gangneung area, Korea and was propagated on a lawn of *Botrytis cinerea* cultured on a potato dextrose agar plate at 28°C. Mixed stages (egg, J1, J2, J3, J4 and adult) were collected on 25 µm sieves. Eggs and nematodes were sterilized with 1% NaOCl and suspended in sterile deionized water. The samples were frozen in liquid nitrogen and ground with a mortar and pestle.

RNA preparation and cDNA library construction

Total RNAs from mixed stages were isolated using TRIzol reagent according to the manufacturer's instructions (Invitrogen, The Netherlands). A full-length cDNA library of *B. xylophilus* was prepared from total RNAs of mixed stages as described previously (Oh et al., 2003).

In brief, the pretreated total RNA with bacterial alkaline phosphatase (Roche Diagnostics, Switzerland) and tobacco acid pyrophosphatase (Wako, Japan) was ligated with a 5'-oligoribonucleotide using RNA ligase (TaKaRa, Japan).

First-strand cDNA synthesis and amplification from purified mRNA were performed as described by Maruyama and Sugano (1994). Amplified PCR products were then digested as described by Kang et al. (2010). The ligated cDNA was then transformed into *Escherichia coli* Top10F' (Invitrogen, USA) by electroporation (Gene Pulser II; Bio-Rad, USA). The *B. xylophilus* cDNA library consisted of 4.8×10^6 colonies. To construct a normalized *B. xylophilus* cDNA library, a single-stranded DNA library was prepared as described previously (Vieira and Messing, 1987). Finally, we obtained a normalized library of 2×10^6 colonies.

Sequencing of plasmids

Each colony from the *B. xylophilus* cDNA libraries was picked into 96-well plates containing 0.5 mL of Luria Bertani (LB) medium containing 75 µg/mL ampicillin. Plates were incubated overnight at 37°C. Plasmids were purified using FB glass-fiber plates (Millipore, USA) to remove protein and cellular debris. Plasmid inserts were sequenced from the 5' end using the primer in the pCNS vector (5'-GGT CTA TAT AAG CAG AGC TC-3') and the BigDye terminator ver. 3.1 kit (Applied Biosystems, USA) on an ABI 3730*xl* DNA sequencer (Applied Biosystems).

EST sequence clustering

Vector trimming and trimmed sequence cleaning for automated trimming, and validation of ESTs or other DNA sequences by screening for various contaminants, low quality and low complexity sequences were performed using the cross_match, SeqClean, and Lucy programs (Xie et al., 2010; Tae et al., 2012; Yang et al., 2012), respectively. The cleanup process included quality assessment, confidence reassurance, vector trimming, and vector removal. ESTs of at least 200 bp after both vector and low-quality trimming were regarded as "high-quality" ESTs. Clustering was performed using TGI clustering tools (TGICL), a software pipeline designed to automate clustering and assembly of a large EST/mRNA data set (Rensing et al., 2003; Menon et al., 2012). Sequence clustering was

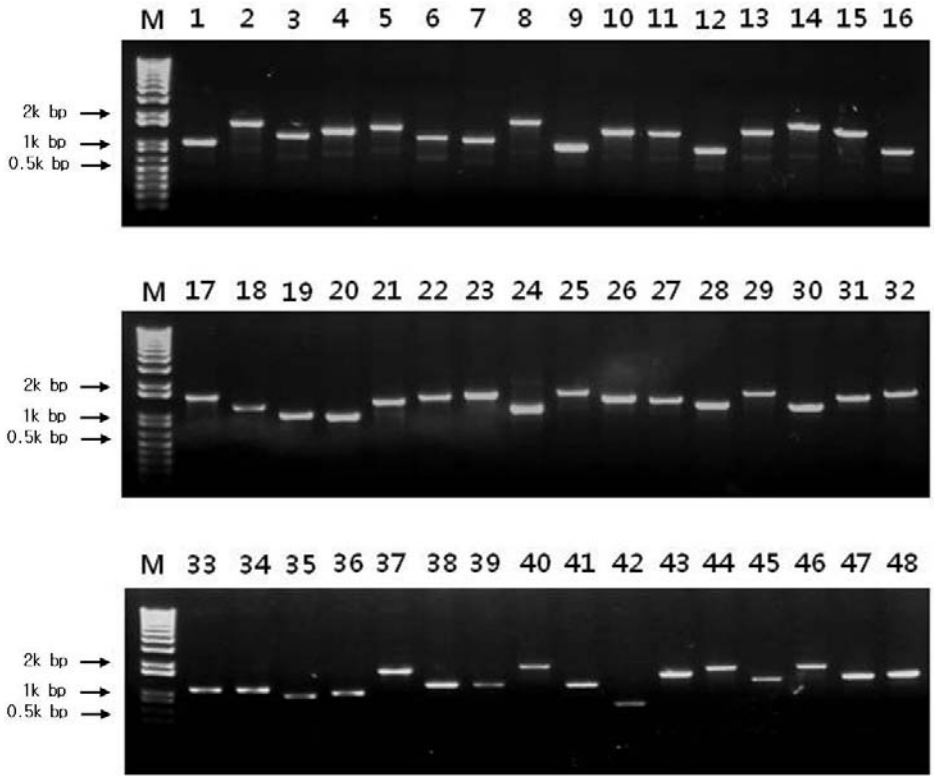

Figure 1. Evaluation of the cDNA library insert size on agarose gel. Colonies were picked at random and colony PCR was performed using T7 and SP6 promoter primers (lanes 1-48). M, DNA size marker (Invitrogen, USA)

was performed with a slightly modified version of NCBI's megablast, and the resulting clusters were then assembled using the CAP3 assembly program. TGICL began with a large multi-FASTA file (an optional peer quality values file) and the output assembly files, as produced by CAP3. Both clustering and assembly phases could be parallelized by distributing the searches and assembly jobs across multiple CPUs since TGICL can take advantage of either SMP machines or parallel virtual machine (PVM) clusters (Lee et al., 2005).

Contig analysis

Each contig sequence was evaluated for similarity and annotation analysis of nucleotide and protein sequences using the Pendant-Pro Sequence Analysis Suite. The Pendant-Pro genome database provides an exhaustive pre-computed analysis using a large variety of established bioinformatics tools. To investigate protein function, BLAST similarity was searched against the complete nonredundant protein sequence database (Altschul et al., 1997). Motifs were searched against Pfam (Bateman et al., 2002), BLOCKS (Henikoff et al., 1999), PROSITE (Falquet et al., 2002), and InterPro (Apweiler et al., 2001) databases. Predictions of cellular roles and functions based on high-stringency BLAST were searched against protein sequences with manually assigned functional categories according to the Functional Catalogue (FunCat), developed by MIPS and Biomax Informatics AG. Enzyme nomenclature (EC) numbers were predicted based on similarity. Keywords and superfamilies were extracted by similarity-based assignments from the PIR-International sequence database (Barker et al., 2000). Sequences were assigned to known clusters of orthologous groups (COGS) (Tatusov et al., 2001). To investigate protein structure, transmembrane regions were predicted using the TMpred algorithm against TMbase (Hofmann and Stoffel, 1993). Local low similarity regions and entire regions were identified using non-globular domains based on the SEG algorithm (Wootton and Federhen 1993). Coiled-coil motifs were also predicted (Lupas et al., 1991). In addition, sequence similarities were searched on the NCBI GenBank and RefSeq databases using BLASTN. BLAST similarity hits were classified based on their taxonomic origin.

RESULTS AND DISCUSSION

Evaluation of *B. xylophilus* cDNA library quality

To confirm and evaluate the insertion and quality of the *B. xylophilus* cDNA library, the range and average plasmid insert lengths were determined by PCR amplification. Forty-eight (48) cDNA clones were randomly picked from the library and colony PCR was performed with T7 and Sp6 promoter primers. Most cDNA inserts in the *B. xylophilus* libraries ranged from 0.9 to 1.8 kb with an average cDNA insert size of 1.5 kb (Figure 1) (1-48). These results are similar to those from our previous study in *Meloidogyne incognita*, as well as results from the library constructed from mixed-stage *B. xylophilus* vigorously growing on fungi (Kikuchi et al., 2007; Kang et al., 2010).

Table 1. Results of *Bursaphelenchus xylophilus* EST clustering.

Parameter	CAP3
Total sequences analyzed	1,902
Number of ESTs in cluster	629
Number of clusters	286
Number of singletons	1,273

The CAP3 program was performed with default parameters. Contigs and singletons were counted as clusters.

EST clustering and protein distribution analysis

ESTs from the *B. xylophilus* cDNA library were assembled into clusters to identify a set of genes. The 1,902 *B. xylophilus* ESTs could be classified into 286 clusters and 1,273 singletons (Table 1). Cluster sizes of *B. xylophilus* ESTs varied from a single EST (1,273 cases) to four ESTs (1 case) (Figure 2). Most clusters consisted of two to four ESTs, demonstrating the high quality of the normalized cDNA library. Also, these results show that abundant transcripts in total RNA during cDNA library preparation were removed and that the full-length cDNA library was successfully normalized. The quality of the cDNA library also showed more efficiency than the results from Kikuchi and colleagues (2011) due to gain probability of the contigs and singletons from analyzed ESTs of each library (our experiment and Kikuchi colleagues study were 82 and 50%, respectively; (Kikuchi et al., 2007; Kang et al., 2010). The sequence distribution of ESTs ranged from 9 to 743 bp with an average size of 336 bp (Figure 2A). The high frequency contigs ranged from 351 to 400 bp and represented 335 (21.5%) of 1,559 contigs. These results matched the consistent quality of the constructed *B. xylophilus* cDNA library in Figure 1.

In addition, protein length frequency values showed high-quality ESTs produced from *B. xylophilus*. The length of predicted proteins from *B. xylophilus* contigs revealed that most proteins ranged from 50 to 149 amino acids (88.1%). The longest proteins ranged from 150 to 299 amino acids and represented 113 (7.2%) of 1,559 total proteins (Figure 2B). In addition, the protein isoelectric point distribution indicated the high quality of ESTs produced from *B. xylophilus*. Putative proteins predicted from contig sequences were classified into nine groups with distinct isoelectric points: very strong basic proteins (>10.5 pI) represented 185 (11.9%) of 1,559 total proteins (Figure 2C); neutral proteins (6.5 < pI < 7.5) represented 153 (9.8%) of the total proteins; very strong acidic proteins (pI < 3.5) represented three (0.2%) of the total proteins (Figure 2C). However, these results only reflected isoelectric points predicted from part of the protein sequences. Furthermore, long-range sequencing of ESTs will need to be performed to determine isoelectric points of *B. xylophilus* full-length proteins.

Identification of highly conserved genes

Highly conserved genes between *B. xylophilus* and other nematodes were annotated by the BLASTP program using the UniProt database. Predicted proteins were classified by BLASTP identity values. The highly-conserved proteins (>90% identity) represented 1.2% of the total predicted proteins. Proteins without homology (0% identity) represented 56.3% of the total predicted proteins.

On the basis of the results of best protein match (BLASTP UniProt) with more than 50% identity, highly conserved transcripts in the *B. xylophilus* cDNA library represented genes encoding body morphogenesis (cuticlin protein), carbohydrate metabolism (pyruvate carboxylase 1, trehalose 6-phosphate synthase, and pectate lyase precursor), cytoskeletons (beta tubulin isotype 1, tubulin alpha chain, and actin-related protein 2), DNA-binding protein (ATP-dependent helicase DDX48), intracellular signaling (CBR-ARF-6 protein, serine/-threonine protein phosphatase, and CBR-TAG-210 protein), ion transporter (NADH-ubiquinone oxidored-uctase 75-kDa subunit), molecular chaperones (heat shock protein 70, heat shock protein 90, and T-complex protein 1 subunit alpha), protein biosynthesis (elongation factor 1-alpha, 60S ribosomal protein L3, lysyl-tRNA synthetase, 40S ribosomal protein S3, 60S acidic ribosomal protein P0, 60S ribosomal protein L11 and CBR-RPS-18 protein), protein targeting (glycoprotein 25L2), protein transport (transport protein Sec61 alpha subunit), proteasomal and proteolytic degradation (proteasome subunit alpha type, 26S proteasome regulatory complex subunit p97, and 26S proteasome regulatory subunit rpn11), and rRNA processing (protein R74.7) (Table 2). These results confirmed that the expression of genes in our library is similar to previously reported cDNA clone sequences involved in the response to the *B. xylophilus* (Kikuchi et al., 2007). Notably, the EST data showed novel EST sequences including trehalose 6-phosphate synthase, transport protein Sec61 alpha subunit, uncharacterized protein gsk-3, SAM-dependant methyltransferase, lysyl-tRNA synthetase, 26S proteasome regulatory complex subunit p97, protein R74.7, T-complex protein 1 subunit alpha and acyl-CoA dehydrogenase.

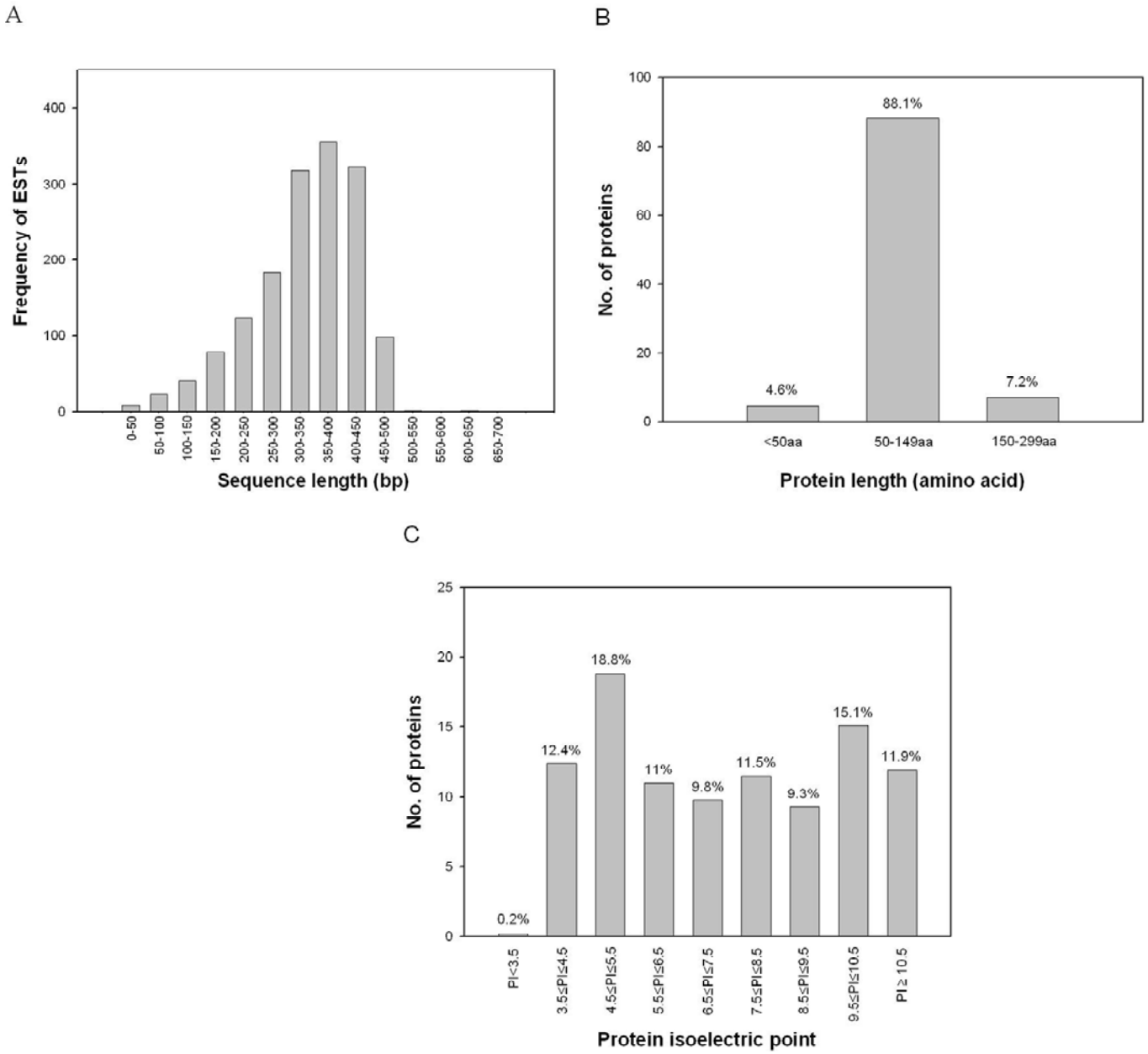

Figure 2. Length and isoelectric point distributions of *Bursaphelenchus xylophilus* cDNA inserts and proteins. Frequency versus sequence length of *B. xylophilus* cDNA inserts (A). The distributions of protein length (B) and isoelectric point (C) were analyzed from a total of 1,559 EST sequences of *B. xylophilus*.

Functional classification of proteins based on GO assignments

Gene ontology (GO) has been widely used to address the need for consistent descriptions of gene products in different databases. It has presented three-structured and controlled ontologies that describe gene products in terms of their associated biological processes, cellular components, and molecular functions in a species-independent manner. Three individual memo methods, gobysimilarity, gofromeckw and gofrominterpro, were calculated to extract GO categories for a protein. The gomerger method integrates the results of the three algorithms (Martin et al., 2004). The gomerger method takes (as input) the GO term assignments for a given genetic element that are the outputs of the three predecessor methods: gofromeckw, gobysimilarity and gofrominterpro. Each GO assignment consists of the GO term number and quality score (BLAST E value or Interpro score). The latter is converted to a negative decimal logarithm. Each GO term number corresponds to a node on the GO tree. The gomerger method then

Table 2. Highly conserved nematode genes between *Bursaphelenchus xylophilus* and other nematodes (*Caenorhabditis* spp. and parasite nematodes).

Parameter	Contig	EST	Best Hit Code	Description	E-value
Body morphogenesis	CL155	1	Q6KFY9_DIRIM	P. Cuticlin protein - *Dirofilaria immitis*	6.80E-62
Carbohydrate metabolism	BXE_1535	1	PYC1_CAEEL	S. Pyruvate carboxylase 1 (EC 6.4.1.1) (Pyruvic carboxylase 1) (PCB 1) - *Caenorhabditis elegans*	2.60E-69
	BXE_421	1	Q5K2C1_APHAV	P. Putative trehalose 6-phosphate synthase (EC 2.4.1.15) - *Aphelenchus avenae*	3.20E-69
	BXE_86	1	Q33CQ4_BURXY	P. Pectate lyase precursor (EC 4.2.2.2) - *Bursaphelenchus xylophilus*	2.70E-59
Cytoskeleton	BXE_449	1	A2TF56_HAECO	P. Beta tubulin isotype 1 - *Haemonchus contortus*	5.90E-63
	BXE_1242	1	A8PYK7_BRUMA	P. Tubulin alpha chain-mouse, putative - *Brugia malayi*	4.20E-58
	BXE_880	1	ARP2_CAEEL	S. Actin-related protein 2 (Actin-like protein 2) (Actin-like protein C) - *Caenorhabditis elegans*	1.30E-52
DNA-binding protein	BXE_1728	1	A8P212_BRUMA	P. ATP-dependent helicase DDX48, putative (Fragment) - *Brugia malayi*	1.00E-57
Intracellular signaling	CL207	1	A8WMU9_CAEBR	P. CBR-ARF-6 protein - *Caenorhabditis briggsae*	4.60E-70
	BXE_1555	1	A8NZM1_BRUMA	P. Serine/threonine protein phosphatase (EC 3.1.3.16) - *Brugia malayi*	6.20E-69
	CL191	1	A8XXM7_CAEBR	P. CBR-TAG-210 protein - *Caenorhabditis briggsae*	1.10E-61
Ion transporter	BXE_1049	1	Q86S77_CAEEL	P. NADH-ubiquinone oxidoreductase 75 kDa subunit (EC 1.6.5.3) - *Caenorhabditis elegans*	1.90E-55
Molecular chaperone	BXE_1864	1	A4UU63_BURXY	P. Heat shock protein 90 (Fragment) - *Bursaphelenchus xylophilus*	3.80E-60
	BXE_747	1	Q8MUA7_HETGL	P. Heat shock protein 70-C - *Heterodera glycines*	6.40E-60
	BXE_1714	1	TCPA_CAEEL	S. T-complex protein 1 subunit alpha (TCP-1-alpha) (CCT-alpha) - *Caenorhabditis elegans*	1.90E-54
	BXE_1301	1	A8XHC9_CAEBR	P. Putative uncharacterized protein - *Caenorhabditis briggsae*	2.90E-53
Protein biosynthesis	CL223	1	A8PJ17_BRUMA	P. Elongation factor 1-alpha (EF-1-alpha), putative - *Brugia malayi*	1.90E-78
	BXE_1507	1	Q95ZQ3_CAEEL	P. Lysyl-tRNA synthetase (EC 6.1.1.6) - *Caenorhabditis elegans*	3.70E-60
	CL150	1	A8NXR7_BRUMA	P. 40S ribosomal protein S3, putative - *Brugia malayi*	5.30E-60
	BXE_271	1	RLA0_CAEEL	S. 60S acidic ribosomal protein P0 - *Caenorhabditis elegans*	1.40E-58

Table 2. Contd.

	BXE_960	1	A8NKQ0_BRUMA	P. 60S ribosomal protein L11, putative - *Brugia malayi*	5.90E-55
	BXE_1101	1	A8Y099_CAEBR	P. CBR-RPS-18 protein - *Caenorhabditis briggsae*	3.50E-54
Electron transport	CL284	2	GCDH_CAEEL	S. Probable glutaryl-CoA dehydrogenase, mitochondrial precurso (EC 1.3.99.7) (GCD) - *Caenorhabditis elegans*	5.50E-53
Protein targeting	CL255	2	A8PU74_BRUMA	P. Glycoprotein 25L2, putative - *Brugia malayi*	1.10E-58
Protein transport	CL110	1	A8Q009_BRUMA	P. Probable transport protein Sec61 alpha subunit, putative - *Brugia malayi*	4.70E-68
	BXE_632	1	A8QCC8_BRUMA	P. Proteasome subunit alpha type (EC 3.4.25.1) - *Brugia malayi*	4.40E-67
	BXE_1164	1	A8PPJ3_BRUMA	P. 26S proteasome regulatory complex subunit p97, putative - *Brugia malayi*	1.00E-59
	CL113	1	A8PAL6_BRUMA	P. 26S proteasome regulatory subunit rpn11, putative - *Brugia malayi*	1.30E-54
rRNA processing	BXE_1063	1	A8Q6F8_BRUMA	P. Protein R74.7, putative - *Brugia malayi*	1.10E-55

The sequence similarities of contigs were searched using the UniProt database.

searches the GO tree (which is kept in memory) upward and finds all ancestors of all GO nodes assigned. Scores from all preceding nodes are then added together, assigning GO categories to a protein sequence (Ashburner and Lewis, 2002; Martin et al., 2004). Using the gomerger method of contigs, we functionally assigned GO terms to 685 (43.9%) of 1,559 contigs (of 1,559 contigs, 1,105 align to InterPro domains and 58 to the keyword method). The 685 contigs with GO annotations from the *B. xylophilus* data set were further annotated, with 621 hits assigned a biological process (BP), 620 hits assigned molecular functions (MF), and 503 hits assigned a cellular component (CC) in GO terms. A summary of GO annotations by biological process, cellular component and molecular function is provided in Figure 3. Among the most common GO categories representing biological processes were cellular process (GO: 0009987) and metabolic process (GO: 0008152). The largest number of GO terms in cellular component was 433 contigs in the cell (GO: 0005623), 433 contigs in a cell part (GO: 0044464), and 399 intracellular contigs (GO: 0005622). The largest number of GO terms in molecular function was 467 contigs in binding (GO: 0005488), 348 contigs in catalytic activity (GO: 0003824), and 328 contigs in protein binding (GO: 0005515). The largest number of GO terms in biological process was 465 contigs in cellular process (GO: 0009987), 415 contigs in metabolic processes (GO: 0008152), and 374 contigs in cellular metabolic processes (GO: 00044237). These results were highly similar to a previous study analyzing ESTs in *Meloidogyne incognita* (Kang et al., 2010). However, in terms of reproduction, reproductive process, and response stimulate in biological processes, a higher frequency was found than in a previous study (Kang et al., 2009). The total transcriptome analysis of *B. xylophilus* will be needed for the complete GO analysis.

Localization of proteins in the cell

Information on subcellular localization of proteins in the cell provides important clues about protein function and can be used to infer the function of predicted proteins. In addition, the subcellular localization of proteins with known function unravels where the corresponding biological processes take place and how they are connected among each other (Shen and Burger 2007). Thirty-one (31) contigs were separated into 12 subcellular structures according to their predicted functions (Figure 4). Putative transcripts in the *B. xylophilus* cDNA library represented genes expressed in the plasma membrane (P. CBR-ARF-6 protein and A8WMU9), cytoplasm (putative uncharacterized protein, A8XHC9; 60S ribosomal protein L3, RL3; ATP-dependent helicase DDX48, A8P212; heat shock protein 90, A4UU63; serine/threonine protein phosphatase, A8PJS7; ps4b-prov protein, A8QBR0; proteasome subunit alpha type, A8QCC8; 60S ribosomal protein L11, A8NKQ0; 26S

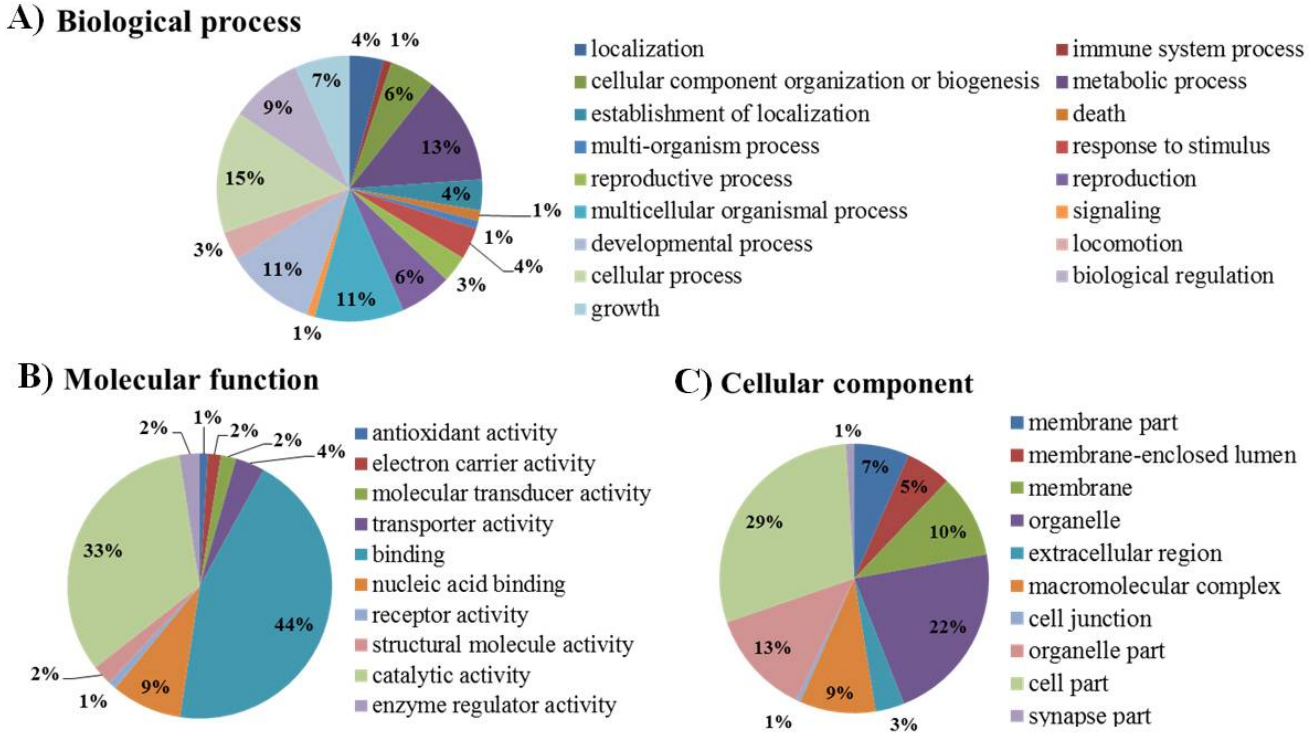

Figure 3. Percentage representation of gene ontology (GO) mappings for *Bursaphelenchus xylophilus* proteins. Biological process (A); Molecular function (B); Cellular component (C). Individual GO categories can have multiple mappings. Percentages shown represent the total categories annotated (not the total sequences annotated under each component).

proteasome regulatory subunit rpn11, A8PAL6; 40S ribosomal protein S3, A8NXR7; and elongation factor 1-alpha, A8PJ17), cytoskeleton (tubulin alpha chain, A8PYK7; RAS-like GTP-binding protein RhoA, A8PJ63; serine/threonine protein phosphatase, A8PJS7; beta tubulin isotype 1, A2TF56; and putative actin, A3QP75), microtubule cytoskeleton (serine/threonine protein phosphatase, A8PJS7), endoplasmic reticulum (heat shock protein 70, Q8MUA7 and probable transport protein Sec61 alpha subunit, A8Q009), golgi (AGAP011363-PA, A0NFB8; CBR-ARF-6 protein, A8WMU9; chromosome 2 SCAF14705, Q4S8K4; glycoprotein 25L2, A8PU74; and Rab fragment, Q6GXB2), intracellular transport vesicles (glycoprotein 25L2, A8PU74), nucleus (putative uncharacterized protein, A8XHC9; putative uncharacterized protein, P90904; 60S ribosomal protein L3, RL3; serine/threonine protein phosphatase, A8PJS7; proteasome subunit alpha type, A8QCC8; nucleolar protein K01G5.5, A8Q703; and uncharacterized protein uev-1, O45495), nucleolus (60S ribosomal protein L3, RL3 and nucleolar protein K01G5.5, A8Q703), other nuclear structures (nucleolar protein K01G5.5, A8Q703), mitochondrion (NADH-ubiquinone oxidoreductase 75-kDa subunit, Q86S77; CBR-RPS-18 protein, A8Y099; pyruvate carboxylase 1, PYC1; probable calcium-binding mitochondrial carrier F55A11.4, CMC2; 60S ribosomal protein L11, A8NKQ0; nucleolar protein K01G5.5, A8Q703; and putative uncharacterized protein, Q9BL46), and the endosome (Vps4b-prov protein, A8QBR0) (Table 2). The appropriate localization of proteins in subcellular structures and compartments plays an important role in their functional integrity. However, determination of subcellular localization by experimental means is not practical for all proteins due to time and cost constraints (Guda 2006). Our results may assist in inferring the function of proteins predicted from the *B. xylophilus* cDNA library.

Enzymatic classification based on EC number

EC numbers were extracted by the EC numbers method from UniProt database hits using the BLASTPGP algorithm. EC numbers were classified for 133 (8.3%) of 1,599 contigs. For the *B. xylophilus* data set, 133 contigs with EC numbers were further annotated, with 44 assigned as oxidoreductases, 35 as transferases, 33 as hydrolases, 9 as lyases, 4 as isomerases, and 8 as ligases (Table 3).

Classification of membrane proteins based on the number of transmembrane domains

The TMpred algorithm predicts membrane-spanning regions and their orientation. The prediction is made

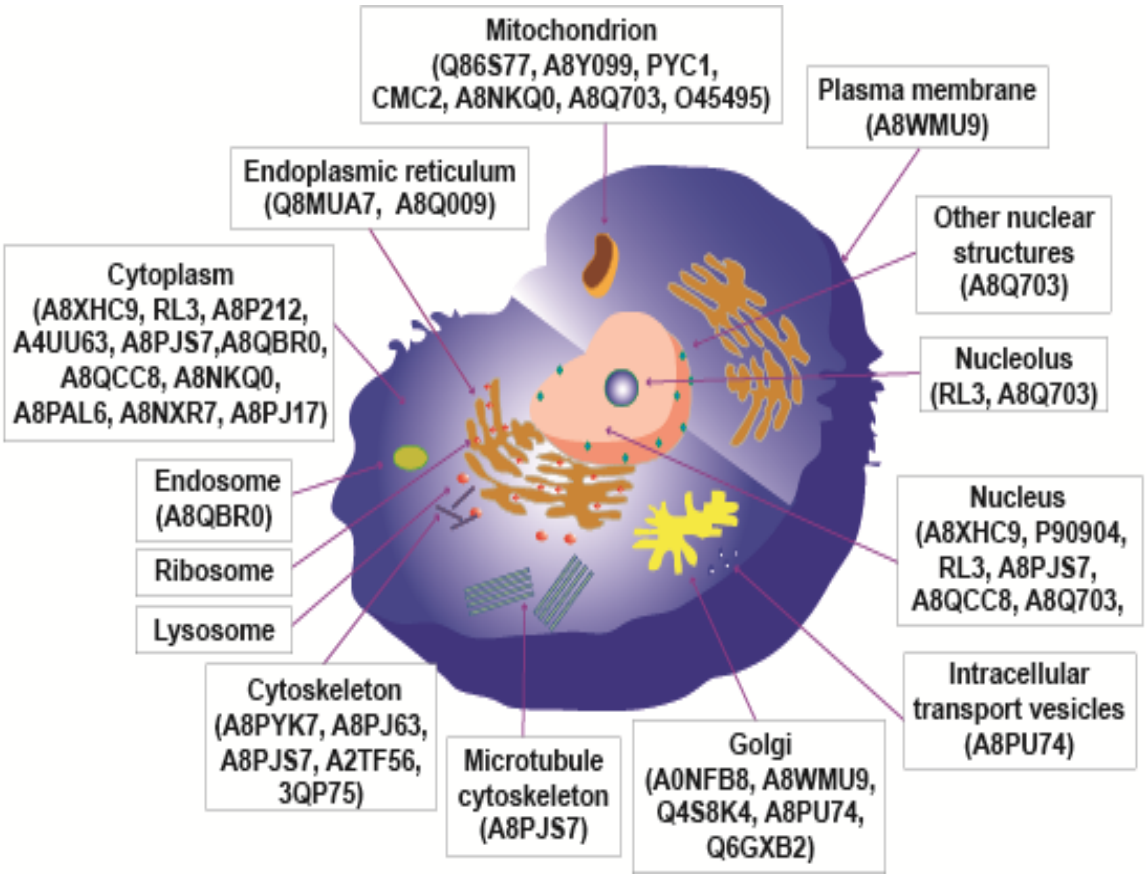

Figure 4. Putative localization of *Bursaphelenchus xylophilus* proteins in the cell. *B. xylophilus* subcellular structures and components were depicted by a single animal cell. The respective thicknesses and size of subcellular components were not accurate. Putative *B. xylophilus* proteins were replaced by annotation of the corresponding protein in the UniProt database.

Table 3. Classification of selected EC numbers.

EC number	EC description	Sorting
1	Oxidoreductases	44
1.1	Acting on the CH-OH group of donors	15
1.1.1	With NAD or NADP as acceptor	15
1.1.1.1	Alcohol dehydrogenase	3
1.1.1.2	Alcohol dehydrogenase (NADP)	3
1.1.1.37	Malate dehydrogenase	3
1.2	Acting on the aldehyde or oxo group of donors	6
1.2.1	With NAD or NADP as acceptor	3
1.2.4	With a disulfide as acceptor	3
1.2.4.1	Pyruvate dehydrogenase (lipoamide)	3
1.3	Acting on the CH-CH group of donors	5
1.3.1	With NAD or NADP as acceptor	3
1.4	Acting on the CH-NH_2 group of donors	3
1.6	Acting on NADH or NADPH	5
1.6.5	With a quinone or similar compound as acceptor	3
1.6.5.3	$NADH_2$ dehydrogenase (ubiquinone)	3
1.13	Acting on single donors with incorporation of molecular oxygen (oxygenases)	3
1.13.11	With incorporation of two atoms of oxygen	3
1.14	Acting on paired donors, with incorporation or reduction of molecular oxygen	4

Table 3. Contd.

2	Transferases	35
2.1	Transferring one-carbon groups	5
2.1.1	Methyltransferases	4
2.3	Acyltransferases	3
2.3.1	Transferring groups other than amino-acyl groups	3
2.4	Glycosyltransferases	4
2.5	Transferring alkyl or aryl groups, other than methyl groups	8
2.7	Transferring phosphorus-containing groups	12
2.7.7	Nucleotidyltransferases	3
3	Hydrolases	33
3.1	Acting on ester bonds	10
3.1.3	Phosphoric monoester hydrolases	7
3.1.3.16	Phosphoprotein phosphatase	6
3.4	Acting on peptide bonds (peptidases)	12
3.4.25	Threonine endopeptidases	4
3.4.25.1	Proteasome endopeptidase complex	4
3.5	Acting on carbon-nitrogen bonds, other than peptide bonds	3
3.5.1	In linear amides	3
3.6	Acting on acid anhydrides	6
3.6.1	In phosphorus-containing anhydrides	4
3.6.1.3	Adenosinetriphosphatase	3
4	Lyases	9
4.1	Carbon-carbon lyases	3
4.2	Carbon-oxygen lyases	5
4.2.1	Hydro-lyases	4
5	Isomerases	4
6	Ligases	8
6.1	Forming carbon-oxygen bonds	3
6.1.1	Ligases forming aminoacyl-tRNA and related compounds	3

EC numbers were extracted from UniProt database hits using the EC numbers method. Six representative EC classes were classified from *B. xylophilus* proteins. Each EC class is illustrated by a representative member. The number of genes associated with each EC class is indicated in the sorting column. The selected EC numbers have at least three hits.

Table 4. Classification of membrane proteins based on the number of transmembrane domains.

Number of domains	Number of proteins	% Protein
≥1 domain	481	30.90
1 domains	390	25.00
2 domains	62	4.00
3 domains	26	1.70
4 domains	3	0.20
none	1,078	69.10

The TMpred algorithm made a prediction of transmembrane helices in protein sequences.

using a combination of several weight matrices for scoring (Hofmann and Stoffel, 1993). Transmembrane regions of 1,599 clusters were grouped. For the *B. xylophilus* data set, 1,599 contigs with transmembrane regions could be further annotated, with 481 (30.9%) assigned to the 'above one' domain and 1,078 (69.1%) assigned as 'none' (Table 4). In the future, the long-ranged sequencing of insert cDNA will be performed to determine complete transmembrane regions of the full-length protein.

Table 5. Taxonomic classification.

Superkingdom (sorting)	Kingdom (sorting)	Phylum (sorting)	Class (sorting)
Eukaryota (665)	Metazoa (648)	Nematoda (564)	Chromadorea (563)
Bacteria (7)	Fungi (6)	Chordata (46)	Insecta (29)
	Viridiplantae (6)	Arthropoda (31)	Mammalia (20)
		Ascomycota (6)	Actinopterygii (14)
		Proteobacteria (5)	Amphibia (9)
		Streptophyta (5)	Saccharomycetes (5)
		Cnidaria (4)	Anthozoa (4)
		Platyhelminthes (3)	Aves (3)
		Apicomplexa (2)	Liliopsida (3)
		Bacteroidetes (1)	Aconoidasida (2)
		Chlorophyta (1)	Alphaproteobacteria (2)
		Firmicutes (1)	Gammaproteobacteria (2)
			Trematoda (2)
			Bacilli (1)
			Chilopoda (1)
			Chlorophyceae (1)
			Deltaproteobacteria (1)
			Enoplea (1)
			Eurotiomycetes (1)
			Malacostraca (1)
			Sphingobacteria (1)
			Spirotrichea (1)
			Turbellaria (1)

Taxonomy information was extracted by BLASTPGP hits from the UniProt database using the Taxon algorithm.

Taxonomic classification

The taxon algorithm extracted taxonomy information from BLASTPGP similarity hits using the UniProt database. Of 1,559 contigs, 672 (43.1%) were classified into taxonomy. For the *B. xylophilus* data set, the 672 contigs with taxonomy classification were further annotated, with seven assigned to bacteria and 665 assigned to eukaryota (Table 5). The number of kingdoms representing Metazoa was 648 (96.4%) of 672 contigs. The number of phylum representing Nematoda was 564 (83.9%) of 672 contigs. The number of classes representing Chromadorea was 563 (83.8%) of 672 contigs.

The class Chromadorea contains the *B. xylophilus*, which belongs to the order Tylenchida. Our results demonstrate that most genes classified in Chromadorea are highly homologous to the genes presented by Lilley and Parkinson and colleagues (Parkinson et al., 2004; Lilley et al., 2005).

Conflict of Interests

The author(s) have not declared any conflict of interests.

ACKNOWLEDGEMENTS

This project was supported by a grant from the National Academy of Agricultural Science (PJ008541), RDA, Korea. This study was supported by the 2014 Postdoctoral Fellowship Program (to H.Y.C. and I.C.C.) of the National Academy of Agricultural Science, RDA, Korea.

REFERENCES

Abelleira A, Picoaga A, Mansilla JP, Aguin O (2011). Detection of *Bursaphelenchus xylophilus*, causal agent of pine wilt disease on *Pinus pinaster* in Northwestern Spain. Plant Dis. 95:776.

Altschul SF, Madden TL, Schaffer AA, Zhang J, Zhang Z, Miller W, Lipman DJ (1997). Gapped BLAST and PSI-BLAST: a new generation of protein database search programs. Nucleic Acids Res. 25:3389-3402.

Apweiler R, Attwood TK, Bairoch A, Bateman A, Birney E, Biswas M, Bucher P, Cerutti L, Corpet F, Croning MD, *et al*. (2001). The InterPro database, an integrated documentation resource for protein families, domains and functional sites. Nucleic Acids Res. 29:37-40.

Ashburner M, Lewis SE (2002). On ontologies for biologists: the Gene Ontology- uncoupling the web. Novartis Found Symp. 247: 66-80.

Barker WC, Garavelli JS, Huang H, McGarvey PB, Orcutt BC, Srinivasarao GY, Xiao C, Yeh LS, Ledley RS, Janda JF, Pfeiffer F, Mewes HW, Tsugita A, Wu C (2000). The protein information resource (PIR). Nucleic Acids Res. 28:41-44.

Bateman A, Birney E, Cerruti L, Durbin R, Etwiller L, Eddy SR, Griffiths-Jones S, Howe KL, Marshall M, Sonnhammer EL (2002). The Pfam

protein families database. Nucleic Acids Res. 30:276-280.
Donald PA, Stamps WT, Linit MJ (2003). Pine wilt disease in APSnet plant disease lessons. The American Phytopathological Society, St. Paul, MN, USA.
Dubreuil G, Magliano M, Deleury E, Abad P, Rosso MN (2007). Transcriptome analysis of root knot nematode functions induced in the early stages of parasitism. N. Phytol. 176:426-436.
Falquet L, Pagni M, Bucher P, Hulo N, Sigrist CJ, Hofmann K, Bairoch A (2002). The PROSITE database, its status in 2002. Nucleic Acids Res. 30:235-238.
Fan J, Kang L, Sun J (2007). Role of host volatiles in mate location by the Japanese pine sawyer, *Monochamus alternatus* Hope (Coleoptera: Cerambycidae). Environ. Entomol. 36:58-63.
Fielding NJ, Evans HF (1996). The pine wood nematode *Bursaphelenchus xylophilus* (Steiner and Buhrer) Nickle (*B. lignicolus* Mamiya and Kiyohara): an assessment of the current position. For. 69:35-46.
Guda C (2006). pTARGET: a web server for predicting protein subcellular localization. Nucleic Acids Res. 34:W210-213.
Henikoff S, Henikoff JG, Pietrokovski S (1999). Blocksþ: a nonredundant database of protein alignment blocks derived from multiple compilations. Bioinform. 15:471-479.
Hofmann K, Stoffel W (1993). TMbase-A database of membrane spanning proteins segments. Biol. Chem. Hoppe-Seyler 374:166.
Kang JS, Lee H, Moon IS, Lee Y, Koh YH, Je YH, Lim KJ, Lee SH (2009). Construction and characterization of subtractive stage-specific expressed sequence tag (EST) libraries of the pinewood nematode *Bursaphelenchus xylophilus*. Genom. 1:70-77.
Kang MJ, Kim YH, Hahn BS (2010). Expressed sequence tag analysis generated from a normalized full-length cDNA library of the root-knot nematode (*Meloidogyne incognita*). Genes Genom. 32:553-562.
Kikuchi T, Aikawa T, Kosaka H, Pritchard L, Ogura N, Jones JT (2007). Expressed sequence tag (EST) analysis of the pine wood nematode *Bursaphelenchus xylophilus* and *B. mucronatus*. Mol. Biochem. Parasitol. 155:9-17.
Kikuchi T, Cotton JA, Dalzell JJ, Hasegawa K, Kanzaki N, McVeigh P, Takanashi T, Tsai IJ, Assefa SA, Cock PJ, Otto TD, Hunt M, Reid AJ, Sanchez-Flores A, Tsuchihara K, Yokoi T, Larsson MC, Miwa J, Maule AG, Sahashi N, Jones JT, Berriman M (2011). Genomic insights into the origin of parasitism in the emerging plant pathogen *Bursaphelenchus xylophilus*. PLoS Pathog. 7:e1002219.
Lee Y, Tsai J, Sunkara S, Karamycheva S, Pertea G, Sultana R, Antonescu V, Chan A, Cheung F, Quackenbush J (2005). The TIGR Gene Indices: clustering and assembling EST and known genes and integration with eukaryotic genomes. Nucleic Acids Res. 1:D71-74.
Lilley CJ, Atkinson HJ, Urwin PE (2005). Molecular aspects of cyst nematodes. Mol. Plant Pathol. 6:577-588.
Linit MJ (1988). Nemtaode-vector relationships in the pine wilt disease system. J. Nematol. 20:227-235.
Lupas A, Van Dyke M, Stock J (1991). Predicting coiled coils from protein sequences. Sci. 24:1162-4116.
Martin DM, Berriman M, Barton GJ (2004). GOtcha: a new method for prediction of protein function assessed by the annotation of seven genomes. BMC Bioinform. 5:178.
Maruyama K, Sugano S (1994). Oligo-capping: a simple method to replace the cap structure of eukaryotic mRNAs with oligoribonucleotides. Gene 138:171-174.
Menon R, Garg G, Gasser RB, Ranganathan S (2012). TranSeqAnnotator: large-scale analysis of transcriptomic data. BMC Bioinformatics 13(Suppl 17):S24.
Mota M, Vieira P (2008). Pine wilt disease: a worldwide threat to forest ecosystems. Springer XVIII, 406 p., ISBN: 978-1-4020-8454-6
Mota MM, Braasch H, Bravo MA, Penas AC, Burgermeister W, Metge K , Sousa E (1999). First report of *Bursaphelenchus xylophilus* in Portugal and in Europe. Nematology 1: 727-734.
Myers RF (1988). Pathogenesis in pine wilt caused by pinewood nematode, *Bursaphelenchus xylophilus*. J. Nematol. 20:236-244.
Nagaraj SH, Gasser RB, Ranganathan S (2008). Needles in the EST Haystack: Large-Scale Identification and Analysis of Excretory-Secretory (ES) Proteins in Parasitic Nematodes Using Expressed Sequence Tags (ESTs). PLoS Negl. Trop. Dis. 2:e301.
Oh JH, Kim YS, Kim NS (2003). An improved method for constructing a full-length enriched cDNA library using small amounts of total RNA as a starting material. Exp. Mol. Med. 35:586-590.
Parkinson J, Mitreva M, Whitton C, Thomson M, Daub J, Martin J, Schmid R, Hall N, Barrell B, Waterston RH, McCarter JP, Blaxter ML (2004). A transcriptomic analysis of the phylum Nematoda. Nat. Genet. 36:1259-1267.
Rensing SA, Lang D, Reski R (2003). *In silico* prediction of UTR repeats using clustered EST data. Proceed. German Conference Bioinform. 117-122.
Rosso MN, Jones JT, Abad P (2008). RNAi and functional genomics in plant parasitic nematodes. Annu. Rev. Phytopathol. 47:207-232.
Sakai M, Yamasaki T (1990). (+)-Juniperol and (+)-pimaral: Attractants for the cerambycid beetle, Monochamus alternatus Hope. J. Chem. Eco. 16:3383-3392.
Scholl EH, Thorne JL, McCarter JP, Bird DM (2003). Horizontally transferred genes in plant-parasitic nematodes: a high-throughput genomic approach. Genome Biol. 4:R39.
Shen YQ, Burger G (2007). 'Unite and conquer': enhanced prediction of protein subcellular localization by integrating multiple specialized tools. BMC Bioinform. 8:420.
Shibata E (1987). Oviposition schedules, survivorship curves, and mortality factors within trees of two cerambycid beetles (Coleoptera: Cerambycidae), the Japanese pine sawyer, *Monochamus alternatus* hope, and sugi bark borer, *Semanotus japonicus* lacordaire. Res. Population Ecol. 29:347-367.
Sriwati R, Takemoto S, Futai K (2007). Cohabitation of the pine wood nematode, *Bursaphelenchus xylophilus*, and fungal species in pine trees inoculated with *B. xylophilus*. Nematol. 9:77-86.
Steiner G, Buhrer EM (1934). *Aphelenchoides xylophilus* n. sp. a nematode associated with bluestain and other fungi in timber. J. Agric. Res. 48:949-951.
Sultana T, Kim J, Lee SH, Han H, Kim S, Min GS, Nadler SA, Park JK (2013). Comparative analysis of complete mitochondrial genome sequences confirms independent origins of plant-parasitic nematodes. BMC Evol. Biol. 13:12.
Tae H, Ryu D, Sureshchandra S, Choi JH (2012). ESTclean: A Cleaning Tool for Next-Gen Transcriptome Shotgun Sequencing. BMC Bioinform. 13:247.
Tatusov RL, Natale DA, Garkavtsev IV, Tatusova TA, Shankavaram UT, Rao BS, Kiryutin B, Galperin MY, Fedorova ND, Koonin EV (2001). The COG database: new developments in phylogenetic classification of proteins from complete genomes. Nucleic Acids Res. 29:22-28.
Vieira J, Messing J (1987). Production of single-stranded plasmid DNA. Methods Enzymol. 153:3-11.
Wootton JC, Federhen S (1993). Statistics of local complexity in amino acid sequences and sequence databases. Comput. Chem. 17:149-163.
Xie G, Chain PS, Lo CC, Liu KL, Gans J, Merritt J, Qi F (2010). Community and gene composition of a human dental plaque microbiota obtained by metagenomic sequencing. Mol. Oral Microbiol. 25:391-405.
Yan X, Cheng XY, Wang YS, Luo J, Mao ZC, Ferris VR, Xie BY (2012). Comparative transcriptomics of two pathogenic pinewood nematodes yields insights into parasitic adaptation to life on pine hosts. Gene 505:81-90.
Yang F, Xu B, Zhao S, Li J, Yang Y, Tang X, Wang F, Peng M, Huang Z (2012). De novo sequencing and analysis of the termite mushroom (*Termitomyces albuminosus*) transcriptome to discover putative genes involved in bioactive component biosynthesis. J. Biosci. Bioeng. 4:228-231.

academicJournals

Vol. 13(33), pp. 3344-3351, 13 August, 2014
DOI: 10.5897/AJB2014.13680
Article Number: 4C4439846615
ISSN 1684-5315

http://www.academicjournals.org/AJB

African Journal of Biotechnology

Full Length Research Paper

A parallel reconfigurable platform for efficient sequence alignment

A. Surendar[1]*, M. Arun[2] and P. S. Periasamy[3]

[1]Research Scholar, Anna University, Chennai-600025, India.
[2]School of Electronics Engineering, VIT University, Vellore-632014, India.
[3]Department of ECE, K.S.R. College of Engineering, Tiruchengode-637215, India.

Received 31 January, 2014; Accepted 4 July, 2014

Bioinformatics is one of the emerging trends in today's world. The major part of bioinformatics is dealing with DNA. Analysis of DNA requires more memory and high efficient computations to produce accurate outputs. Researchers use various bioinformatics algorithms for sequencing and pattern detection techniques, but still now it takes enormous amount of time for computations. In our method we are going to propose a time, memory and speed optimized algorithms for efficient repetitive finding in genomes and proteins. Then, another major aspect is the hardware implementation. It is a platform which reduces the complexity of process further. Therefore, we have proposed to implement the optimized algorithm in the reconfigurable and user friendly FPGA platform. Thus, our proposal mainly focuses on an efficient and optimized computation, analysis and sequencing of DNA pattern. The distinct feature is reducing the time consumption from several hours to few seconds.

Key words: DNA, sequencing, bioinformatics, efficient computations, repetitive finding, optimized sequencing.

INTRODUCTION

In the world of expanding set of biological species, finding repetitive structures in genomes and proteins is important to understand their biological functions. DNA sequencing is the process of determining the precise order of nucleotides within a DNA molecule. It includes any method or technology that is used to determine the order of the four bases Adenine, Guanine, Cytosine and Thymine in a strand of DNA (Surendar et al., 2013). The advent of rapid DNA sequencing methods has greatly accelerated biological and medical research and discovery. If the number of maximal repeat increases, then finding those structures becomes tedious. In existing method, Burrows Wheeler Transform and Wavelet Coding, the major disadvantage is time consumption. And it also needs huge computer space for processing the structures. One of the most important thing that decides our heredity is DNA. One of the well-known features of DNA is its repetitive structures. Many existing methods proposed different data compression formats to reduce the space consumption. Even though the method saves memory, time and speed efficiency cannot be obtained. To obtain optimization of the bioinformatics algorithms used: i) bloom filter; ii) content-addressable memory; iii) Aho-Corasick algorithm are used.

*Corresponding author. E-mail: surendararavindhan@gmail.com.

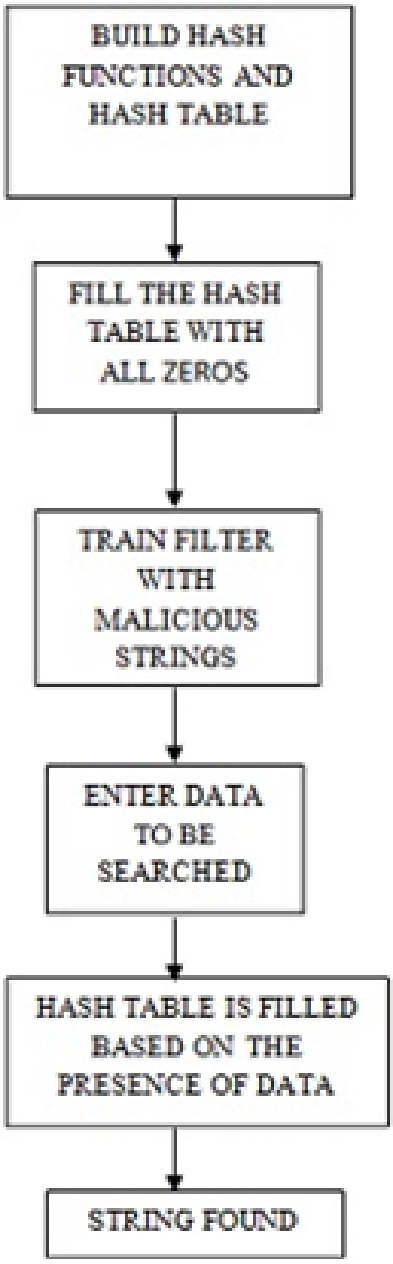

Figure 1. Flow of bloom filter.

TOOLS FOR OPTIMIZATION

A field-programmable gate array (FPGA)

A field-programmable gate array (FPGA) is an integrated circuit designed to be configured by a customer or a designer. The FPGA configuration is generally specified using a hardware description language (HDL). FPGAs are reprogrammable silicon chips. It provides hardware-timed speed and reliability. FPGAs are truly parallel in nature. Previously, a design may have included 6 to 10 ASICs, the same design can now be achieved using only one FPGA (Surendar et al., 2013).

Altium - 3000 nanoboard-XILINX variant

Altium - 3000 nanoboard-XILINX variant is a perfect entry-point to discover and explore the world of soft design. It is a programmable hardware platform. Rapid and interactive implementation and debugging of digital designs can be achieved. It has a fixed user FPGA's on the motherboard and so, speed of processing is increased. Circuit can be probed, analyzed and debugged interactively using an array of virtual instruments and JTAG-based monitoring features.

Bloom filter

Bloom filter (Arun and Krishnan, 2011) is a space-efficient probabilistic data structure that is used to test whether an element is a member of a set (Figure 1). This compact representation is the payoff for allowing a small rate of false positives in membership queries; that is, queries might incorrectly recognize an element as member of the set which can be made negligible by the intensive design effort. It consists of number of hash tables and hash functions that easily store and handle the incoming strings. Each hash table entry stores only a single bit of data, thus a hash table of size M would be made up of M entries, each of size one bit. A bloom filter must be trained with a dictionary of malicious strings before it can be used in a system. All hash table entries are initialized to 0 before training begins. During the training phase malicious strings are fed one at a time to the bloom filter. Each of the k hash functions then acts on every incoming dictionary string (Table 1) and computes an output in the range 0 to M − 1. Entries corresponding to these k outputs are set to 1 in the hash table. The bloom filter reports the current string in its window as a member of the dictionary on which the bloom filter was trained. If a non dictionary input string (Table 2) is such that it hashes to k hash table entries, each of which was set to 1 by one or more dictionary elements during the training phase, the bloom filter will erroneously report this string to be a member of the dictionary on which the bloom filter was trained. The bloom filter thus reports a false positive in this case. Though a bloom filter may occasionally report false positives, it does not allow for false negatives. Even though a bloom filter may sometimes report a non member to be a part of the dictionary set, it will never happen that a true member goes unreported. Thus, the working of bloom filter can be explained in following steps: 1) training the bloom filter with various strings; 2) defining the hash functions and building hash testing the incoming strings for the finding of given string with the help of hash functions; 4) determination of result using the behavior of the filter.

The part of code to hash the values to the hash table to

Table 1. Dictionary.

Path	In dictionary	Suffix link	Dict. suffix link
()	-		
(a)	+	()	
(ab)	+	(b)	
(b)	-	()	
(bc)	+	(c)	(c)
(bca)	+	(ca)	(a)
(c)	+	()	
(ca)	-	(a)	(a)
(caa)	+	(a)	(a)

Dictionary {a, ab, bc, bca, c, caa}

Table 2. Input string analysis.

Node	Remaining string	Output end position	Transition	Output
()	abccab		Start at root	
(a)	bccab	A:1	() to child (a)	Current node
(ab)	ccab	Ab:2	(a) to child (ab)	Current node
(bc)	cab	bc:3, c:3	(ab) to suffix (b) to child (bc)	Current node, Dict suffix node
(c)	ab	c:4	(bc) to suffix (c) to suffix () to child (c)	Current node
(ca)	b	a:5	(c) to child (ca)	Dict suffix node
(ab)		ab:6	(ca) to suffix (a) to child (ab)	Current node

Analysis of Input string analysis.

the filter is as:

hash1:=hash(present_state(1),d); hash2:=hash(present_state(2),d); a<=hash1; b<=hash2; y(hash1)<='1'; y(hash2)<='1'; if(hashd_bitvectr(hash1)='1'and hashd_bitvectr(hash2)='1')then state<="positive"; shft_out :='0'; match<=input(pos-1 to pos+4); -- elsif(hashd_bitvectr(hash1)='1' or hashd_bitvectr(hash2)='1')then --- state<="fals_pos"; -- shft_out :='1'; else state<="negative"; shft_out :='1'; end if The VHDL simulation of the filter yields the waveform shown in Figure 2.

Content addressable memory

Manuscript of content-addressable memory (CAM) was received on July 17, 1987 and revised October 5, 1987. A content-addressable memory (CAM) is a high speed matching unit because it has parallel matching capability (Yoshiki et al., 2002). It speeds up the data searching and pattern matching. CAMs are storage devices that allow its contents to be accessible on the basis of a match between a specified key and the contents, a process called "content addressing". CAM architectures fall between two extremes: the bit serial CAM and the fully parallel CAM. In the bit serial CAM, the matching logic is associated with one bit position, and shared among all the bits in a word, in effect matching one bit at-a-time simultaneously in all the CAM words. In the fully parallel CAM, each word has its own bit-parallel matching logic, allowing that match of all words to process. Here, initially the device is trained with certain 8 bit binary database. And then the input binary parameter is given. The number of 1's in the parameter is extracted by parameter extraction then it is stored in the parameter memory. Then 1's in the input parameter is compare with the trained database and produce a required result else next input parameter is given. Thus, the working of CAM filter can be expressed in following steps. Castelo et al., 2002

1. The device is trained with database,
2. Input is given,

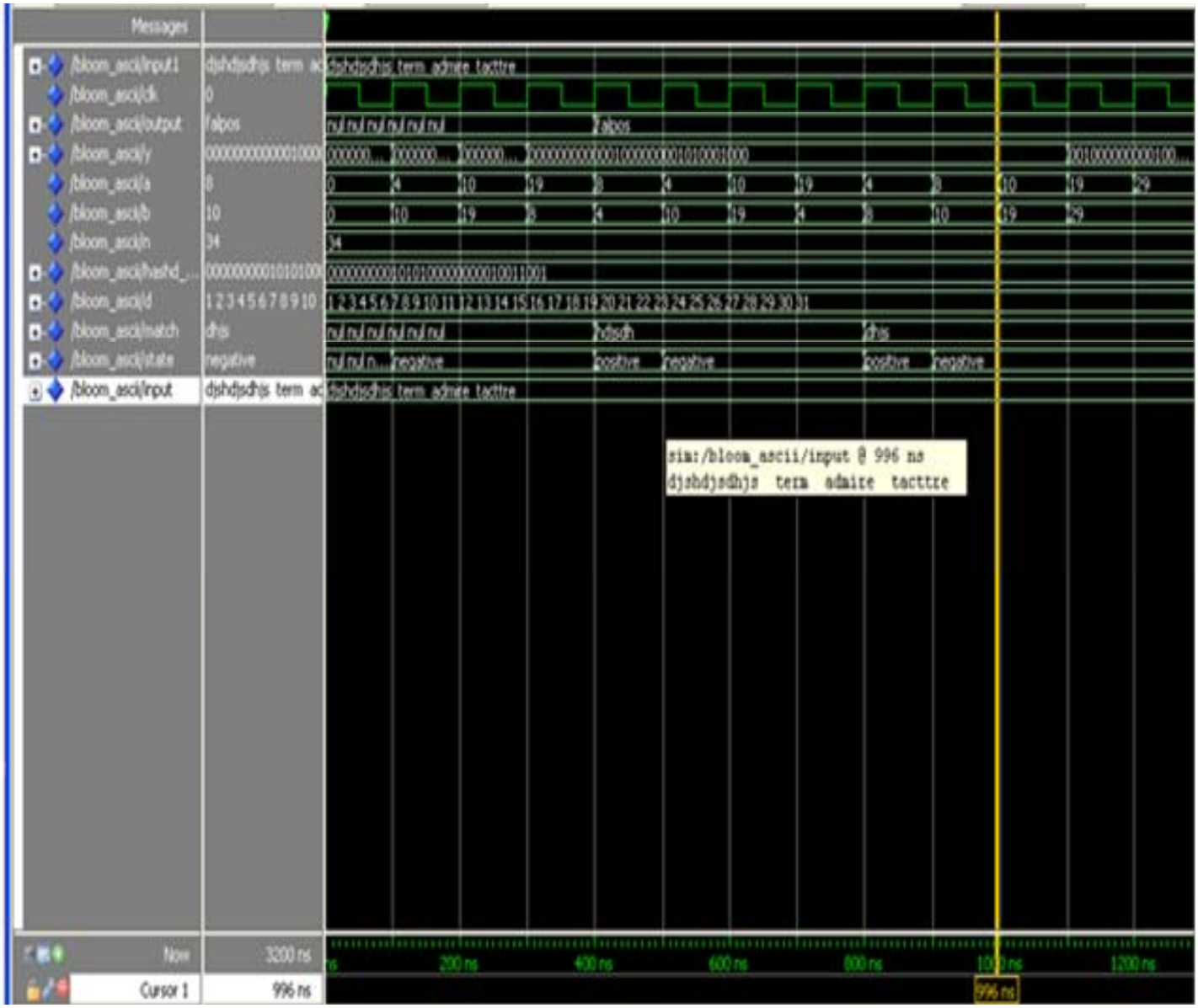

Figure 2. Output waveform of bloom filter.

3. The number of 1's and 0's is extracted by parameter extraction,
4. It is stored in memory,
5. Compare 1's in the given input with database,
6. Finally, it produced the required input if it is matched (Figure 3).

The code to train CAM is given as process (clk,fail,sram_out,ss)

begin; if rising_edge(clk) then; tcam_in.input<=input; tcam_in.current_state<=sram_out;
end if; end process; x2:tcam port map(tcam_in,tcam_out); x3:sram port map(tcam_out,sram_out,fail); process(sram_out); begin; if sram_out=2 then; output<=" pattern he matched "; elsif sram_out=9 then; output<="pattern hers matched"; elsif sram_out=7 then; output<="pattern his matched "; elsif sram_out=5 then; output<="pattern she matched "; end if; end process; The VHDL simulation of the filter yields the waveforms shown in (Figures 4 and 5).

Aho-Corasick

Aho-Corasick algorithm (Komodia, 2012) is a dictionary matching algorithm that searches for elements of a finite set of strings in the input text, developed by Alfred V. Aho

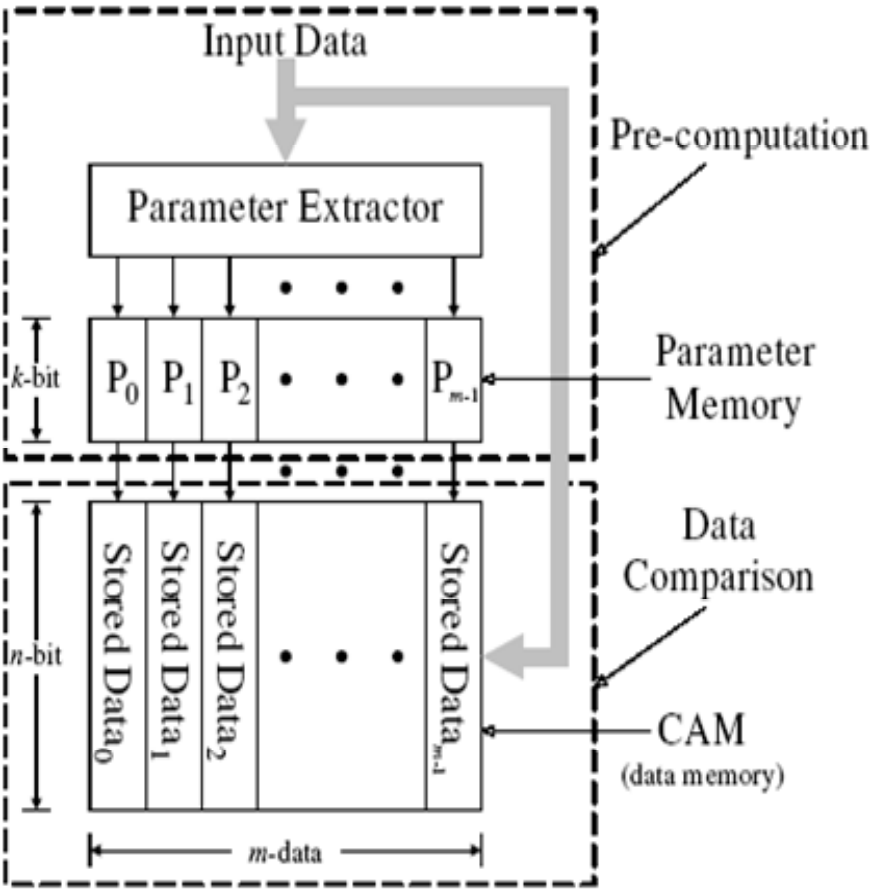

Figure 3. Pre-computation block of CAM.

and Margaret J. Corasick. Since, it locates all patterns in one time, the time complexity of the algorithm (Jung et al., 2006) is proportional to sum of the length of the patterns, length of the input text and the number of matches. In this algorithm, a trie with suffix tree-like set of links is established from each node representing a string to the node corresponding to the longest proper suffix. Since, it also consists of links from each node to the longest suffix node that connect to a match string; all of the matches can be traversed by going along the resulting linked list. The trie is utilized at runtime to keep track of the longest match and the suffix links are used to make sure the computation is proportional to the length of the input. For every link along the dictionary suffix linked list and every node in the dictionary located, a match is found. Since most of the time, the pattern database is known ahead, program can be created to build the trie, compile it and save it for later use. In this case, the computational complexity in the runtime is proportional to the sum of the length of the inputs and the number of matched entries. Figure 6 shows an example of data structure made up from a couple of strings. Each row represents a node in the trie while each column indicates the distinct order of characters from root to the node. In every step, the current node will try to find its child recursively if the suffix child does not exist until it reach the root node. Steps taken when scanning “abccab” are shown below.

Simulation on an input text

Since there may be two or more dictionary entries at a character location in the input text, more than one dictionary suffix link may need to be followed. The working of Aho-Corasick can be explained as follows.

1. The data pattern to be analyzed is built as a dictionary,
2. The pattern to be find is given as input,
3. The node built based on suffix matching,
4. The input for next string is taken from previous node.

Hence, all the pattern is matched at same time. The critical part of code to train the filter is given as, architecture behave of aho_Corasick is

type state_node is;
(state_0,state_1,state_2,state_3,state_4,state_5,state_6,

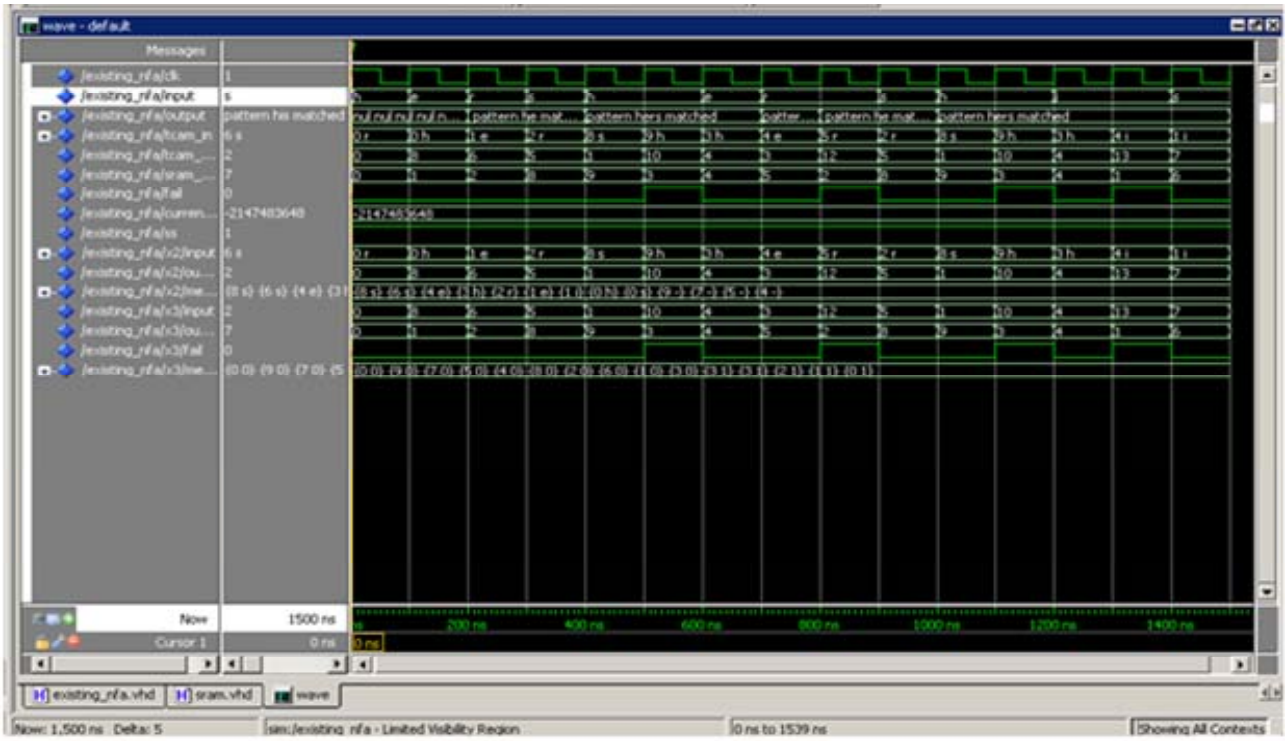

Figure 4. Output waveform of CAM.

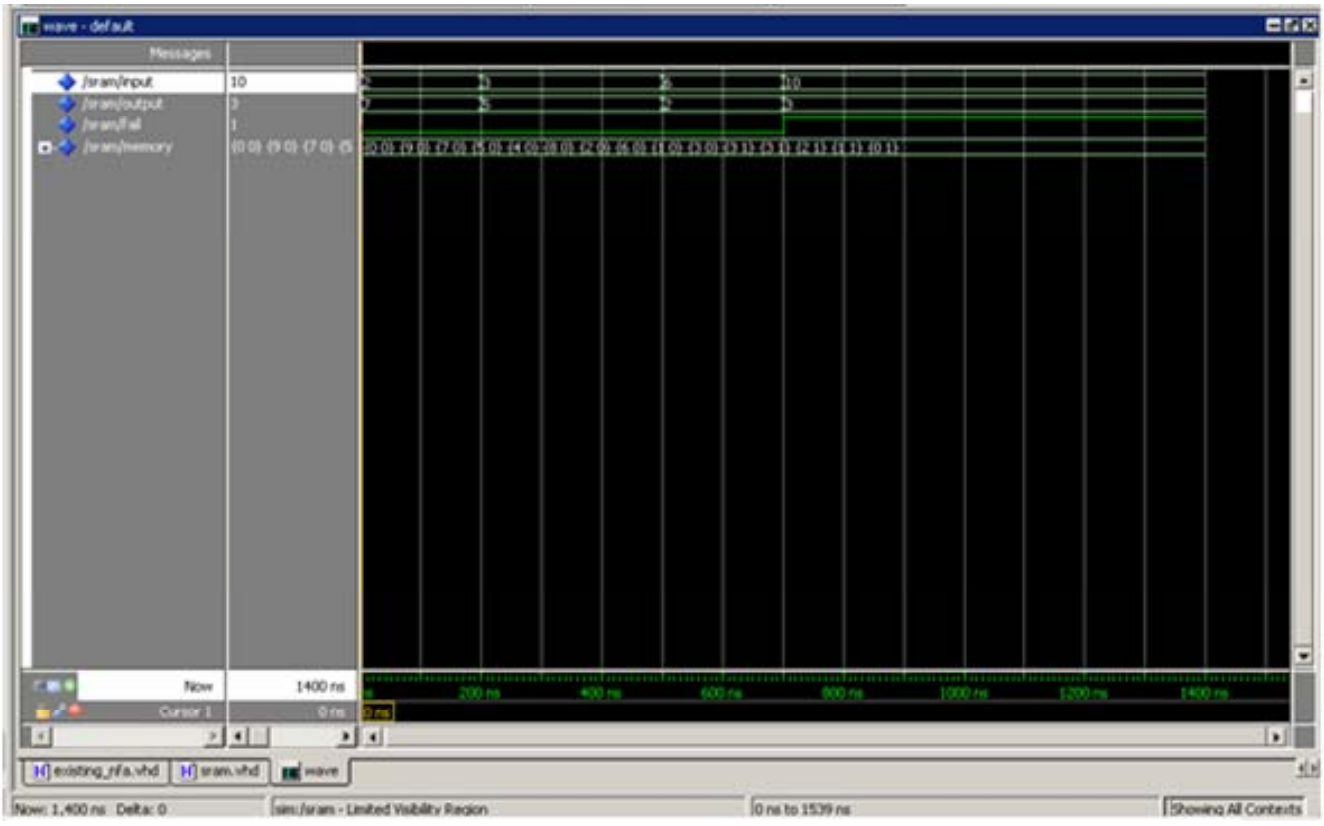

Figure 5. Output waveform of SRAM.

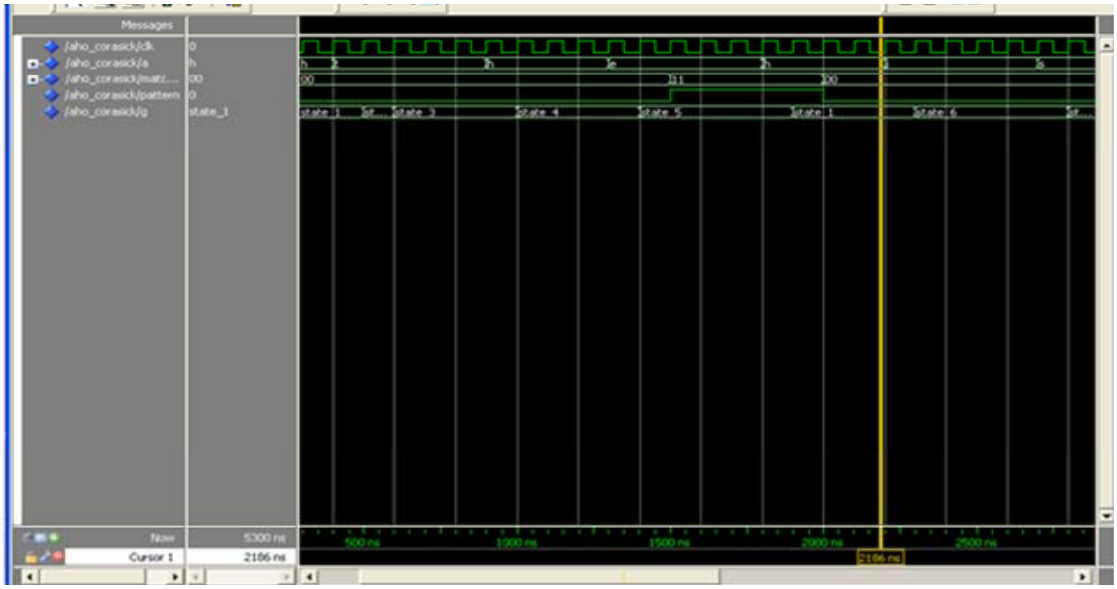

Figure 6. Output waveform of Aho-Corasick.

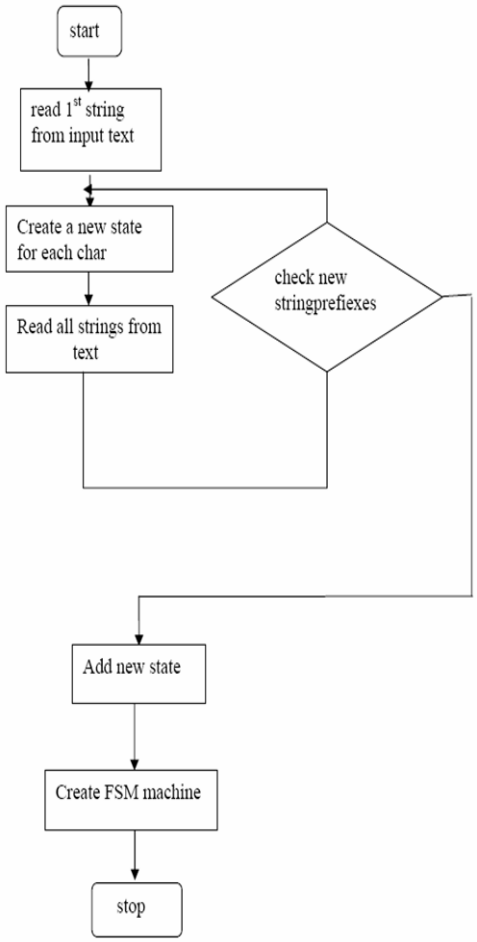

Figure 7. Flow of Aho-Corasick string matching.

PERFORMANCE RESULTS

PARAMETERS	AHO	BLOOM	CAM	TCAM	SRAM
IOs	12	321	169	65	72
CELL USAGE	111	9004	221	41	325
FF/LATCHES	13	104	20	-	-
IO BUFFERS	12	321	169	37	72
TOTAL REAL TIME	3s	10s	5s	3s	4s
TOTAL CPU TIME	3.23s	10.2s	5.4s	2.93s	4.28s
TOTAL MEMORY USED	234872Kb	26239Kb	24408Kb	232120Kb	233464Kb

Figure 8. Performance summary of filters.

state_7,state_8,state_9); signal g:state_node; begin; process(clk,g,a); begin; if rising_edge(clk) then; case g is; when state_0 =>; match_vector<="00"; pattern<='0'; if a(1)='h' then; g<=state_1; elsif a(1)='t' then; g<=state_3; else; -- g<=state_0; end if; The VHDL simulation of the filter yields the below waveform (Figure 7).

Conclusion

The filter used not only reduces the execution performance time but it stands out most in saving the memory. The flip flops and the latches used are triggered efficiently using perfect clocks. The total I/O ports used for this process are very less. The time of CPU processing is reduced very much and thus it enhances the output processing capability. The below table shows the requirements of optimized filters. The optimized algorithms are implemented in reconfigurable FPGA platform. The FPGA platform is in Altium Nanoboard 3000- Xilinx Spartan. The above proposed algorithms are analyzed to be efficient from their performance. When it is implemented in a reconfigurable platform it will work in more optimized way that produces accurate outputs. The Nano Board 3000 is a programmable design environment so it will be efficient for analysis.

Conflict of Interests

The author(s) have not declared any conflict of interests.

REFERENCES

Arun M, Krishnan A (2011). Functional Verification of Signature Detection Architectures for High Speed Network Applications. International Journal of Automation and Computing, Springer 9(4):395-402.

Arun M, Krishnan A (2011). Low Power Bloom Filter Architectures Using Multi Stage Lookup Techniques. Aust. J. Elect. Electronics Engineering, 8(3):1-10.

Castelo AT, Martins W, Gao GR (2002). Troll-Tandem Repeat Occurrence Locator. Bioinformatics. 18(4): 634-636.

Jung HJ, Baker ZK, Prasanna VK (2006). Performance of FPGA Implementation of Bit-split Architecture for Intrusion Detection Systems.

Komodia (2012). Aho-Corasick source code. Available: http://www.komodia.com/aho-corasick

Surendar A, Arun M, Periasamy PS (2013). Hardware Based Algorithms for Bioinformatics Applications - A Survey. Int. J. Appl. Eng. Res. (6):745-754.

Surendar A, Arun M, Bagavathi C (2013). Evolution of Reconfigurable Based Algorithms for Bioinformatics Applications: An Investigation. Int. J. Life Sci. Bt & Pharm. Res. 2(4):17-27. Symposium on Biocomputing. 7: 271-282.

Yoshiki Y, Tsutomu M (2002). High Speed Homology Search with FPGAs. Pacific

academicJournals

Vol. 13(33), pp. 3352-3359, 13 August, 2014
DOI: 10.5897/AJB2013.13530
Article Number: FEB0DFF46616
ISSN 1684-5315

http://www.academicjournals.org/AJB

African Journal of Biotechnology

Full Length Research Paper

Genetic variability among 'Kashmiri Nakh' pear (*Pyrus pyrifolia*): A local variety grown in North- Western Himalayan region of India

M. K. Verma*, S. Lal, J. I. Mir, H. A. Bhat and M. A. Sheikh

Division of Fruits and Horticultural Technology, Indian Agricultural Research Institute, New Delhi-110012, India.

Received 3 December, 2013; Accepted 20 June, 2014

Twenty four (24) 'Kashmiri Nakh' pear (*Pyrus pyrifolia*) genotypes were studied to assess the overall degree of polymorphism, detect similarities among important tree, pomological, fruit quality and yield parameters. Eleven (11) variables were scored and subjected to multivariate analysis. Results show a considerable phenotypic diversity among 'Kashmiri Nakh' pear genotypes and differed significantly for the above traits. The cluster analysis classified the genotypes into two major groups according to their potential characteristics. The first group was found superior in terms of fruits total soluble solids (TSS), TSS/acidity and yield related characteristics and second group in fruits morphological (length, diameter, weight) and tree characteristics attributes. Principal component analysis (PCA) revealed that traits positively related to tree height, tree spread (N-S), tree spread (E-W), yield per tree, fruit weight, fruit length, fruit diameter and acidity, however negatively related to TSS and TSS/acidity. The first principal components expressed 33.58% of the total variation and second PC2 accounted for 23.76% of the total variation. A large proportion of variability observed in genotypes 'TB-3, CHB-4, TBP-3, THP-7, TB-1, THP-1, TBP-1 and TB-2 were found unique for tree, fruit and yield attributing traits during PCA.

Key words: Genetic variability, genotypes, cluster analysis, principal component analysis (PCA).

INTRODUCTION

Pear is the third most important fruit crop grown in temperate region after grapes and apples (Oliveira et al., 1999) in world. In India, it is grown in an area of about 0.4 lakh ha and productivity 8.82 t/ha (FAO, 2012). The genus *Pyrus*, with common name pear, belongs to subfamily Pomoideae, and the family Rosaceae. Geographically, pears are divided in to Occidental and Oriental groups. Occidental pears found in Europe, northern Africa, Asia Minor, Iran, central Asia, and Afghanistan; the majority of cultivars originated primarily from *Pyrus communis*. The Oriental pears grown mainly in Tian-Shan and Hindu-Kush Mountains eastward to Japan and further divided into five groups, that is, Ussurian pear, Chinese white pear, Chinese sand pear, Xinjiang pear (*Pyrus sinkiangensis* Yu) and Japanese pear. Chinese sandpears are botanically *Pyrus pyrifolia*

*Corresponding author. E-mail: mahenicar10@gamil.com. Tel: +91-11-25843214.

Abbreviations: PCA, Principal component analysis; **TSS,** total soluble solids; **PC,** principal components.

and native to China, Japan and Korea. Himalayan region in Asia is known for its biological richness and has always been a botanist's paradise. Several native species that are commonly grown wild are*Pyrus pashia* Buch. & Ham. ex. D. Don (Himalayan Pear, Indian wild pear, Mehal, Mole, Kainath, Soh jhur Shegal, Chhota kainth, wild pear), *P. serotina* Rehd., *Pyrus kumaonii* (Decne.) Stapf., *Pyrus verruculosa* (Indian pear), *Pyrus griffithi* Decne., *Pyrus jacquemontiana* Decne., *Pyrus khasiana* Decne., *Pyrus polycarpa* Hook. F., and *P. pyrifolia* (Burm. F.) Nakai var. culta (Makino) Nakai. In India, pear cultivars commercially grown belong to both *P. pyrifolia* and *P. communis* group. Cultivated occidental pears introduced in the 19th century from Europe and America, where as oriental pears (Chinese sand pears) came from Eastern Asian countries. The 'Chinese Sand Pears' were widely grown in North Western Himalayan region including Jammu and Kashmir, Himachal Pradesh and Uttarakhand. The maximum area under cultivation of 'Chinese Sand Pear' is existed in Kashmir valley. Therefore, it is locally known as 'Kashmiri Nakh". It is also believed that the 'Kashmiri Nakh' is one of the naturalized indigenous cultivar grown since ancient time in India.

Genetic diversity is the key component of any agricultural production system. It plays vital roles for efficient selection of parents for plant improvement in which genetically diverse parents are likely to contribute desirable segregants and or to produce high heterotic crosses. Parents identification based on divergence are more promising for any breeding program (Arunachalam, 1981). Grouping or classification of genotypes based on suitable scale is quite imperative to understand the usable variability existing among them.

The value of genetic diversity, in its various forms has been extensively discussed (Smale, 2006; Rausser and Small, 2011). Moreover, plant breeders require genetic variation (genotypes) for crop/plant improvement. Morphological characters and isozyme analysis have been the two major tools used to assess the genetic variation in *Pyrus* spp. However, isozyme markers and morphological characters are still limited in number (Karimi et al., 2008; Yamamoto et al., 2004). These traits are in common use for elucidation of wide genetic diversity in different field and horticultural crops (Blazek, 2007). Although, newly developed molecular markers are valuable techniques in gene based diversity studies, however the procedures used for molecular analysis have disadvantage of high cost (Ahmad et al., 2004; Bouhadida et al., 2005). The North Western region of Himalayas possesses a high level of heterozygosity created through natural and artificial reproductions (Srivastava et al., 2012). The potential of genetic variability is vast and need to be explored for genetic enhancement of pear genotypes in North West Himalayan region to meet the demand for more food and to find particular characters such as variability in fruit traits especially in size and shape (round, oblong and pyriform) and colour of fruits. In contrast, morphological traits could feasibly be used for parental selection and along with molecular techniques are of highly appreciated procedures for description and germplasm classification of plants. Statistical method such as: principal component analysis and cluster analysis have been employed as powerful options for plant cultivar and accession screenings. Morphological criteria have been widely used as important markers in plant breeding programs (Kaufmane et al., 2002; Ogasanovic et al., 2007; Karimi et al., 2008). Keeping in view these facts, the present studies were carried out to investigate the extent of genetic diversity in germplasm based on pomological, yield and quality traits using multivariate analysis.

MATERIALS AND METHODS

This study was conducted during year 2006 to 2009 on 24 diverse genotypes of 'Kashmiri Nakh' pear collected from different sites of Kashmir valley, India (Table 1). The primary selection criterion was based on fruit yield and quality attributes. Individual genotypes were marked in the field. The data were recorded at the time of fruit maturity during summer (August to September) seasons of each year, that is, 2006 to 2009 and data pooled for analysis. Tree height was measured by pole method, and tree spread in N-S and E-W have been recorded by measuring tape. Morphological features and physico-chemical parameters of the fruits were recorded in the laboratory. Twenty fruits from each genotype were randomly chosen and measured. The data were collected on fruit length (mm), fruit weight (g), fruit diameter (mm), pulp (%) , TSS (^{o} Brix), acidity (%), ascorbic acid (mg/100 g) and fruit yield (kg/plant). Weight was measured by Sartorius balance of accuracy of 0.001 g. The length and diameter of the fruit was measured with a digital vernier caliper. The measurement of fruit length was made on the polar axis, that is, between the apex and the end of stem. The maximum width of the fruit, as measured in the direction perpendicular to the polar axis, is defined as the diameter. Total soluble solids (T.S.S), titrable acidity, and sugars were determined by method given in AOAC (1994). The experiment was conducted under randomized block design replicated three times and pooled data of two years were analyzed as per the method suggested by Gomez and Gomez (1984).

To explore the diversity and relationship among 24 genotypes, their vital morphological characteristics were studied by the multivariate factor analysis. The determination of the states of the morphological and chemical characters was carried out on samples collected. To find out significance level, analysis of variance (ANOVA) performed using PROC GLM, clustering of genotypes into similarity groups was performed using the method tree procedure PROC CLUSTER based on average distance. In order to identify the patterns of morphological variation and contribution of traits, principal component analysis (PCA) was conducted as PROC PRINCOP in the SAS 9.3 software (SAS Institute, 2012, Cary, NC).

RESULTS AND DISCUSSION

Analysis of variance showed significant differences among the genotypes for all the characters studied and extent of variability is given in Table 2. The tree height was ranged from 3.15 to 14.15 m and maximum recorded in 'CHB-4' followed by 'TBP-3' and minimum in 'TB-3' m.

Table 1. List of genotypes used in studied.

S/N	Genotype	S/N	Genotype
1	THP-1	13	TBP-3
2	THP-2	14	CB-1
3	THP-3	15	CB-2
4	THP-4	16	CB-3
5	THP-5	17	CHB-4
6	THP-6	18	CB-5
7	THP-7	19	CB-6
8	TB-1	20	CB-7
9	TB-2	21	CB-8
10	TB-3	22	CHB-1
11	TBP-1	23	CHB-2
12	TBP-2	24	CHB-3

Table 2. Tree fruit and yield characteristic of 'Kashmiri Nakh' pear genotypes grown commercially in North West Himalayan region of India.

Genotype	Tree height (m)	Tree spread (m) N-S	Tree spread (m) E-W	Fruit weight (g)	Fruit length (mm)	Fruit Diameter (mm)	TSS (°Brix)	TSS/Acidity ratio (%)	Acidity (%)	Vit-C (mg/100 gm pulp)	Yield/tree (kg)
THP-1	10.25	12.25	10.25	115.07	61.65	58.84	13.1	52.40	0.25	4.94	250
THP-2	9.45	10.25	8.45	128.58	65.39	60.66	13.2	37.71	0.35	2.86	210
THP-3	10.45	10.56	9.58	124.41	60.76	58.43	12.9	67.89	0.19	2.34	510
THP-4	8.78	9.45	8.45	128.61	61.90	61.9	13.3	110.83	0.12	1.17	600
THP-5	3.45	2.45	3.45	119.91	60.23	60.77	15.7	65.41	0.24	2.21	240
THP-6	4.45	4.46	5.12	105.92	58.65	58.31	16.5	91.66	0.18	3.25	280
THP-7	3.58	4.58	5.45	137.18	66.44	62.71	16.5	68.75	0.24	1.95	215
TB-1	6.25	7.16	6.89	122.37	62.11	61.79	15.9	66.25	0.24	2.73	315
TB-2	11.15	10.13	9.45	93.95	54.96	57.45	15.7	82.63	0.19	1.69	800
TB-3	3.15	3.09	4.56	58.82	46.17	51.56	16.5	71.73	0.23	2.73	245
TBP-1	11.45	11.07	10.58	114.35	58.37	60.17	17.8	136.92	0.13	2.73	1600
TBP-2	12.25	14.45	11.25	116.80	59.41	59.71	13.8	125.45	0.11	2.34	815
TBP-3	13.55	15.56	14.20	96.01	56.28	57.65	13.4	33.50	0.4	2.34	1614
CB-1	8.45	6.78	7.14	115.03	65.32	52.13	14.4	120.00	0.12	2.73	250
CB-2	10.15	7.89	8.10	126.26	58.13	42.14	17.2	95.55	0.18	2.99	230
CB-3	6.45	8.46	7.45	125.13	52.14	58.21	16.3	95.88	0.17	2.34	280
CB-4	9.45	10.25	9.45	111.10	60.34	52.42	13.4	78.82	0.17	1.69	514
CB-5	6.47	11.45	10.45	119.50	62.12	60.31	14.6	63.47	0.23	1.69	612
CB-6	4.48	4.45	5.46	96.34	62.31	55.24	15.6	141.81	0.11	3.25	210
CB-7	11.13	10.25	10.25	98.42	42.35	48.34	17.4	145.00	0.12	3.12	330
CB-8	7.45	6.58	7.45	112.31	48.14	47.21	16.3	135.83	0.12	2.73	220
CHB-1	8.75	8.45	8.46	119.12	52.13	55.14	14.2	88.75	0.16	2.08	190
CHB-2	9.12	8.46	8.41	96.52	58.14	52.33	15.2	89.41	0.17	2.73	230
CHB-3	14.15	12.25	12.25	116.21	60.24	58.34	14.3	110.00	0.13	2.47	280
CD at 5%	3.13	3.16	2.87	15.74	4.23	2.89	1.23	30.65	0.09	1.16	60.76

The tree spread measured as North-South and East-West extension. The North-South spread ranged from 2.45 to 15.56 m and maximum in genotype 'TBP-3' followed by 'TBP-2' and minimum in 'THP-5'; whereas, East-West tree spared ranged from 3.45 to 14.20 m and maximum in genotype 'TBP-3' followed by 'CHB-3' and minimum in 'THP-5'. The findings were in agreement with (Prakash 2000; Singh et al*.*, 2001).

The maximum fruit weight was recorded in 'THP-7' (137.18 g) followed by 'THP-4' (128.61 g) and minimum in 'TB-3' (58.82 g); wherein, fruit length was ranged between 42.35 to 66.44 and maximum measured in

Table 3. Descriptive statistics for eleven tree, fruit quality, and yield traits of 24 'Kashmiri Nakh' pear genotypes.

Variable	Range	Mean	Std. Dev	CV	Skewness	Kurtosis	Bimodality
Tree height (m)	3.15-14.15	8.51	3.17	37.25	-0.19	-0.80	0.39
Tree spread (m) N-S	2.45-15.56	8.78	3.40	38.72	-0.09	-0.39	0.33
Tree spread (m) E-W	3.45-14.20	8.44	2.55	30.21	0.06	0.02	0.29
Fruit weight (g)	58.82-137.18	112.41	16.38	14.57	-1.55	3.80	0.47
Fruit length (mm)	42.35-66.44	58.07	6.08	10.47	-1.12	0.93	0.51
Fruit Diameter (mm)	42.14-62.71	56.32	5.23	9.29	-1.14	0.91	0.53
TSS	12.9-17.80	15.13	1.51	9.98	0.05	-1.28	0.47
TSS/acidity ratio (%)	33.5-145	90.65	32.12	35.43	0.14	-0.81	0.39
Acidity (%)	0.11-0.40	0.19	0.07	36.84	1.33	1.96	0.51
Vit-C (mg/100 gm)	1.17-4.94	2.55	0.74	29.02	1.17	4.00	0.32
Yield/tree (kg)	190-1614	460.00	398.93	86.72	2.20	4.44	0.74

genotype 'THP-7' followed by 'THP-2' and lowest in 'CB-7'. Fruit diameter also varied considerably from 42.14 to 62.71 and maximum in genotype 'THP-7' followed by 'TB-1' and least in 'CB-2'. The total soluble solids (TSS) ranged from 12.90 to 17.80 °Brix and maximum TSS expressed by genotype 'THB-1' followed by 'CB-7', 'CB-2' least in 'THP-3'. However, fruit acidity was varied from 0.11 to 0.40% and maximum found in 'TBP-3' followed by 'THP-2' and least in 'TBP-2'. The sugar acid ratio ranged from 33.50 to 145 and maximum in 'CB-7' and lowest in 'TBP-3'. Ascorbic acid varied between 1.17 to 4.94 mg/100 g of pulp and highest was recorded in 'THP-1' followed by 'THP-6' and 'CB-6' and lowest in 'THP-4'. These results are in agreement with the values reported by (Nergiz and Yildiz, 1997; Robertson et al., 1992) in European plum and (Prakash 2000; Singh et al., 2001) in pear genotypes.

Yield is the economic potential of plants considered most important while making selection and further improvement. A wide range of variability noticed among the twenty three genotypes which range from (190 to 1614 kg/tree). The most productive selections 'TBP-3' yielded 1614 kg/tree followed by 'TBP-1' (1600 kg/tree)' and 'TB-2 (800 kg/tree)'. Low yielding genotype 'CHB-1' produces only 190 kg/plant. Previous studies on pear also reported a high variability among pear cultivars for above, these parameters and findings are in conformity with (Mann and Singh, 1985; Prakash, 2000; Singh et al., 2001).

Data on extent of diversity for eleven pomological, chemical and yield variables are presented in Table 3. The variability of each trait was expressed by standard deviation and the coefficients of variation. Studied genotypes showed highest coefficient of variation for fruit yield (86.72) followed by tree spread N-S (38.72), tree height (37.25), acidity (36.84), tree spread E-W (30.21) and lowest in fruit diameter (9.29). Maximum standard deviation was recorded in fruit yield (398.93) followed by TSS/Acidity (32.12), fruit weight (16.38); however, lowest in acidity (0.07). These results are in line with the findings of Brown and Walker (1990) and Chen et al. (2007) who reported genotypic variations for fruit quality in apricots and pear cultivars, respectively. Skewness describes the symmetrical distribution pattern with respect to its dispersion from the mean. The positive skewness was recorded for the traits like tree spread (m) E-W, TSS, TSS/acidity, acidity, vitamin C and fruit yield per plant and negative skewness in traits like tree height , tree spread, tree spread (m) N-S, fruit weight, fruit length and fruit diameter. Kurtosis tells the weight of the tails of a distribution. In the present set of data it was recorded that platykurtic distribution pattern for the traits like tree spread, tree height, TSS, TSS/acidity, however lepto-kurtic distribution for the traits like tree spread, fruit weight, fruit length, fruit diameter, acidity, vitamin C and yield per plant. Bimodality of genetic admixture values provides evidence of strong isolation between two morphological and genetic clusters, supporting the existence of a sympatric genotypes pair within the gene pool. It clearly showed that these genotypes existed in the same geographic area and thus regularly encounters one another. An initially interbreeding population that splits into two or more distinct species sharing a common range exemplifies sympatric speciation. Such speciation may be a product of reproductive isolation which prevents hybrid offspring from being viable or able to reproduce, thereby reducing gene flow that results in genetic divergence.

From the above result, it can be concluded that all the 24 pear genotypes are having wide variability for studied traits. Genetic variability in 'Kashmiri Nakh' is probably due to heterogeneity, diversity in environments and hybrid progeny (Katayama and Uematsu, 2006). The obtained evidences as a result of the present study indicated prospects of some accessions to exploit for commercialization and use in breeding programmes for improvement of existing and evolution of new cultivars. The dendrogram generated from the average linkage cluster analysis based on average distance, classified 24 genotypes in to two major groups at 2.23 NRMS distance

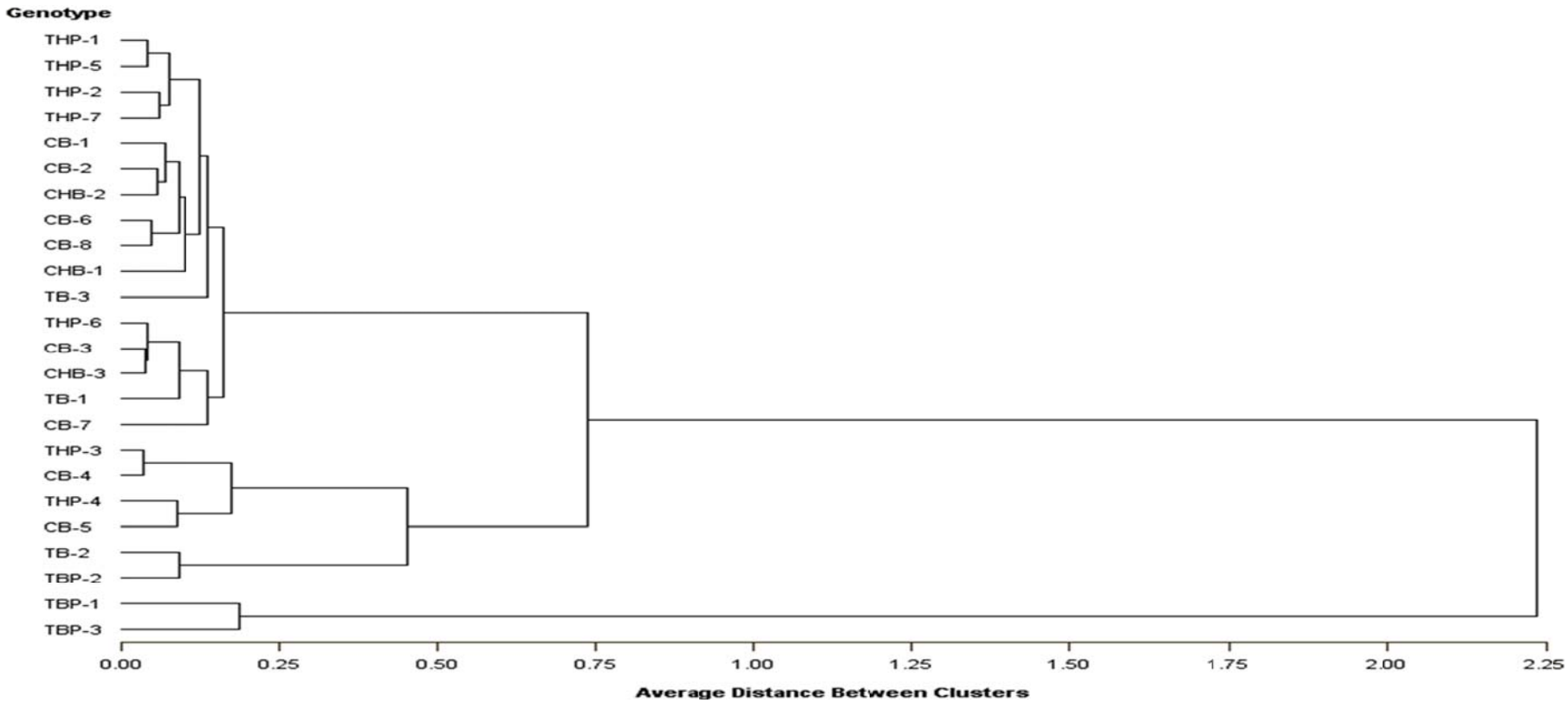

Figure 1. Dendrogram of 24 'Kashmiri Nakh'pear *genotypes* obtained by average distance between cluster analyses based on 11 tree, pomological, fruit quality, and yield traits.

(Figure 1). The first group included two genotypes (TBP-1, TBP-3) contributes 8.33% of the total genotypes in this population. It had the maximum fruit yield per plant and high TSS and TSS/Acidity. The second group comprised 22 genotypes (THP-1, THP-5, THP-2, THP-7, CB-1, CB-2, CHB-2, CB-6, CB-8, CHB-1, TB-3, THP-6, CB-3, CHB-3, TB-1, CB-7, THP-3, CB-4, THP-4, CB-5, TB-2, TBP-2) contributes 91.66% of the total genotypes. This group further divided in to two major clusters at 0.73 NRMS distance. In first cluster, six genotypes exist and contributes 25.00% of the total genotypes which is further divided in to two sub clusters at 0.45 NRMS distance in which first sub cluster comprised two genotypes which possess medium fruit length, fruit diameter, fruit weight, TSS, mid to high fruit yield and lower fruit acidity however second sub-cluster consists four genotypes that is, THP-3, CB-4, THP-4, CB-5 having lowest fruit acidity, high tree spread, tree height, high fruit weight, medium fruit length. The second cluster also further divided into two sub clusters segregated at 0.16 NRMS distance comprised 16 genotype (THP-1, THP-5, THP-2, THP-7, CB-1, CB-2, CHB-2, CB-6, CB-8, CHB-1, TB-3, THP-6, CB-3, CHB-3, TB-1, CB-7) contributes 66.66% of the total genotypes.

The first sub cluster consists five genotype, that is, (CB-7, TB-1, CHB-3, CB-3 and THP-6) and possess medium to high tree height, TSS, TSS/-acidity and low fruit yield attributes however second sub cluster comprised 11 genotypes in 2 sub-sub clusters. The second sub cluster divided

Table 4. Principal component analysis of the "Kashmiri Nakh' pear genotypes showing the eigen vectors, eigen values and percentage total variance accounted for by the eleven principal component axes.

Parameter	Eigen vector										
	PRIN1	PRIN2	PRIN3	PRIN4	PRIN5	PRIN6	PRIN7	PRIN8	PRIN9	PRIN10	PRIN11
Tree height (m)	0.406022	0.326143	0.050758	0.181451	-0.033762	0.104402	0.068807	0.347342	0.742690	-0.008537	0.064772
Tree spread (m) N-S	0.479381	0.200321	0.010391	0.095263	0.006716	0.029149	-0.169550	0.049329	-0.446632	-0.055181	0.697339
Tree spread (m) E-W	0.457938	0.267753	-0.019804	0.060031	-0.006041	0.072890	-0.073575	0.198018	-0.415908	0.113716	-0.691896
Yield/tree (kg)	0.336776	0.165463	-0.080281	-0.507138	0.410679	-0.042198	0.325698	-0.511623	0.107660	-0.209418	-0.042997
Fruit weight (g)	0.130493	-0.259580	0.528155	0.203767	0.092763	0.643076	-0.197203	-0.352975	0.059309	-0.039011	-0.066699
Fruit length (mm)	0.158184	-0.421594	0.331439	0.180502	0.230292	-0.167720	0.672541	0.310847	-0.144694	0.046448	0.040098
Fruit Diameter (mm)	0.201869	-0.387988	0.175355	-0.284337	0.362074	-0.379036	-0.590803	0.218787	0.143896	0.054954	-0.041343
TSS °B	-0.341807	0.205363	-0.045366	-0.278608	0.503672	0.490445	0.004516	0.491999	-0.116154	-0.076557	0.075206
TSS/Acidity ratio (%)	-0.188391	0.435174	0.435338	-0.010566	0.175608	-0.199654	0.017933	-0.163422	-0.003026	0.694358	0.075036
Acidity (%)	0.197839	-0.348471	-0.538057	-0.052657	0.057030	0.302102	0.058178	-0.049448	0.072748	0.659314	0.082543
Eigen value	3.694005	2.613585	1.569189	1.136287	0.76194	0.575275	0.357612	0.138637	0.08329	0.05411	0.016071
Difference	1.08042	1.044396	0.432902	0.374347	0.186665	0.217663	0.218975	0.055348	0.029179	0.038039	
Proportion	0.3358	0.2376	0.1427	0.1033	0.0693	0.0523	0.0325	0.0126	0.0076	0.0049	0.0015
Cumulative	0.3358	0.5734	0.7161	0.8194	0.8886	0.9409	0.9734	0.986	0.9936	0.9985	1

into two sub-sub clusters. The first sub-sub cluster includes only single genotypes TB-3 which is characterized by lowest tree height, tree spread, fruit weight, fruit length but high in TSS, vitamin C and yield per plant whereas second sub-sub cluster consists 10 genotypes (THP-1, THP-5, THP-2, THP-7, CB-1, CB-2, CHB-2, CB-6, CB-8, CHB-1) which were characterized by moderate to high in tree height, tree spread, fruit weight, length, diameter, TSS, TSS/acidity, vitamin C and low to moderate in fruit yield per plant.

The dissimilarity level in terms of genetic distance ranged from (0.0.33 to 2.236) based on NRMS (Figure 1) indicating a high degree of dissimilarity between genotypes and high genetic distance between genotypes and if chosen for hybridization program, may give high heterotic F_1s and broad spectrum of variability in segregating generations (Mratinić et al., 2007). This grouping pattern of genotypes based on pomological and yield attributes confirmed the results obtained by cluster analysis and that the crosses involving parents belonging to the maximum divergent clusters were expected to manifest maximum heterosis and also wide variability in genetic architecture. The results of present study are thus useful as it gives information about the groups where certain traits are more important allowing breeder to conduct specific breeding programme.

Principal components (PC) analysis is a way of identifying patterns in data, which expresses data in such a way as to highlight their similarities and differences (Milosevic and Milosevic, 2010). Therefore, PC was carried out to determine the characters more strongly contributed to the principal components. Principal components analysis reduced the original 11 characters in experiment to 4 principal components. The first four principal components with Eigen values >1 explained 81.94% of variation among 24 accessions (Table 4). Other PCs had Eigen values <1 and have not been interpreted.

The first PC, which is the most important component, explained 33.58% of the total variation and was positively related to tree height, tree spread (N-S), tree spread (E-W), yield per tree, fruit weight, fruit length, fruit diameter and acidity however PC1 negatively related to TSS and TSS/acidity. The PC2 accounted of 23.76% of the total variation and the characters with the greatest weight on this component was TSS. The PC3 accounted for 14.27% and highest positively related to TSS/acidity. However, PC4 is accounted for only 10.33%. This situation confirms the suitability of using morphology as a basis for selecting parental sources; nevertheless, studies through several years must be conducted

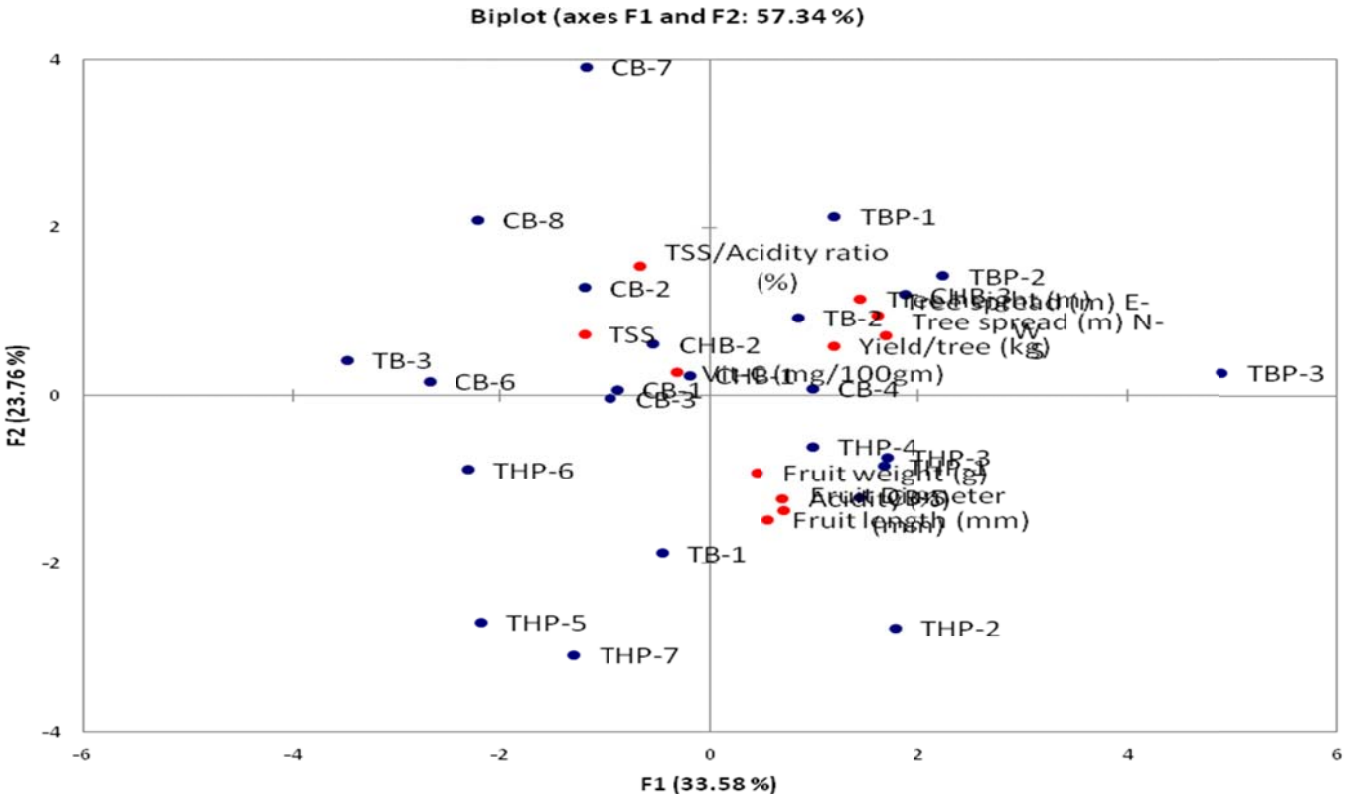

Figure 2. Segregation of 24 'Kashmiri Nakh' pear genotypes according to their fruit quality and yield characteristics determined by principal component analysis (PCA). Vectors represent the loadings of phenological, quality and yield traits data along with the principal component scores.

before parental selection for a possible plant breeding.

The PC analysis provided a simplified classification of the pear genotypes for collecting and breeding programme. The biplot axes also shows geometrical distances among cultivars that reflect similarity among them in terms of variables measured. The first three principal component scores were plotted to aid visualization of accessions grouping (Figure 2). The derived cluster and subgroups are very similar to those identified from average distance between cluster analyses. More interesting genotypes were 'CHB-4, THP-3, THP-7, THP-1, TBP-1 and TB-2,' that were disposed in gaps means more diverse than others and are the most promising ones. Genotype 'TB-3' characterized by smallest tree height minimum plant spread minimum fruit weight and fruit length however 'TBP-3' is characterized by highest tree height of the tree. Genotype 'TBP-1' had the maximum TSS and TBP-3 highest yield per plant. THP-1 was richest in vitamin C however TBP-3 in acidity. The THP-7 genotype had highest fruit weight and fruit diameter compared to others genotypes.

So, it can be intended for further utilization for introducing these traits in desired genotypes. Identification and description of the genetic variability available in the genotypes of *Prunus* sp. are preliminary requirements for the exploitation of useful traits in plant breeding. The multivariate analysis was found useful for detection of phenotypic differences among the pear genotypes. The results of the present work may also help breeders in selecting the most diverse accessions with similar pomological, fruit quality and yield related traits to begin crossing and breeding programs which may results in increased in desired traits. The results are certainly representative and valuable, and will provide some guidance for screening breeding resources for improving fruit quality and serve as a base for economically valuable phenotypes. The cluster analysis classified genotypes into two major groups and further in clusters according to their potential characteristics. The first (TBP-1 and TBP-3) genotypes were superior in terms of fruit yield and second group (22) genotypes in quality attributes. Genotypes and high genetic distance between genotypes and if chosen for hybridization program, may give high heterotic F_1s and broad spectrum of variability in segregating generations PC analysis may help in selection of a set of genotypes with better fruit qualities, which, in our study, were observed in 'TB-3, CHB-4, TBP-3, THP-7, TBP-3, THP-1, TBP-1 and TB-2. They can be used as directly new cultivars or potential may be utilized for desirable crop improvement programme to breed a

variety with high yield and fruit quality.

Conflict of Interests

The author(s) have not declared any conflict of interest.

REFERENCES

Ahmad R, Potter D, Southwick SM (2004). Identification and characterization of plum and Pluto cultivars by microsatellite markers. J. Hort. Sci. Biotech. 79(1):164-169.

AOAC (1994). Official Methods of Analysis, Association of Official Analytical Chemists. 111 North 19th street, suite 20, Ed. 16th, Arlington, Virginia, USA., 2209.

Arunachalam V (1981). Genetic distances in plant breeding. Indian J. Genet. Pl. Breed 41: 226-236.

Blazek J (2007). A survey of the genetic resources used in plum breeding. Acta Hort. 771:25-31.

Bouhadida M, Casas AM, Moreno MA, Gogorcena Y (2005). Genetic diversity *of Prunus* rootstocks using microsatellite markers. Acta Hort. 663:167-171.

Brown GS, Walker TD (1990). Indicators of maturity in apricots using biplot multivariate analysis. J. Sci. Food Agric. 53: 321-331.

Chen J, Wang Z, Wu J, Wang Q, Hu X (2007). Chemical compositional characterization of eight pear cultivars grown in China. Food Chem. 104: 268-275.

FAO (2012). Food and Agricultural Organization of the United Nations. 17 August 2013th August 2013.

Gomez KA, Gomez AA (1984). Statistical Procedures for Agricultural Research, 2nd John Wiley and Sons Inc., New York.

Karimi HR, Zamani Z, Ebadi A, Fatahi MR (2008). Morphological diversity of *Pistacia* species in Iran. Genet. Resour. Crop 44:76-81.

Katayama HC, Uematsu C (2006). Pear (*Pyrus* species) genetic resources in Iwate, Japan. Genet. Resour. Crop Evol. 53:483-498.

Kaufmane E, Ikase L, Trajkovski V, Lacis G (2002). Evaluation and characterization of plum genetic resources in Sweden and Lativa. Acta Hort. 577:207-213.

Mann SS, Singh B (1985). Some aspects of developmental physiology of LeConte pear. Acta Hort. 158: 211-215.

Miloševic T, Miloševic N, Glišic I, Krška B (2010). Characteristics of promising apricot (*Prunus armeniaca* L.) genetic resources in central Serbia based on blossoming period and fruit quality. HortScience 37:46-55.

Mratinić E, Rakonjac V, Milatović D (2007). Genetic parameters of yield and morphological fruit and stone properties in apricot. Genetika 39: 315-324.

Nergiz C, Yildiz H (1997). Research on chemical composition of some varieties of European plums (*Prunus domestica*) adapted to the Aegean district of Turkey. J. Agri. Food Chem. 45:2820-2823.

Ogasanovic D, Plazinic R, Rankovic M, Stamenkovic S, Milinkovic V (2007). Pomological characteristics of new plum cultivars developed in Cacak. Acta Hort. 734:165-168.

Prakash C (2000). Evaluation of low-chill pear (*Pyrus* spp.) cultivars under tarai conditions of U.P. *M.Sc. Thesis* submitted to GB Pant University of Agriculture and Technology, Pantnagar, 82 p.

Rausser GC, AA Small (2011). Valuing research leads: Bioprospecting and conservation of genetic resources. J. Political Economy 108:173-206.

Robertson JA, Meredith FI, Senter SS, Okie WR, Norton JD (1992). Physical, chemical and sensory characteristics of Japanese-type plums growing in Georgia and Alabama. J. Sci. Food Agric. 60: 339-347.

SAS Institute (2012). SAS Enterprise Guide, Version 9.3. SAS Inst., Cary, NC, USA.

Singh J, Dillon WW, Singh SN (2001). Studies on flowering and fruiting behaviour in *Pyrus* spp. Indian J. Hort. 58(4): 332-335.

Smale M (2006). Valuing crop biodiversity on-farm genetic resources and economic change. UK: CABI.

Srivastava KK, Singh SR, Ahmad N, Das B, Sharma OC, Rather JA, Bhat SK (2012). Genetic divergence analysis of pear using qualitative traits as per DUS guidelines. Indian J. Hort. 69(3): 432-434.

Yamamoto T, Kimura T, Soejima J, Sanada T, Hayashi T, Ban Y (2004). Identification of quince varieties using SSR markers developed from pear and apple. Breed. Sci. 54:239-244.

academicJournals

Vol. 13(33), pp. 3360-3365, 13 August, 2014
DOI: 10.5897/AJB2014.13835
Article Number: 95A23BF46618
ISSN 1684-5315

http://www.academicjournals.org/AJB

African Journal of Biotechnology

Full Length Research Paper

Plant growth promoting potential of endophytic bacteria isolated from cashew leaves

Milca Rachel da Costa Ribeiro Lins[1], Jéssica Martins Fontes[1], Nataliane Marques de Vasconcelos[1], Danilo Mamede da Silva Santos[2], Ozias Elias Ferreira[3], João Lúcio de Azevedo[4], Janete Magali de Araújo[1] and Gláucia Manoella de Souza Lima[1]*

[1]Department of Antibiotics of Universidade Federal de Pernambuco - UFPE, Avenida Prof. Moraes Rego, s/n - Cidade Universitária, CEP: 50670-901, Recife, Pernambuco, Brazil.
[2]Education Department of Universidade do Estado da Bahia - UNEB, Rua do Bom Conselho, 179, Alvez de Souza, CEP: 46800-000, Paulo Afonso - Bahia, Brazil.
[3]Federal Institute of Pernambuco - IFPE, Av. Prof. Luiz Freire, 500 - *CEP* 50740-540, Cidade Universitária, *Recife*-PE.
[4]Luiz de Queiroz" College of Agriculture, Universidade de São Paulo - ESALQ/USP, Av. Pádua Dias, 11 - CEP 13418-900, Piracicaba, Sao Paulo, Brazil.

Received 17 April, 2014; Accepted 21 July, 2014

Endophytic microorganisms are able to promote plant growth through various mechanisms, such as production of plant hormones and antimicrobial substances, as well as to provide the soil with nutrients, for instance, inorganic phosphate. This study aimed to evaluate the potential of endophytic bacteria isolated from cashew leaves to produce substances involved in the promotion of plant growth, such as indole-3-acetic acid, the phosphate solubilization capacity, and the antimicrobial activity. For this, 31 isolate samples were used, out of which 17 (54.8%) produce indole-3-acetic acid in concentrations ranging from 11.79 to 145.85 µg.mL^{-1}. In turn, four (12.9%) were able to solubilize phosphate and the solubilization halos range from 5 to 19 mm. Soluble phosphorus concentrations range from 62.5 to 1,605.2 mg.L^{-1}. It was observed that *Fusarium oxysporum* and *Colletotrichum* sp. were inhibited by 70 and 40% of the strains, respectively. It was found out that five bacteria (25%) were Gram-positive, predominantly the species *Staphylococcus saprophyticus* (100%), while 15 bacteria (75%) were Gram-negative. Out of these, 4 (26.6%) and 3 (20%) belong to the species *Escherichia coli* and *Shigella flexneri*, respectively. Studying the endophytic population is something important due its biotechnological applications, because it has a great potential for promoting plant growth.

Key words: *Anacardium occidentale*, auxin, endophytic microorganisms, secondary metabolites, phosphate solubilization.

INTRODUCTION

In recent decades, the search for new compounds with applications to health and agriculture has increased and

*Corresponding author. E-mail: gmslima@yahoo.com.br. Tel: +558121268347. Fax: +558121268346.

in this context, endophytic microorganisms have shown a great potential, since they represent an important genetic diversity source and bioactive compounds (Zhao et al., 2010; Joseph and Priya, 2011).

Endophytes microorganisms spend at least one period of their life cycle beneficially associated to plants' tissues and/or organs, such as roots, branches, and leaves, and they can be isolated after disinfecting the surface of these plants. Bacteria and fungi, which are commonly found as endophytes, do not cause harm to their hosts; instead, they play important roles with regard to the plant's health (Azevedo et al., 2000; Azevedo et al., 2006; Nair and Padmavathy, 2014).

During a long co-evolution period, a friendly relationship was formed between endophytes and the host plant. Some endophytes can produce the same or similar bioactive compounds from the host plant, presenting a mutualistic association, as they receive nutrients, protection by the plant, and other benefits, such as pathogenic microorganism control, insect control, and protection against herbivores (Zhao et al., 2011).

These microorganisms facilitate the plant's growth and development through two mechanisms: Direct: when it involves in the supply of compounds which are synthesized and make easier the absorption of nutrients from the environment; and Indirect: when the microorganism reduces or prevents the harmful effects of pathogens by producing inhibitory substances or increasing the host's natural resistance.

The direct mechanisms are nitrogen fixation (N_2), phosphate solubilization, insoluble iron chelation through the production of siderophores and phytohormones, such as auxins, cytokinins, and gibberellins (Oliveira et al., 2003; Tsavkelova et al., 2007; Jha et al., 2012).

Auxins are hormones produced by endophytes which regulate plant growth and act on the cell division, elongation, and differentiation (Shokri and Emtiazi, 2010). However, the interaction of bacteria with the host plant for promoting growth depends on the concentration of hormones available to the plant cells (Oliveira et al., 2003).

Indole-3-acetic acid (IAA) is the most important auxin for the growth of roots and stems by stretching the cells (Tsavkelova et al., 2007). This hormone is usually produced by several bacteria genera which promote plant growth, such as *Actinomyces*, *Agrobacterium*, *Arthrobacter, Azospirillum, Azotobacter*, *Bacillus*, *Burkholderia*, *Caulobacter*, *Chromobacterium*, *Enterobacter, Gluconacetobacter, Klebsiella, Methylobacterium, Pantoea*, *Pseudomonas*, *Rhizobium*, *Salmonella*, *Sthaphylococcus* and among others (Hayat et al., 2010; Bhattacharyya et al., 2012; Oliveira et al., 2013; Zheng et al., 2013; Rangjaroen et al., 2014).

Another important function of endophytic bacteria is related to the phosphorus cycle, being responsible for the hydrolysis of phosphorus to its soluble form. These microorganisms use different mechanisms to convert forms insoluble in soluble phosphate through the activity of enzymes such as phosphatases or phosphohydrolases with processes of acidification, chelation, exchange reactions, but usually, the main mechanism of solubilization is the release of metabolites such as organic acids (Hameeda et al., 2008; Young et al., 2013).

The ability of endophytic bacteria with regard to the solubilization of inorganic phosphate raised interest in agricultural practices and because of this, the endophytic microorganisms have been studied. They play an important role in the conversion of phosphorus to soluble phosphate.

Studying the endophytic population is important not only for acquiring knowledge on its ecological role, but also with regards to its biotechnological applications to the production of bioactive substances which can be used in the field in order to increase the agricultural production. This study aimed to evaluate endophytic bacteria producing indole acetic acid and solubilized phosphorus as well as identify them by biochemical characteristics.

MATERIALS AND METHODS

Microorganisms

We used 31 endophytic bacteria from cashew leaves (*Anacardium occidentale* L.) that belonged to the Microorganism Collection - UFPEDA, Brazil. The strains were inoculated in BHI broth (Dadook et al., 2013) for reactivation and incubated for 24 h/30°C. Afterwards, the biochemical characteristics were analyzed as described above.

Classical taxonomy (phenotypic features and microscopic analysis)

Bacteria were cultivated on Agar Nutrient (Verma et al., 2001) and after 24 h, Gram staining and biochemical tests were performed using the systems Bactray I and II (Gram-negative negative oxidase) and III (Gram-negative positive oxidase), in accordance with the manufacturer's instructions (LaborClin). Gram positive bacteria were identified by specific tests including catalase test, DNase agar, mannitol salt agar and sensitivity to novobiocin according to Winn et al. (2006).

Production of indole-3-acetic acid

The production of IAA was analyzed according to the method developed by Sarwar and Kremer (1995); inoculating 31 endophytic bacteria padronized 1.0 $\times 10^8$ UFC/ml (λ=625nm) in tubes with 10% TSA (Kuklinsky-Sobral et al., 2004) supplemented with 5 mmol.L^{-1} of L-tryptophan and cultivated for 24h/30°C in the dark under a 110 × g shake. After growth, the samples were centrifuged at 8 000 × *g* for 15 min and to the supernatant, the reagent Salkowski (0.5 mol.L^{-1} $FeCl_3$ + 7.9 mol.L^{-1} H_2SO_4) was added in a 1:1 ratio (v/v) and left in the dark for 30 min at room temperature. The emergence of pink-red color indicated the production of auxins. For quantifying IAA, spectrophotometer at 530 nm was used. A standard curve was obtained with commercial IAA solutions (Vetec) at different concentrations. Tests were performed in triplicate and *Pantoea agglomerans* UFPEDA 774 was used as the positive control and

Table 1. Concentration of indole-3-acetic acid produced by endophytic bacteria of cashew leaves.

Bacterial strain	Concentration of IAA (µg.mL^{-1})	Bacterial Strain	Concentration of IAA (µg.mL^{-1})
Pantoea agglomerans	76.31 ± 4.15	BC-26	37.29 ± 9.00
BC-1	23.12 ± 3.24	BC-46	132.79 ± 3.53
BC-2	36.95 ± 4.64	BC-47	131.73 ± 17.58
BC-8	144.43 ± 0.50	BC-48	130.7 ± 6.49
BC-9	38.81 ± 0.23	BC-49	106.63 ± 0.22
BC-10	145.85 ± 0.44	BC-51	11.79 ± 2.81
BC-21	135.29 ± 0.00	BC-55	108.91 ± 14.67
BC-22	132.79 ± 3.53	BC-63	104.29 ± 13.17
BC-24	16.66 ± 4.68	BC-147	62.07 ± 0.31

± Standard deviation.

the negative control consisted of the same medium supplemented with L-tryptophan, with no bacterial growth.

Evaluation of inorganic phosphate solubilization

For the semiquantitative assessment of phosphate solubilization, the bacteria (1.0 × 10^8 UFC/ml, λ 625 nm) were inoculated in spots on plates containing three different media: 'National Botanical Research Institute's Phosphate Solubilization' - NBRIP (Kumar et al., 2012); the medium according to Verma et al. (2001) and Phosphate medium (Kuklinsky-Sobral et al., 2004). After 120 h of incubation, clear zones around the colonies were indicative of solubilization of inorganic phosphate and the phosphate solubilization index (PSI) was calculated according to Sarkar et al. (2012). *P. agglomerans* UFPEDA 774 was used as the positive control.

Evaluation of phosphate solubilization in liquid medium

Each strain containing 1.0 × 10^8 UFC/ml (λ 625 nm), were inoculated on NBRIP and VERMA medium (previously described), according to Kumar et al. (2012) and Verma et al. (2001). After 144 h, the supernatants were analysed according molybdate-vanadate method (Inui-Kishi et al., 2012). Afterwards, the absorbance was estimated the absorbance at 420 nm. A standard curve was obtained from potassium phosphate solutions (1.0; 2.0; 4.0; 5.0; 6.0; 8.0; 10.0 mg.L^{-1}) in accordance with the Standard Methods (Clesceri et al., 1999). *P. agglomerans* UFPEDA 774 was used as the positive control.

Statistical analyses

Each experiment was performed in triplicate and analysis of variance was performed (ANOVA) at $p \leq 0.05$ and the Tukey test ($p \leq 0.05$) on the program Excel 2010 and Minitab version 15 to analyze the results of IAA's production, semiquantitative and quantitative phosphate solubilizing on VERMA and NBRIP media by bacteria of Cashew tree was done (Bluman, 2001).

Antimicrobial activity

The solubilizing phosphate and/or producing IAA strains were tested against the activity of *A. niger* UFPEDA 2003, *Colletotrichum* sp. UFPEDA 2561 and *F. oxysporum* UFPEDA 2456 (1.0 x10^6 spores/mL). The fungi were inoculated on potato dextrose agar (Ribeiro and Cardoso, 2012) and the antagonistic activity was evaluated after seven days at 28°C.

RESULTS AND DISCUSSION

Production of IAA and quantitative assessment

Out of the 31 strains tested with regards to the production of auxin, 17 (54.83%) showed reddish pink coloration after addition of the reagent Salkowski, indicating that they produce IAA through tryptophan, with concentrations ranging from 11.79 to 145.85 µg.mL^{-1} (Table 1).

The plant hormone production is part of the metabolism of several microorganisms associated to plants and they may be regarded as important agents in the regulation of the plant's growth and development (Oliveira et al., 2003). The auxin synthesized by bacteria affects the root system by increasing the number and size of adventitious roots (Gutierrez et al., 2012). One should take into account the fact that the IAA effect may vary according to their concentrations. Depending on the plant's variety, higher concentrations of IAA can have an inhibiting effect on plant growth inducing callus tissues (Ribeiro and Cardoso, 2012).

The colorimetric method for observing the production of auxins by microorganisms uses the reagent Salkowski and it is based on the oxidation of indole compounds by ferric salts (Mayer, 1958). Variation in the concentration of auxin produced by the endophytic bacteria may have been caused by differences in the behavior of each bacterium, and one needs to better understand the IAA synthesis at different times of bacterial growth, thus determining the time when the maximum synthesis of the product took place.

ANOVA indicated that the averages obtained in relation to production of IAA are not statistically equal ($p > 0.05$). Then, the Tukey shows the strain BC-10 has good potential to produce this important metabolite for plants growth.

Table 2. Phosphate solubilization index (PSI) of solubilized phosphorus in plate assay of endophytic bacteria.

Bacterial strain	VERMA	NBRIP	Phosphate medium
BC-51	-	-	2.85 ± 0.51
BC-52	-	-	1.9 ± 0.09
BC-53	2.21 ± 0.21	2.29 ± 0.66	2.31 ± 0.09
BC-56	1.54 ± 0.04	1.83 ± 0.14	3.92 ± 0.09
P. agglomerans	3.02 ± 0.42	2.00 ± 0.00	2.19 ± 0.26

± Standard deviation.

Table 3. Concentration ($mg.L^{-1}$) of phosphorus solubilized by endophytic bacteria of cashew leaves.

Bacterial strain (media)	Concentration of solubilized phosphate ($mg.L^{-1}$)
BC-51 (NBRIP)	36.73 ± 1.00
BC-51 (VERMA)	126.89 ± 21.00
BC-52 (NBRIP)	113.53 ± 15.99
BC-52 (VERMA)	400.70 ± 25.05
BC-53 (NBRIP)	1569.41 ± 11.00
BC-53 (VERMA)	1349.02 ± 62.31
BC-56 (NBRIP)	1389.09 ± 62.31
BC-56 (VERMA)	1395.77 ± 32.17
Pantoea agglomerans (NBRIP)	1095.25 ± 84.00
Pantoea agglomerans (VERMA)	808.08 ± 34.28

± Standard deviation.

Kuklinsky-Sobral et al. (2004) observed that 34% of the endophytic bacteria associated to soybean are auxin producers, standing out in the production of important substances for promoting plant growth. In this study, the BC-10 isolate showed auxin production with a 145.85 $\mu g.mL^{-1}$ concentration, higher than the result obtained by Kochar et al. (2011) through the *P. fluorescens* isolate (25.82 $\mu g.mL^{-1}$) in a culture medium containing the same tryptophan concentration (5 $mmol.L^{-1}$).

Therefore, the results found in the literature corroborate those obtained through the endophytic bacteria of cashew leaves analyzed in this study.

Phosphate solubilization assessment

The tested bacteria showed low phosphate solubilization, only 4 strains (12.9%) were able to solubilize phosphorus in the Phosphate medium (BC-52, BC-53, BC-56, and BC-51), highlighting the strain BC-51 which also produces IAA. Only two out of the four strains were able to solubilize phosphate in the VERMA and NBRIP media.

The PSI was calculated through the ratio between the phosphate solubilization halo (mm) and the colony diameter (mm), and it was observed that it ranged from 1.90 to 3.92 in the Phosphate medium and, among the four strains, three (BC-51, BC-53, and BC-56) showed a phosphate solubilization higher than the positive control, *P. agglomerans*. In the VERMA medium, PSI ranged from 1.53 to 2.21 and in NBRIP it ranged from 1.83 to 2.29 (Table 2).

After analyses of variance, it was cleared that the averages of PSI are not statistically equal ($p > 0.05$) in relation to phosphate solubilization in solid media with phosphate insoluble.

Regarding the phosphate solubilization, according to Chagas-Junior et al. (2010), the PSI is measured through the ratio solubilization halo (mm)/colony diameter (mm). Thus, the solubilization may be classified as low solubility ($PSI < 2$), middle solubilization ($2 \leq PSI < 4$), and high solubility ($PSI > 4$). Then, all of the endophytic bacteria of cashew tree have low or medium capability to solubilize phosphate.

The phosphorus concentrations solubilized by the isolates ranged from 36.73 to 1,569.41 $mg.L^{-1}$. The strains BC-53 and BC-56 solubilized phosphate at a higher concentration than the positive control in the NBRIP and VERMA media (Table 3). In liquid media, the *p*-value of ANOVA was less than 0.05 showing that there was difference between the averages of phosphate solubilization in liquid media. The Turkey test indicated that BC-53, BC-56 and the control *P. agglomerans* have

Table 4. Identification of endophytic bacterial strains which produced IAA and solubilized phosphate.

Bacterial strain	Species	Bacterial strain	Species
BC-1	*Staphylococcus saprophyticus*	BC-47	*E. coli*
BC-2	*S. saprophyticus*	BC-48	*E. coli*
BC-8	*Shigella flexneri*	BC-49	*E. coli*
BC-9	*S. flexneri*	BC-51	*Enterobacter cloacae*
BC-10	*S. flexneri*	BC-52	*Pseudomonas maltophilia*
BC-21	*Yersinia psedotuberculosis*	BC-53	*Escherichia fergusonii*
BC-22	*Escherichia coli*	BC-55	*Pseudomonas stutzeri*
BC-24	*S. saprophyticus*	BC-56	*Enterobacter sakazakii*
BC-26	*S. saprophyticus*	BC-63	*S. saprophyticus*
BC-46	*Klebsiella* sp.	BC-147	*Hafnia alvei*

the same capability to solubilize phosphate and they had higher concentrations of soluble phosphorus than BC-51 and BC-52.

The changes observed in the soluble phosphorus concentration are due to the features and requirements of each bacterial growth, for instance, different nutrient compositions in the culture medium influence the microbial development. Sarkar et al. (2012) isolated bacteria from roots of rice seedlings and tested the phosphate solubilization ability in a Pikovskaya liquid media and the concentrations ranged from 87.8 to 140.1 $mg.L^{-1}$. For this reason, the endophytic bacteria of cashew leaves have higher concentrations of soluble phosphate and because of this, they have characteristics that might promote plant growth.

Antimicrobial activity assessment

Out of the 20 endophytic bacteria which produced auxin and/or solubilized phosphate, did not observe an antimicrobial activity against *A. niger* UFPEDA 2003 was not observed. However, 14 (70%) showed activity against *F. oxysporum* UFPEDA 2456, while eight (40%) showed activity against *Colletotrichum* sp. UFPEDA 2561.

Regarding the antimicrobial activity, the term antagonist is used for the biological agents with potential to interfere in the life processes of pathogenic microorganisms, inhibiting their growth. Further studies with a deeper investigation involving biological control are needed, since the endophytic bacteria can show an activity against other pathogen types.

Characterization of classical taxonomy

Biochemical characterization showed that five (25%) are Gram-positive bacteria and the results suggest that all of them belong to species *S. saprophyticus*. It was found that 15 (75%) are Gram-negative bacteria and, among the Gram-negative bacteria with negative oxidase, it was suggested that 26.6% belong to the species *E. coli* and 20% *S. flexneri*. Other species, such as *E. fergusoni*, *H. alvei*, *Y. pseudotuberculosis*, and those from the genus *Klebsiella* sp were observed. Among the Gram-negative bacteria with positive oxidase, species *E. cloacae*, *P. maltophilia*, and *P. stutzeri* (Table 4) were observed. However, the confirmation with molecular tools needs to be done.

Stamford et al. (1998) identified the genus *Staphylococcus* as endophytic of yam bean. A similar phenomenon was observed by Velásquez et al. (2008), who were also able to identify the genus *Staphylococcus* as being endophytic of sugar cane through the analysis of 16S rRNA. Vendan et al. (2010) also identified endophytic bacteria from ginseng and observed that the genus *Staphylococcus*, confirm the results obtained in this study.

Several studies reported the occurrence of enterobacteria as plant endophytes. The presence of these microorganisms, such as *Klebsiella* spp., is usually observed in the endophytic community playing important roles in the host plants, since they are able to produce phytohormones and provide nitrogen (Dong et al., 2003; Durán et al., 2014; Guo et al., 2014).

The genus *Pseudomonas* and *Burkholderia* was identified as endophytic through biochemical and molecular tools; also they had the ability to produce some phytohormones and solubilized phosphate to growth plant (Mendes et al., 2007; Chauhan et al., 2013; Allu et al., 2014).

The assessed strains have higher potential for promoting plant growth and/or being used as biofertilizers through the production of phytohormones, such as auxins, as well as the conversion of insoluble phosphorus into soluble one, making it accessible to plant absorption. Therefore, research involving endophytes which have more than one feature for promoting plant growth is important for a better understanding of their interaction with the plant, something useful for analyzing the use of microorganisms in agriculture.

Conflict of Interests

The author(s) have not declared any conflict of interest.

REFERENCES

Allu S, Kumar NP, Audipudi AV (2014). Isolation, biochemical and PGP characterization of endophytic *Pseudomonas aeruginosa* isolated from chilli red fruit antagonistic against chilli anthracnose disease. Int. J. Curr. Microbiol. App. Sci. 3(2):318-329.

Azevedo JL, Araújo WL, Lacava PT, Andreote FD (2006). Caracterização da comunidade bacteriana endofítica de citros por isolamento, PCR específico e DGGE. Pesqui. Agropec. Bras. 41:637-642.

Azevedo JL, Maccheroni-Jr W, Pereira JO, Araújo WL (2000). Endophytic microorganisms: a review on insect control and recent advances on tropical plants. Electr. J. Biotechn. 3:40-65.

Bhattacharyya PN, Jha DK (2012). Plant growth-promoting rhizobacteria (PGPR): emergence in agriculture. World J. Micro. Biot. 28:1327-1350.

Bluman AG (2001). Elementary statistics: a step by step approach. 4th ed. chapter 13.

Chagas-Junior AF, Oliveira LA, Oliveira AN, Willerding AL (2010). Capacidade de solubilização de fosfatos e eficiência simbiótica de rizóbios isolados de solos da Amazônia. Acta Sci. Agron. 32(2):359-366.

Chauhan H, Bagyaraj DJ, Sharma A (2013). Plant growth-promoting bacterial endophytes from sugarcane and their potential in promoting growth of the host under field conditions. Exp Agri 49(1):43-52.

Clesceri LS, Greenberg AE, Eaton AD (1999). Standard methods for the examination of water and wastewater, 20th ed.

Dadook M, Mehrabian S, Irian S (2013). Identification of ten N2-fixing bacteria using 16S rRNA and their response to various zinc concentrations. Inter. J. Cell. Mol. Biotech. 1-8.

Dong Y, Iniguez AL, Triplett EW (2003). Quantitative assessments of the host range and strain specificity of endophytic colonization by *Klebsiella pneumoniae* 342. Plant Soil 257:49-59.

Durán P, Acuña JJ, Jorquera MA, Azcón R, Paredes C, Rengel Z, Mora ML (2014). Endophytic bacteria from selenium-supplemented wheat plants could be useful for plant-growth promotion, biofortification and Gaeumannomyces graminis biocontrol in wheat production. Biol. Fert. Soils 50(6):983-990.

Guo C, Sun L, Kong D, Sun M, Zhao K (2014). *Klebsiella variicola*, a nitrogen fixing activity endophytic bacterium isolated from the gut of *Odontotermes formosanus*. Afr. J. Micrbiol. Res. 8(12):1322-1330.

Gutierrez L, Mongelard G, Floková K, Păcurar DI, Novák O, Staswick P, Kowalczyk M, Păcurar M, Demailly H, Geiss G, Bellinid C (2012). Auxin controls *Arabidopsis* adventitious root initiation by regulating jasmonic acid homeostasis. Plant Cell 24:2515-2527.

Hameeda B, Harini G, Rupela, OP, Wani, SP, Reddy G (2008). Growth promotion of maize by phosphate-solubilizing bacteria isolated from composts and macrofauna. Microbiol. Res. 163(2):234-242.

Hayat R, Ali S, Amara U, Khalid R, Ahmed I (2010). Soil beneficial bacteria and their role in plant growth promotion: a review. Ann. Microbiol. 60:579-598.

Inui-Kishi RN, Kishi LT, Picchi SC, Barbosa JC, Lemos MTO, Marcondes J, Lemos EGM (2012). Phosphorus solubilizing and IAA production activities in plant growth promoting rhizobacteria from brazilian soils under sugarcane cultivation. J. Eng. Appl. Sci. 7(11):1446-1454.

Jha B, Gontia I, Hartmann A (2012). The roots of the halophyte *Salicornia brachiata* are a source of new halotolerant diazotrophic bacteria with plant growth-promoting potential. Plant Soil 356:265-277.

Joseph B, Priya RM (2011). Bioactive compounds from endophytes and their potential in pharmaceutical effect: a review. Am. J. Biochem. Mol. Biol. 1(3):291-309.

Kochar M, Upadhyay A, Srivastava S (2011). Indole-3-acetic acid biosynthesis in the biocontrol strain *Pseudomonas fluorescens* Psd and plant growth regulation by hormone overexpression. Res. Microbiol. 162:426-435.

Kuklinsky-Sobral J, Araújo WL, Mendes R, Geraldi IO, Pizzirani-Kleiner AA, Azevedo JL (2004). Isolation and characterization of soybean-associated bacteria and their potential for plant growth promotion. Environ. Microbiol. 6:1244-1251.

Kumar P, Dubey RC, Maheshwari DK (2012). Bacillus strains isolated from rhizosphere showed plant growth promoting and antagonistic activity against phytopathogens. Microbiol. Res. 167:493-499.

Mayer AM (1958). Determination of indole acetic acid by the Salkowsky reaction. Nature 162:1670-1671.

Mendes R, Pizzirani-Kleiner AA, Araújo WL, Raaijmakers JM (2007). Diversity of cultivated endophytic bacteria from sugarcane: genetic and biochemical characterization of *Burkholderia cepacia* complex isolates. Appl. Environ. Microbiol. 73:7259-7267.

Nair DN, Padmavathy S (2014). Impact of endophytic microorganisms on plants, environment and humans. Scientific World J.

Oliveira ALM, Urquiaga S, Baldani JI (2003). Processos e mecanismos envolvidos na influência de microrganismos sobre o crescimento vegetal. Embrapa Agrobiologia Documentos 161:1-5.

Oliveira MNV, Santos TMA, Vale HMM, Delvaux JC, Cordero AP, Ferreira AB, Miguel PSB, Tótola MR, Costa MD, Moraes CA, Borges AC (2013). Endophytic microbial diversity in coffee cherries of *Coffea arabica* from southeastern Brazil. Can. J. Microbiol. 59(4):221-230.

Rangjaroen C, Rekarsem B, Teaumroong N, Noisangiam R, Lumyong S (2014). Promoting plant growth in a commercial rice cultivar by endophytic diazotrophic bacteria isolated from rice landraces. Ann. Microbiol. 1-14.

Ribeiro CM, Cardoso EJBN (2012). Isolation selection and characterization of root-associated growth promoting bacteria in Brazil Pine (*Araucaria angustifolia*). Microbiol. Res. 167:69-78.

Sarkar A, Islam T, Biswas GC, Alam S, Hossain M, Talukder NM (2012). Screening for phosphate solubilizing bacteria inhabiting the rhizoplane of rice grown in acidic soil in Bangladesh. Acta Microbiol. Imm. H. 59:199-213.

Sarwar M, Kremer RJ (1995). Determination of bacterially derived auxins using a microplate method. Lett. Appl. Microbiol. 20:282-285.

Stamford TLM, Araújo JM, Stamford NP (1998). Atividade enzimática de microrganismos isolados do jacatupé (*Pachyrhizus erosus* L Urban). Ciênc. Tecnol. Aliment. 18:4-10.

Tsavkelova EA, Cherdyntseva TA, Botina SG, Netrusov AI (2007). Bacteria associated with orchid roots and microbial production of auxin. Microbiol. Res. 162:69-76.

Velásquez E, Rojas M, Lorite MJ, Rivas R, Zurdo-Piñeiro JL, Heydrich M, Bedmar EJ (2008). Genetic diversity of endophytic bacteria which could be found in the apoplastic sap of the medullary parenchym of the stem of healthy sugarcane plants. J. Basic Microbiol. 48:118-124.

Vendan RT, Yu YJ, Lee SH, Rhee YH (2010). Diversity of endophytic bacteria in ginseng and their potential for plant growth promotion. J. Microbiol. 48(5):559-565.

Verma SC, Ladha JK, Tripathi AK (2001). Evaluation of plant growth promoting and colonization ability of endophytic diazotrophs from deep water rice. J. Biotechnol. 91:127-141.

Winn WC, Allen S, Janda W, Koneman E, Procop G, Schreckenberger P (2006). Koneman's color ctlas and textbook of diagnostic microbiology. 6 th ed. Philadelphia: Lippincott Williams and Wilkins.

Young LS, Hameed A, Peng SY, Shan YH, Wu SP (2013). Endophytic establishment of the soil isolate *Burkholderia* sp. CC-Al74 enhances growth and P-utilization rate in raize (*Zea mays* L.). Appl. Soil Ecol., 66:40-47.

Zhao J, Shan T, Mou Y, Zhou L (2011). Plant-derived bioactive compounds produced by endophytic fungi. Mini Rev. Med. Chem. 11:159-168.

Zhao J, Zhou L, Wang J, Shan T, Zhong L, Liu X, Gao X (2010). Endophytic fungi for producing bioactive compounds originally from their host plants. Curr. Res., Technol. Educ. Trop. Appl. Microbiol. Microbial. Biotechnol. 1:567-576.

Zheng J, Allarda S, Reynoldsb S, Millnerb P, Arcea G, Blodgetta RJ, Browna EW (2013). Colonization and internalization of *Salmonella enterica* in tomato plants. Appl. Environ. Microbiol. 79(8):2494-2502.

academicJournals

Vol. 13(33), pp. 3366-3375, 13 August, 2014
DOI: 10.5897/AJB2013.13365
Article Number: 15CE98146619
ISSN 1684-5315

http://www.academicjournals.org/AJB

African Journal of Biotechnology

Full Length Research Paper

The effect of natural antioxidant(s) on date palm (*Phoenix dactylifera* L.) *in vitro*

Gehan Safwat[1]*, Sherif El-Sharabasy[2], Abd El-Moneam El-Banna[3], Saleh Khede Zardah[1] and Nashwa Hamido[1]

[1]Faculty of Biotechnology, October University for Modern Science an d Art University, Cairo, Egypt.
[2]The Central Laboratory for Date Palm Research and Development, Giza, Egypt.
[3]Aricultural Research Centre, Giza, Egypt.

Received 9 October, 2013; Accepted 14 July, 2014

Date palm (Phoenix *dactylifera L.*) is one of the most valuable economic resources in the Middle East and North Africa that grow on monocotyledonous trees. To increase crop yield of palm trees, *in vitro* micro-propagation has become an attractive alternative for large-scale production of date palm. A problem that frequently damages tissues in the early micro-propagation is the brown color that advances in the callus culture due to the creation of quinones. Quinones seize plant cellular developments which lead to cellular decay. This study advocates the use of antioxidant factors found in spinach, kale and strawberries within various concentrations (50, 150 and 300 mg/L) with respect to the medium culture, in an attempt to reduce the level of total phenol and browning which occurs, and also to improve growth and development in different *in vitro* stages of date palm (*P. dactylifera L.*). The results indicate that better growth value of callus was achieved using 150 mg/L of kale concentration; allowing the total phenol level to be reduced to 0.9237 mg/g D.W, presenting a significant growth value in comparison to the other treatments in the embryonic callus stage. In the date palm's somatic embryogenesis stage, the results show that the use of 50 mg/L of spinach, 50 mg/L of kale, 150 mg/L of strawberries, achieved a high number of somatic embryos and the total phenol level was reduced to 0.6167 mg/g D.W. Results from date palm shoot proliferation shows that high numbers of shoot (16.3) was achieved using 50 to 300 mg/L of kale; however, total phenol level was reduced to 0.04567 at 150 mg/L of spinach concentration. The fluctuation of reducing total phenol level in date palm was recorded when the explants were grown on medium supplemented with 50 mg/L of kale concentration.

Key words: Date palm, tissue culture, natural antioxidants, browning, quionones.

INTRODUCTION

Date palm (*Phoenix dactylifera L.*) is an important crop that grows in the arid regions of North Africa, Middle East and the Arabian Peninsula. Date palm is a chief nutriment for the locals and plays substantial roles in the industrial, economic and environmental aspects of these areas. Furthermore, date palms have the ability to be manipulated in numerous ways making them a crop that adds ease to its production (Al-Khateeb, 2008).

The ecological aspects of date palm tree is that it has the ability to be grown ideally where permanent water

table is present within the soil surface; minimally 8 to 9 acre feet of irrigation water per year is required for fine palm production. The mean temperature between the flowering and the ripening period should be above 2°C rising to 26°C for at least a month, to ensure proper fruit ripening. It takes about six months for the dates to ripe. There are certain regulators that withhold irrigation during fall and winter. There must be no rain during flowering time; extreme winter temperatures are harmful to this crop. Its cultivation process may be propagated through seeds or off shots. It takes about eight years in Egypt for an offshoot to yield economically (Chao and Krueger, 2007).

Through recent breakthroughs in tissue culturing methods, culture propagation is ideal for the expansion of date production. Date palm *in vitro* plant regeneration occurs through organogenesis and somatic embryogenesis relying on the genotype and hormonal manipulations. The utmost method for date palm regeneration used by various cultivators is somatic embryogenesis from shoot tip derived callus; since it has feasibility in micropropagation scale-up for commercial requirements. Date palm somatic embryogenesis involves series of consecutive stages beginning with callus induction, embryogenic callus multiplication, somatic embryo formation, shoot formation and finally rooting (Al-Khateeb, 2008).

There is a major problem that encounters tissue culturing techniques, which is the “browning color” that advances in the callus. This phenomenon results from physiological changes in the cultured tissues that lead to gradual browning and death of the tissues eventually. The brown color that advances in callus cultures of various plant cultures is due to the creation of quinines, which prevent plant cellular growth. The increase of quinones to a certain level harms *in vitro* growth especially in explants from woody plants (Mustafa et al., 2013).

Phenol oxidation frequently damages tissues in the early stage of micropropagation and advances in browning of explants which slows down growth or leads to death of the explants. Oxidative browning can sometimes be evaded by washing, soaking or stirring the explants in antioxidant solutions as a pretreatment before moving them on the media.

To be precise, adopting certain measures with the culturing of plant parts during winter and spring seasons, incubation of tissues in the dark especially in the first three months and adding charcoal to the medium can reduce this phenomenon (Mustafa et al., 2013; Panaia et al., 2000; Wu and du Toit, 2004).

The proposition of the use of caffeine, activated charcoal and polyvinylpyrrolidone (PVP) in the culture media of Eucalyptus was tested not to assist in avoiding exudation of phenolic compounds (Gill and Gill, 1994). Similarly, the proposition of adding PVP and ammonium citrate aids in reducing the explants of date palm shoots from browning (Mustafa et al., 2013).

This study investigate the alternative ways to avoid the browning phenomenon drawback in date palm (*P. dactylifera L.*) explants during tissue culturing procedures, through the use of natural antioxidants (kale, spinach and strawberries).

MATERIALS AND METHODS

The work was carried out in The Central Laboratory for Research and Development of Date Palm, Agriculture Research Center, Ministry of Agriculture, Giza, Egypt, throughout the year of 2010.

Callus formation

The embryogenic callus produced and established from the shoot tip were transferred and cultured on Murashige and Skoog (1962) basal media supplemented with 200 mg of glutamine, 2 mg/L of glycine, 30 g/L of sucrose, 6 g/L of agar, and 0.1 mg/L of NAA. The formed callus was sub-cultured to fresh media with three different concentrations that is, 50, 150, and 300 mg/L from each extraction juice of spinach, kale and strawberry. For the control, 2 g/L PVP were added to the media instead of antioxidant source. All culture jars were maintained in complete darkness at 27 ± 2°C for four weeks.

The data was excerpted as an average per explant according to Pottino (1981) for growth value of the culture visual calculations; while total phenols were calculated with the use of the spectrophotometer.

Embryoids initiation

The investigation of effect of different concentration of spinach, kale and strawberry extraction juice on callus differentiation and initiation of embryoids was carried out through white friable embryonic nodular callus (0.1 g in weight and 1 to 2 mm in diameter) which were obtained from embryonic callus formation medium. They were transferred and cultured on embryoids differentiation medium which consisted of MS basal media supplemented with 200 mg of glutamine, 2 mg/L of glycine, 30 g/L of sucrose, 6 g/L of agar, 0.1 mg/L of NAA, 0.5 mg/L of ABA with three different concentrations that is, 50, 150, and 300 mg/L from each extraction juice of spinach, kale and strawberry. PVP was used as the control of antioxidant source by adding 2 g/L to the medium culture. All culture jars were kept in the complete darkness at 27 ±2°C for four weeks. After four weeks, data was collected through the counted number of embryos; while total phenols were calculated with the use of the spectrophotometer.

*Corresponding author. E-mail: gehan.safwat@hotmail.co.uk.

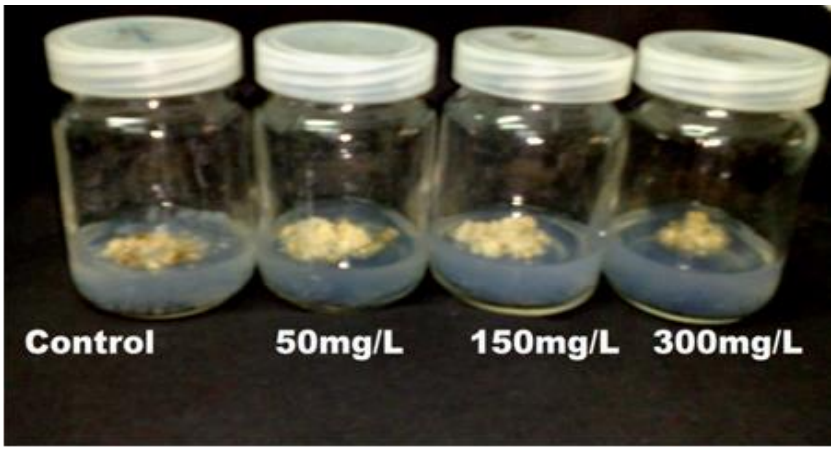

Plate 1. Date palm *c.v. Malakaby* embryogenic callus treated with different concentrations of Spanish juice (50, 150 and 300 mg/L) as antioxidants. The control was treated with PVP.

Shoot proliferation

The investigation of the effect of different concentration of spinach, kale and strawberry extraction juice on shoot proliferation was conducted by developing two to three shoots in a small cluster. They were developed from germinated mature embryos of *Malakaby*, then cultured on MS basal nutrient media, supplemented with 200 mg/L of glutamine, 2 mg/L of glycine, 30 g/L of sucrose, 6 g/L of agar, 0.05 mg/L of BA, 0.1 mg/L of NAA and three different concentration from each of spinach, kale and strawberry extraction juice (that is, 50, 150 and 300 mg/L), and 2 g/L PVP were added. Small jars (150 ml) were used to dispense the nutrient medium of each treatment and 2 g/L of PVP was used as the control of antioxidant source. All culture jars were kept in the complete darkness at 27± 2°C for four weeks. After four weeks of culturing, data was collected through the counted number of shoots; while total phenols were calculated with the use of the spectrophotometer

Total soluble phenols determination

Phenols were determined by the colorimetric method described by Snell and Snell (1953). A procedure of folin (A.O.A.C, 1980) was adapted for determining the total soluble phenols in the ethanolic extract from 0.05 g of dry materials. Folin-Denis reagent was prepared by transferring 100 g of sodium tungstate to 25 g of sodium molybdate and 700 ml water was added to a 1500 ml flask. The mixture was also supplied with 50 ml of 85% phosphoric acid and 100 ml of concentrated hydrochloric acid attached to reflux condenser, then boiled gently for 10 h, after which 150 g of lithium sulphate, 50 ml water, and a few drops of liquid bromine were added. To remove the bromine excess, the mixture was boiled without attaching the condenser, cooled and diluted to one liter. The total soluble phenols were calculated as mg pyrogallol/g of dry weight.

Statistical analysis

The experiments were carried out using completely randomized blocks design and three replicates. The results were analyzed using variance analysis, while the means were compared using L.S.D. at 5% level. The entire data were subjected to variance analysis with completely randomized blocks according to Snedecor and Cochran (1980).

RESULTS

This study advocates the use of antioxidant factors to reduce the level of total phenol and browning which occurs, and to improve growth and development in different *in vitro* stages of date palm (*P. dactylifera L.*). The effects of the different antioxidants on the growth values and total phenols levels were evaluated. The following data exposes the results obtained.

The effect of the antioxidants with various concentrations on the embryonic callus of date palm

The effect of three different concentrations (50, 150, or 300 mg/L) of spinach, strawberry and kale juice as antioxidants on embryogenic callus browning are presented in Plates 1 to 3 respectively. Generally, by adding the antioxidants, browning were reduced compared to the control. The best result was shown with the use of 150 mg/L of the strawberry extraction and 50 mg/L from spinach and kale extractions as antioxidants and callus appeared healthier with less browning. For callus formation, using the 300 mg/L from the antioxidants affected negatively the callus formation. However, the medium supplemented with 50 mg/L of both strawberry and spinach extraction juices gave almost 20% growth value of the embryogenic callus compared to the control (Figure 1). In the case of using kale extraction juice, 150 mg increased the growth value

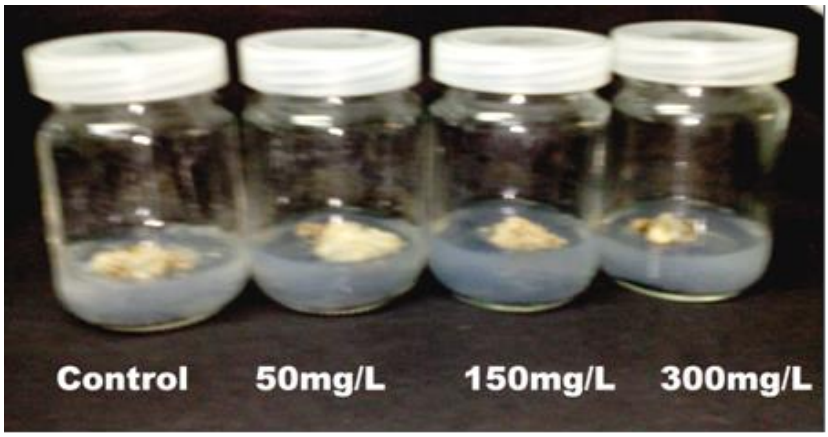

Plate 2. Date palm *c.v. Malakaby* embryogenic callus treated with different concentrations of Strawberry juice (50, 150 and 300 mg/L) as antioxidants. The control was treated with PVP.

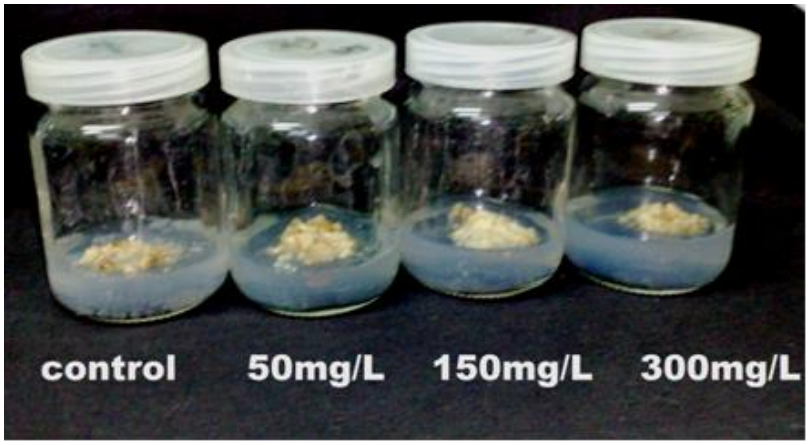

Plate 3. Date palm *c.v. Malakaby* embryogenic callus treated with different concentrations of Kale juice (50, 150 and 300 mg/L) as antioxidants. The control was treated with PVP.

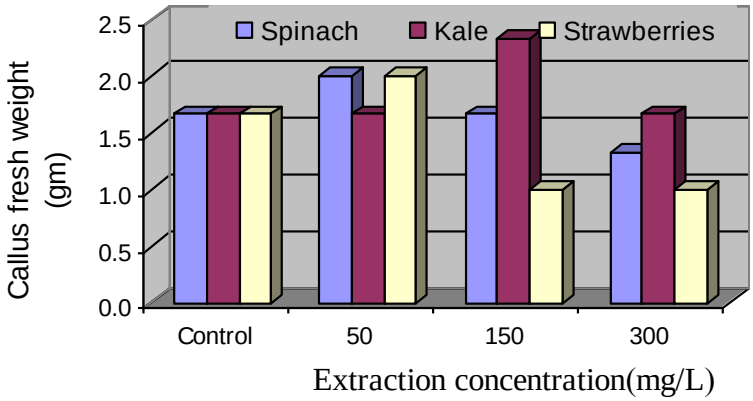

Figure 1. Effect of different concentrations of spinach, kale and strawberry juice as antioxidants on the growth value of embryogenic callus of date palm *c.v. Malakaby.*

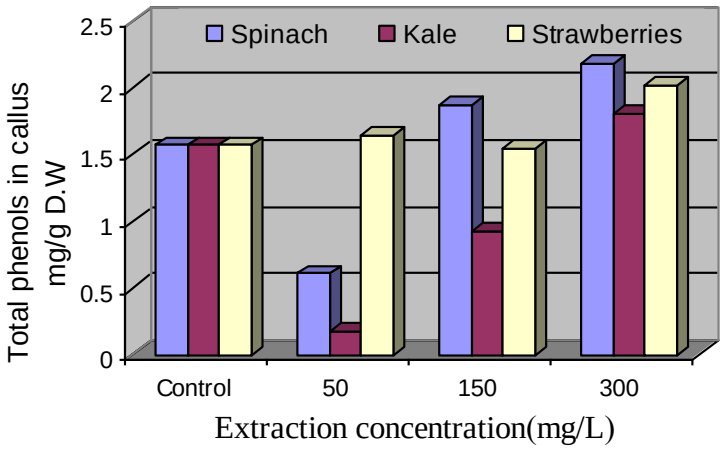

Figure 2. Effect of different concentrations of spinach, kale and strawberry juice as antioxidants on the total phenols of embryogenic callus of date palm *c.v. Malakaby.*

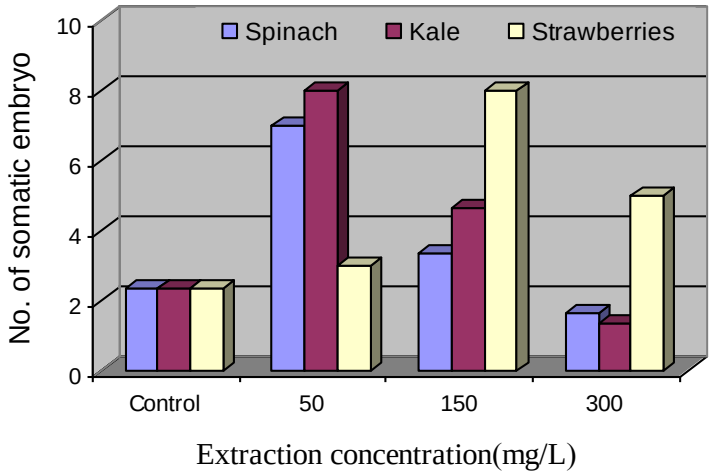

Figure 3. Effect of different concentrations of spinach, kale and strawberry juice as antioxidants on number of embryo of somatic embryo of date palms *c.v. Malakaby*.

by almost 35% (Figure 1). Concerning the total phenol levels, it was clear that treating the embryonic callus cultures with kale at the concentration of 50 and 150 mg/L gave the value of 0.17 mg/g D.W. and 0.92 mg/g D.W, which reduced the total phenol by 79.1 and 41.2% respectively, and had the preeminent results amongst other antioxidants (Figure 2). Overall, for these results, the better type of antioxidant for callus formation was kale at the concentration of 150 mg/L (Figures 1 and 2).

The effect of the antioxidants with various concentrations on the somatic embryos of date palm

In the date palm's somatic embryogenesis stage, the results show that the use of 50 mg/L of spinach and 150 mg/L of strawberries elevated the number of somatic embryos to almost 4 times the control. Meanwhile, using 50 mg/L of kale extraction achieved almost 3 times the number of somatic embryos for date palm with the control (Figure 3). The effect of the three antioxidants on total phenol level is presented in Figure 4. Two of the extraction juices that is strawberries and spinach at the lowest concentration (50 mg/L) gave the significant reduction on the total phenol level to the extent of 60 and 46% with the value of 0.6167 and 0.862 mg/g D.W respectively compared to the control. These percentages become lesser when the concentration increased to 150 and 300 mg/L. For the kale extraction juice the level of total phenol was decreased to the lowest value (0.549

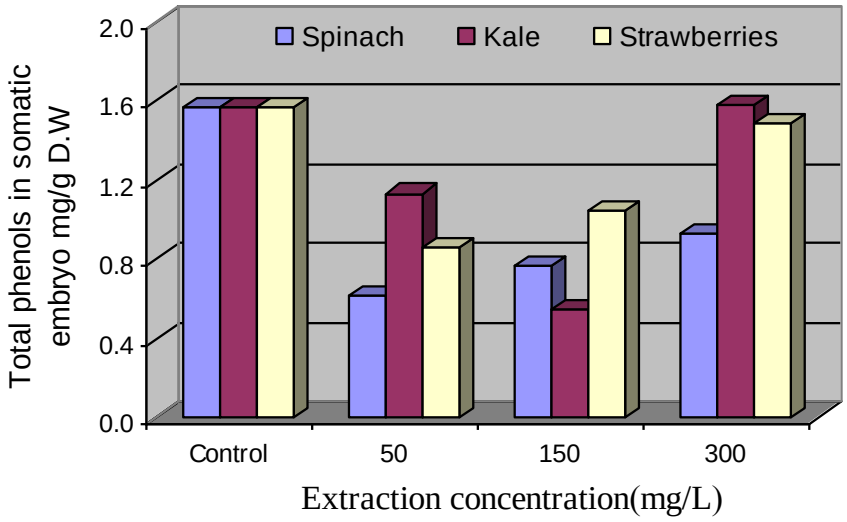

Figure 4. Effect of different concentrations of spinach, kale and strawberry juice as antioxidants on total phenols of somatic embryo of date palm *c.v. Malakaby.*

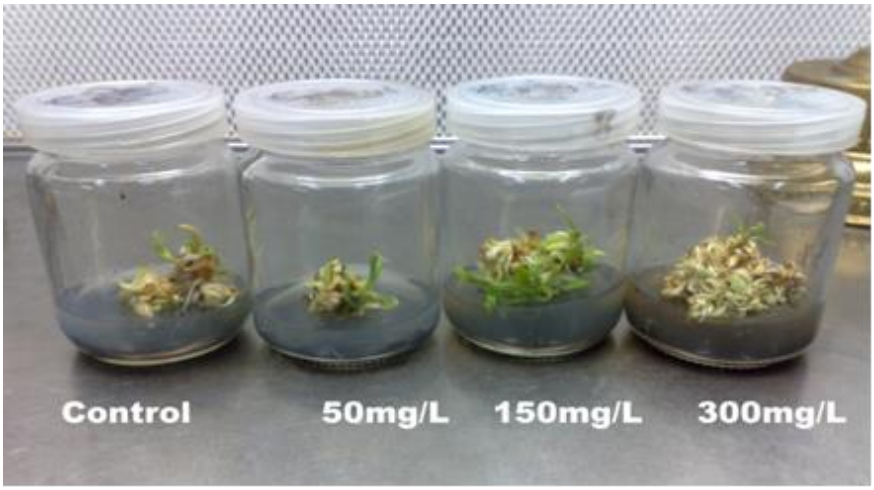

Plate 4. Date palm *c.v. Malakaby* embryogenic somatic embryo treated with different concentrations of strawberry juice (50, 150 and 300 mg/L) as antioxidants. The control was treated with PVP.

mg/g D.W) over all the nine treatments when concentration of 150 mg/L was added. This significant reduction was calculated as 66% from the total phenol in the control. The level of browning are illustrated in Plates 4 to 6 which reflect the results. When calculating the mean per type of antioxidant, strawberries presented the finest results; while calculating the mean per concentration, 50 mg/L gave the best results. These results suggest that for somatic embryos initiation, the better antioxidant was Kale extraction juice at the concentration of 50 or 100 mg/L (Figures 3 and 4).

The effect of the antioxidants with various concentrations on the shoot proliferation of date palm

Results from date palm shoot proliferation shows increase value with all treatments for the three antioxidants than control (Figure 5). Among the three antioxidants, high numbers of shoot (16 and16.3) were achieved using 50 and 300 mg/L of kale extraction juices followed by the three concentrations of strawberry juice (Figure 5 and Plates 7 and 8), in addition, the spinach

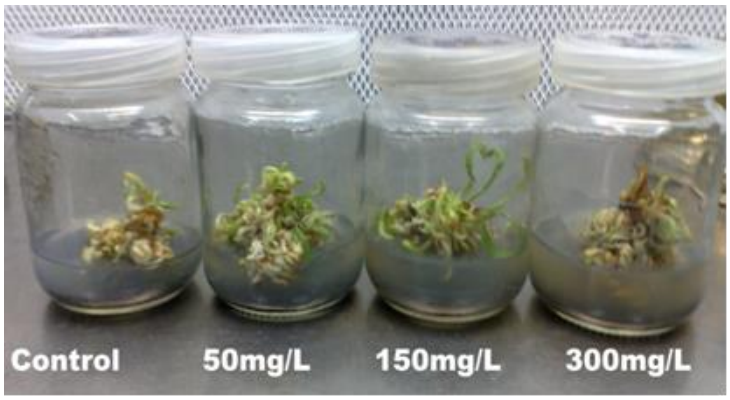

Plate 5. Date palm *c.v. Malakaby* embryogenic somatic embryo treated with different concentrations of kale juice (50, 150 and 300 mg/L) as antioxidants. The control was treated with PVP

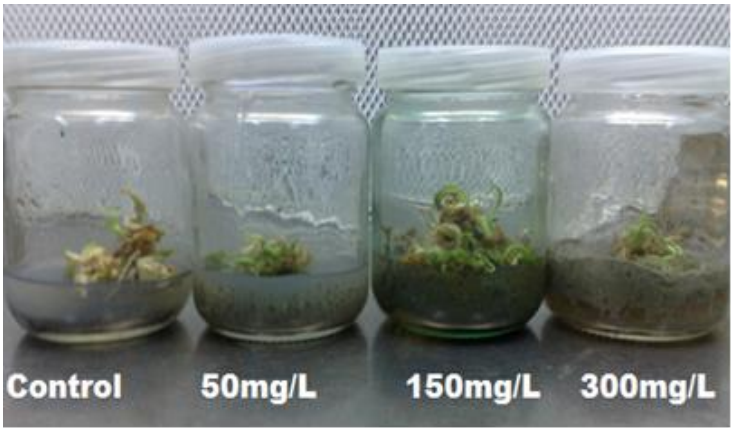

Plate 6. Date palm *c.v. Malakaby* embryogenic somatic embryo treated with different concentrations of spinach juice (50, 150 and 300 mg/L) as antioxidants. The control was treated with PVP

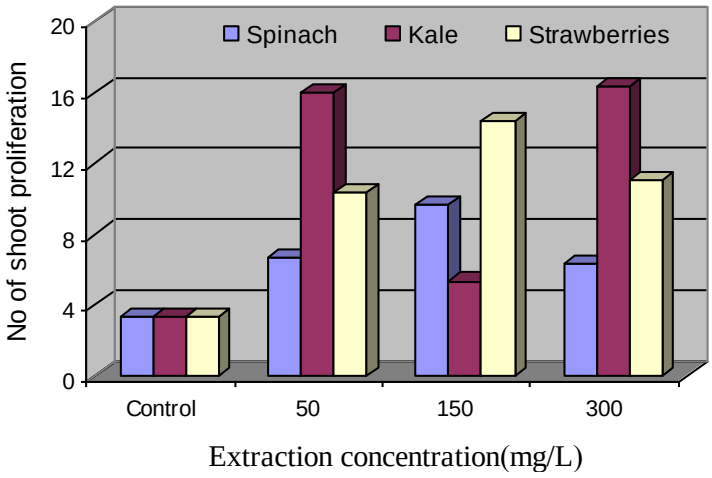

Figure 5. Effect of different concentrations of spinach, kale and strawberry juice as antioxidants on number of shoots of shoot proliferation of date palm *c.v. Malakaby*.

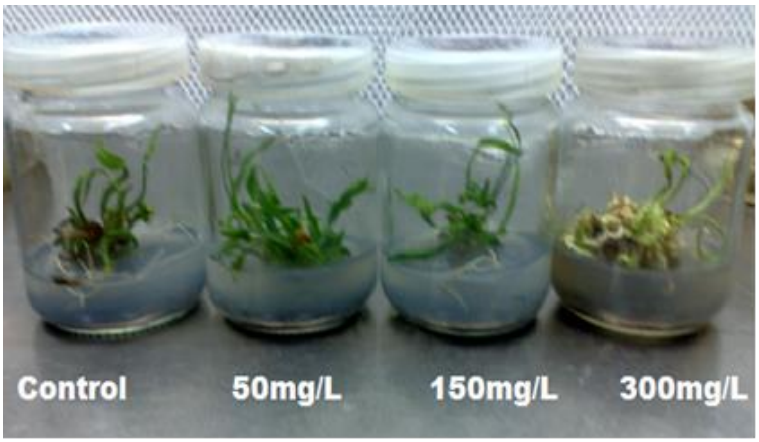

Plate 7. Date palm *c.v. Malakaby* embryogenic shoot proliferation after treated with different concentrations of kale juice (50, 150 and 300 mg/L) as antioxidants. The control was treated with PVP.

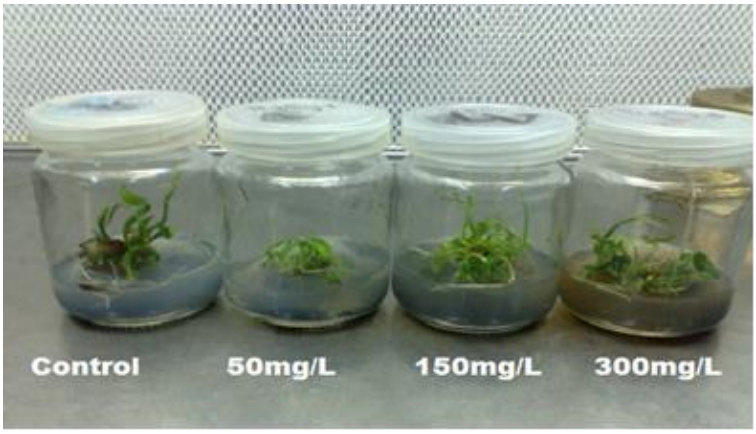

Plate 8. Date palm *c.v. Malakaby* embryogenic shoot proliferation after treated with different concentrations of strawberry juice (50, 150 and 300 mg/L) as antioxidants. The control was treated with PVP.

antioxidant showed the lowest effect amongst them (Figure 5 and Plate 9). Total phenol level in shoots was highly significantly reduced (95%) to the value of 0.04567 mg/g D.W at 150 mg/L of spinach concentration (Figure 6). Moreover, a significant reduction in total phenol by almost 75% was calculated with two treatments from strawberry antioxidant (150 and 300 mg/L) (Figure 6), meanwhile, no more than 24% of reduction of total phenol level in date palm was recorded when the shoots were grown on the medium containing any of the kale different concentrations (Figure 6). When calculating the mean per type of antioxidant, kale conveyed preeminent results with the shoot proliferation, while combining that with results of total phenol level, it was suggested that treating the shoot proliferation cultures with strawberry at the concentration of 150 mg/L might give the best result (Figures 5 and 6).

DISCUSSION

Commercial cultivation and expansion of date palm (*P. dactylifera L.)* had unsatisfactory upshots due to varieties of undesired contamination, the incidence of contamination in the culture could sometime lead to important losses. An obstacle caused by phenol oxidation during the callus phase, and the callus was subjected to browning.

In this study, callus initiation, somatic embryoids and shoot proliferation have been subjected to three different concentrations of various antioxidants, which consist of spinach, kale and strawberries. The growing or dipping of the explants in the antioxidant concentrations has proved to be efficient with almost negligible or no browning noted. The results were parallel with those of Abdel Sattar's (1999), which describes the effect of reducing

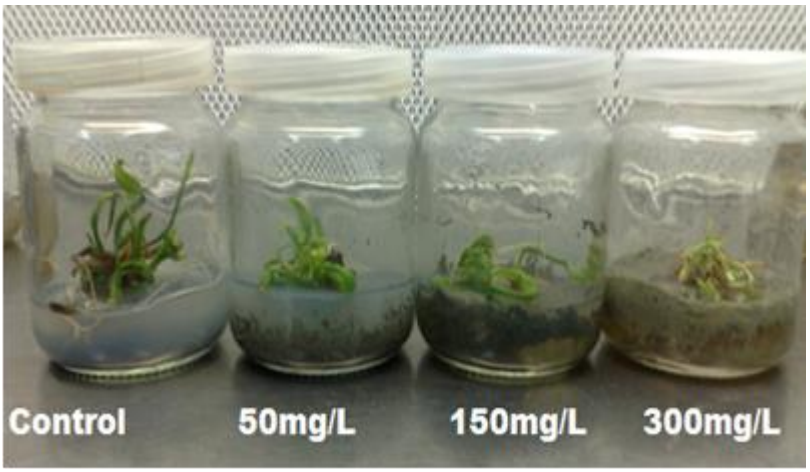

Plate 9. Date palm *c.v. Malakaby* embryogenic shoot proliferation after treated with different concentrations of spinach juice (50, 150 and 300 mg/L) as antioxidants. The control was treated with PVP.

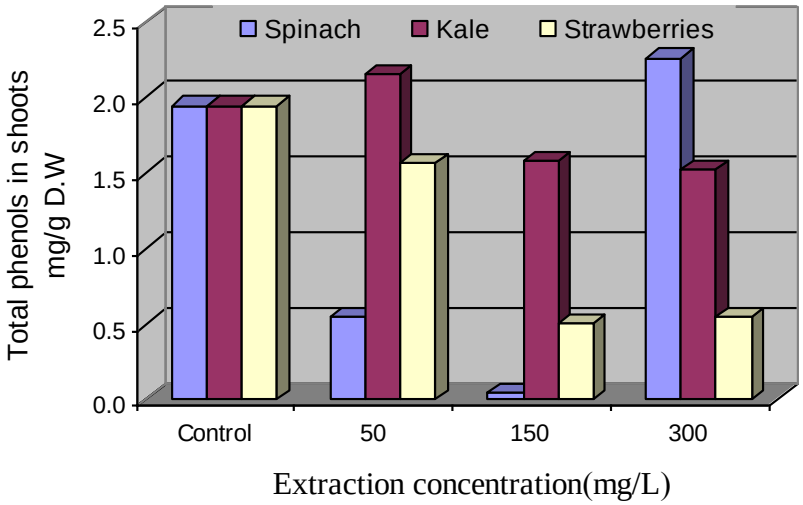

Figure 6. The effect of different concentrations of antioxidants on the total phenols of the shoot proliferation: the figure represents Spinach, kale and strawberry juice as antioxidants on total phenols of shoot proliferation of date palm *c.v. Malakaby*.

the browning on the callus induction rate.

The effect of kale as an antioxidant on the treatment was to reduce the phenolic compounds as compared with the control, which used PVP as the factor of reducing the browning color in the cultures.

It has been tested in various studies conducted in immature date embryo culture that the liquid endosperm of *Cocos nucifera* (coconut milk) showed stimulation in cell division in other cultured tissues and is used as an antioxidant to overcome contamination problems, in comparison to applying the tested antioxidants (kale, spinach and strawberry) (Duhamet and Gautheret, 1950; Morel, 1950; Nickell, 1950; Duhamet, 1951; Henderson et al., 1952; De Ropp et al., 1952; Archibald, 1954; Wiggans, 1954). Also, other complex plant juices and liquid endosperms have been shown to possess stimulatory properties more or less similar to those of coconut milk. These include liquid endosperm from immature corn (Netien et al., 1951), tomato juice (Nitsch, 1951; Straus and La Rue, 1954), immature fruits and seeds (Steward and Caplin, 1952; Steward and Shantz, 1959), orange juice, malt extract, yeast extract, casein hydrolysate, leaf

extracts, sap from a number of plants and tumor extracts (Butenko, 1968) in comparison to date palm. Similarly, Straus (1960) has shown that tomato juice, yeast extract or casein hydrolysate function by supplying a form of organic nitrogen (a mixture of amino acids) while malt extract provide an auxin, kinetin, minositol, urea and arginine to *in vitro* cultured explants (Steinhart et al., 1961). The mentioned experiments serve as a support to the hypothesis that natural antioxidants have positive preeminent impact on the date palm culture and rate of callus induction.

Conclusion

It could be concluded that treatments with antioxidants from natural sources did have favorable results in reducing the total phenol levels, which plays a role in the browning that occurs in cultures. In addition, those observed at high concentrations of antioxidants had no positive effects in reducing the phenol levels. It is recommended to use concentrations between 50 to 150 mg/L of the stated antioxidants for utmost results. Furthermore, it was also revealed that for the date palm cultures kept in the dark, the explants' tissues started numbering and swelling for callus formations at a higher rate than the ones kept in the light.

Conflict of Interests

The author(s) have not declared any conflict of interests.

ACKNOWLEDGEMENTS

We would like to thank the members of the Central Laboratory for date palm, especially Dr. Zainab El-Sayed, and Dr. Ibrahim Shams, for their guidance and useful advices. We would also like to send a token of our appreciation to whoever had a helping hand in making this work possible and showed us support in every way possible.

REFERENCES

A.O.A.C (1980). Official Methods of Analysis 13th ed. Association of Office Agricultural Chemists, Washington D. C.

Abdel Sattar M (1999). Physiological studies on date palm by using tissue culture. Department of Pomology, Faculty of Agriculture, Cairo University, Egypt.

Archibald JF (1954). Culture *in vitro* of cambial tissues of cacao. Nature 173:351-353.

Butenko RG (1968). In Plant Tissue Culture and Plant Morphogenesis, Israel Program for Scientific Translations, Jerusalem.10: 40-45.

Chao C, Krueger R (2007).The date palm ((*Phoneonix dactylifera L.)*, the overview of biology, uses and cultivation. HortScience 42:1077:1082.

De Ropp RS, Vitucci JC, Hutchings BL, Williams JM (1952). Effect of coconut fractions on growth of carrot tissues. Proc. Soc. Exp. Biol. 81:704-709.

Duhamet L (1951). Action du lait de coco sur la croissance des cultives de tissus de crown-gall de vign, de tabac, de topinambour et de scorsonere. Comp. Rendus de la Soc. deBiol. 145:1781-1785.

Duhamet L, Gautheret RJ (1950). Structure anatomique de fragments de tubercules de topinambour cultives en presence de lait de coco. Comp. Rendus de la Soc. De Biol. 144:177-184.

Gill R, Gill S (1994). *In vitro* exudation of phenols in Eucalyptus. Indian. Forester.120 (6):504-509.

Henderson J, Durrell ME, Bonner J (1952). The cultures of normal sunflower callus. Am. J. Bot. 39:467-472.

Morel G (1950). Sur la culture des tissus de deux monocotyledons. Comp. Rendus de L` Acad. Des Sci. 230:1099-1105.

Murashige T, Skoog FA (1962). A revised medium for rapid growth and biooassays with tobacco tissue cultures. Plant Physiol. 15: 473-479.

Netien G, Beauchesne G, Mentzer C (1951). Influence du `lait de mais` sur la croissance des tissus de carotte *in vitro*. Comp. Rendus de L` Acad. Des Sci. 233:92-98.

Nickell LG (1950). Effect of coconut milk on the growth *in vitro* of plant virus tumour tissue. Bot. Gaz.112:225-229.

Nitsch JP (1951). Growth and development *in vitro* of excises ovaries. Am. J. Bot. 38:566-571.

Panaia M, Senaratna T, Bunn E, Dixon K W, Sivasithamparam K (2000). Micropropagation of the critically endangered Western Australian species, *Symonanthus bancroftii (F. Muell.) L. Haegi (Solanaceae)*. Plant Cell Tissue Organ Cult. 63(1):23-29.

Pottino BG (1981). Methods in plant tissue culture. Dep. Hort. Agric. College (1):8-29.

Snedecor W, Cochran W (1980). Statistical methods 7th ed . Iowa State University Press. Ames Iowa.

Snell FD, Snell CT (1953). Colorimetric Methods of Analysis Including some Turbidimetric and Nephelometric Methods. D.Van Noster Company Inc. Toronto New York.London Organic. 3 (1): 116-117.

Steinhart CE, Standifer LG, Skoog F (1961). Nutrient requirements for *in vitro* growth of spruce tissue. Am. J. Bot. 48:465-472.

Steward FC, Caplin SM (1952). Investigation on growth and metabolism of plant cells Evidence on the role of coconut milk factor in development. Ann. Bot. 16:491-498.

Steward FC, Shantz EM (1959). The chemical regulation of growth some substances and extracts which induce growth and morphogenesis. Ann. Rev. Plant. Physiol. 10: 379-386.

Straus J (1960). Maize endosperm tissue grown *in vitro* Development of a synthetic medium. Am. J Bot. 47: 641-646.

Straus J, La Rue CD (1954). Maize endosperm tissue grown *in vitro* Cultural requirements. Am. J. Bot. 41:687-692.

Wiggans SC (1954). Growth and organ formation on callus tissues derived from Daucus carota. Am. J. Bot. 41:321-326.

Wu HC,Du Toit ES (2004). Reducing oxidative browning during *in vitro* establishment of *Protea cynatoides.* Sci. Hortic. 100(14):355-358.

academicJournals

Vol. 13(33), pp. 3376-3384, 13 August, 2014
DOI: 10.5897/AJB2014.13790
Article Number: 64A511E46620
ISSN 1684-5315

http://www.academicjournals.org/AJB

AfricanJournalofBiotechnology

Full Length Research Paper

CO_2 emissions from soil incubated with sugarcane straw and nitrogen fertilizer

Risely Ferraz de Almeida[1]*, Camila Haddad Silveira[2], Joseph Elias Rodrigues Mikhael[2], Fernando Oliveira Franco[1],Bruno Teixeira Ribeiro[2], Adão de Siqueira Ferreira[2], Eduardo de Sá Mendonça[3] and Beno Wendling[2]

[1]Universidade Estadual Paulista"Júlio de Mesquita Filho"-UNESP, Jaboticabal, Brazil.
[2]Universidade Federal de Uberlândia-UFU/Iciag, Uberlândia/MG, Brazil.
[3]Universidade Federal do Espírito Santo-UFES, Alegre/ES, Brazil.

Received 11 March, 2014; Accepted 14 July, 2014

The decomposition/mineralization of organic material from crop residues constitutes an important nutrient reservoir for plants. This process produces CO_2 and is influenced by biophysical and environmental conditions such as temperature, oxygen availability and the chemical composition of the crop residue. We studied the effect of temperature and nitrogen fertilization on CO_2 emissions and the distinct contributions of C from sugarcane residue either left on the surface or incorporated into the red-yellow Oxisol. Incorporated sugarcane residue and N applications produce higher total organic carbon (TOC) mineralization rates when compared to application on the soil surface and without N. Nevertheless, there was no difference between TOC and C in the humin fraction (C-HU) 80 days after incubation. CO_2 emissions peaked at 5.45, 10.82, 14.00, 11.92 and 11.20, 14.47, 15.98,and 14.74 µg mol of CO_2 g^{-1} s^{-1} within the first four days of incubation for unincorporated and incorporated residues, respectively. After these first four days, emissions decreased until stabilizing at 40 days after incubation.

Key words: Greenhouse gases,organic matter, urea.

INTRODUCTION

Increasing atmospheric CO_2 will bring about serious global warming, which is expected to affect crop production (Fan et al., 2008). The soils are important reservoirs of active C and play an important role in the global C cycle. Decomposed and mineralized crop residue is an important source of available nutrients for sugarcane crops. Aerobic organotrophs decompose and mineralize organic matter, which produces energy for these organisms and liberates H_2O and CO_2 to the atmosphere (Brady and Weil, 2008).

Soil and vegetation management practices and the addition of organic residue (Wu et al., 2012) can affect CO_2 production from the soil. In addition, the chemical composition of the residue (C/N ratio and levels of lignin, cellulose, hemicellulose, various carbohydrates and polyphenols), temperature, soil moisture (Adachi et al.,

*Corresponding author. E-mail: rizely@gmail.com.

Table 1. Sugarcane residue attributes (chemical attributes) and red-yellow Oxisol (physical and chemical characteristics) used in the experiment.

Attribute	Soil	Attribute	Soil	Residue
Sand (g kg^{-1})	630	TN (g kg-^{1})	0.69	1.44
Silt (g kg^{-1})	140	TOC (g kg^{-1})	7.40	142.0
Clay (g kg^{-1})	230	C/N	-	99.0
pH (H_2O)	5.6	P (mg dm^{-3})	2.47	0.8
H+Al ($cmol_c$ dm^{-3})	15.8	K^+ (mg dm^{-3})	208.0	9.0
S-SO_4 (mg dm^{-3})	51.00	Mg^{2+} ($cmol_c$ dm^{-3})	0.56	1.3
CEC	5.53	Ca^{2+} ($cmol_c$ dm^{-3})	2.20	5.4

CEC, Cation exchange capacity.

2006; Fu et al., 2010) and oxygen availability (Herman et al., 1977) directly affect the decomposition/mineralization of organic material and CO_2 efflux, (Johnson et al., 2008). Among these the CO_2 emission is highly sensitive to changes in temperature because of its effects on almost all aspects of CO_2 emission processes (Townsend et al., 1992; Mikan et al., 2002; Luo and Zhou, 2006).

Additionally, physical and chemical characteristics of the soil, such as density, porosity, pore saturation and nutrient availability, influence CO_2 emissions (Brady and Weil, 2008). Accumulated soil residue is the main source of mineral N for plants and microorganisms. The immobilization or mineralization of N depends on the quality of the residue and can result in significant quantities during decomposition (Mengel and Schmeer, 1985).

Mechanized surgarcane harvesting in Brazil deposits crop residue on the soil surface (Panosso et al., 2009) at an average of 10 Mg ha^{-1} $year^{-1}$ and at a depth of 10 to 15 cm (Urquiaga et al., 1991). A 2002 federal law bans the burning of crop residue, which was a common practice for removing crop residue and facilitating sugarcane harvesting. Sugarcane residue in the soil and CO_2 emissions are linked to the various C sources in the soil. Understanding the proportion and dynamics of C is essential for understanding how different agricultural systems are sustained and the consequences for the C cycle (Liu et al., 2013).

The objective of this studywas to determine the effect of temperature and nitrogen fertilizer on CO_2 emissions and specific C contributions in soils managed with sugarcane residue in a red-yellow Oxisol.

MATERIALS AND METHODS

Soil sampling and analysis

The incubation experiment was carried out in lab conditions. The soil was collected in April, 2012 under sugarcane cropland (19°13'00,22″S latitude and 48º08'24,80″W longitude) and classified red yellow Latosol according to Brazilian System of Soil Classification (Embrapa, 2014). Before the experiment, the soil samples were air-dried, sieved (<2 mm) to obtain TFSA, and moistened to 60% of its water-holding capacity (WHC).

An aliquot of the resulting samples was used to characterize the chemical and physical attributes of the soil. The pipette method (Kilmer and Alexander, 1949) was used to determine soil texture. Total nitrogen (TN) was measured using Kjeldahl method (Black, 1965), available phosphorus (P) by Sommers and Nelson (1972) method and total organic carbon (TOC) according to Yeomans and Bremner (1988). The methodology recommended by Carter and Gregorich (2007) was used to determine potassium (K^+), calcium (Ca^{2+}), magnesium (Mg^{2+}),sulphur (S-SO_4), potential acidity (H + Al), and in pH (water) (Table 1).

Soil incubation

700 g of soil sample were packed into a PVC column (15 cm height; 10.5 internal diameter; total volume of 1.298.2 cm^3) and incubated using a BOD incubator. The experiment was set up completely randomized, with three replicates (3×2×2 factorial) corresponding to: three temperatures (20, 25 and 30°C), two sugarcane straw conditions (surface and incorporated) and two nitrogen doses: 0 kg N ha^{-1} (control) and 120 kg N ha^{-1}, separated into two groups(Table 2).In addition, treatment controlswere incubated at 20, 25 and 30°C, without straw and fertilizer.

A recommended 120 Kg N ha^{-1} of granulated urea ($(NH_2)_2CO$) was added as solid and incorporated into the soil used in the treatments. Afterwards, 17 g of sugarcane straw (20 Mg of crop residue ha^{-1}) was either incorporated or added to the surface (depending on treatment).

For ratoon cane in Sao Paulo state, surface applications of 120 kg N $ha^{-1}$are recommended to achieve stalk productivity greater than 100 Mg ha^{-1} (Raij andCantarella, 1997). The temperatures used in these treatments are within the optimum range (20to40°C) for mesophilic microorganism growth and activity (Moreira and Siqueira, 2006). These temperatures also encompass soil temperatures found in the Triângulo Mineiro region of Brazil (average of 18°C in winter and 23°C in the hottest months) (Silva et al., 2003). The climate of this region is classified as Aw tropical hot and humid with cool and dry winters (Köppen).

After setting up the experiment, the samples were divided among the three different BOD temperatures. Soil moisture was maintained throughout the experiment at 60% of soil field capacity by measuring differences in sample weight. The soil water content and soil temperature are considered important abiotic factors regulating soil CO_2 efflux (Fu et al., 2010).

Measuring CO_2 emissions and organic carbon

An IRGA (Li-Cor 8100A) was used to measure CO_2 emissions from

Table 2. Treatment in experiment.

Temperature (°C)	Group 1 (surface sugarcane straw condition)	Group 2 (Incorporated sugarcane straw condition)
	Nitrogen fertilizer	Nitrogen fertilizer
20	0 kg N ha^{-1} (control)	0 kg N ha^{-1} (control)
25	0 kg N ha^{-1} (control)	0 kg N ha^{-1} (control)
30	0 kg N ha^{-1} (control)	0 kg N ha^{-1} (control)
20	120 kg N ha^{-1}	120 kg N ha^{-1}
25	120 kg N ha^{-1}	120 kg N ha^{-1}
30	120 kg N ha^{-1}	120 kg N ha^{-1}

the soil on the 1st, 2nd, 3rd, 4th, 6th, 8th, 10th, 13th, 16th, 19th, 22nd, 25th, 28th, 31st, 34th, 37th, 44th, 51st, 58th, 65th, 72nd, and 79th day after incubation (DAI) in the BODs. The IRGA has a closed internal volume of 854.20 and 83.70 cm² area of contact with the soil (Li-Cor Inc. Linclon, NE, USA). The device quantifies the concentration of CO_2 using optical absorption spectroscopy in the infrared range.

CO_2 emissions variables were used to calculate final accumulated respiration (Σ-CO_2 until the 79th DAI) and initial accumulated respiration (Σ-CO_2 until the 5th DAI).

Analytical procedures

At the 80th DAI, the incubated soils were sieved (2 mm opening) to remove the remaining crop residue from the soil. TOC (crop residue and soil) was determined by oxidation of potassium dichromate in an acid medium (Yeomans and Bremner, 1988). The same methodology was also used to characterize TOC in the soil and in the crop residue before incubation (Table 1).

Quantitative extraction and fractionation of C from the humic substances - HS (humin/C-HU, fulvic acid/C-FA and humic acid/C-HA) was determined by differential solubility, established by the International Society of Humic Substances (Swift, 1996).The same methodology was also used to characterize the soil before incubation (Table 1).

Microbial biomass C (Cmic) was determined with the method described by Vance et al. (1987), using a microwave oven to irradiate the samples (Islam and Weil, 1998). Labile C was determined according to Mendonça and Matos (2005) and N, P_2O_5, Ca^{+2} and Mg^{+2} levels according to the methodologies of Carter and Gregorich (2007) (Table 1).

Statistical analysis

The results were tested for normality of residuals (Shapiro-Wilk Test, SPSS Inc., USA) and homogeneity of variances (Bartlett Test, SPSS Inc., USA). Next, significant results (t-test) were then compared by a Tukey test at 5 % probability.

RESULTS AND DISCUSSION

CO_2emissions

In treatments with surface residue management, CO_2 emissions peaked within the first four days after incubation and were highest when incubated at 30°C with average daily emissions of 5.45, 10.82, 14.00, 11.92 and 9.66 µmol of CO_2 m^2 s^{-1} on the 1st, 2nd, 3rd, 4th and 5th DAI, respectively. Emissions decreased after the 6th DAI with small peaks until it reached stability after the 40th DAI at an average of 1.22 µmol de CO_2 m^2 s^{-1} (Figures 1A, C, E).The control treatment had the lowest CO2 emissions in all treatment (Figures 1A).

CO_2 emissions in treatments with incorporated crop residue also peaked within the first 5 DAI. However, daily average emissions were higher at 11.20, 14.47, 15.98, 14.74 and 11.42 µmol of CO2 m^2 s^{-1}. Emissions also decreased after the fifth DAI until reaching stability after the 40th DAI (Figure 1B, D and F). The tillage accelerates CO_2 emissions by increasing contact between soil and crop residue and speeding organic carbon decomposition (Gregorich et al., 2005; Bilen et al., 2010).

Similar CO_2 emissions rates were found with surface wheat residue in Luvisol with a peak emission at the 3rd DAI and an exponential decrease until the end of the experiment at 56 DAI (Guillou et al., 2011). Cayuela et al. (2009) found similar peaks in CO_2 emissions working with surface cotton residue on Regosol incubated for 25 days.

Fu et al. (2010) found that CO_2 emissions by soil temperature were described by multiple regression models. It can be seen from the regression equations that soil temperatures were more closely correlated with soil CO_2 efflux. The CO_2 emissions stabilized after the 40th DAI because the majority of labile C had been consumed. The remaining C is recalcitrant and associated with structural and more lignified crop residue (< 2 mm).

Oscillations in CO_2 emission peaks in the management of sugarcane residue, especially at 20°C (Figure 1A and B) are due to the succession and stability of soil micro-organism communities (Moreira andSiqueira, 2006). Opportunistic and colonizer organisms grow and reproduce rapidly in environments with abundant plant material.

High initial CO_2 emissions can be explained by the rapid mineralization of C-labile from vegetative tissue that quickly decomposes (Cayuela et al., 2009) over a few days or a few years (Brady and Weil, 2008). At 79 DAI, there was no correlation between C-labile with initial (r= - 0.12) and final (r= - 0.16) respiration. However, there was a positive correlation between the initial and final respiration (r=0.95), Table 3. Panosso et al. (2009) found decreases in C-labile with decreases in CO_2 in soils

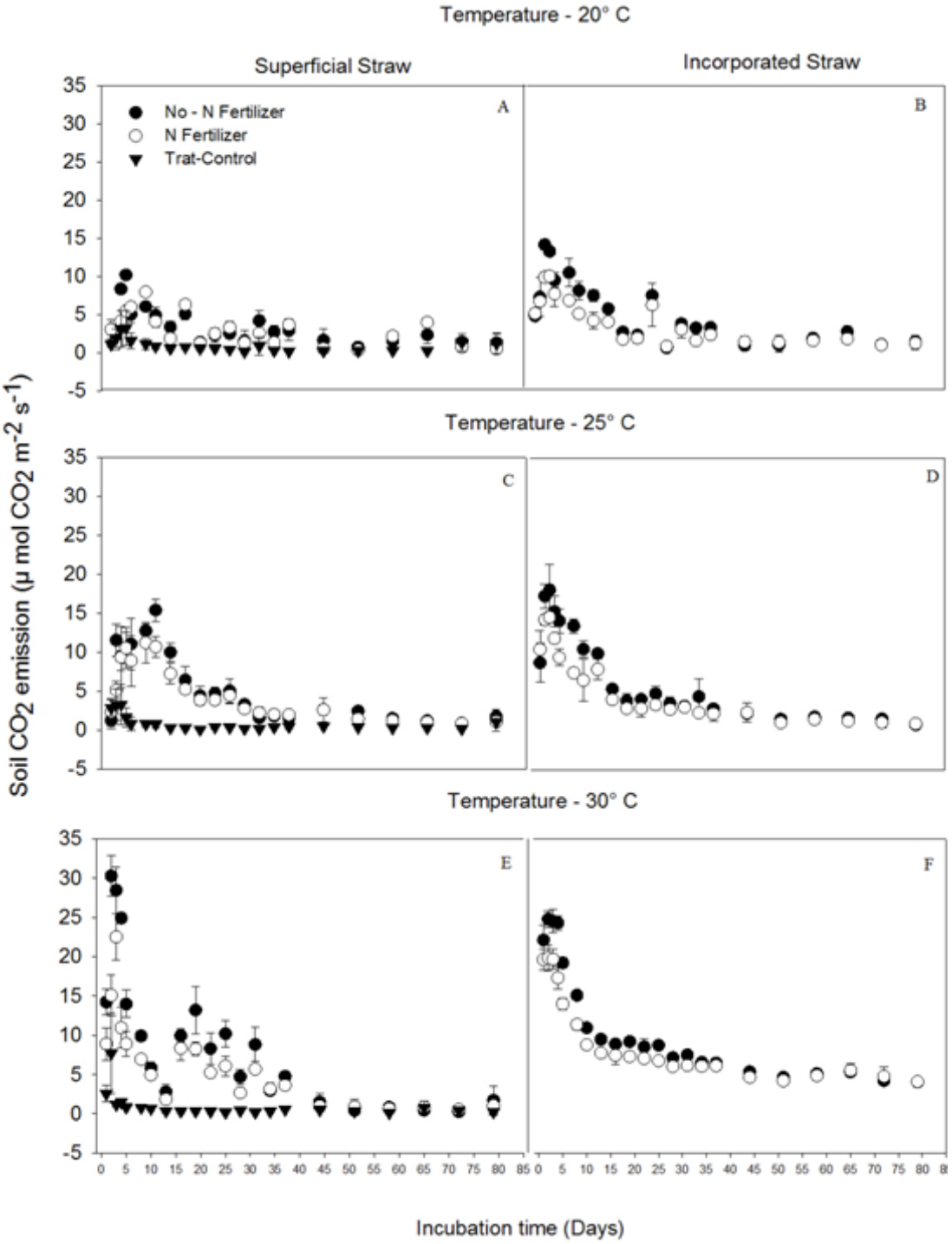

Figure 1. CO_2 emissions (microbial respiration) during incubation of soils with surface, Treatment control (Trat-Control) (Figures A, C, and E) and incorporated (Figures B, D and F) sugarcane residue, combined with nitrogen fertilization at 0 and 120 kg N ha^{-1} and incubated at 20, 25 and 30°C.

cultivated with sugarcane.

After incubation, Cmic, C-labile and Ca^{+2}, Mg^{+2} and P_2O_5 levels in the soil did not differ by management types (Table 4). However, C in the crop residue added to the soil decreased by 10.0 to 21.8 g Kg^{-1} of C (Table 4) with CO_2 emissions (Table 5). According to Brady and Wiel (2008), approximately 80% of total decomposed soil organic matter is emitted to the atmosphere as CO_2.

Table 3. Correlation coefficient and p value between variables: carbon in the humin fraction (C-HU), carbon in the humic acid fraction (C-HA) and fulvic acid (C-FA), total organic carbon (TOC), Labile carbon (C-Labile), HA/FA ratio (HA/FA), initial accumulated respiration (AR-I) and final accumulated respiration (AR-F).

Variable	C-HA	C-FA	TOC	C-labile	HA/FA	AR - F	AR - I
C-HU	0.35 (0.033)	0.16 (0.347)	0.39* (0.016)	-0.22 (0.185)	-0.06 (0.690)	-0.005 (0.97)	0.05 (0.767)
C-HA	-	0.37 (0.026)	0.11 (0.504)	-0.18 (0.294)	0.06 (0.693)	0.21 (0.210)	0.32 (0.051)
C-FA	-	-	0.09 (0.577)	0.11 (0.521)	0.29 (0.082)	-0.14 (0.405)	-0.07 (0.666)
TOC	-	-	-	-0.06 (0.690)	-0.50** (0.001)	0.02 (0.864)	-0.02 (0.885)
C-Labile	-	-	-	-	0.14 (0.407)	-0.12 (0.463)	-0.16 (0.327)
HA/FA	-	-	-	-	-	-0.46** (0.004)	-0.38** (0.021)
AR - F	-	-	-	-	-	-	0.95* ($7.84\ 10^{-19}$)

Variables are considered significant at $p < 0.050$. Correlation in bold: Positive correlation (*) and Negative (**). p value in table are in parentheses.

Table 4. Soil levels of microbial biomass carbon (Cmic), labile carbon (C-labile), nitrogen(N), carbon/nitrogen ratio (C/N), calcium (Ca^{+2}), magnesium (Mg^{+2}), phosphorus (P_2O_5) and crop residue carbon (RC) after 79 days of incubation.

Soil level	Cmic* (ug g^{-1} ha^{-1})	C-labile*	N*	RC	C/N	Ca^{2+}*	Mg^{2+}*	P_2O_5*
		----------g kg^{-1}----------				-----$cmol_c$ dcm^{-3}----		
Residue management								
Surface	238.30	5.05	0.81	132.0^{A}	9.6^{A}	1.94	0.88	3.00
Incorporated	289.07	4.77	0.87	118.1^{B}	10.2^{A}	2.05	0.94	2.94
Nitrogen fertilizer								
0Kg N ha^{-1}	245.22	5.11	0.83	128.9^{A}	9.7^{A}	2.05	0.94	3.0
120Kg N ha^{-1}	282.15	4.72	0.84	121.1^{A}	10.1^{A}	1.94	0.88	2.94
Temperature								
20º C	285.11	4.66	0.82	127.3^{A}	10.3^{A}	2.00	0.83	2.91
25º C	299.14	5.25	0.85	127.3^{A}	10.8^{A}	2.00	0.91	3.00
30º C	306.81	4.83	0.84	120.1^{A}	8.6^{B}	2.00	1.00	3.00

*Variables are not significantly different, whereas C/N and RC averages with distinct uppercase letters within the same column are significantly different (Turkey, P>0.05).

Soils incubated at 30°C, unlike soils incubated at the other temperatures, had greater CO_2 emissions (C losses) and thus significantly lower C/N ratios (Table 4). Soils with lower C/N ratios have fewer nutrients and greater competition among microorganisms for resources. This condition causes some microorganism deaths and lower CO_2 emissions to the atmosphere. Small microorganism populations survive by slowly digesting stable and resistant organic tissue (lignin and cellulose) in the soil (Brady andWiel, 2008).

Accumulated CO_2 emissions in the first five DAI represent 20.45% of total emissions from the soil under surface residue management and 25.53% from the incorporated management system. Rezende et al. (2004) achieved similar results (34 to 67% of total CO_2 emissions in the first 14 DAI) working with Alfisol, TypicKandiustalf and Oxisol, TypicHaplustox, which had been incubated with distillery yeast. During this period, average CO_2 emissions from incorporated residue incubated at 30°C increased 72.72% more than emissions from surface management incubated at 20°C. Emissions were 70.92% higher in a treatment incubated at 30°C with 120 Kg N ha^{-1} relative to a treatment without added N and incubated at 20°C (Table 5).

Temperature increases from 20 to 25°C and from 25 to 30°C raised CO_2 emissions by 40.00 % and 50.00% in treatments with surface crop residue. However, for treatments with incorporated residue, these same increases were lower, 37.50 and 27.27%, respectively (Table 5). This occurred because soil temperature is

Table 5. Accumulated CO_2 emissions from 5 to 79 DAI (days after incubation) in soils with surface and incorporated sugarcane residue with two nitrogen application rates (0 Kg N ha^{-1} and 120 Kg N ha^{-1}) and three incubation temperatures (20, 25 and 30° C).

Temperature (°C)*	Residue management[1]		Nitrogen fertilizer[2]	
	Surface	Incorporated	0 Kg N ha^{-1}	120 Kg N ha^{-1}
Accumulated emissions at 5 DAI				
20	24.1^{Bc}	42.8^{Ac}	29.0^{Bc}	38.0^{Ac}
25	42.1^{Bb}	67.1^{Ab}	48.3^{Bb}	61.0^{Ab}
30	89.1^{Aa}	93.6^{Aa}	73.1^{Ba}	109.6^{Aa}
Accumulated emissions at 79 DAI				
20	73.8^{Bc}	91.1^{Ac}	74.5^{Bc}	95.5^{Ac}
25	112.6^{Bb}	130.6^{Ab}	107.3^{Bb}	136.0^{Ab}
30	163.1^{Aa}	151.8^{Aa}	128.0^{Ba}	187.0^{Aa}

Accumulated Emissions at 5 DAI, CV: 9.6; [1]DMS, Residue management: 6.8; [2]DMS, Nitrogen fertilizer: 8.3. Accumulated Emissions at 79 DAI - CV: 7.9; [1]DMS - Residue management: 11.5; [2]DMS - Nitrogen application rates: 13.9. *CO_2 emissions in µmol CO_2 m^{-2} s^{-1}. Averages followed by distinct lowercase letters within a column and uppercase letters within a row are significantly different for temperature/residue management and temperature/nitrogen rate interactions (Tukey, P>0.05).

considered an important abiotic factor regulating soil CO_2 efflux (Fu et al., 2010).

According to Stanford et al. (1973), C mineralization increases in soils when incubation temperatures rise from 5 to 35°C. However, soil temperature and CO_2 emissions are not positively correlated under normal conditions for sugarcane cultivation in Brazil (Panosso et al., 2009). It is thought that soil temperatures in this environment remain near optimal levels for microbial activity without major fluctuations.

At 20 and 25°C, CO_2 emissions were higher with incorporated residue than with surface residue. However, at 30°C, there was no difference between management types. Incorporated residue produces greater emissions because it has greater contact area with microorganisms and reaches soil depths with higher microbial populations (Brady and Weil, 2008).

CO_2 emissions were 25.00% higher in treatments with N applications than in treatments without. Sugarcane residue is nitrogen deficient given that it contains 12.30% N and has a C/N ratio of 120g Kg^{-1} (Table 1). Microorganism development requires high levels of N for compounds such as enzymes and DNA. Therefore, applying N to the soil increases biological activity and consequently raises CO_2 emissions (Gifford et al., 2000). Management systems that add crop residue with high C/N ratios, such as sugarcane, must also add N to avoid N immobilization, which makes N unavailable for plants and soil microorganisms (Brady and Weil, 2008).

Total organic carbon (TOC) and humic substances (HS) in the soil

TOC levels varied erratically and thus it was not possible to identify positive interactions with management systems (Figure 2). This result is due to the low C/N ratio of sugarcane residue (Table 1) and the short observation period (79 days of incubation). There is a direct relationship between the C contribution to the soil and the addition rate of each type of organic residue. Deposition of vegetative material can significantly increase soil TOC over decades (Harrison et al., 1995).

C from humic substances (HS) represented 71.00% of the TOC concentration. More than 70.00% of TOC was in the form of more stable humic substances (Luo and Zhou, 2006; Stevenson, 1994).The humic substance with the highest average concentration was C-HU (7.0 g C kg^{-1}) followed by C-FA (1.63 g C kg^{-1}) and C-HA (1.36 g C kg^{-1}) (Figure 3). Other studies have also shown that in various classes of tropical soils with various types of management and usage, C-HU concentrations are higher than concentrations of other C-HS (Conteh and Blair, 1998). C-HU concentrations are higher because these substances are more insoluble (acid and base), more stable and more closely associated with the soil mineral fraction (Stevenson, 1994; Sparks, 2001). Additionally, the majority of TOC in sandy, low-fertility soils (Tables 1 and 3) is concentrated in the C-HU with greater C-HA and C-FA losses due to greater soil mobility (Andreux and Becerra, 1975).

Canellas et al. (2003) also found low C-HA concentrations in soils with surface management of sugarcane residue (raw cane). The predominance of C-FA over C-HA results from conditions that limit humification such as a low sum of bases and low Al^{3+} levels (Castillo and Wright, 2008).

C-HU did not vary by management type. However, there was a significant positive correlation between C-HU with soil TOC(r= 0.39) and C-HA (r= 0.35)(Table 3), C-

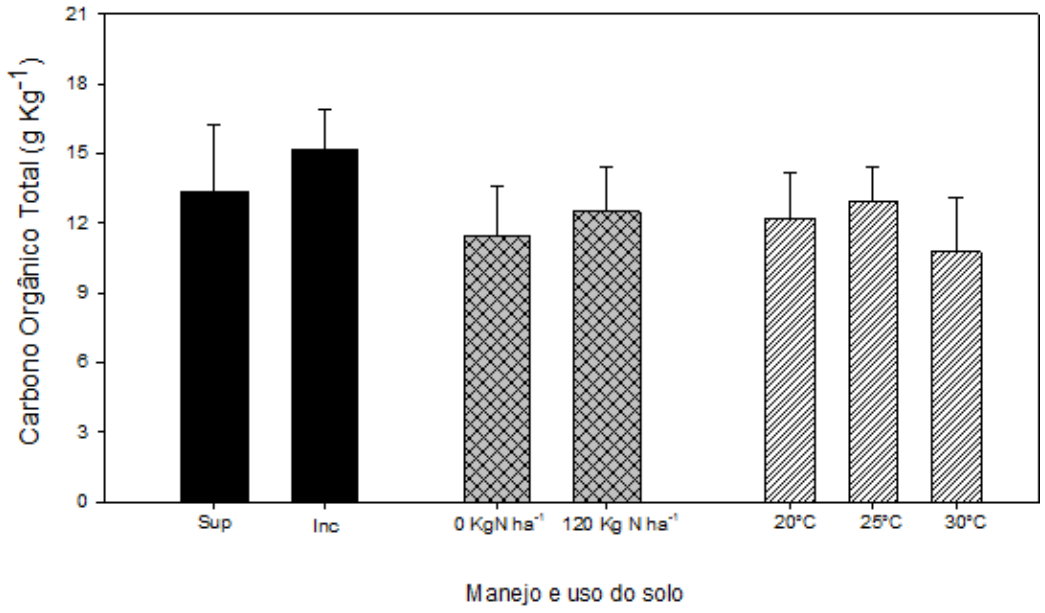

Figure 2. Total organic carbon in soils (gKg^{-1}) with surface (Sur) and incorporated (Inc) management of sugarcane residue and different nitrogen sources (0 and 120 Kg ha^{-1}), incubated for 79 days at three different temperatures (20, 25 and 30°C). Error bars represent the standard deviation from the mean for the averages (P>0.05).

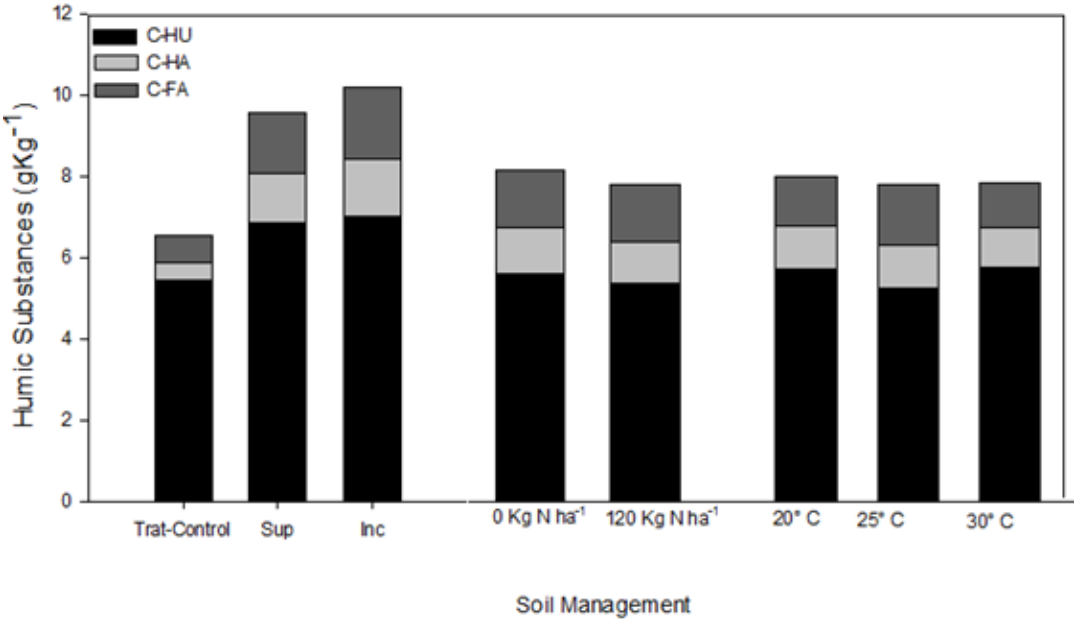

Figure 3. Carbon from humic substances (HS): humin(C-HU), fulvic acid (C-FA) and humic acid (C-HA) in the soil (g Kg^{-1}), with surface (Sur) and incorporated (Inc) sugarcane residue management, different nitrogen sources (0 and 120Kg N ha^{-1}) and Treatment control (Trat-Control) incubated for 79 days at three different temperatures (20, 25 and 30°C).

HU varying randomly and averaging 79.60% of soil TOC (Figure 3). Canellas et al. (2003) found the same positive correlation with C-HU concentrations ranging from 30 to 80% of soil TOC (Brady and Weil, 2008; Stevenson, 1994).

Higher levels of lignin in sugarcane residue form more

phenolic compounds during decomposition. This means that higher quantities of C remain in the soil, especially in the C-HU fraction, but over a longer time (Stevenson, 1994). Among the alkaline fractions (C-FA and C-HA), C-FA did not interact significantly with management type, but did vary randomly. However, C-HA was 6.15% greater with incorporated residue than with surface residue.

There was a positive correlation between the alkaline fractions (r= 0.37), negative interactions between the HA/FA ratio and initial (r= 0.38) and final respiration (r= 0.46) and a negative correlation between the HA/FA ratio and TOC (r= -0.50)(Table 3). This shows that HS plays an important role in the transfer of nutrients through ecological systems and the emission of CO_2 to the atmosphere. According to Fontaine et al. (2007), higher respiration is associated with reductions in the more stable fractions of SOM.These negative correlations probably result from the priming effect in which, according to Brady and Weil (2008), higher soil respiration with the addition of plant residue is stimulated by the breakdown of more resilient organic matter.

Conclusion

The CO_2 emission apex was present in the first 5 DAI and a subsequent decrease to acquire stability from 40 DAI. There was no correlation between the emissions of CO_2 to the C-Labile after 79 DAI but there was a negative correlation with HA/FA. The management with incorporated straw, nitrogen fertilization and increased of T°C contribute to higher CO_2 emissions. For TOC, C-HU, C-HA, there were no significant differences after 79 DAI and no correlation with the CO_2emission.

Conflict of Interests

The author(s) have not declared any conflict of interests.

ACKNOWLEDGEMENT

The authors acknowledge the Foundation for Research Support of the State of Minas Gerais (FAPEMIG), Coordination for the Improvement of Higher Education Personnel (CAPES), National Council for Scientific and Technological Development (CNPq) for support and encouragement to production.

REFERENCES

Adachi M, Bekku YS, Rashidah W, Okuda T, Koizumi H (2006). Differences in soil respiration between different tropical ecosystems.Appl. Soil Ecol. 34: 258-265.

Andreux F, Becerra SP (1975) Fraccionamiento y caracterizacióndelmaterialhúmicoenalgunossuelosde sabanadelaOrinoquia Colombiana. Turrialba 25(1):191-198.

Bilen S, Celik A, Altikat S (2010) Effects of strip and full-width tillage on soil carbon IV Oxide-carbon (CO2-C) fluxes and on bacterial and fungal populations in sunflower. Afr. J. Biotechnol. 9(38): 6312-6319.

Black CA (1965) Methods of Soil Analisys: Part 2 - Chemical and Microbiological Properties. Madison: American Society of Agronomy, 1159.

Brady NC, Weil RR (2008). The nature and properties of soils. 14th ed. New Jersey: Prentice Hall

Canellas LP, Velloso ACX,Marciano, CR, Ramalho JFGP, RumjanekVM, Rezende CE, Santos GA (2003) Propriedades químicas de um cambissolo cultivado com cana-de-açúcar, com preservação do palhiço e adição de vinhaça por longo tempo. Revista Brasileira de Ciência do Solo. 27(1):935-944.

Carter MR, Gregorich EG (Editors) (2007) Soil Sampling and Methods of Analysis. CRC Press, Inc. Boca Raton, FL, USA.

Castillo MS, Wright AL (2008) Soil phosphorus pools for Histosols under sugarcane and pasture in the Everglades, USA. Geoderma 14(1):130-135.

Cayuela ML, Sinicco T, Mondini C (2009) Mineralization dynamics and biochemical properties during initial decomposition of plant and animal residues in soil. Appl. Soil Ecol. 41(1):118-127.

Conteh A, Blair GJ (1998) The distribution and relative losses of soil organic carbon fractions in aggregate size fractions from cracking clay soils (vertisols) under cotton production. Aust. J. Soil Res. 36(1):257-271.

Embrapa- EmpresaBrasileira de PesquisaAgropecuária. (2014) SistemaBrasileiro de Classificação de Solos. 3° Edição. Rio de Janeiro/RJ, Brasil

Fan G, Li X, Cai Q., Zhu J. (2008) Detection of elevated CO2 responsive QTLs for yield and its components in rice.Afr. J. Biotechnol. 7(11): 1707-1711.

Fontaine S, Barot S, Barre P, Bdioui N, Mary B, Rumpel C (2007) Stability of organic carbon in deep soil layers controlled by fresh carbon supply. Nature 408(1): 277-280.

Fu W, Huang M, Shao M, Horton R (2010) Soil carbon dioxide (CO2) efflux of two shrubs inresponse to plant density in the northern Loess Plateau of China. Afr. J. Biotechnol. 9(41): 6916-6926.

Gifford RM, Barrett DJ, LutzeJL(2000) The effects of elevated [CO2] on the C:N and C:P mass ratios of plant tissues. Plant Soil 224 (1):1-14.

Gregorich EG, Rochette P., Van den Bygaart AJ, Angers DA (2005) Greenhouse gas contributions of agricultural soils and potential mitigation practices in Eastern Canada.Soil Tillage Res. 82(1):53-72.

Guillou CL, Angers DA, Leterme P, Menasseri-Aubry S (2011) Differential and successive effects of residue quality and soil mineral N on water-stable aggregation during crop residue decomposition. Soil Biol. Biochem. 43(1):1955-1960.

Harrison KG, Post WM, Richter DD (1995) Soil carbon turnover in a recovering termperate forest.Global Biogeochem. Cycles9(1):449-454

Herman WA, Mcgill WB, Dormaar JF (1977) Effects of initial chemical composition on decomposition of roots of three grass species.Can. J. Soil Sci. 57(1):205-215

Islam KR, Weil RR (1998) Microwave irradiation of soil for routine measurement of microbial biomass carbon. Biol. Fertil. Soils 27(1):408-416.

Johnson MS, Lehmann J, Riha SJ, Krusche AV, Richey JE, et al. (2008) CO2 efflux from Amazonian headwater streams represents a significant fate for deep soil respiration. Geophys. Res. Lett. 35:L17401.

Kilmer VJ, Alexander LT (1949). Methods of making mechanical analyses of soils.Soil Sci. 68(1): 15-24.

Liu Y, Wan KY, Tao Y, Li ZG, Zhang GS, LI SL, Chen F (2013) Carbon Dioxide Flux from Rice Paddy Soils in Central China: Effects of Intermittent Flooding and Draining Cycles. Plos one 8(2): 56562

Luo Y, Zhou X (2006) Soil Respiration and the Environment. Burlington, MA, 333p.

Mendonça ES, Matos ES (2005) Matéria orgânica do solo; métodos de análises. Viçosa, MG, Universidade Federal de Viçosa, 107p.

Mengel K, Schmeer H (1985), Effect of straw, cellulose and lignin on the turnover and availability of labelled ammonium nitrate. Biol. Fertil. Soils (1):175-181.

Mikan CJ, Schimel JP, Doyle AP (2002). Temperature controls of microbial respiration in arctic tundra soils above and below freezing. Soil Biol. Biochem. 34:1785-1795.
Moreira FMS, Siqueira JO (2006) Microbiologia e Bioquímica do Solo. 2.ed. Lavras: Ufla, 729p.
Panosso, AR, Larques Jr, Pereira J, La Scala Jr N (2009) Spatialand temporal variability os foil CO_2emission in a sugarcane área under Green andslash-and-burn managements. Soil Tillage Res. 105 (1):275-282.
Raij BV, Cantarella H (1997) Outras culturas industriais. In: RAIJ, B. Van.;Cantarella, H.; Quaggio, J.A.; Furlani, A.M.C. Recomendações de adubação e calagem para o estado de São Paulo. 2. ed. Campinas: InstitutoAgronômico, B-100 (1):233-239.
Rezende LA, AssisLC,Nahas E (2004) Carbon, nitrogen and phosphorus mineralization in two soils amended with distillery yeast.Bioresour. Technol. 94(1):159-167.
Silva JW, Guimarães EC, Tavares M (2003) Variabilidade temporal da precipitação mensal e anual na estação climatológica de Uberaba, MG. Ciência e Agrotecnologia 27(1):665-674.
Sommers LE, Nelson DW(1972). Determination of total phosphorus in soils: a rapid perchloric acid digestion procedure. Soil Sci. Soc. Am. J. 36(1):902-904
Sparks DL(2001) Elucidating the fundamental chemistry of soils: Past and recent achievements and future frontiers. Geoderma 100(1):303-319.
Stanford G, Frere MH, Shwaninger DH (1973) Temperature coefficient of soil nitrogen mineralization.Soil Sci. 115(1):321-323
Stevenson FJ (1994) Humus chemistry: genesis, composition, reactions. New York: J. Wiley.p. 496.
Swift RS (1996) Organic matter characterization. In: Sparks, D.L.; Page, A.L.; Helmke, P.A.; Loeppert, R.H.; Soltanpour, P.N.; Tabatabai, M.A.; Johnston, C.T.; Sumner, M.E. (Eds.) Methods of soil analysis: chimical methods. Vol. 3.Soil Science Society of America; American Society of Agronomy, Madison.(SSSA.Book Series, 5). pp.1011-1020.
Townsend AR, Vitousek PM, Holland EA (1992). Tropical soils could dominate the shortterm carbon cycle feedbacks to increased global temperatures. Clim. Change 22:293-303.
Urquiaga S, Bodey M, Oliveira OC, Lima E, Guimarães DHVA (1991) Importância de não queimar a palha na cultura de cana-de-açúcar. *Comunicado técnico da Empresa Nacional de Pesquisa Agropecuária* / EMBRAPA 5(1):1-6.
Vance ED, Brookes PC, Jenkinson DS (1987) Anextractionmethod for measuringsoil microbial biomass-C. Soil Biol. Biochem. 19(1):703-707
WuF, Jia Z, Wang S, Chang SX, Startsev A (2012) Contrasting effects of wheat straw and its biochar on greenhouse gas emissions and enzyme activities in a Chernozemic soil. Biol. Fertil. Soils 49(1):555-565.
Yeomans J, Bremner JM (1988) A rapid and precise method four routine determination of organic carbon in soil.Commun. Soil Sci. Plant Anal. 19(1):1467-1476.

academicJournals

Vol. 13(33), pp. 3385-3393, 13 August, 2014
DOI: 10.5897/AJB2014.13964
Article Number: 75D442346622
ISSN 1684-5315

http://www.academicjournals.org/AJB

African Journal of Biotechnology

Full Length Research Paper

Biodegradation of hydrocarbons exploiting spent substrate from *Pleurotus ostreatus* in agricultural soils

A. Mauricio-Gutiérrez[1], T. Jiménez-Salgado[2], A. Tapia-Hernández[2], J. Cavazos-Arroyo[1] and B. Pérez-Armendáriz[1*]

[1]Interdisciplinary Research and Consulting, Autonomus Popular University of State of Puebla, 21 Sur 1103, Barrio Santiago, C.P. 72410, Puebla, Puebla, Mexico.
[2]Research Center for Microbial Sciences, Laboratory of soil microbiology "Jesús Caballero Mellado". Autonomous University of Puebla, Edificio 103 J 2do. Piso, 14 Sur y Av. San Claudio, Ciudad Universitaria Apdo. postal 1622 C.P. 72570, Puebla, Puebla, Mexico.

Received 5 June, 2014; Accepted 21 July, 2014

In Acatzingo, Puebla, Mexico (east-central), oil spills have mainly affected agricultural fields. *Pleurotus ostreatus* is a white rot basidiomycete and produces extracellular enzymes (lacasses, manganese peroxidases, versatile peroxidases and veratryl alcohol oxidases). The production of edible mushrooms generates spent mushroom substrate that may have a biotechnological application. The aim of this study was to evaluate the mushroom substrate of *P. ostreatus* in a microcosm for the bioremediation of an agricultural soil contaminated with diesel. We evaluated the participation of microbial populations and specific enzymatic lacasses, manganese peroxidases, versatile peroxidases, veratryl alcohol oxidases activities of mushroom substrate in the biodegradation of a soil contaminated with 11030 ppm of diesel in four treatments: E1, E2, E3 and E4. All the experiments were performed in triplicate at 25 and 37°C for 28 days, with a soil:substrate ratio of 4:1. The treatments incubated at 37°C were quantified for diesel-tolerant bacteria, and treatments incubated at 25°C were quantified for diesel-tolerant fungi. Mushroom substrate participated in the biostimulation (91% organic material, 0.56% total nitrogen and 0.3% phosphorus) and bioaugmentation of the microorganisms of the mirocosm. Bacteria-tolerant populations increased significantly (p = 0.000) in all the treatments. Lacasses (8.62 U g^{-1}) activity was stimulated at 25°C and was the only one related to biodegradation; however, the highest biodegradation rate (72%) was at 37°C (bacterial biodegradation) being promising for future research.

Key words: Bioremediation, diesel, laccase, veratryl alcohol oxidase, *Pleurotus ostreatus*.

INTRODUCTION

Mexico is one of the world's important oil producers and the activity has had repercussions on the environment. In Acatzingo, Puebla (east-central Mexico) agricultural soil has been affected by hydrocarbon spills. The region's

*Corresponding author. E-mail: beatriz.perez@upaep.mx. Tel: +52-222-229-9400. Fax: +52-222-229-9400.

Abbreviations: Lac, Laccases; **MnP,** Manganese peroxidases; **VP,** versatile peroxidases; **VAO,** veratryl alcohol oxidases; **SMS,** spent mushroom substrate; **TPH**, total petroleum hydrocarbons; **PAHs,** polyaromatic hydrocarbons.

main economic activity is farming, producing mainly alfalfa, cabbage, lettuce, corn, nopal, green tomato, prickly pear and carrots.

However, agro-food production and safety has been affected by the dispersion and spillage of recalcitrant pollutants due to the pipelines crossing extensive zones of agricultural fields trans-porting diesel, gasoline, fuel oil and crude oil. The lack of maintenance facilities for the pipelines, fuel theft, vehicular transport and even topographic, orographic and hydrological conditions of the site, cause a high incidence of pollution on agricultural land. These hydrocarbon spills have affected the fertility and structure of agricultural soils, reducing crop yields, and altering biological systems, irrigation systems and the peasant economy in the region (Rivera-Pineda et al., 2012).

Petroleum hydrocarbons are comprised of alkanes (linear or branched), cycloalkanes, polycyclic aromatic hydrocarbons (PAHs) and the most complex heavy fraction such as asphaltenes (Polichtchouk and Yashchenko, 2006). Diesel is a complex mixture of linear (C_{10}-C_{28}), branched and cyclic alkanes and PAHs, which is obtained from the middle distillate during the separation of the petroleum and is recognized for causing health problems (Gallego et al., 2001; Bento et al., 2005) due to its content of benzo[a]anthracene, benzo[a]pyrene and dibenzo[a,h]anthracene which are considered highly toxic and reported as mutagenic and carcinogenic (Das and Chandran, 2011).

Among the different technologies available for the remediation of petroleum hydrocarbons, bioremediation uses living beings such as plants and microorganisms to restore or decontaminate soils, using the enzymatic capacity of bacteria and fungi to mineralize the complex hydrocarbon mixtures (Alexander, 1971).

Ligninolytic fungi like *Phanerochaete chrysosporium*, *Bjerkandera adusta* and *Pleurotus ostreatus*, possess the capacity to express enzymes which are incorporated into the environment to degrade compounds of complex molecular composition, and are known as extracellular. *P. ostreatus* is a white rot basidiomycete; it produces laccases (Lac), manganese peroxidases (MnP), versatile peroxidases (VP) and veratryl alcohol oxidases (VAO) (Bourbonnais and Paice, 1988; Palmieri et al., 2001; Wong, 2009). These enzymes are capable of degrading, and even partially mineralizing, recalcitrant pollutants (dyes, endocrine disruptors, PAHs, halogenated compounds, and various agrochemicals) (Gayosso-Canales et al., 2011).

The isolation of these enzymes in *in vitro* cultures for bioremediation purposes is costly and therefore limits their application. SMS is a source of mycelium and ligninolytic enzymes produced during the growth of the fungus; unused lignocellulosic substrate is inexpensive and readily available (Singh et al., 2011), and its reuse minimizes the adverse impact on the environment (Pardo-Giménez and Pardo-González, 2008). In addition, 62,374 ton of fresh edible mushrooms are produced in Mexico every year, and *P. ostreatus* represents 4.86% of domestic production (Martínez-Carrera et al., 2010). Crude extracts of SMS from white rot fungi have been used for the biodegradation of PAHs (Lau et al., 2003), bleaching of textile dyes (Singh et al., 2010; Singh et al., 2011), and immobilization of heavy metals (Garcia-Delgado et al., 2013), as well as the application of SMS in the biodegradation of PAHs in soil (Eggen, 1999).

In addition, the hydrocarbon degrading enzymes from SMS as well as laccase and manganese peroxidase have been evaluated to biodegrade total petroleum hydrocarbons (TPH) and PAHs. The SMS of mushroom *P. pulmonarius* were evaluated at a concentration of laccases of 1.7-2.0 U mg^{-1} and 880 U g^{-1} and a concentration of manganese peroxidases of 1.8-1.9 U mg^{-1} and 580 U g^{-1}; these enzymes could act directly and immediately to degrade 40% TPH (at 1.2 ±0.2 g kg^{-1} initial concentration) (Chiu et al., 2009), and completely biodegrade naphthalene, phenanthrene, benzo[α]pyrene and benzo[*g,h,i*]perylene (200 ppm of PAHs initial concentration) (Lau et al., 2003).

The aim of this investigation, then, was to evaluate the SMS of *P. ostreatus* under microcosm conditions for the bioremediation of an agricultural soil contaminated with diesel, through microbial characterization, bioaugmentation (microorganisms present in the SMS) and biostimulation (co-substrate of the lignocellulosic material of the SMS).

MATERIALS AND METHODS

Sampling

A non-contaminated soil sample was taken from the following geographic coordinates: 18° 57' 01" N 97° 43' 40" W in the municipality of Acatzingo, Puebla, Mexico. The spent *P. ostreatus* substrate samples were donated by local producers from the Puebla region.

Physicochemical and microbiological characterization in soil and spent mushroom substrate (SMS) of *P. ostreatus*

The physicochemical characterization of the agricultural soil and of *P. ostreatus* SMS was done according to Arshad and Coen (1992).

The microbiological characterization of the soil and substrate was performed using serial dilution and the plate count technique in culture media suitable for quantification of cultivable populations of bacteria, fungi, actinomycetes and diesel-tolerant bacteria (Taylor et al., 2002). The different microorganisms were quantified using differential culture media and different growth conditions, additionally were differentiated morphologically. The bacteria population was quantified by pour plate technique using 0.1 ml aliquots of appropriate dilution into nutrient agar (Bioxon Mexico) plates with pH 7 and incubated at 37°C for 24 h. The fungi populations were quantified by plating out the diluents on potato dextrose agar (Bioxon Mexico) added with streptomycin (0.05 g l^{-1}), pH 5.5 and were incubated at 25°C for five days. The actinomycetes were quantified using congo-red medium (Fisher-Scientific, Mexico), grown at 25°C for five days.

The determination of bacteria diesel-tolerant were grown in basal medium (g l^{-1}): NH_4NO_3, 1; K_2HPO_4, 1; KH_2PO_4, 1; $MgSO_47H_2O$, 0.409; $CaCl_2$, 0.02; $FeCl_3$, 0.00005, supplemented with 100 µl of sterile diesel and pH 7.0, incubated at 37°C for 24 h. The microorganisms were reported as Log cfu g^{-1} of dry soil.

Experiments in microcosms to evaluate the enzymatic activities of SMS of *P. ostreatus* in the biodegradation of diesel

An experimental design in microcosm was used to evaluate the participation in microbial populations and enzymatic activities (laccases, veratryl alcohol oxidases, manganese peroxidases, versatile peroxidases) present in the study system. The treatments in the design were: sterile contaminated soil and sterile SMS (E1); sterile contaminated soil and non-sterile SMS (E2); non-sterile contaminated soil and sterile SMS (E3); non-sterile contaminated soil and non-sterile SMS (E4). The soil and SMS were sterilized three times at 10 PSI for 2 h every other day. The soil used was spiked with 11030 ppm diesel and weathered for three months. For each treatment, 120 ml serological flasks were used, with 30 g of the soil-substrate mixture and adjusted to a C:N:P ratio of 100:10:1, the initial values of the organic matter and nitrogen from mixture were used for the adjustment, using sterile solutions of NH_4SO_4 1 N and K_2HPO_4 1 N. Humidity was maintained between 23.8 and 25.6% ± 5.23. The atmosphere of the flasks was changed every third day with an air flow (1.8 ml air/sec) through a sterile membrane (0.22 µm). The treatments were incubated for 28 days at 25 and 37°C. Diesel's biodegradation (%), the initial and final population of bacteria and fungi tolerant to diesel were determined for the treatments incubated at 25 and 37°C respectively. All the treatments were performed in triplicate. The % of biodegradation was determined according to the following equation:

The % of biodegradation = [(initial diesel concentration – final diesel concentration) / initial diesel concentration] * 100.

Microbiological analysis

The quantification of the initial and final population of diesel-tolerant bacteria and fungi was done by direct plate count. The determination of bacteria was done for the treatments incubated at 37°C grown in basal medium (g l^{-1}): NH_4NO_3, 1; K_2HPO_4, 1; KH_2PO_4, 1; $MgSO_47H_2O$, 0.409; $CaCl_2$, 0.02; $FeCl_3$, 0.00005; pH 7.0. The determination of fungi was done for the treatments incubated at 25°C using minimal medium with the following chemical composition (g l^{-1}): $(NH_4)_2SO_4$, 7; K_2HPO_4, 1; KH_2PO_4, 1; $MgSO_47H_2O$, 0.409; dextrose, 0.1; Sol. E 100x, 100 µl; rose bengal, 0.05; Streptomycin sulfate, 0.05; pH 5.5. diesel, previously sterilized by filtration, was used as carbon source, adding 100 µl over the Petri dish. The microorganisms were reported as Log cfu g^{-1} of dry soil.

Quantification of diesel

Initial and residual diesel was quantified based on the EPA method 8015 C (nonhalogenated organics by gas chromatography) using a gas chromatograph-mass spectrometry (GC-MS Mainframe, HP Model 6890 System-FID) with an HP-5 (30 m x 0.25 mm x 0.25 µm) capillary column, with the following parameters: the injector temperature was 250°C, column was set at an initial temperature of 50°C for one minute followed by a 14°C increment per minute to 275°C and the isothermal held for 8 min. Carrier gas (He) flow was 1.0 ml/min, and makeup N_2 gas was used with a total run time of 25 min.

Quantification of enzymes

An extract was prepared from the sample of the SMS of *P. ostreatus* and from the mixture soil: substrate (5 g) with 20 ml sodium acetate buffer (50 mM, pH 5.0), by shaking for 2 h at 80 rev/min and at 4°C, and then filtered through Whatman 1 paper. The extracts were stored at 4°C to determine the enzymatic activities (Isikhuemhen and Mikiashvilli, 2009).

Lac activity was determined by oxidation of 2,2'-azinobis, 3-ethylbenzothiazoline-6-sulphonic acid (ABTS) at 25°C and read at 420 nm (ε_{420}= 36000 $M^{-1}cm^{-1}$). MnP was determined by the formation of Mn^{3+}-malonate complex at 25°C in malonate buffer (sodium malonate) 50 mM (pH 4.5), with 1 mM $MnSO_4$ as substrate, and 0.1 mM H_2O_2; they were determined at an absorbance of 270 nm (ε_{270}= 11590 $M^{-1}cm^{-1}$). VP activity was monitored by the formation of Mn^{3+}-tartrate complex at 25°C and read at 238 nm (ε_{238}= 6500 $M^{-1}cm^{-1}$) during the oxidation of 0.1 mM Mn^{2+} ($MnSO_4$) in 0.1 M of the sodium tartrate buffer (pH 5), and 0.1 mM H_2O_2. For the determination of VAO, the reaction mixture contained 1 mM veratryl alcohol, 0.25 M sodium tartrate buffer pH 5.0, and was monitored at an absorbance of 310 nm for the formation of veratraldehyde (ε_{310}= 9300 M^{-1} cm^{-1}). Therefore, one unit of enzymatic activity is defined as the amount of enzyme activity that transforms 1 μmol min^{-1} of substrate; the enzymatic activities were reported with specific activities (U g $soil^{-1}$) (Bollag and Leonowicz, 1984; Bourbonnais and Paice, 1988; Palmieri et al., 2001; Gayosso-Canales et al., 2011).

Statistical analysis

A variance analysis (means test) was made to compare the different treatments and Tukey's multiple comparison test ($p \leq 0.05$) using the Minitab statistical package Versión 16.1.0 (licensed to the UPAEP).

RESULTS

Physicochemical characterization and microbiological analysis of non-contaminated soil and spent substrate (SMS) of *P. ostreatus*

The agricultural soil presented a sandy loam texture, moderately alkaline (pH= 8.01), with 2.04% organic material, 0.032% total nitrogen and 0.00256% phosphorus. In addition, the humidity percentage (17.35%) was low compared to the spent mushroom substrate (SMS) of *P. ostreatus* (76.77%). With regard to the characterization of SMS, it presented an acid pH (pH= 5.68) and a high content of organic material (91%), total nitrogen (0.56%) and phosphorus (0.3%) compared to agricultural soil.

Bacteria were the most abundant cultivable microorganisms in the non-contaminated soil and in the SMS (6.02 and 4.8 Log cfu g^{-1}, respectively); however, diesel-tolerant bacteria were reduced in these samples, being more populous in soil (5.05 Log cfu g^{-1}) than in SMS (4.71 Log cfu g^{-1}). The group of actinomycetes in soil was about 2.9 Log cfu g^{-1} and was absent in the SMS, but the group of fungi remained in the same order in these samples (3.45 to 3.68 Log cfu g^{-1}).

The SMS of *P. ostreatus* presented different ligninolytic

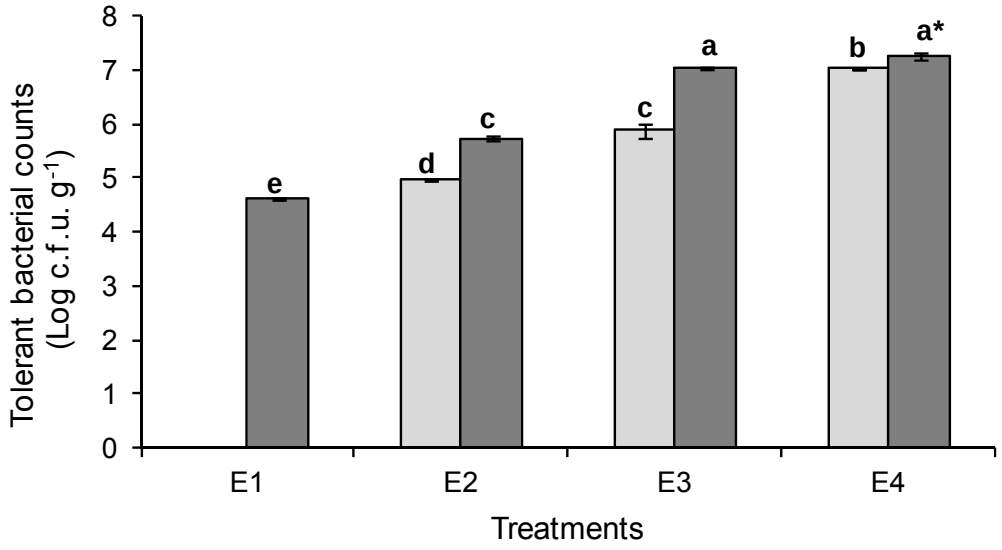

Figure 1. Population dynamics of tolerant diesel bacteria in microcosm using farm soil contaminated with diesel and SMS (4:1): treatments were E1, contaminated sterile soil and sterile substrate; E2, contaminated sterile soil and non sterile substrate; E3, contaminated non sterile soil and sterile substrate; E4, contaminated non sterile soil and non sterile substrate. Values were the mean of triplicate treatments incubated at 37°C at the beginning (light bars) and end (dark bars) of the experiment. *Different letters represent highly significant differences (p = 0.000) between treatments (Tukey's test).

enzymes such as Lac with a specific enzymatic activity of 263 U g^{-1}, VP (5.6 U g^{-1}) and VAO (9.5 U g^{-1}); MnP was not detected.

Evaluation in a microcosm of the enzymatic activities of SMS in the biodegradation of diesel in agricultural soil (11030 ppm)

In the microcosm, the tolerant bacteria increased significantly in all the treatments evaluated, the highest being E4 with 7.26 Log cfu g^{-1} (Figure 1). In contrast, the tolerant fungi populations presented a significant reduction (p = 0.000) according to system conditions and ranged from 2.82-5.22 Log cfu g^{-1} (Figure 2). However, biodegradation at 25°C was significantly lower (p = 0.000) than at 37°C, and E4 achieved the highest biodegradation of diesel (72%) (Table 1).

In the evaluation of extracellular enzymes in the microcosm, Lac activity was significantly stimulated (p = 0.000) in treatments E2, E3, and E4 with contaminated soil (11030 ppm diesel) at 25°C (0.92, 7.62 and 8.62 U g^{-1}, respectively) (Figure 3); no activity was detected in treatments at 37°C. VAO activity was also significantly stimulated (p = 0.000) at 25 and 37°C. The highest VAO activity was in treatment E4 at 25°C with 0.55 U g^{-1}, and at 37°C with 0.83 U g^{-1} (Figures 4 and 5). Manganese peroxidase and versatile peroxidase were undetectable in any treatment. In treatment E1 (sterile soil and sterile SMS) no enzymatic activity was detected, as shown in Figures 3, 4 and 5; but the tolerant bacterial and fungal population was stimulated at the end of the experiment with 4.63 and 2.82 Log cfu g^{-1} respectively (Figures 1 and 2).

DISCUSSION

The agricultural soil from Acatzingo, Puebla, Mexico presented a low nutritional content that is inadequate for farming activity according to Arshad and Coen (1992), and the SMS, being composed mainly of wheat straw, contains high doses of total nitrogen (0.56%) and organic material (91%); the physicochemical characteristics vary depending on the origin of the substrate and can contribute from 0.11 to 10.85% total nitrogen and 18.66 to 51.00% organic carbon for the development of the mushroom according to López-Rodrigez et al. (2008). The total nitrogen (0.56%), organic carbon (52.78%) and phosphorus (0.3%) content of the SMS of *P. ostreatus* was similar to that reported by García-Delgado et al. (2013) with 42% organic carbon and 0.7% total nitrogen.

The role of SMS, besides being a soil texturizer, is as co-substrate because of the incorporation of C, N and P, necessary for microbial metabolism whereby the treatment E3 increased native populations of tolerant diesel bacteria. In addition, the SMS of *P. ostreatus* bioaugmented the diesel-tolerant bacterial populations to 5.74 Log cfu g^{-1} in treatment E2 (Figure 1). Chiu et al. (2009) reported similar results during a bioremediation

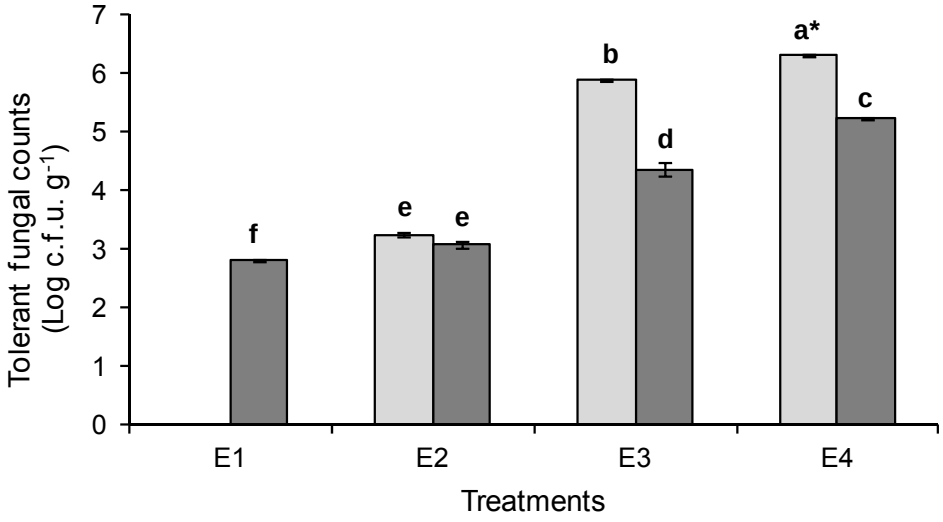

Figure 2. Population dynamics of tolerant diesel fungus in microcosm using farm soil contaminated with diesel and SMS (4:1), treatments were E1, contaminated sterile soil and sterile substrate; E2, contaminated sterile soil and non sterile substrate; E3, contaminated non sterile soil and sterile substrate; E4, contaminated non sterile soil and non sterile substrate. Values were the mean of triplicate treatments incubated at 25°C at the beginning (light bars) and end (dark bars) of the experiment. *Different letters represent highly significant differences (p = 0.000) between treatments (Tukey's test).

Table 1. Evaluation of diesel´s biodegradation in microcosm using farm soil contaminated and SMS (4:1).

Treatment	Temperature (°C)	Residual diesel (mg/kg)[1, 2]	± SD (mg/kg)	Diesel's biodegradation (%)	*F*-value
E1	25	10044[a]	30.3	8.9	3442.77
E1	37	9368.1[b]	56.2	15.1	
E2	25	7012.6[c]	66.6	36.4	
E2	37	4835.4[d]	49.9	56.2	
E3	25	4776.6[d]	40.2	56.7	
E3	37	3454.6[e]	79.6	68.7	
E4	25	3695.0[e]	37.6	66.5	
E4	37	3086.2[f]	117.5	72.0	

[1]Each value represents the average of triplicate with initial concentration of 11030 ppm diesel, treatments: E1, contaminated sterile soil and sterile substrate; E2, contaminated sterile soil and non sterile substrate; E3, contaminated non sterile soil and sterile substrate; E4, contaminated non sterile soil and non sterile substrate. [2]Different letters in the column indicate statistically significant differences according to the Tukey test (p = 0.000). SD, Standard deviation.

process when using SMS of *P. pulmonarius;* the substrates contributed macronutrients for the biostimulation of microbial populations giving, in addition, a bioaugmentation effect. Furthermore, Martens and Zadrazil (1998) suggest that organic substrates contribute nutrients that stimulate native microflora in the soil through products formed by the lysis of such substrates increasing degradation rates.

In this work, a reduction in the fungal population (Figure 2) was observed at the end of the experiment, associated with less biodegradation of diesel. Despite evidence of the biodegradation of contaminants by native fungi (Pérez-Armendáriz et al., 2010), the metabolic activity of native microorganisms is unpredictable; it can be affected by, among other things, the presence of the contaminant (Bento et al., 2005). However, the bacterial populations were significantly stimulated (p = 0.000) (Figure 1) and the highest biodegradation obtained (72%) (Table 1). Under the conditions studied in this work, the bacteria showed more ability to biodegrade diesel compared to fungi. It is possible that bacterial metabolism, the system of oxidation by monooxygenase and dioxygenase enzymes is more efficient than that of fungal enzymes (Das and Chandran, 2011). The biodegradation of diesel in treatment E1 (Table 1) was due to the loss and chemical degradation of diesel, and to the microorganisms

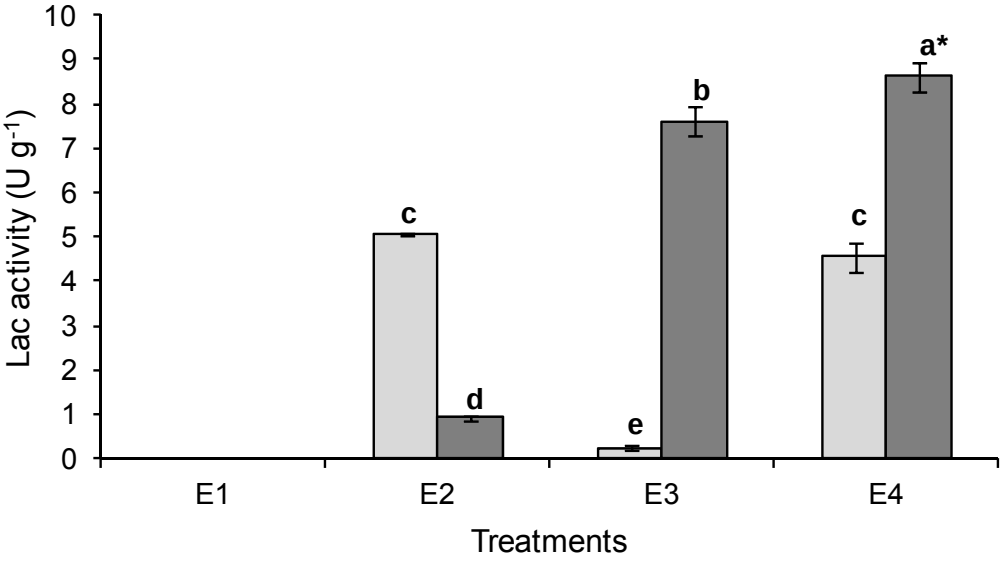

Figure 3. Laccase activity in microcosm using farm soil contaminated with diesel and SMS (4:1). Treatments correspond E1, contaminated sterile soil and sterile substrate; E2, contaminated sterile soil and non sterile substrate; E3, contaminated non sterile soil and sterile substrate; E4, contaminated non sterile soil and non sterile substrate. Values were the mean of triplicate treatments incubated at 25°C at the beginning (light bars) and end (dark bars) of the experiment. *Different letters represent highly significant differences (p = 0.000) between treatments (Tukey's test).

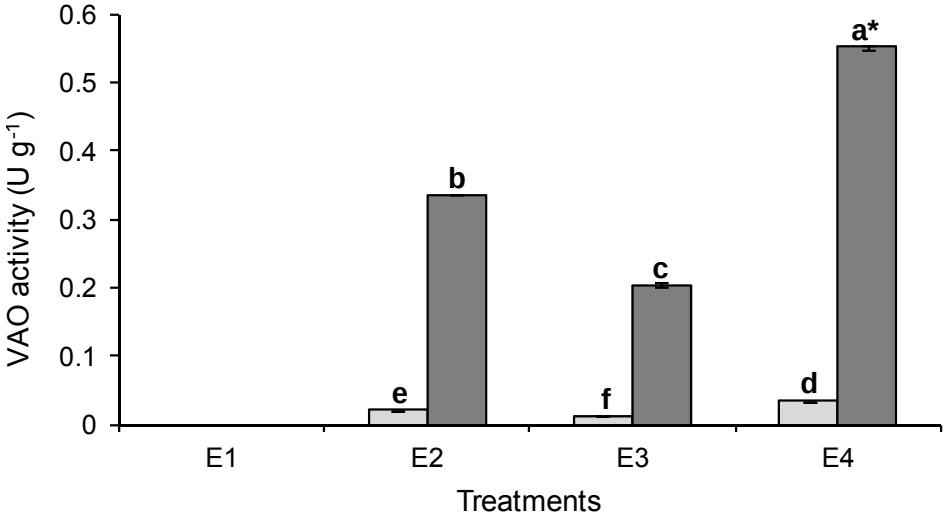

Figure 4. Veratryl alcohol oxidase activity in microcosm using farm soil contaminated with diesel. Treatments correspond E1, contaminated sterile soil and sterile substrate; E2, contaminated sterile soil and non sterile substrate; E3, contaminated non sterile soil and sterile substrate; E4, contaminated non sterile soil and non sterile substrate. Values were the mean of triplicate treatments incubated at 25°C at the beginning (light bars) and end (dark bars) of the experiment. *Different letters represent highly significant differences (p = 0.000) between treatments (Tukey´s test).

that withstood the soil sterilization process (Figures 1 and 2). With the results obtained, the SMS of *P. ostreatus* enabled high (72%) percentages of diesel biodegradation (11030 ppm initial concentration) at 37°C for 28 days (Table 1) which is promising for an escalation and subsequent physiological studies, since the application

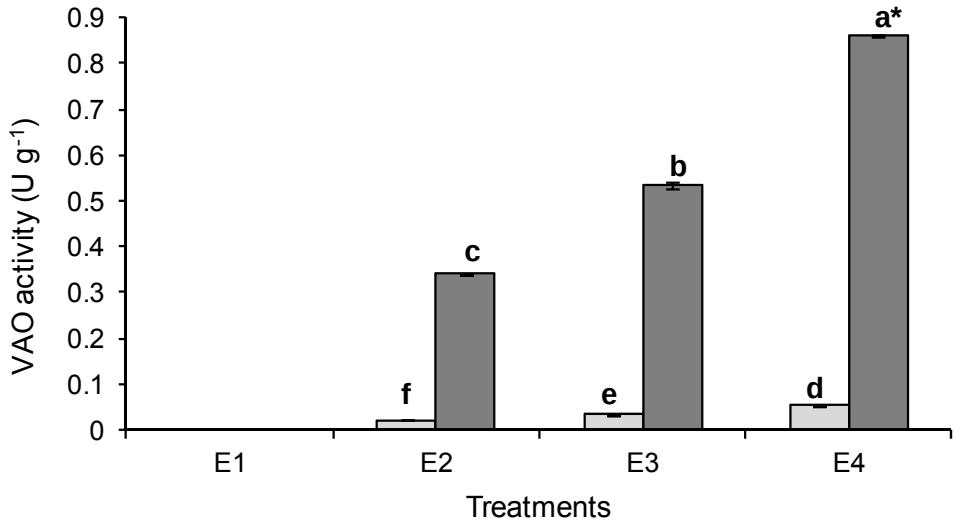

Figure 5. Veratryl alcohol oxidase activity in microcosm using farm soil contaminated with diesel. Treatments correspond E1, contaminated sterile soil and sterile substrate; E2, contaminated sterile soil and non sterile substrate; E3, contaminated non sterile soil and sterile substrate; E4, contaminated non sterile soil and non sterile substrate. Values were the mean of triplicate treatments incubated at 37°C at the beginning (light bars) and end (dark bars) of the experiment. *Different letters represent highly significant differences (p = 0.000) between treatments (Tukey's test).

of other SMS (*P. pulmonarius*) (3%) achieve the biodegradation of 40-45% of TPH (1200 ppm initial concentration) for 22 days in *ex situ* treatments (Chiu et al., 2009).

In addition, the SMS of *P. ostratus* was a source of ligninolytic enzymes (263 U g^{-1} Lac, 5.6 U g^{-1} VP and 9.5 U g^{-1} VAO) for the biodegradation of diesel in the microcosm. Singh et al. (2003) reported 7.59 U g^{-1} Lac in SMS of *P. sajor-caju*. Furthermore, Lau et al. (2003) reported Lac activities of 880 ± 40 U g^{-1} and of MnP 580 ± 20 U g^{-1} in SMS of *P. pulmonarius* to be higher than our results, and when applied (5% of SMS) to a contaminated soil (200 ppm of PAHs), presented a biodegradation of 100% after two days under constant agitation (at 80°C). Law et al. (2003) reported 89% biodegradation of pentachlorophenol (100 mg l^{-1} initial concentration) in water system by the SMS of *P. pulmonarius* (5%) after two days of incubation at 250 rev/min in darkness at room temperature. Also, enzymatic extracts from SMS of *A. bisporus* (0.43 ± 0.02 U ml^{-1} Lac) have been used *in vitro* to evaluate the biodegradation of PAHs in the presence of heavy metals (Cd or Pb), which affected degradation with a reduction in Lac activity (García-Delgado et al., 2013). In our study, the application of the SMS of *P. ostreatus* to a contaminated agricultural soil (11030 ppm diesel) contributed extracellular enzymes like Lac (0.92 U g^{-1}) and VAO (0.34 U g^{-1}) in the microcosm (Figures 3, 4 and 5) which suggests that they are part of the bioremediation process.

Lignocellulosic residues also have the role of cosubstrate since they stimulate microbial activity in general (Eggen, 1999); in our study, it was observed that the SMS increased the Lac production 30.85 times and the VAO production 15.83 times (Figures 3 and 5). The highest Lac activity (8.62 U g^{-1}) was at 25°C (E4) with a high diesel biodegradation of 66.5% (Table 1) suggesting Laccase stimulation due to the presence of the contaminant; similar results were reported by Eggen (1999) for a soil contaminated with creosote, showing the Lac activity of 0.57 U g^{-1}. Other studies conducted with different enzymatic extracts of SMS of different basidiomycetes (*Agaricus bisporus*, *P. eryngii, P. ostreatus* and *Coprinus comatus*) have presented the same effect (Li et al., 2010). In addition, in *in vitro* cultures of strains of *P. eryngii, P. ostreatus, P. pulmonarius* and *P. sajor-cajur,* Lac and VP activities were related to biodegradation (Rodríguez et al., 2004).

The stimulation of Lac expression in soils contaminated with recalcitrant substances for *P. ostreatus* has been widely reported; Gayosso-Canales et al. (2011) showed that this basidiomycete was producing 19.1 U mg of Lac $protein^{-1}$ when polychlorinated biphenyls were present in soil.

An interesting result in this work was the concentration of VAO at 37°C (0.83 U g^{-1}), also found in contaminated soils at 25°C (0.55 U g^{-1}) (Figures 4 and 5). These results suggest that the expression of VAO enzyme can be by both bacteria and fungi, due to the presence of intermediary compounds like veratrylic alcohol, resulting from the biodegradation of lignocellulosic substrates and

hydrocarbons. VAO is an enzyme that oxidizes two O_2 electrons to H_2O_2 for the formation of a free radical followed by the loss of a proton, in lignin biodegradation with characteristics similar to the majority of peroxidases but with the ability to biodegrade aromatic alcohol compounds such as veratrylic alcohol (Bourbonnais and Paice, 1988).

The presence of VAO has been reported *in vitro* in fungi such as *P. sajor-caju*, *P. ostreatus*, *P. cornucopiae*, *P. eryngii*, *P. floridanus*, and *P. pulmonarius* (Bourbonnais and Paice, 1988; Gutiérrez et al., 1994; Marzullo et al., 1995), and in the unicellular bacteria *Comamonas* sp*.,* VAO has been purified with the ability to decolorize textile dyes (Jadhav et al., 2009; Chen et al., 2012).

In conclusion, this study investigates different factors associated with the use of spent substrate of *Pleurotus ostreatus* in the bioremediation of an agricultural soil contaminated with diesel. The best treatment was obtained with the non-sterile mixture at 11030 ppm diesel with 72% biodegradation, evaluated after 28 days of incubation at 37°C. Therefore, the SMS of *P. ostreatus* contributed extracellular enzymes such as Lac (0.92 U g^{-1}) and VAO (0.34 U g^{-1}) in the microcosm system used. The SMS also functioned as a biostimulant agent by contributing the residues of ligninolytic origin increasing the production of Lac (30.85 times) and VAO (15.83 times) and as biostimulant by increasing the number of cfu of microorganisms in the bioremediation system.

Conflict of Interests

The author(s) have not declared any conflict of interest.

REFERENCES

Alexander M (1971). Interspecific relationship. In: Microbial Ecology (Alexander, M., Ed.). John Wiley and Sons. Press, New York.

Arshad MA, Coen GM (1992). Characterization of soil quality: Physical and chemical criteria. Am. J. Alternative Agr. 7(1-2):25-31.

Bento FM, Camargo FAO, Okeke BC, Frankenberger WT (2005). Comparative bioremediation of soils contaminated with diesel oil by natural attenuation, biostimulation and bioaugmentation. Bioresour. Technol. 96(9):1049-1055.

Bollag J, Leonowicz A (1984). Comparative studies of extracelular fungal laccases. Appl. Environ. Microbiol. 48(4):849-854.

Bourbonnais R, Paice GM (1988). Veratryl alcohol oxidases from the lignin-degrading basidiomycete *Pleurotus sajor-caju*. Biochem. J. 255(2):445-450.

Chen YH, Chai LY, Zhu YH, Yang ZH, Zheng Y, Zhang H (2012). Biodegradation of kraft lignin by a bacterial strain *Comamonas sp.* B-9 isolated from eroded bamboo slips. J. Appl. Microbiol. 112(5):900-906.

Chiu S-W, Gao T, Chan CS, Ho CK (2009). Removal of spilled petroleum in industrial soils by spent compost of mushroom *Pleurotus pulmonarius*. Chemosphere 75(6):837-842.

Das N, Chandran P (2011). Microbial degradation of petroleum hydrocarbon contaminants: an overview. Biotechnol Res Int. 2011:1-13.

Eggen T (1999). Application of fungal substrate from commercial mushroom production –*Pleurotus ostreatus*- for bioremediation of creosote contaminated soil. Int. Biodeter. Biodegr. 44(2):117-126.

Gallego JLR, Loredo J, Llamas JF, Vázquez F, Sánchez J (2001). Bioremedation of diesel-contaminated soils: Evaluation of potential *in situ* techniques by study of bacterial degradation. Biodegradation 12(5):325-335.

García-Delgado C, Jiménez-Ayuso N, Frutos I, Gárate A, Eymar E (2013). Cadmium and lead bioavailability and their effects on polycyclic aromatic hydrocarbons biodegradation by spent mushroom substrate. Environ. Sci. Pollut. Res. 20(12):8690-8699.

Gayosso-Canales M, Esparza-García FJ, Bermúdez-Cruz RM, Tomasini A, Ruíz-Aguilar GM, Rodríguez-Vázquez R (2011). Application of 2III7-3 fractional factorial experimental design to enhance enzymatic activities of *Pleurotus ostreatus* with high concentrations of polychlorinated biphenyls. J. Environ. Sci. Health A 46(3):298-305.

Gutiérrez A, Caramelo L, Prieto A, Martínez MJ, Martínez AT (1994). Anisaldehyde Production and Ary-Alcohol Oxidase and Dehydrogenase Activities in Ligninolytic Fungi of the Genus *Pleurotus*. Appl. Environ. Microbiol. 60(6):1783-1788.

Isikhuemhen OS, Mikiashvilli NA (2009). Lignocellulolytic enzyme activity, substrate utilization, and mushroom yield by *Pleurotus ostreatus* cultivated on substrate containing anaerobic digester solids. J. Ind. Microbiol. Biotechnol. 36(1): 1353-1362.

Jadhav UU, Dawkar VV, Tamboli DP, Govindwar SP (2009). Purification and characterization of veratryl alcohol oxidase from *Comamonas sp.* UVS and its role in decolorization of textile dyes. Biotechnol. Bioproc. Eng. 14(3):369-376.

Lau KL, Tsang YY, Chiu SW (2003). Use of spent mushroom compost to bioremediate PHA-contaminated samples. Chemosphere 52(9): 1539-1546.

Law WM, Lau WN, Lo KL, Wai LM, Chiu SW (2003). Removal of biocide pentchlorophenol in water system by the spent mushroom compost of *Pleurotus pulmonarius*. Chemosphere 52(9): 1531-1537.

Li X, Lin X, Zhang J, Wu Y, Yin R, Feng Y, Wang Y (2010). Degradation of polycyclic aromactic hydrocarbons by crude extracts from spent mushroom substrate and its possible mechanisms. Curr. Microbiol. 60(5):336-342.

López-Rodríguez C, Hernández-Corredor R, Suárez-Franco C, Borrero M (2008). Evaluación del crecimiento y producción de *Pleurotus ostreatus* sobre diferentes residuos agroindustriales del departamento de Cundinamarca. Universitas Scientiarum 13(2): 128-137.

Martens R, Zadrazil F (1998). Screening of white-rot fungi for their ability to mineralize polycyclic aromatic hydrocarbons in soil. Folia Microbiol. 43(1):97-103.

Martínez-Carrera D, Curvertto N, Sobal M, Morales P, Mora V (2010). Hacia un desarrollo sostenible del sistema de producción-consumo de los hongos comestibles y medicinales en Latinoamérica: Avances y perspectivas en el siglo XXI. Red Latinoamericana de Hongos Comestibles y Medicinales. COLPOS-UNS-CONACYT-AMC-UAEM-UPAEP-IMINAP, Mexico.

Marzullo L, Cannio R, Giardina P, Santini MT (1995). Veratryl alcohol oxidase from *Pleurotus ostreatus* participates in lignin biodegradation and prevents polymerization of laccase-oxidized substrates. J. Biol. Chem. 270(8):3823-3827.

Palmieri G, Bianco C, Cennamo G, Giardina P, Marino G, Monti M, Sannia G (2001). Purification, characterization, and functional role of a novel extracellular protease from *Pleurotus ostreatus*. Appl. Environ. Microbiol. 67(6):2754-2759.

Pardo-Giménez A, Pardo-González JE (2008). Evaluation of casing materials made from spent mushroom substrate and coconut fibre pith for use in production of *Agaricus bisporus* (Lange) Imbach. Span J. Agric. Res. 6(4):683-690.

Pérez-Armendáriz B, Martínez-Carrera D, Calixto-Mosqueda M, Alba J, Rodríguez-Vázquez R (2010). Filamentous fungi remove weathered hydrocarbons from polluted soil of tropical Mexico. Rev. Int. Contam. Ambie. 26(3):193-199.

Polichtchouk YM, Yashchenko IG (2006). Possible correlations between crude oil chemical composition and reservoir age. J. Petrol. Geol. 29(2):189-194.

Rivera-Pineda F, Ramírez-Valverde B, Juárez-Sánchez JP, Pérez-Armendáriz B, Estrella-Chulim N, Escobedo-Castillo F, Ramírez-Valverde G (2012). Implicaciones en la agricultura por el derrame de

hidrocarburo en Acatzingo, México. In: Martínez RR, Ramírez VB, Rojo MGE (eds.) Recursos naturales y contaminación ambiental, 1st edn. UAIM-ANCA. Mexico. pp. 203-218.

Rodríguez E, Nuero O, Guillén F, Martínez AT, Martínez MJ (2004). Degradation of phenolic and non-phenolic aromatic pollutants by four *Pleurotus* species: the role of laccase and versatile peroxidase. Soil Biol. Biochem. 36(6):909-916.

Singh AD, Abdullah N, Vikineswary S (2003). Optimization of extraction of bulk enzymes from spent mushroom compost. J. Chem. Tech. Biotechnol. 78(7):743-752.

Singh AD, Sabaratnam V, Abdullah N, Annuar MSM, Ramachandran KB (2010). Decolourisation of chemically different dyes by enzymes from spent compost of *Pleurotus sajor-caju* and their kinetics. Afr. J. Biotechnol. 9(1):41-54.

Singh AD, Sabaratnam V, Abdullah N, Sekaran M (2011). Enzymes from spent mushroom substrate of *Pleurotus sajor-caju* for the decolourisation and detoxification of textile dyes. World J. Microbiol. Biotechnol. 27(3): 535-545.

Taylor JP, Wilson B, Mills MS, Burns RG (2002). Comparison of microbial numbers and enzymatic activities in surface soils and subsoils using various techniques. Soil Biol. Biochem. 34(3):387-401.

Wong DWS (2009). Structure and action mechanism of ligninolytic enzymes. Appl. Biochem. Biotechnol. 157(2):174-209.

academicJournals

Vol. 13(33), pp. 3394-3401, 13 August, 2014
DOI: 10.5897/AJB2014.13843
Article Number: 6BEFAD946623
ISSN 1684-5315

http://www.academicjournals.org/AJB

African Journal of Biotechnology

Full Length Research Paper

Production and characterization of biosurfactant from *Pseudomonas aeruginosa* PBSC1 isolated from mangrove ecosystem

Anna Joice, P.[1]* and Parthasarathi, R.[2]

[1]Division of Microbiology, Faculty of Science, Annamalai University, Annamalai Nagar-608 002, Chidambaram, Tamil Nadu 608002, India.
[2]Department of Microbiology, Faculty of Agriculture, Annamalai University, Annamalai Nagar-608 002, Chidambaram, Tamil Nadu 608002, India.

Received 9 April, 2014; Accepted 4 August, 2014

In this present study, biosurfactant-producing microorganisms *Pseudomonas aeruginosa* PBSC1, was isolated from mangrove ecosystem in Pichavaram (Boat house), Tamil Nadu, India. The biosurfactant production was done using a minimal salt medium (MSM) with crude oil as the hydrocarbon. The microbial growths were investigated, and the best cultivation times for the biosurfactant production by *P. aeruginosa* PBSC1 was found to be 144 h. The biosurfactant was extracted and characterized. The critical micelle concentrations (CMCs) of extracted biosurfactant was found to be 78 mg l^{-1}. Stability studies were done at various pH, temperature and NaCl concentrations. The emulsification activity was stable at lower and higher pH and temperature respectively. NaCl concentration does not affect the emulsification activity of the biosurfactant. The emulsion formed by the biosurfactant against each hydrocarbon was stable for one month. Further characterization of biosurfactant using Fourier transform infrared spectroscopy (FTIR) revealed it as a rhamnolipid.

Key words: Mangrove ecosystems, *Pseudomonas aeruginosa*, biosurfactant, critical micelle concentration (CMC), FT-IR fourier transform infrared spectroscopy (FTIR).

INTRODUCTION

Microbial biosurfactants are extracellular compounds produced by microbes such as bacteria, fungi and actinomycetes when grown in culture medium containing hydrophobic/hydrophilic substrates. Biosurfactants are surface active molecules having hydrophilic and hydrophobic moieties as their constituents which allow them to interact at interfaces and reduce the surface tension. They are classified based on their chemical composition into many groups such as fatty acids, glycolipids, glycolipopeptides, glycoproteins, lipopeptides, phospholipids, polymeric and particulate biosurfactants (Desai and Banat, 1997).

The biosurfactants properties includes excellent detergency, emulsification, foaming, dispersing traits,

*Corresponding author. E-mail: hannahjoice@gmail.com. Tel: +91- 9952520289.

wetting, penetrating, thickening, microbial growth enhancement, metal sequestering and resource recovering (oil) which make surfactants replace some of the most versatile process chemicals (Rosenberg, 1986). They are promising natural surfactants that offer several advantages over chemically synthesized surfactants, such as lower toxicity, biodegradability and ecological acceptability. Although biosurfactants exhibit such important advantages, they have not been yet employed extensively in industry because of relatively high production cost. One possible strategy for reducing cost is the utilization of alternative substrates such as agro industrial wastes (Mercade and Manresa, 1994). The establishment of waste-based medium for biosurfactant production also faces another problem; that is, the kind and the properties of final product depend on the composition of culture media (Besson and Michel, 1992).

Mangrove ecosystem is a bridge between terrestrial and marine ecosystem and harbours unique microbial diversity. Mangroves are present in the coastal areas of tropical countries and supports abundant life through a food chain that starts with the trees and the micro-biota (Smith et al., 1991). Although mangrove ecosystem is rich in organic matter, by and large they are nutrient-deficient especially in nitrogen and phosphorus. Diversity of microbial communities inhabiting this unique swampy, saline, partially anaerobic environment is useful as it provides clue of the microorganism and their adaptability in such habitats (Semenov et al., 1999). The biosurfactant producing organisms are isolated from the mangrove ecosystems.

In this present study, biosurfactant-producing micro-organism *P. aeruginosa* PBSC1 was isolated from mangrove ecosystems. The production of biosurfactant was carried out using the MSM. The cell free culture broth was extracted for the biosurfactant and quantified. To confirm the type of biosurfactant, the characterization study was conducted.

MATERIALS AND METHODS

Isolation, screening and identification of the microorganism

The mangrove soil samples were collected from various places of Cuddalore district of Tamil Nadu, India. The places are Pichavaram (boat house), South Pichavaram, Kodiyampalayam, Muzhukuthurai and Artificial Mangrove forest. From these five places, a total of 21 soil samples were collected from sediments and rhizosphere of the mangrove plant. One hundred gram of freshly collected soil samples was taken in a 250 ml Erlenmeyer flask. It was added to 10 ml of crude oil (to selectly enrich the biosurfactant producers) and thoroughly mixed and kept for incubation at room temperature (28 ± 2°C) for 30 days. The samples were moistened with water to avoid desiccation when necessary. The screening of bacterial isolates was done using hemolytic assay (Mulligan et al., 1984), drop collapse assay (Jain et al., 1991; Bodour and Miller-Maier, 1998), oil speading test (Morikawa et al., 2000), and emulsification (Cooper and Goldenberg, 1987). Best biosurfactant producing strain was identified and used for the production and characterization.

Identification of bacterial isolates

The isolated bacterial strains were identified using standard biochemical and sugar fermentation test. The species level identification was done using 16S rRNA sequencing.

16S rRNA sequencing

It is important to use a pure cultivated bacterium for identification. The purification of PCR products were done by removing unincorporated PCR primers and dNTPs from PCR products by using Montage PCR Clean up kit (Millipore). The sequencing was carried out by purifying the PCR products of approximately 1,400 bp and was sequenced using 2 primers. Sequencing products were resolved on an Applied Biosystems model 3730XL automated DNA sequencing system (Applied BioSystems, USA).

The partial sequencing of the 16S rRNA gene was commercially carried out at the Yazhl Xenomics, Chennai, using universal amplification and sequencing primers and Sequencing reactions were performed in a MJ Research PTC-225 Peltier Thermal Cycler using a ABI PRISM® BigDyeTM Terminator Cycle Sequencing Kits with AmpliTaq® DNA polymerase (FS enzyme) (Applied Biosystems), following the protocols provided by the manufacturer.

Phylogenetic analysis

The partial sequencing was analyzed and compared with nucleotide sequence databases in the National Center for Biotechnology Information (NCBI) website using basic local alignment search tool (BLAST) program (http://www. ncbi.nlm.nih.gov/BLAST), in order to confer percentage sequence similarities. The evolutionary history of SOL-10 strain was inferred using the Neighbor-Joining (NJ) method. The evolutionary distances were computed using the maximum composite likelihood (MCL) method. Phylogenetic analyses were conducted in Molecular Evolutionary Genetics Analysis (MEGA) software (Version 4.0).

Growth and biosurfactant production

Bacteria were grown in Minimal Salt Medium (g L^{-1}) containing 1.0 K_2HPO_4, 0.2 $MgSO_4.7H_2O$, 0.05 $FeSO_4.7H_2O$, 0.1 $CaCl_2.2H_2O$, 0.001 $Na_2MoO_4.2H_2O$, and 30 NaCl was added with crude oil (1.0%, w/v). Flasks containing sterilized MSM were inoculated with a loopful of bacteria and flasks were maintained in an Orbital shaker for seven days at 120 rpm, 30°C. After seven days of incubation, culture broth from each flask was centrifuged at 6000 rpm, 4°C for 15 min and the supernatant was filtered through 0.45 µm pore size filter paper (Millipore, India). This cell free culture broth was used for drop collapse assay, oil spreading assay, emulsification assay and surface tension measurement. All the screening experiments were performed in triplicates (until otherwise mentioned) and the mean values were recorded.

Biosurfactant extraction and characterization

The MSM broth with the culture inoculums was centrifuged at 10,000 × *g* for 30 min to discard the cells and extracted twice with chloroform and methanol (2:1 v/v). The solvents were removed by rotary evaporation and the residue was partially purified in silica gel (60-120 mesh) column eluted with chloroform and methanol ranging from 20:1 to 2:1 (v/v) in a gradient manner. The fractions were pooled and solvents were evaporated; resulting residue was dialyzed against distilled water and lyophilized. The crude biosurfactant was expressed in g L^{-1} (Thavasi et al., 2011).

The critical micelle dilution (CMD) is defined as the solubility of a surfactant in an aqueous phase and is commonly used to measure the efficiency of a surfactant (Desai and Banat, 1997). The extracted biosurfactant was dissolved in distilled water at concentrations ranging from 1.0 to 200 mg L^{-1} for calculation of critical micelle concentration (CMC). This is a direct measurement of surfactant concentration corresponding to the concentration of an amphiphilic component at which the formation of micelles is initiated in the solution (Abouseoud et al., 2008). The CMC of the produced biosurfactant was determined following standard methods (Kim et al., 1997; Bonilla et al., 2005). CMD^{-1} and CMD^{-2} were determined by measuring the surface tensions of cell free supernatant diluted 10-times and 100-times in distilled water (Kosaric, 1993).

Carbohydrate moieties in the biosurfactant molecule were assayed using rhamnose (Dubois et al., 1956) and Molisch's test. The rhamnose test was performed by adding 0.5 mL cell supernatant to 0.5 ml 5% phenol solution and 2.5 ml sulfuric acid and incubating the sample for 15 min before measuring absorbance at 490 nm. Molisch's test was performed by adding 3 mL cell free supernatant to 1 mL 10% α-naphthol. This was followed by the addition of 1 mL concentrated sulfuric acid to the sample without disturbing it.

The crude biosurfactant extracted with chloroform: methanol was analyzed by thin layer chromatography (TLC). The TLC tank was filled with a solvent mixture of chloroform:methanol:acetic acid:water (25:15:4:2 v/v/v/v). The chromatogram was sprayed with α-naphthol and sulfuric acid.

Activity characterization

Foam was produced by hand shaking a two-day-old culture supernatant for a few minutes. The stability of the foam was monitored by observing it for 48 h. To determine the thermal stability of the biosurfactant, cell-free broth of the isolate was maintained at a constant temperature range of 20-100°C for 15 min, followed by cooling at room temperature (28 ± 2°C). The effect of pH and salinity on stability of the biosurfactant was evaluated by altering the pH (2-12) and the concentration of NaCl (0-1%, 5%) of the cell free culture supernatant and measuring the surface tension and Emulsification index (E_{24}, %) (Rashmi et al., 2012).

Emulsification

Cell free culture broth was used as the biosurfactant source to check the emulsification of crude oil. 1 ml of cell free culture broth was added to 5 ml of 50 mM Tris buffer (pH 8.0) in a 30 ml screw-capped test tube. Five milligram of hydrocarbon was added to the above solution and vortex-shaken for 1 min and the emulsion mixture was allowed to stand for 20 min. A negative control was maintained only with buffer solution and crude oil and Triton X-100 was used as the positive control. Various hydrocarbons like xylene, crude oil, benzene, kerosene, coconut oil, heptanes, n-hexadecane, diesel and petrol were used to check the emulsification activity of the isolate.

$$E_{24}\ (\%) = \frac{The\ heig\,ht\ of\ emulsion\ \ layer}{The\ heig\,ht\ of\ total\ \ solution} \times 100$$

FTIR

The FT-IR spectra was recorded in a Thermo Niocolet, AVATAR 330 FT-IR system, Madison WI 53711-4495, in the spectral region of 4000-400 cm^{-1} using potassium bromide (KBr) pellets. The air dried biosurfactant sample was ground with a purified potassium bromide salt to remove scattering effects from large crystals. This powdered mixture is then pressed in a mechanical press to form a translucent pellet through which the beam from spectrometer passed.

Statistical analysis

All the results related to determination of emulsification activity, biosurfactants quantity and CFU counts were the average of three replicates of two separate experiments for each cultural condition. They were statistically analyzed by SPSS software (version 100) using the Duncan test performed after analysis of variance (ANOVA).

RESULTS AND DISCUSSION

Among the 21 soil samples, the higher microbial population was observed with Pichavaram (boat house) soil samples. All the 63 bacterial strains isolated were subjected to screening for their biosurfactant production. Results on identification of 63 bacterial strains revealed that out of 63 isolates, 29 strains belong to Gram positive and 34 strains to Gram negative group represented by 5 genera. The genera were as followed: *Bacillus* (18), *Escherichia coli* (6), *Klebsiella* (5), *Lactobacillus* (3), *Proteus* (6), *Pseudomonas* (21) and *Staphylococcus aureus* (4). Species dominance results showed that among the 63 strains isolated, 21 strains belong to the genus *Pseudomonas* (33.3%). From 63 bacterial strains tested, 34 (53.97%) strains were positive for hemolysis and the promising isolate PBSC1 showed the maximum hemolytic activity of 2.9 cm followed by isolate KBSB1 (2.5 cm). Among the 63 strains screened, 41 (65.1 %) strains were positive for drop collapse activity. 12 isolates showed positive to hemolytic and negative to the drop collapse test. The isolate PBSC1 reduced the surface tension greatly to 30.20 mN/m, which was selected as the most potent biosurfactant producer.

16S rRNA sequencing

The isolate PBSC1 was initially identified using standard biochemical and sugar fermentation test and further subjected to 16S rRNA sequencing. The isolate PBSC1 was identified by the 16S rRNA sequence as *Pseudomonas aeruginosa* PBSC1and deposited under the accession no JQ314422 in the Gen bank. The isolate PBSC1 has 99% similarity with the *P. aeruginosa*. The Figure 1 represents the phylogentic tree of *P. aeruginosa* PBSC1.

Estimation of growth and biosurfactant production

The biosurfactant production was studied using 2.0% crude oil supplemented with 1% mannitol in the MSM medium. Figure 2 shows the time-course of biosurfactant production by *P. aeruginosa* PBSC1 with crude oil as the

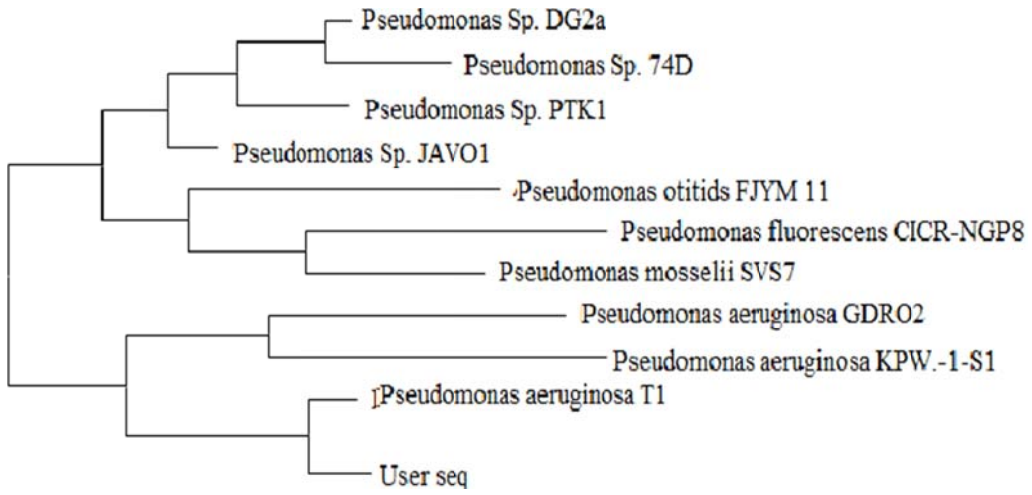

Figure 1. 16S rRNA sequence analysis of isolate PBSC1 and phylogenetic tree.

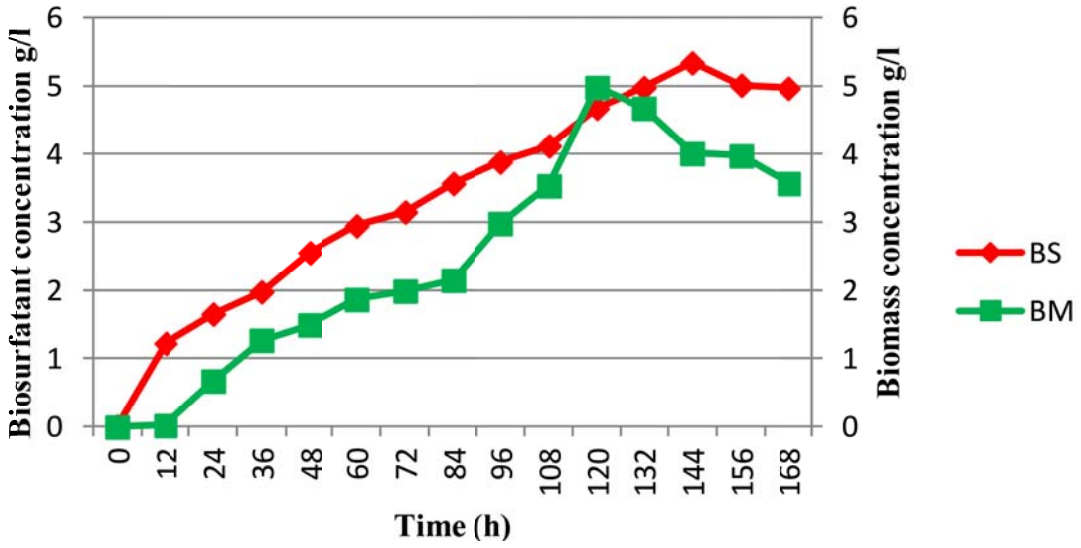

Figure 2. Growth kinetics of biosurfactant production by *Pseudomonas aeruginosa* PBSC1 under optimized conditions.

substrate. Maximum biosurfactant concentration of biosurfactant of 5.34 g L^{-1} occurred at 144 h of incubation, when the cells reached their early stationary phase. Maximum biomass was observed at 120 h (4.98 g L^{-1}). The biosurfactant was extracted from the cell free broth and further characterized to confirm the biosurfactant as rhamnolipid (a type of glycolipid) biosurfactant.

Characterization of biosurfactant

The CMC value of *P. aeruginosa* PBSC1was found to be 78 mg L^{-1}. Biosurfactant concentrations above the CMC could not decrease the surface tension further, indicating that biosurfactant molecules had begun to aggregate (Karsa et al., 1999). In the case of *P. aeruginosa* SP4, the excreted biosurfactant in the culture supernatant could decrease the surface tension of pure water from 72.0 to 28.3 mN m^{-1}, and the CMC was estimated to be 120 mg L^{-1} (Pornsunthorntawee et al., 2008). For *Pseudomonas fluorescens*, the CMC recorded for the isolated biosurfactant was 290 mg l^{-1} and the corresponding surface tension was 32 mN m^{-1}. The biosurfactant produced by *P. aeruginosa* PBSC1 exhibits better properties in terms of higher surface tension reduction and a lower CMC. The results of CMD^{-1} and CMD^{-2} of the biosurfactant containing cell-free medium were 30.3 and 42.0 mN m^{-1}, respectively, depicting non-significant change in efficiency. The results suggest that a sufficient amount of biosurfactant was present in the

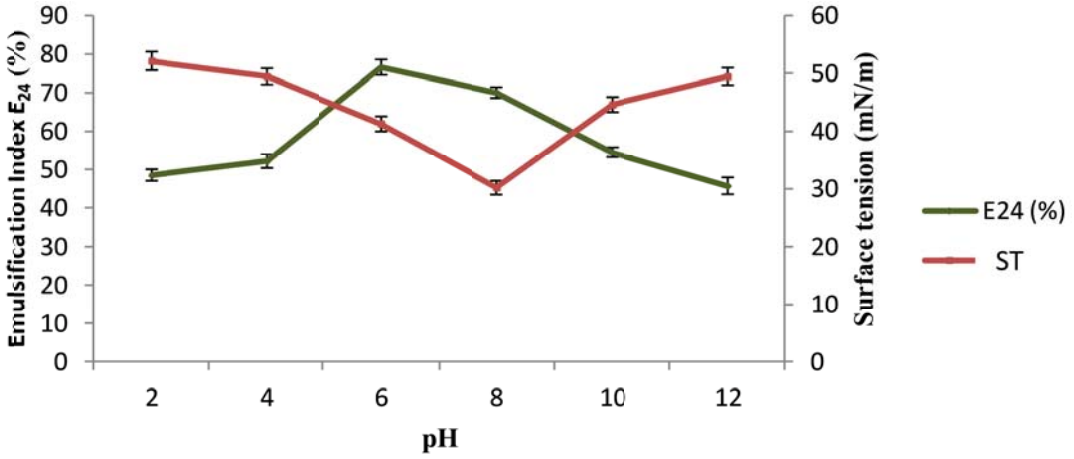

Figure 3. Stability of biosurfactant towards the changes in pH.

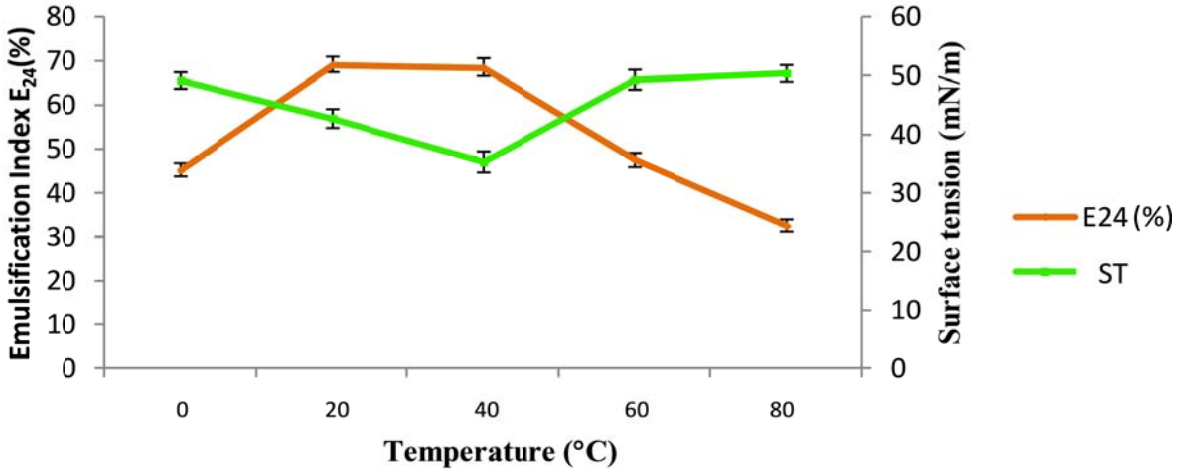

Figure 4. Stability of biosurfactant towards the changes in temperature.

culture medium, and thus its surface activity was retained even at such a high dilution.

Molisch's test showed a clear purple ring between the layers of solvent and the sample, indicating that the sample contained sugar moieties. The rhamnose test was positive, indicating that the separated biosurfactant could be of the glycolipid type. Red spots appeared on the TLC plate after spraying with α-naphthol and sulfuric acid, indicating the presence of carbohydrates in the sample. The production of glycolipid-type biosurfactant was previously reported for *Pseudomonas* sp. (Wilson and Bradley, 1996).

Activity characterization

Biosurfactant containing culture supernatant showed good foaming stability. The foam produced was stable for 48 h. Stable foam indicates that the produced biosurfactant can be used as a good foaming agent. Similar findings were reported for 48-h-old culture of *P. aeruginosa* PTCC 1561 grown in nutrient broth, which showed foam stability for 48 h (Noudeh et al., 2010).

In the case of stability of the biosurfactant towards the variations in the pH may alter the emulsification activity of the surfactant (Figure 3). pH range between 6-8, the highest emulsification activity was found. In the pH level of 2 and 12 the emulsification activity was greatly reduced and moderate activity was observed with the pH 4 and 10. The temperature may also have a significant role in the activity of emulsification of biosurfactant (Figure 4). In the lowest and highest temperature the activity was greatly reduced but good activity was observed with 20 and 40°C. When compared with pH and temperature the sodium chloride concentration does not produce any major differences in the emulsification activity (Figure 5). 5%

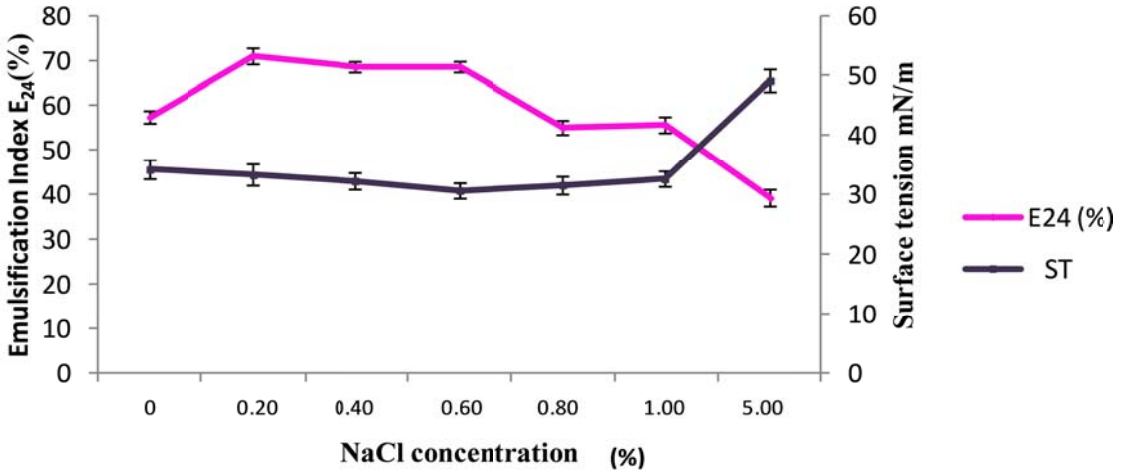

Figure 5. Stability of biosurfactant toward the changes in NaCl Concentration.

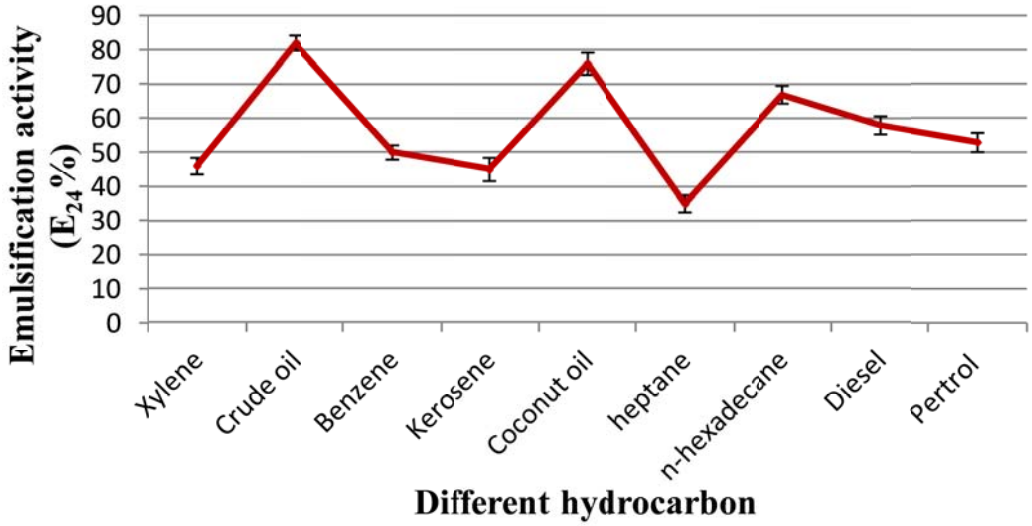

Figure 6. Emulsification activity of *P. aeruginosa* PBSC1 with various hydrocarbon.

concentration of NaCl showed highest emulsification activity followed by 10 and 15 %. From these results the biosurfactant was stable in the different pH levels with various temperatures and various concentration of sodium chloride.

This indicated that Surface tension and the E_{24} were stable even at a high temperature, in contrast to synthetic surfactants such as Sodium Dodecyl Sulphate, which exhibits a significant loss of emulsification activity above 70°C (Kim et al., 1997). Similar findings were reported for *P. aeruginosa* isolate Bs20, which exhibited excellent stability at high temperature (heating at 100°C for 1 h and autoclaving at 121°C for 10 min), salinities up to 6% NaCl, and pH values up to pH 13 (Abdel-Mawgoud et al., 2009).

Emulsification assay

Bio surfactant isolated from *P. aeruginosa* PBSC1 showed maximum emulsification activity against crude oil. Emulsification activities of the biosurfactant with different hydrocarbons were illustrated in Figure 6. The emulsion formed by the biosurfactant against each hydrocarbons were stable for one month.

Fourier transform Infrared (FT-IR) spectral analysis

The organism *P. aeruginosa* PBSC1 produced a rhamnolipid biosurfatant and it was confirmed with the FT-IR analysis based on the presence of functional

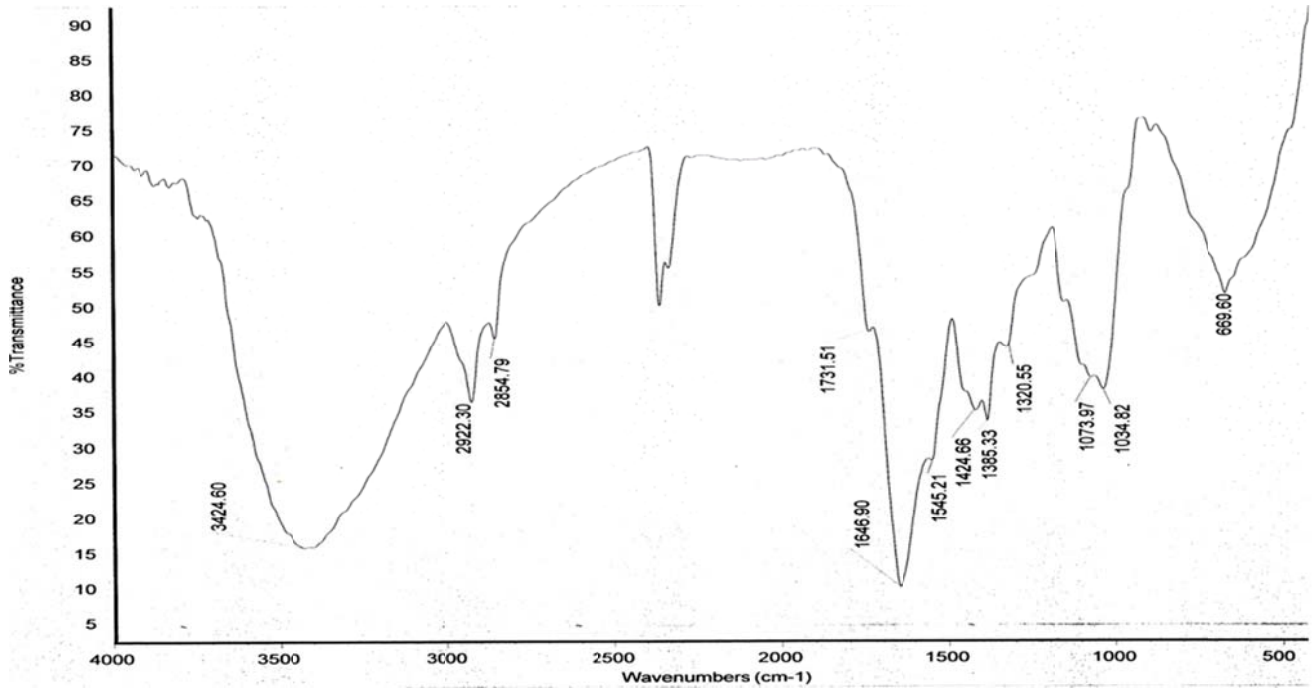

Figure 7. FT-IR spectra of biosurfactant produced by *P. aeruginosa* PBSC1.

group. FT-IR spectrum (Figure 7) revealed that, the most important adsorption bands were located at 3424.60 (OH bond, typical polysaccharides), 2922.30 and 2854.79 (CH band: CH2-CH3, hydrocarbon chains), 1731.51 and1646.90 cm^{-1} (for C=O, C=O ester bond), 1424.66 cm^{-1}(C-N amide groups). The C-O stretching bands at 1034.82-1320.55 cm^{-1} confirm the presence of bonds formed between carbon atoms and hydroxyl groups in the chemical structures of the rhamnose rings and 669.60 (for the CH2 groups) . According to Govindammal and Parthasarathi (2013) the most important adsorption bands were located at 3466.24 cm^{-1} which indicate the presence of OH bond, 2926.45 and 2856.23 cm^{-1} (CH band: CH2-CH3, hydrocarbon chains), and 1743.47 and1601.26 cm^{-1} (for C=O, C=O ester bond). The C-O stretching bands at 1162.26 to 1232.88 cm^{-1} showed the presence of bonds formed between carbon atoms and hydroxyl groups in the chemical structures of the rhamnose rings and 846.93 and 652.05 for CH_2 groups.

Conclusion

The isolated *P. aeruginosa* PBSC1 is a potent biosurfactant-producing native strain. The amount of crude biosurfactant recovered (5.34 g L^{-1}) from the culture medium. The CMC value (78 mg l^{-1}) of the produced biosurfactant is superior to many other biosurfactants. The tensioactive properties and stability of the biosurfactant to high temperature, pH and salinity reveal good prospects for this product in industrial applications. The emulsifying and foaming activity of the biosurfactant indicate that it can be used as a good emulsion-forming and foaming agent in different industries. The FT-IR spectrum reveals that the produced biosurfactant is a rhamnolipid. This strain can be further used in large scale production with alternative agroindustrial substrates for the better yield of biosurfactant. The optimization of the substrate may be studied elaborately using Response Surface Methodology (RSM).

ACKNOWLEDGEMENT

The authors would like to acknowledge the University Grants Commision (UGC), Government of India, for the financial assistance and Annamalai University, Tamil Nadu, India for providing the necessary facilities to conduct the research experiment.

Conflict of Interests

The author(s) have not declared any conflict of interests.

REFERENCES

Abdel-Mawgoud AM, Aboulwafa MM, Hassouna NA (2009). Characterization of Rhamnolipid Produced by *Pseudomonas aeruginosa* Isolate Bs20. Appl. Biochem. Biotechnol. 157:329-345.

Abouseoud M, Yataghene A, Amrane A, Maachi R (2008). Biosurfactant production by free and alginate entrapped cells of *Pseudomonas fluorescens*. J. Ind. Microbiol. Biotechnol. 35:1303-1308.

Besson F, Michel G (1992). Biosynthesis of iturin and surfactin by *Bacillus subtilis*. Evidence for amino acid activating enzymes. Biotechnol. Lett. 14:1013-1018.

Bodour AA, Miller-Maier R (1998). Application of a modified drop collapse technique for surfactant quantification and screening of biosurfactant-producing microorganisms. J. Microbiol. Methods 32: 273-280.

Bonilla M, Olivaro C, Corona M, Vazquez A, Soubes M (2005). Production and characterization of a new bioemulsifier from *Pseudomonas putida* ML2. J. Appl. Microbiol. 98:456-463.

Cooper DG, Goldenberg BG (1987). Surface-active agents from two *Bacillus* species. Appl. Environ. Microbiol. 53:224-229.

Desai JD, Banat IM (1997). Microbial production of surfactants and their commercial potential. Microbiol. Mol. Biol. Rev. 61:47-64

Dubois M, Gills KA, Hamilton JK, Rebers PA, Smith F (1956). Colorimetric method for determination of sugar and related substances. Anal. Chem. 28:350-356.

Govindammal M, Parthasarathi R (2013). Production and Characterization of Biosurfactant Using Renewable Substrates by *Pseudomonas fluorescence* Isolated from Mangrove Ecosystem. J. Appl. Chem. 2(1):55-62.

Jain DK, Collins-Thompson DL, Lee H, Trevors JT (1991). A drop collapsing test for screening surfactant-producing microorganisms. J. Microbiol. Methods 13:271-279.

Karsa DR, Bailey RM, Shelmerdine B, McCann SA (1999). Overview: A decade of change in the surfactant industry. In: Karsa DR (ed) Industrial applications of surfactants. Vol. 4. Royal Society of Chemistry, London. pp. 1-22.

Kim H, Yoon B, Lee C, Suh H, Oh H, Katsuragi T, Tani Y (1997). Production and properties of a lipopeptide biosurfactant from *Bacillus subtilis* C9. J. Ferment. Bioeng. 84(1):41-46

Kosaric N (1993). Biosurfactants. Production, property, application, surfactant sciences series, 48. Dekker, New York.

Mercade ME, Manresa MA (1994). The use of agroindustrial byproducts for biosurfactant production. J. Am. Oil Chem. Soc. 71:61-64

Morikawa M, Hirata Y, Imanaka TA (2000). A study on the structure-function relationship of lipopeptide biosurfactants. Biochem. Biophys. Acta 1488:211-218.

Mulligan CN, Cooper DG, Neufeld RJ (1984). Selection of microbes producing biosurfactants in media without hydrocarbons. J. Ferment. Technol. 62:311-314.

Noudeh GD, Noodeh AD, Moshafi MH, Behravan E, Afzadi MA, Sodagar M (2010). Investigation of cellular hydrophobicity andsurface activity effects of biosynthesed biosurfactant from broth media of PTCC 1561. Afr. J. Microbiol. Res. 4(17):1814-1822.

Pornsunthorntawee O, Arttaweeporna N, Paisanjit S, Somboonthanatea P, Abeb M, Rujiravanita R, Chavadeja S (2008). Isolation and comparison of biosurfactants produced by *Bacillus subtilis* PT2 and *Pseudomonas aeruginosa* SP4 for microbial surfactant enhanced oil recovery. Biochem. Eng. J. 42:172-179.

Rashmi RS, Suresh D, Manab D, Ibrahim MB (2012). Isolation of biosurfactant-producing *Pseudomonas aeruginosa* RS29 from oil-contaminated soil and evaluation of different nitrogen sources in biosurfactant production. Ann. Microbiol. 62:753-763.

Rosenberg E (1986). Microbial biosurfactants. Crit. Rev. Biotechnol. 3: 109-132.

Semenov AM, Van Bruggen AH, Zelenev VV (1999). Moving waves of bacterial populations and total organic carbon along roots of wheat. Microbial. Ecol. 37:116-128.

Smith TJ, Boto KG, Frusher SD, Giddins RL (1991). Keystone species and mangrove forest dynamics: the influence of burrowing by crabs on soil nutrient status and forest productivity. Estuar. Coast. Shelf Sci. 33:419-432.

Thavasi R, Subramanyam Nambaru VRM, Jayalakshmi S, Balasubramanian T, Ibrahim MB (2011). Biosurfactant Production by *Pseudomonas aeruginosa* from renewable resources. Ind. J. Microbiol. 51(1):30-36.

Wilson NG, Bradley G (1996). The effect of immobilization on rhamnolipid production by *Pseudomonas fluorescens*. J. Appl. Bacteriol. 81(5):525-530.

academicJournals

Vol. 13(33), pp. 3402-3412, 13 August, 2014
DOI: 10.5897/AJB2013.12195
Article Number: D9B84D046624
ISSN 1684-5315

http://www.academicjournals.org/AJB

African Journal of Biotechnology

Full Length Research Paper

In vitro inhibition of pathogenic *Verticillium dahliae*, causal agent of potato wilt disease in China by *Trichoderma* isolates

Chen Xiaojun[1,2], Sopone Wongkaew[1], Yuan Jie[2], Yang Xuehui[2], He Haiyong[1,2], Wu Shiping[2], Tai Qigqun[2], Wang Lishuang[2], Dusit Athinuwat[3] and Natthiya Buensanteai[1]*

[1]School of Crop Production Technology, Institute of Agriculture Technology, Suranaree University of Technology, Nakhon Ratchasima, 30000 Thailand.
[2]Guizhou Institute of Plant Protection, Guizhou Academy of Agricultural Sciences, Guiyang, 550006 China.
[3]Major of Organic Farming Management, Faculty of Science and Technology, Thammasat University, Pathumthani, 12121, Thailand.

Received 27 February, 2013; Accepted 24 March, 2014

Twenty (20) of *Verticillium dahliae* were isolated from wilted potato specimens collected from six districts in Guizhou, China. All the isolates were evaluated for pathogenicity on two potato cultivars, Favorita (susceptible) and Hui-2 (resistant) using the root dip inoculation (RDI) and microsclerotia inoculation (MI). All of the *V. dahliae* isolates appeared to be pathogenic on both cultivars but VGZ-HZ-4 isolate gave the highest wilt incidence comparing to the others, seconded by VGZ-SC-1 and VGZ-XW-1. Combined analysis of wilt incidence resulting from using two inoculation methods for VGZ-HZ-4 and VGZ-XW-1 isolates on the two potato cultivars showed that the MI gave a higher wilt incidence than that of the RDI and cultivar Favorita had a higher wilt incidence than that of Hui-2. These two *V. dahliae* isolates were further used as representative isolates for mycelial inhibition (MyI) test with 33 *Trichoderma* isolates under a dual culture condition on potato dextrose agar plate. The 33 *Trichoderma* isolates consisting of 21 isolates isolated from potato soils from seven districts of Guizhou, 11 isolates from single spore isolates of the TGZ-150 isolate preserved at Guizhou Institute of Plant Protection (GZIPP) and one isolate TGZ-OLD-81 also preserved at the GZIPP. Most of the single spore isolates and TGZ-SC-4 were found to have higher MyI efficiency than that of the rest. The results indicate that the *Trichoderma* isolates in this study have initial modes of action of biological control to protect potato crop against *V. dahlia*.

Key words: *Trichoderma*, potato wilt disease, growth inhibition, *Verticillium dahliae*, antagonistic fungi.

INTRODUCTION

Trichoderma species as biocontrol agents of plant pathogen were first recognized in the early 1930's and subsequently they were applied successfully as biocontrol agents against several plant diseases in commercial agriculture (Hjeljord and Tronsmo, 1998; Harman, 2006; Schubert and Fink, 2008). *Trichoderma* is a genus which include species of free- living soil fungi, opportunistic, avirulent plant symbionts (Harman et al., 2004), asympto-

matic endophytes (Williama et al., 2003), and parasites of other fungi (Harman, 2006). It is often the major component of the microflora in soils of various ecosystems, such as agricultural farm soil, grassland, forest, marshes, deserts and water (Danielson and Davey, 1973). It possesses high reproductive capacity, ability to survive under very unfavorable conditions, efficiency in the utilization of nutrients, and capability to modify the rhizosphere. They produce a variety of compounds that induce localized or systemic resistance responses in plants (Brunner et al., 2005).

Potato (*Solanum tuberosum* L.) is the World's and China's fourth largest staple crop after rice, wheat and maize. China is the largest potato producer worldwide, accounting for 26.3 and 22.2% of the global total area and yield (Wang et al., 2011). However, the potato yield and quality has been seriously influenced by various diseases. Among problems of potato, *Verticillium* wilt is one of the most destructive diseases that occurs in major potato growing regions worldwide and has been reported in many countries, like USA, New Zealand, the Pacific North-West, Canada and China (Rowe and Powelson, 2002; Mpofu and Hall, 2002). *Verticillium* wilt is a complex disease caused by many species of *Verticillium*, such as *Verticillium dahliae* Kleb or *Verticillium alboatrum* (Francl et al., 1990; Rowe and Powelson, 2002). However, it is mainly caused by *V. dahliae* which can cause wilt, severe yield and quality losses in more than 160 plant species, such as potato (*S. tuberosum* L.), cotton (*Gossypium* spp.), tomato (*Lycopersicon esculentum* Mill.), alfalfa (*Medicago sativa* L.), strawberry (*Fragaria grandiflora* Ehrh.), mint (*Mentha piperita* L.), sunflower (*Helianthus annuus* L.) and eggplant (*Solanum melongena* L.) (Gazendam et al., 2004; Uppal et al., 2008; Cirulli, 1981). This disease continues to have a considerable impact on the potato industry, worth about US$ 44 million annually (Mpofu and Hall, 2002) and *Verticillium* spp. were present over 60% of potato fields in the USA (Slattery and Eide, 1980). Furthermore, it can cause total loss in individual field. *V. dahliae* is one of the most destructive soil/seed-borne fungal pathogen (Uppal et al., 2008) and can survive in the soil for 5 to 14 years (http://www.crop.cri.nz/home/ products-services/publications/ broadsheets/126-Potato.pdf). The management of *Verticillium* wilt is challenging not only due to the endogenous growth of the pathogen, but also to its ability to infect multiple hosts and to the multi-year longevity of its propagules in the soil (AlstrÖm, 2001).

The soil-borne pathogens like *Verticillium* spp. are difficult to control, even by chemicals. One reason could be the complicated ecosystem of the soil, where a number of interactions occur. Under favorable conditions such diseases spread rapidly, almost without any possibility of control by fungicides (Galletti et al., 2008). Although, the agricultural chemical fungicides have been used for so long and the effects were prominent, they could induce the pathogen to develop resistance. Moreover, although the disease had been so controlled, some beneficial microbes have also been killed, thus disturbing the ecological balance. There is now a need for other methods of control as fungicidal use may be limited in the future by governmental regulations (Hanson, 2000; Kexiang et al., 2002).

In recent years, sustainable agricultural systems aimed at safeguarding the environment have gained more and more interest, and considerable efforts have been made to adopt strategies which reduce chemical inputs (Gamliel et al., 2000; Zamanian et al., 2005). *Trichoderma* spp. are widely used as commercial biofungicides for control of soil-borne and foliar pathogens (Chet and Baker, 1981; Cook and Baker, 1982; Papavizas, 1985; Verma et al., 2007; Buensanteai et al., 2010; Akinbode and Ikotun, 2011). In addition, plant pathogens directly affected through antibiosis and mycoparasitism, *Trichoderma* spp. can colonize roots and trigger systemic resistance against bacterial and fungal pathogens (Liansheng and Weihua, 2000; Harman et al., 2004). Induced resistance caused by treating plants with a biologically active elicitor is the phenol-menon of priming and sensitizing plants to exhibit a more rapid and elevated expression of defense-related responses upon pathogen infection compared to unprimed plants. These responses may include an accumulation of PR proteins associated with the SA-dependent and the pathogen-induced JA-dependent pathways, as well as phenylalanine ammonia-lyase and redox regulating proteins (Mittler et al., 2004; Fobert and Despres, 2005; Heil and Silva Bueno, 2007; Buensanteai et al., 2010).

The aim of this study was to evaluate the efficacy of *Trichoderma* strains for antagonistic activity on the fungal pathogen *V. dahliae,* causal agent of potato wilt disease.

MATERIALS AND METHODS

Pathogen isolation

Ten (10) potato wilt diseased samples were collected from Shuicheng, Hezhang, Changshun, Weining, Guiyang (GZAAS and Xiuwen) in Guizhou province, China. Subsequently, the samples were washed in running water for 15-20 min, immersed in 1% sodium hypochlorite (NaOCl) for 2-3 min, rinsed with sterile distilled water for 30 to 45 s and then dipped in 70% ethyl alcohol for 20 to

*Corresponding author. E-mail: natthiya@sut.ac.th. Tel: 66 4 422 4204. Fax: 66 4 422 4281.

30 s. Cross sections were then made under an aseptic condition and transferred onto acidified potato-dextrose agar (APDA). The APDA contained 2 ml of 25% lactic acid per liter. The stem sections were incubated for 14 to 20 days at 22 to 24°C as reported by Slattery and Eide (1980). After four days, the *V. dahliae* hyphal tip grown out from each piece of tissue of potato was picked and transferred onto the new potato dextrose agar (PDA) for further experiment.

Pathogenicity test of *V. dahliae* isolates

Root dip inoculation (RDI)

Twenty (20) of the *V. dahliae* isolates obtained were tested for their pathogenicity in potato seedlings. All cultures were grown on PDA at 24±2°C prior to inoculation. Spore suspensions were prepared from 3-week-old cultures by adding 10 ml of sterile distilled water to each plate and scraping the cultures with a rubber spatula. Using a haemacytometer, the inoculum concentration was adjusted to 10^7 conidia/ml. Potato seedlings of the Favorita and Hui-2 cultivars were used as test plants. Favorita had been observed to be susceptible to *V. dahliae*, while Hui-2 was resistant. These potato seedlings were uprooted and inoculated by using the root-dip technique. Roots were washed with running water, and submerged for 60 min in conidia suspension. The inoculated seedlings were subsequently transplanted into 20 cm pots with sterilized soil (autoclaved 1 h, 121°C -or whatever it is). Three replications of five plants for each isolate were used. The plants were kept on a room bench at 21 to 23°C. Daylight was supplemented by fluorescent lamps to provide a 12 h day length; wilt incidence was checked at four weeks after inoculation.

Microsclerotia inoculation (MI)

The same 20 isolates of *V. dahliae* were used for this experiment. After microsclerotia having formed on PDA, the whole agar piece was removed from the plate and put in the soil beneath the roots of transplanted potato seedlings of the Favorita and Hui-2 cultivars in a 20 cm pot. Three replications of five plants for each isolate were used. The plants were kept under the same condition as in previous experiment; wilt incidence was observed four weeks after inoculation. The experimental trials were conducted following a three-factor complete randomized design (CRD).

Trichoderma origin and isolation

Trichoderma-selective medium (TSM)

The TSM consisted of a basal medium comprising (all amount is per liter) 0.2 g $MgSO_4$ ($7H_2O$), 0.9 g K_2HPO_4, 0.15 g KCl, 1.0 g NH_4NO_3, 3 g glucose, 0.15 g rose Bengal, and 20 g agar. These constituents were added to 950 ml of distilled water and autoclaved at 121°C for 15 min. The antimicrobial and fungicidal ingredients (all amount were per liter) were 0.25 g chloramphenicol, 9.0 ml streptomycin stock solution (1% w/v), 0.2 g quintozene, and 1.2 ml propamocarb (772 g of active ingredient per liter), all in 20 ml of sterile distilled water, and the mixtures were added to the cooled basal medium (40 to 50°C) (Williams et al., 2003).

***Trichoderma* isolation from soil**

Ten (10) soil samples of each field were taken from each *Verticillium* wilt diseased field in Shuicheng, Weining, Hezhang, Zunyi and Guiyang of Guizhou province, China and 10 fields were sampled. Five soil sub samples were taken from the area around the healthy potato roots, pooled and placed in polyethylene bags and stored at 4°C. Ten gram of the soil sample was suspended in 50 ml of sterile distilled water and incubated for 30 min at 200 rpm in a rotary shaker. Serial dilutions (5×1:9 ml) were then made. Subsequently, 0.1 ml of each dilution was spread on the TSM surface with a glass rod, two replications for each dilution and incubated at 28°C. Five to ten *Trichoderma* single colonies were collected from each sample and transferred onto PDA for further study. The isolates were primarily selected according to their differences in colony characters.

Single spore isolates

Trichoderma harzianum TGZ-150 was isolated from rhizosphere soil of tobacco damaged by tobacco root rot (*Fusarium oxysporum*) in Bijie city of Guizhou province in 2011 and preserved at the Plant Pathology Laboratory of Guizhou Institute of Plant Protection (GZIPP). The 0.03 ml of TGZ-150 *Trichoderma* spore suspension (10^3 conidia/ml) was spread on 10 PDA medium, incubated at 28±2°C for 12 h and examined frequently every 12 h under a microscope for germinating spores which were picked and transferred with a sterile cork borer to fresh PDA. The single spore isolates were maintained in PDA slant for the future experiment.

In vitro* inhibition of *V. dahliae* by *Trichoderma

Mycelial inhibition (Myl)

Trichoderma isolates used for this study were from two origins. One was the 11 single spore isolates of TGZ150, and the strain TGZ-OLD-81 preserved at GZIPP, the others were those isolated from the fields. The *T. harzianum* and the *V. dahliae* isolates tested were VGZ HZ4 and VGZ XW1 which previously showed the highest levels of pathogenicity in potato. *Trichoderma* isolates were tested *in vitro* for their highest antagonistic ability over *V. dahliae* colony in dual culture. One mycelial disc (5 mm) of each *Trichoderma* isolate and *V. dahliae* was put together in a Petri dish with PDA medium, 6 cm apart. Three replications (dishes) were used for each *Verticillium*-*Trichoderma* combination. The *V. dahliae* mycelial growth inhibition rate was calculated three days after incubation. The percent of growth inhibition was calculated as follows:

Growth inhibition (%) = [(RCK-RT/RCK) ×100]

Where, RCK is the radius of *V. dahliae* colony, and RT is the radius of *V. dahliae* colony cultured with *Trichoderma* in the same Petri dish.

Microsclerotia disintegration (MD)

Based on the fact that microsclerotia are the main inocula of V. dahliae in the soil, their elimination can reduce wilt incidence in the subsequently growing season. Therefore, Trichoderma isolates having microsclertia disintegration ability (MDA) would be more desirable. This experiment was aimed at testing the MDA of some selected Trichoderma isolates. Microsclerotia paper discs (MPD) were prepared. A sterile filter paper disc (5 mm) was put at the edge of each growing colony of V. dahliae in order to collect microsclerotia. Numerous microsclerotia were produced on the

Table 1. Isolates of *Verticillium dahliae* isolated from the wilted potato grown in Guizhou Province, China used in the experiment.

Isolate	Site	Host	Isolate	Site	Host
VGZ-SC-1	Shuicheng	Favorita	VGZ-HZ-1	Hezhang	WeiYu-3
VGZ-SC-2	Shuicheng	Favorita	VGZ-HZ-3	Hezhang	Favorita
VGZ-SC-3	Shuicheng	WeiYu-3	VGZ-HZ-4	Hezhang	Favorita
VGZ-SC-4	Shuicheng	WeiYu-3	VGZ-HZ-9	Hezhang	Favorita
VGZ-SC-5	Shuicheng	WeiYu-3	VGZ-HZ-10	Hezhang	Favorita
VGZ-SC-6	Shuicheng	Favorita	VGZ-XW-1	Xiuwen	WeiYu-3
VGZ-SC-7	Shuicheng	Favorita	VGZ-WN-1	Weining	Favorita
VGZ-CS-1	Changshun	Favorita	VGZ-WN-2	Weining	WeiYu-3
VGZ-CS-2	Changshun	Favorita	VGZ-NKY-2	GZAAS[1]	Favorita
VGZ-CS-5	Changshun	Favorita	VGZ-NKY-4	GZAAS	Favorita

[1]GZAAS: Guizhou academy of agricultural sciences.

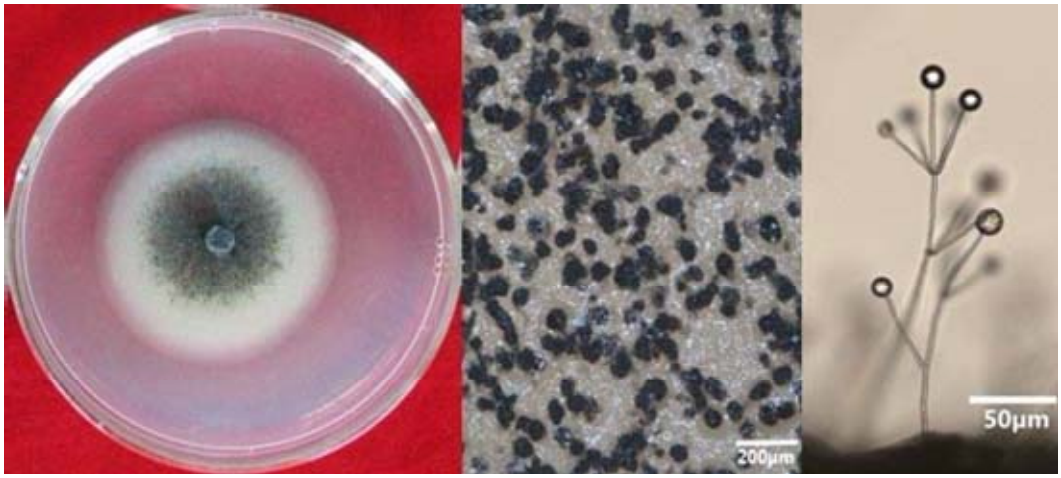

Figure 1. Colony character (left), microsclerotia (middle) and conidia (right) of *Verticillium dahliae* on APDA medium.

paper disc after one week. Ten (10) Trichoderma isolates having highly inhibition ability on V. dahliae mycelial growth were tested for their ability to disintegrate V. dahliae microsclerotia. One mycelial disc (5 mm) of each Trichoderma isolate was put in the middle of the PDA. After 1 day, 30 MPDs were put at the edge of the growing colony in three replications. The MPD was pretested for their sensitivity to surface disinfectant (1% NaOCl and 75% ethyl alcohol) before the actual experiment was conducted. The best condition of MPD treatment was applied to the MPD for this test. After 1 week, the MPD from each treatment was recovered and checked for the viability. All of the MPDs were put in the PDA after disinfectant (75% ethyl alcohol 3 min and 1% NaOCl 5 min) treatment. With this treatment, only viable microsclerotia survived but all Trichoderma propagules were killed. Percentage of non-germinating microsclerotia reflected the ability of Trichoderma to disintegrate the microsclerotia.

Statistics analysis

The data was analyzed by SPSS 16.0 software. To ensure that the homogeneity of the variances and the symmetry of the distribution of each variable, data recorded as percentages were arcsine-transformed before ANOVA analysis in this research. Statistical differences were determined by DMRT (Duncan) test.

RESULTS

Isolation of *V. dahliae* and *Trichoderma*

Twenty (20) isolates of *V. dahliae* were obtained from the planting areas of Guizhou province (Table 1). Colony character showed white mycelia and produced black microsclerotia on APDA (Figure 1). From the soil samples collected from different location in Guizhou, 21 *Trichoderma* isolates were obtained (Table 2). Additional 11 isolates were single-spore isolated from *T. harzianum* TGZ-150, a commercial isolate preserved at GZIPP. All

Table 2. Isolates of *Trichoderma* from the GZIPP collection and obtained from the soil in Guizhou Province, China.

Isolate	Site	Isolate	Site
TGZ-SC-3	Shuicheng	TGZ-CH-1	Weining
TGZ-SC-4	Shuicheng	TGZ-CH-2	Weining
TGZ-SC-5	Shuicheng	TGZ-CH-3	Weining
TGZ-HZ-3	Hezhang	TGZ-CH-4	Weining
TGZ-NKY-1	GZAAS	TGZ-OLD-81[1]	Guanling
TGZ- NKY -2	GZAAS		
TGZ- NKY -3	GZAAS	TGZ-150-1	
TGZ- NKY -5	GZAAS	TGZ-150-4	
TGZ- NKY -7	GZAAS	TGZ-150-5	
TGZ- NKY -8	GZAAS	TGZ-150-6	
TGZ-TC-3	Changshun	TGZ-150-33	
TGZ-TC-4	Changshun	TGZ-150-37	Single spore isolate of TGZ-150[2]
TGZ-TV-1	Xingyi	TGZ-150-38	
TGZ-TV-2	Xingyi	TGZ-150-41	
TGZ-TV-3	Xingyi	TGZ-150-50	
TGZ-ZY-2	Zunyi	TGZ-150-51	
TGZ-ZY-4	Zunyi	TGZ-150-55	

[1]TGZ-OLD-81 was isolated by baiting from the soil of a pepper field. [2]TGZ-150 was isolated from rhizosphere of tobacco roots and preserved at GZIPP.

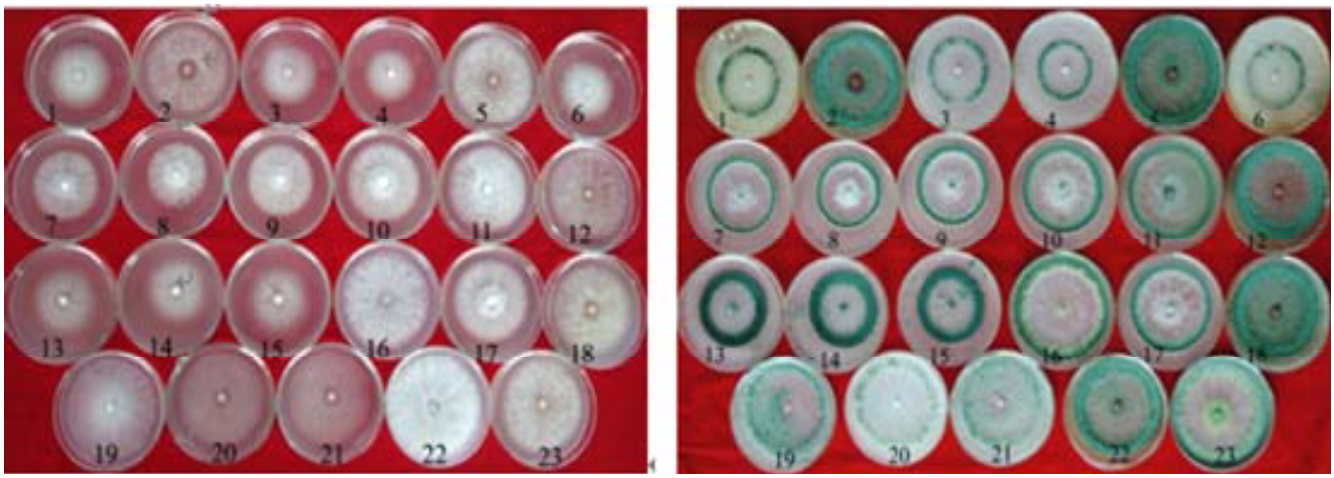

Figure 2. The character of *Trichoderma* isolates cultured for 2 days (left) and 7 days (right) on PDA. (1 TGZ-TV-1, 2 TGZ-150-37, 3 TGZ-TV-2, 4 TGZ-TV-3, 5 TGZ-150-5, 6 TGZ-150-33, 7 TGZ-CH-1, 8 TGZ-CH-2, 9 TGZ-CH-3, 10 TGZ-CH-4, 11 TGZ-ZY-2, 12 TGZ-ZY-4, 13 TGZ-NKY-1, 14 TGZ-NKY-2, 15 TGZ-NKY-3, 16 TGZ-NKY-5, 17 TGZ-HZ-4, 18 TGZ-OLD-81, 19 TGZ-NKY-7, 20 TGZ-SC-5, 21 TGZ- SC-3, 22 TGZ-SC-4 and 23 TGZ-150-38).

these isolates and TGZ-OLD-81 were included in the up-coming experiment (Figure 2).

Pathogenicity test of *V. dahliae* isolates

The 20 isolates of *V. dahliae* were tested for pathogenicity on two potato cultivars by root dip inoculation (RDI) and microsclerotia inoculation (MI). All of the *V. dahliae* isolates could infect potato cultivar Favorita (Table 3). When results of pathogenicity of the 20 *V. dahliae* isolates on the two potato cultivars were combined, it appeared that VGZ-HZ-4 gave the highest wilt incidence of 39.71%, seconded by VGZ-SC-1 and VGZ-XW-1

Table 3. Wilt incidence on potato cultivars favorita and Hui-2 inoculated with *Verticillium dahliae* isolates by root dip inoculation (RDI) and microsclerotia inoculation (MI).

Treatment	Wilt incidence (%)			
	Favorita		Hui-2	
	RDI[1]	MI	RDI	MI
VGZ-SC-1	26.67^{ab}	33.33^{bcd}	0.00^{a}	6.67^{ab}
VGZ-SC-2	40.00^{ab}	40.00^{abcd}	6.67^{a}	6.67^{ab}
VGZ-SC-3	46.67^{ab}	33.33^{bcd}	0.00^{a}	0.00^{b}
VGZ-SC-4	33.33^{ab}	40.00^{abcd}	13.33^{a}	13.33^{ab}
VGZ-SC-5	46.67^{ab}	46.67^{abcd}	0.00^{a}	6.67^{ab}
VGZ-SC-6	20.00^{bc}	46.67^{abcd}	6.67^{a}	6.67^{ab}
VGZ-SC-7	46.67^{ab}	53.33^{abc}	0.00^{a}	0.00^{b}
VGZ-HZ-1	20.00^{bc}	6.67^{ef}	0.00^{a}	6.67^{ab}
VGZ-HZ-3	53.33^{ab}	46.67^{abcd}	6.67^{a}	0.00^{b}
VGZ-HZ-4	60.00^{a}	73.33^{a}	20.00^{a}	20.00^{a}
VGZ-HZ-9	20.00^{bc}	20.00^{de}	0.00^{a}	0.00^{b}
VGZ-HZ-10	40.00^{ab}	66.67^{ab}	6.67^{a}	0.00^{b}
VGZ-CS-1	66.67^{a}	73.33^{a}	13.33^{a}	13.33^{ab}
VGZ-CS-2	40.00^{ab}	53.33^{abc}	0.00^{a}	6.67^{ab}
VGZ-CS-5	33.33^{ab}	26.67^{cd}	0.00^{a}	13.33^{ab}
VGZ-WN-1	40.00^{ab}	53.33^{abc}	13.33^{a}	13.33^{ab}
VGZ_WN-2	40.00^{ab}	60.00^{abc}	6.67^{a}	6.67^{ab}
VGZ-NKY-2	46.67^{ab}	46.67^{abcd}	6.67^{a}	13.33^{ab}
VGZ-NKY-4	20.00^{bc}	40.00^{abcd}	0.00^{a}	0.00^{b}
VGZ-XW-1	46.67^{ab}	60.00^{abc}	13.33^{a}	20.00^{a}
Control[2]	0.00^{c}	6.67^{f}	0.00^{a}	0.00^{b}
F-test	**	**	NS	*
CV (%)	27.23	20.43	35.95	30.54

[1]Means in the same column followed by different letters are statistically different at P≤0.05 by DMRT.
[2]Control: without *Verticillium.*

which gave wilt incidence that were not statistically different (37.41 and 34.62%, respectively) (Table 4). The combined average wilt incidence of RDI and MI on the cultivar Favorita was higher than cultivar Hui-2 (Table 5) which was 39.63 and 8.62%, respectively. Table 6 shows the combined wilt incidence resulting from the use of 2 inoculation techniques on the two cultivars. It appears that the MI gave a higher wilt incidence (25.92%) compared to that of the RDI. VGZ-HZ-4 and VGZ-XW-1 were selected as representative isolates for further experiment.

In vitro inhibition of *V. dahliae* by *Trichoderma* isolates

In this experiment, the 33 *Trichoderma* isolates were tested for mycelia growth inhibition of the *V. dahliae* isolates VGZ-HZ-4 and VGZ-XW-1. All of *Trichoderma* isolates could grow and occupy the whole colony of *V. dahliae* within four days (Figure 3). Most of the *Trichoderma* isolates grew so fast and had the averaged colony radius of 41.86, 54.08 and 65.98 mm after two, three and four days, respectively. After seven days, all of them could produce spores at the average of 1.38×10^{10} cfu/dish.

After three days of dual culture at 28°C, most of the isolates had performed noticeably well on inhibition ability. The inhibition percentage measured at three days after the dual culture is shown in Table 7. It can be seen that most of single spore-isolates of TGZ-150 and the TGZ-OLD-81 had higher inhibition efficacy than the average but the one isolated from soil of Shuicheng, TGZ-SC-4 isolate gave the highest inhibition percentage of 38.37%.

Microsclerotia disintegration test

After pretesting the disinfection time for *Trichoderma* and *V. dahliae*, it was found that immersing paper dices containing the fungal propagules in 75% EtOH for 3 min followed by NaOCl for 5 min could kill the *Trichoderma*

Table 4. Combined wilt incidence on favorita and Hui-2 potato cultivars inoculated by root dip technique and microsclerotia inoculation with different *Verticillium dahliae* isolates.

V. dahlia isolate	Wilt incidence (%)[1]
VGZ-HZ-4	39.71[a]
VGZ-CS-1	37.41[ab]
VGZ-XW-1	34.62[ab]
VGZ-WN-1	30.30[abcd]
VGZ-NKY-2	28.18[abcd]
VGZ-SC-4	27.42[abcd]
VGZ-WN-2	26.93[bcde]
VGZ-HZ-10	25.77[cde]
VGZ-HZ-3	24.81[cde]
VGZ-SC-2	23.95[cde]
VGZ-CS-2	23.75[cde]
VGZ-SC-5	23.66[cde]
VGZ-SC-7	22.50[de]
VGZ-SC-6	20.68[def]
VGZ-SC-3	19.52[def]
VGZ-SC-1	18.66[def]
VGZ-CS-5	18.47[def]
VGZ-NKY-4	15.29[ef]
VGZ-HZ-9	10.97[fg]
VGZ-HZ-1	9.91f[g]
F-test	**
CV (%)	19.81

[1]Means in the same column followed by different letters are statistically different at P≤0.05 by DMRT.

Table 5. Combined wilt incidence on two potato cultivars inoculated with *Verticillium dahliae* by two inoculation methods.

Potato cultivar	Wilt incidence (%)[1]
Favorita	39.63[a]
Hui-2	8.62[b]
F-test	**
CV (%)	19.81

[1]Means in the same column followed by different letter are statistically different at P≤0.05 by DMRT.

completely but not the microsclerotia of *V. dahliae*. This disinfection condition was subsequently applied for the microsclerotia disintegration test. The 10 *Trichoderma* isolates having high mycelial inhibition ability could disintegrate microcsclerotia of both *V. dahliae* isolates completely (Table 8).

DISCUSSION

Twenty (20) isolates of *V. dahliae* could be isolated from diseased samples from various potato growing areas in Guizhou. The isolates were similar in morphology and growth characteristics but different in pathogenicity reflecting their diversity. Among them, isolate VGZ-HZ-4 gave the highest wilt incidence of 39.71% while VGZ-HZ-1 gave the lowest incidence of 9.91% when the averaged from the 2 potato cultivars were inoculated with the two methods, root dipping (RDI) and microsclerotia inoculations (MI). It is interesting that both of them came from the same location, Hezhang but VGZ-HZ-1 was isolated from diseased WeiYu-3 potato cultivar. Biodiversity among *V. dahliae* isolates is a common phenomena that has been observed by many researchers (Schubert et al., 2008). Both crop species and planting areas could have an effect on the diversity (Steven et al., 2009). Such finding indicates the necessity of screening *V. dahliae* for pathogenicity before any research of this nature could be conducted.

Table 6. Combined wilt incidence of two inoculation methods on two potato cultivars.

Inoculation method	Wilt incidence[1]
Microsclerotia inoculation (MI)	25.92[a]
Root dip inoculation (RDI)	22.31[b]
F-test	*
CV (%)	19.81

[1]Means in the same column followed by different letters are statistically different at P≤0.05 by DMRT.

For the inoculation, when the results were combined and analyzed, MI appeared to have a higher efficacy than that of the RDI using conidia suspension. However, when the single factor was analyzed it was obvious that both inoculation methods were equally effective on the Favorita cultivar and only on Hui-2 that RDI was less effective. It appears that inoculation methods do not affect the efficacy if the test cultivar is susceptible but will have a significant effect if the test cultivar is resistant. Results of this observation could be used to explain why some researchers were more successful using RDI while other found that MI was better (Maas et al., 1985). Both inoculation methods have advantages and disadvantages. The MI is more natural considering that microsclerotia are the fungal propagules over seasoning in the soil and are the main inocula that start the disease cycle (Maas et al., 1985). But to prepare microsclerotia as inocula is rather difficult and time consuming. In contrast to the RDI in which conidia suspension is used as inoculum, the conidia can be prepared at ease but they may not survive the field condition. Based on the result of this experiment, root or seed dipping in conidia suspension was used in the upcoming experiment because Favorita would be used as test cultivar.

As regard to the two cultivars tested, it was evident that

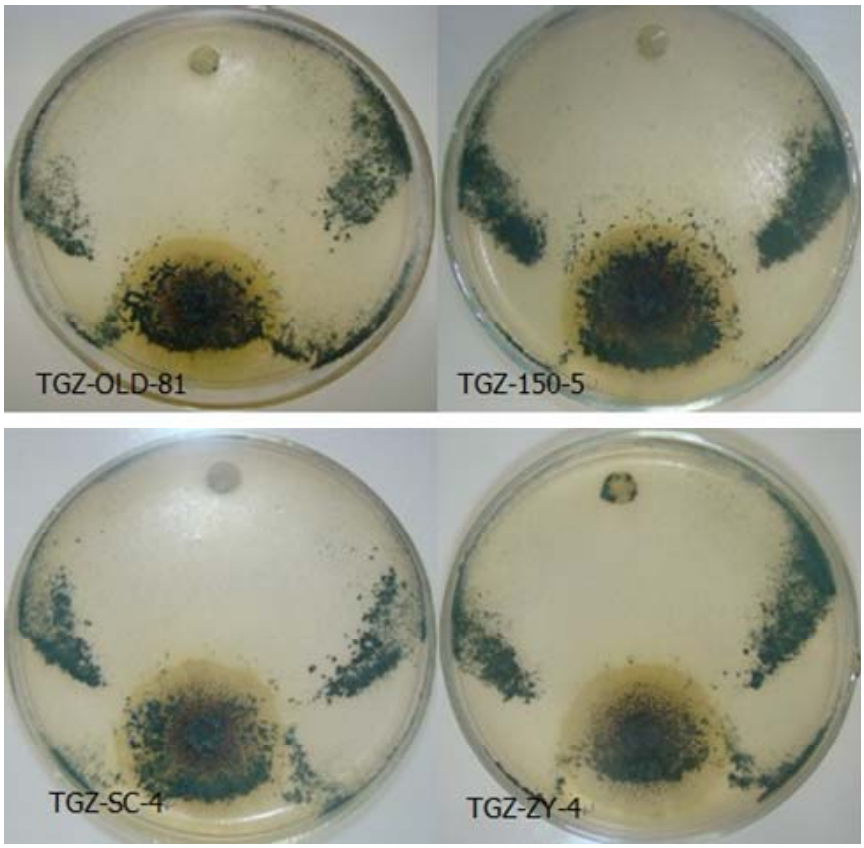

Figure 3. Inhibition of mycelia growth of *Verticillium dahliae* by *Trichoderma* isolates after 4 days.

Table 7. Inhibition of mycelial growth of *Verticillium dahliae* VGZ-HZ-4 and VGZ-XW-1 by 33*Trichoderma* isolates under a dual culture test condition.

***Trichoderma* isolate**	**Mycelial inhibition[1] (%)**		**Average (%)**
	VGZ-HZ-4	**VGZ-XW-1**	
TGZ-SC-4	38.98^{a}	37.76^{abd}	38.37^{a}
TGZ-150-5	36.51^{abc}	40.20^{a}	38.36^{a}
TGZ-150-33	35.26^{abcd}	38.98^{ab}	37.12^{ab}
TGZ-OLD-81	37.76^{ab}	35.26^{bcd}	36.51^{abc}
TGZ-150-51	35.26^{abcd}	37.76^{abc}	36.51^{abc}
TGZ-ZY-4	36.51^{abc}	35.26^{bcd}	35.89^{abcd}
TGZ-150-38	33.98^{bcde}	37.76^{abc}	35.87^{abcd}
TGZ-150-55	32.69^{cde}	38.98^{ab}	35.84^{abcd}
TGZ-150-37	36.51^{abc}	33.98^{cde}	35.24^{bcd}
TGZ-NKY-5	35.26^{abcd}	33.98^{cde}	34.62^{bcd}
TGZ-150-41	33.98^{bcde}	35.26^{bcd}	34.62^{bcd}
TGZ-150-4	35.23^{abcde}	33.98^{cde}	34.60^{bcd}
TGZ-NKY-2	36.51^{abc}	32.69^{def}	34.60^{bcd}
TGZ-150-1	33.98^{bcde}	33.98^{cde}	33.98^{cde}
TGZ-150-6	35.26^{abcd}	32.69^{def}	33.98^{cde}
TGZ-HZ-3	32.69^{cde}	35.26^{bcd}	33.98^{cde}
TGZ-150-50	32.69^{cde}	33.98^{cde}	33.33^{def}

Table 7. Contd.

TGZ-CH-3	31.35^{def}	35.26^{bcd}	33.30^{def}
TGZ-CH-2	31.35^{def}	31.35^{defg}	31.35^{efg}
TGZ-CH-4	32.69^{cde}	27.05^{hi}	29.87^{gh}
TGZ-SC-5	28.58^{fg}	30.00^{efgh}	29.29^{ghi}
TGZ-CH-1	28.58^{fg}	30.00^{efgh}	29.29^{ghi}
TGZ-TC-3	25.63^{ghi}	32.69^{def}	29.16^{ghi}
TGZ-SC-3	27.16^{gh}	30.00^{efgh}	28.58^{hij}
TGZ-NKY-1	27.16^{gh}	30.00^{efgh}	28.58^{hij}
TGZ-TC-4	27.05^{gh}	30.00^{efgh}	28.52^{hij}
TGZ-NKY-7	24.10^{hij}	32.69^{def}	28.39^{hij}
TGZ-TV-1	22.40^{ij}	31.35^{defg}	26.87^{ijk}
TGZ-ZY-2	25.63^{ghi}	27.16^{hi}	26.39^{jk}
TGZ-TV-2	22.40^{ij}	28.58^{ghi}	25.49^{k}
TGZ-TV-3	20.44^{j}	30.00^{efgh}	25.22^{k}
TGZ-NKY-8	24.10^{hij}	25.63^{i}	24.86^{k}
TGZ-NKY-3	22.40^{ij}	27.16^{hi}	24.78^{k}
Average	30.91	32.93	31.92
F-test	**	**	**
CV (%)	8.29	6.68	5.65

[1]Means in the same column followed by different letters are statistically different at P≤0.05 by DMRT. The inhibition percentage was calculated at 3 days after the incubation.

Table 8. Microsclerotia germination (MG) and disintegration (MD) of *Verticillium dahliae* by isolates of *Trichoderma*.

***Trichoderma* isolate**	**VGZ-HZ-4**		**VGZ-XW-1**	
	MG	**MD**	**MG**	**MD**
TGZ-150-51	0	100	0	100
TGZ-OLD-81	0	100	0	100
TGZ-150-5	0	100	0	100
TGZ-150-37	0	100	0	100
TGZ-ZY-4	0	100	0	100
TGZ-NKY-2	0	100	0	100
TGZ-NKY-5	0	100	0	100
TGZ-150-33	0	100	0	100
TGZ-SC-4	0	100	0	100
TGZ-150-6	0	100	0	100
Control[1]	100	0	100	0

[1]Paper discs containing *V. dahliae* microsclerotia immersed in 75% EtOH for 3 min followed by 1% NaOCl for 5 min.

Favorita was highly susceptible while Hui-2 was highly resistant to *V. dahliae*. The response observes in the experiment had confirmed what had been observed in the field. Favorita, although the most popular and widely grown in Guizhou always had bad records with *Verticillium* wilt. It was also reported to be susceptible to *Phytophthora imfestans.* From results of this experiment growing Favorita should be discouraged in Guizhou and be replaced by Hui-2. It is interesting to note that Hui-2 had 100% survival when inoculated with conidia suspension of many *V. dahliae* isolates when those isolates caused 100% wilt incidence in Favorita inoculated in the same way. The wilt incidence found on Hui-2 mainly came from the result of MI. There should be

further investigation to find out why Hui-2 was susceptible when inoculated with microsclerotia but resistant to infection by conidia.

The 21 *Trichoderma* isolates obtained from the soil samples and 11 single-spore isolates obtained from re-isolation of the TGZ-150 isolate preserved at GZIPP could inhibit mycelial growth of both VGZ-HZ-4 and VGZ-XW-1 *V. dahliae* isolates but with different degree of efficacy. Most of the single-spore isolates and the TGZ-OLD-81 isolate had higher than the average mycelial inhibition percentage of all test isolates. Among them, only TGZ-SC-4 isolates from Shuicheng soil had a better efficacy than that of the GZIPP isolates. This isolate, TGZ-OLD-81 and most single-spore isolates could overgrow the *V. dahliae* within two days at 28°C. The selected 10 isolates of this group could be 100% disintegrate the *V. dahliae* microsclerotia. The rapid growth of *Trichoderma* over *Verticillium* suggests that competition for space and nutrients could be one of the mechanisms implied in the antagonist action of Trichoderma in this essay. Both mycelia inhibition and microsclerotia disintegration are important mode of actions in controlling fungal disease (Hartman et al., 1981; Papavizas, 1985) apart from other mechanisms such as mycoparasitism (Papavizas, 1985; Harman et al., 2004; Mishra, 2010) and antibiosis (Papavizas, 1985). Considering microsclerotia an important source of initial inoculum, the ability of *Trichoderma* isolates to disintegrate them should be most desirable as a biocontrol agent.

Conclusion

The results of this experiment could be concluded at this point that the most effective *Trichoderma* isolates for controlling *Verticillium* wilt in potato are TGZ-150-5 and TGZ-ZY-4. There should be further investigation on field application of these two strains before they could be recommended for commercial use in the near future.

Conflict of Interests

The author(s) have not declared any conflict of interests.

ACKNOWLEDGEMENTS

The authors wish to express our special thanks to the Suranaree University of Technology, Thailand for providing the partial grant support. Also, this research is partial support by funds from the Guizhou Academy of Agricultural Sciences in China and Science and Technology Department of Guizhou Province [QKHNGZ(2007)4007] and [QNKH(08017)].

REFERENCES

Akinbode OA, Ikotun T (2011). Potential of two *Tricroderma* species as antagonistic agents against *Colletotrichum destructivum* of cowpea. Afr. J. Mocrobiol Res. 5(5):551-554.

AlstrÖm S (2001). Characteristics of bacteria from oilseed rape in relation to their biocontrol activity against *Verticillium dahlia*.Phyto., 149:56-2001.

Brunner K, Zeilinger S, Ciliento R, Woo SL, Lorita M, Kubicek CP, Mach RL (2005). Improvement of the fungal biocontrol agent *Trichoderma atroviride* to enhance both antagonism and induction of plant systemic disease resistance. Appl. Eniviron. Microbiol. 71(7):3959-3965.

Buensanteai N, Mukherjee PK, Horwitz BA, Cheng C, Dangott LJ, Kenerley CM (2010). Expression and purification of biologically active *Trichoderma virens* proteinaceous elicitor Sm1 in *Pichia pastoris*. Protein Expr. Purif. 72(1):131-138.

Chet I, Baker R (1981). Isolation and biocontrol potential of *Trichoderma hamatum* from soil naturally suppressive to *Rhizoctonia solani*. Phytopathol. 71:281-290.

Cirulli M (1981). Attuali cognizioni sulla verticilliosi dell'olivo. Informatore Fitopatologio, 3:101-105 (in Italian).

Cook RJ, Baker KF (1982). Biological control of plant pathogens. W.H Freeman San Francisco. p. 433.

Danielson RM, Davey CB (1973) The abundance of *Trichoderma* propagules and the distribution of species in forest soils. Soil Biol. Biochem. 5(5):485-494.

Fobert PR, Despres C (2005). Redox control of systemic acquired resistance. Curr. Opin. Plant Biol. 8:378-382.

Francl LJ, Madden LV, Rowe RC Riedel RM (1990). Correlation of growing season environmental variables and the effect of early dying on potato yield. Phyt. Path. 80:425- 432.

Galletti R, Denoux C, Gambetta S, Dewdney J, Ausubel FM, D Lorenzo G, Ferrari S (2008).The AtrbohD - mediated oxidative brust elicited by oligogalacturonides in Arabidopsis is dispensable for the activation of defense responses effective against *Botritis cinerea*. Plant Physiol.148:1695-1706.

Gamliel A, Austerweil M, Kritzman G (2002). Non chemical Approach to soilborne pest management - organic amendments. Crop Prot. 19:847-853.

Hanson LE (2000). Reduction of Verticillium wilt symtoms in cotton following seed treatment with *Trichoderma virens*. J. Cotton Sci.,4: 224 - 231.

Hartman GE, Chet I, Baker R (1981). *Trichoderma hamatum* effects on seed and seedling diseases induced in radish and peas by *Pythium* sp. or *Rhizoctonia solani*. Phytopathology 70:1167-1172.

Harman GE, Howell CR, Viterbo A, Chet I, Lorito M (2004). *Trichoderma* species - opportunistic, avirulent plant symbionts. Nat. Rev. Microbiol. 2:43-56.

Harman GE (2006). Overview of mechanisms and uses of *Trichoderma* spp. Phythology 96:190-194.

Heil M, Silva Bueno JC (2007). Within-plant signaling by volatiles leads to induction and priming of an indirect plant defense in nature. Proc. Natl. Acad. Sci. USA. 104:5467-5472.

Hjeljord L, Tronsmo A (1998). Trochoderma and Gliocladium - enzymes, biological control and commercial applications (Eds): G.E.Hama & C.P. Kubicek Taylor & Francis Ltd.,London Great Britain, pp. 131-151.

Kexiang G, Xiaoguang L, Yonghong L, Tianbo Z, Shuliang W (2002). Potential of *Trichoderma hazianum* and *T. atrovidie* to control Botryosphaeria berengeriana f.sp.piricola. the cause of apple ring rot. J. Phytopathol. 150:271-276.

Liansheng T, Wweihua W (2000). Control of *Trichoderma* against *Botrytis cinera* of strawberries in greenhouse, Plant Prot. 16(3):294-298.

Maas JL, Draper AD, Galletta GI (1985) Inoculation methods for evaluating *Verticillium* wilt resistance in strawberry germ-tube. Hort Sci. 20:739-741.

Mishra VK (2010). *In vitro* antagonism of *Trichoderma* species against *Pythium aphanidermatum*. J. Phytol. 2(9):28-35.

Mittler R, Vanderauwera S, Gollery M, Van Breusegem F (2004). Reactive oxygen gene network of plants. Trends Plant Sci. 9:490-498.

Mpofu SI, Hall R (2002). Effect of annual sequence of removing or flaming potato vines and fumigating soil on *Verticillium* wilt of potato. Am. J. potato Res. 79:1-7.

Papavizas GC (1985). Trichoderma and Gliocladium: Biology, ecology and potential for biocontrol. Ann. Rev. Phytopathol. 23:23-54.

Rowe RC, Powelson ML (2002). Potato early dying: management challenges in a changing production environment. Plant Disease 86:1184-1193.

SAS Institute (1989). SAS user's guide, version 5. SAS inc., Cary, NC. p. 231.

Schubert P, Fink F (2008). Evaluation of *Trichoderma* spp. as biocontrol agent against wood decay fungi in urban trees. Bio Cont. 45:111-123.

Schubert P, Golldack J, Schwärzel H, Lentzsch P (2008) Pathogenicity in *Verticillium* on strawberry plants. 13th International Conference on Cultivation Technique and Phytopathological Problems in Organic Fruit-Growing: 138-143. Fördergemeinschaft Ökologischer Obstbau e.V., Weinsberg.

Slattery RJ, Eide CJ (1980). Prevalence of Verticillium wilt in potatoes in the Red River valley area of Minnesota. Am. Potato J. 57:293-299.

Steven BC, Gregory DM (2009). Three sequenced legume genomes and many crop species: rich opportunities for translational genomics. Plant Physiol. 151(3):970-977.

Uppal AK, El Hadrami A, Adam LR, Tenuta M, Dayf F (2008). Biological control potato verticillium wilt under controlled and field conditions using selected bacterial antagonists and plant extracts. Biol Control., 44:90-100.

Verma M, Brar SK, Tyagi RD, Surampalli RY, Val´ero JR (2007) Antagonistic fungi, *Trichoderma* spp.: panoply of biological control. Biochem Eng J. 37:1-20.

Wang F, Li F, Wang J, Zhou Y, Sun H (2011). Genetic diversity of the selected 64 potato germplasms revealed by AFLP markers. Mol Plant Breed. pp. 1923-8226.

Williams J, Clarkson JM, Mils PR, Cooper RM (2003). Saprotrophic and mycoparasitic components of aggressiveness of Trichoderma harzianum groups toward the commercial mushroom Agaricus bisporus. Appl. Environ. Microbiol. 69(7):4192-4199.

Zamanian S, Shahidi GH, Saadoun (2005). Report of antibacterial properties of a new strain of Streptomyces plicatus (strain 101) against *Erwinia carotovora* subsp. *carotovora* from Iran. Biotechnol. 4:114-120.

academicJournals

Vol. 13(33), pp. 3413-3425, 13 August, 2014
DOI: 10.5897/AJB2013.13450
Article Number: C85924C46625
ISSN 1684-5315

http://www.academicjournals.org/AJB

African Journal of Biotechnology

Full Length Research Paper

Adsorption of essential oil components of *Lavandula angustifolia* on sodium modified bentonite from Nador (North-East Morocco)

M. EL MIZ[1]*, S. SALHI[1], A. EL BACHIRI[1], J. P. WATHELET[2] and A. TAHANI[1]*

[1]LACPRENE, Bloc de recherche 2ème étage, Faculté des Sciences Oujda, Université Mohamed 1[er], Route de Sidi Maâfa, BP 524-Oujda- Morocco.
[2]Gembloux Agricultural Faculty - FUSAGx. Unité de Chimie générale et organique. Passage des Déportés 2. B-5030 Gembloux, Belgium.

Received 5 November, 2013; Accepted 26 May, 2014

The analysis of essential oil has basically one technical goal: to achieve the best possible separation performance by using the most effective, available and current technology of chromatography. The present work aimed to study the formulation created by the adsorption of active components of *Lavandula angustifolia* essential oil on sodium modified bentonite. Essential oils were obtained from dried leaves of *L. angustifolia*; they were extracted by hydro distillation and were analyzed by gas chromatography-mass spectrometry (GC-MS) and gas chromatography flame ionization detector (GC-FID). The retention indices (RI) were calculated for each detected component. Besides, the characterization of the individual components making up the oils was performed with the use of a mass spectrometry (MS) library. The quantitative analysis was made by GC-FID. The identified components accounted for more than 95% for each essential oil. The results of these studies show that organic contaminant adsorption is dependent, to some degree, on solid-liquid ratio and the competition system of mixture. The adsorption amount of terpenics and the others components could be the results of many factors. The selectivity was affected by the abundance of each component in the crude essential dependent on the particle size fractions; the finer fractions adsorbed higher amounts. The selectivity of adsorption was affected by the polarity of terpenic components.

Key words: Clays, bentonite, essential oil, adsorption, *Lavande angustifolia*.

INTRODUCTION

Clays are widely used in pesticide formulation as adsorbents or particulate fillers. Many researchers studied the adsorption of pesticide on clay material (Lagaly, 2001) to limit pest damages. Therefore, the common method used to prevent stored products from insect attacks is the one that make use of synthetic insecticides. The use of such insecticides is increasing year after year. It is evident that the intensive and

*Corresponding authors. E-mail: elmiz.mohamed@gmail.com, abdesstaha@yahoo.fr.

uncontrolled use of chemical insecticides has direct effect on consumers and on the environment. Therefore, there is a need to develop environment friendly products that present less dangerous effect on both the environment and the consumer.

Essential oils of aromatic plants currently used are considered to be a good tool to prevent insect attacks on stored grains (Ngamo et al., 2007). The most important difficulty to popularise this new tool is to produce a new formulation of a chemical active insecticide with moderate persistence (Lajide et al., 1995; Keita et al., 2001). Due to the higher volatility of essentials oils, the duration of their activities is very short. The local material suitable for the formulation of the essential oils seemed to be bentonite type clay. It is cited as good adsorbent and is currently used in medicine, in cosmetics and in other insecticide. Yet, there are no adsorption studies of terpenic compounds on this clay material.

Clays, used in different fields of application such as ceramics, paper, paint, barrier, adsorbent, catalyst are among the most important industrial raw materials (Grim and Güven, 1978; Murray, 2000; Bergaya and Vayer, 2006). These clays are composed of minerals belonging generally to the clay stone groups. They are used either in the natural state or treated by various methods to improve some of their characteristics.

This paper presents the study of the adsorption of active components of *Lavandula angustifolia* essential oil on sodium purified bentonite. *L. angustifolia* is an important member of Lamiaceae family. It is an indigenous plant of the Mediterranean South Region, tropical Africa and the Southeast Regions of India. The genus includes annuals, herbaceous plants and small shrubs, having aromatic foliage and flowers.

It is cultivated in France, Spain and Italy. Among these plants, the most common species believed to have medicinal value are *Lavandula dentata*, *L. angustifolia*, *Lavandula latifolia*, *Lavan-dula intermedia*, *Lavandula stoechas* and *Lavandula dhofarensis* (Hanamanthagouda et al., 2010). Lavender's essential oil is popular as a complementary medicine in its own right and as an additive to many over the counter complementary medicine and cosmetic products (Muyima et al., 2002). These have been used for centuries as a therapeutic agent, with the more recent addition; the essential oils derived from these plants were widely used as an antibacterial in World War I (Cavanagh and Wilkinson, 2005).

Lavandula essential oils are obtained from the flowering tips of the plants *L. angustifolia* (lavender). These essential oils have a popular and easily recognisable fragrance. Pure *L. angustifolia* essential oils are used in aromatherapy, and are thought to have calmative, anti-flatulence, and anti-colic properties (Lis-Balchin and Hart, 1999).

Lavandula essential oil contains various components depending on the species, but there is usually linalyl acetate and linalool, geraniol, pinene, cineol, coumarin and ethylamyl-cetone (behind its refreshing scent). Lavender essential oil used in this study is the *angustifolia* type, from Al Hoceima (North region of Morocco).

MATERIALS AND METHODS

Plant material (*Lavandula angustifolia*) and hydrodistillation procedure

The air dried material (200 g) was hydrodistilled in a Clevenger like apparatus for 2 h and the essential oil was collected and analyzed by gas chromatography-mass spectrometry (GC-MS).

Chromatographic analysis of essential oil

The GC-MS analyses were done using a HP-6890 Series II instrument equipped with Agilent 19091S-433 and HP-5 capillary columns (30 m 0.25 mm, 0.25 um film thickness), working with the following temperature program: from 60°C for 1 min to 240°C for 10 min hold time, ramp of 10°C/min up to 220°C; injector and detector temperatures 280°C; injector Split/splitless N°7673, detector MSD (transfer line heater), carrier gas helium (1.2 ml/min); with splitless mode and the pressure in the column was 0.629 Bar.

Quantitative results were obtained using GC-FID, HP 6890 series, with the same type of column, the same parameters and the same temperature program. The detector temperature was 300°C, the hydrogen and air flows rate are 30 ml/min and 450 ml/min.

The identification of the compounds was made by comparison of the retention time (Rt) and Kovats indices with respect to a series of n-hydrocarbons. The relative proportions of the constituents of essential oils are obtained by GC-FID. Table 1 shows the chemical composition of the essential oil of lavender, and the percentage of each compound.

Preparation of the sodium modified bentonite

The clay samples used for these analyses were collected from Nador (North-East Morocco, North Africa). The bentonite was purified and modified by sodium before it was used. Adsorption isotherms which represent the adsorbed amount versus the equilibrium concentration have been identified for each compound.

Natural clay from North-East Morocco (Nador), was used in a purified form. The clay is an industrial bentonite rich with bentonite clay type. Purification was done by removing all the crystalline phases (quartz, feldspar, calcite, ...), by a preliminary treatment of the raw sample by ionization homo-sodium, and it began first with a series of washings to remove impurities and thereby have a granular fraction of a well defined size $\leq$ 2 microns. The sodium modified clay are subjected to analysis and identification by X-ray diffraction (XRD), infrared spectroscopy (IR) and textural characteristics.

X-ray diffractograms were recorded in a Shimadzu XRD diffractometer D6000 stations working on the monochromatic copper Kα1 radiation (1.54 Å) (Figure 1). Infra red (IR) spectra were acquired using a Shimadzu Fourier Transform spectrometer over a range from 400 to 4000 cm^{-1} with a resolution of 2 cm^{-1}, and the samples were prepared in the form of a dispersion in a vial KBr (1/200 by weight) (Figure 2).

Thermal analysis was carried out in a SHIMATZU D6000 coupled to a DC ampler and temperature controller. Data from DTA-TG were obtained in all cases at a heating rate of 5°C/min between

Table 1. Identification results of the components and the percentage of each compound in essential oil.

Product name	QI	Rt	Surface	C_x (µg/ml)	KI	% in samples
Alpha Pinene	95	10.09	282.35	24.43	942	6.05
Camphene	97	10.40	33.98	2.940	957	0.72
Verbenene	96	10.52	10.88	0.94	963	0.23
Sabinene	81	10.92	22.11	1.91	982	0.47
2-Beta Pinene	97	10.98	924.1	79.96	985	19.81
Limonene	99	11.89	29.03	2.51	1033	0.62
M-Cymene	87	11.97	99.10	8.57	1038	2.12
1,8 Cineole	97	12.03	1092.38	94.52	1041	23.42
Cis Linalol oxide	97	12.75	42.67	3.69	1082	0.91
Alpha Thujone	98	13.04	428.84	37.107	1097	9.19
L-Linalool	94	13.17	155.95	13.49	1105	3.34
(+) Carvone	95	13.25	9.156	0.79	1110	0.19
Perille Alcohol	83	13.35	11.85	1.02	1117	0.25
(Z E) Alpha Farnesene	94	13.46	79.02	6.83	1124	1.69
Fenchol	96	14.31	65.198	5.64	1157	1.39
1-Methyl adamantane	93	14.38	5.557	0.480	1183	0.11
Cryptone	96	14.47	30.81	2.66	1189	0.66
1-Alpha Terpineol	72	14.57	21.28	1.841	1195	0.45
Alpha Campholene Aldehyde	58	14.67	40.32	3.48	1201	0.86
Camphor	98	14.78	215.14	18.61	1209	4.61
1-4-Terpineol	98	14.99	17.09	1.478	1224	0.36
Verbenone	99	15.08	11.12	0.96	1230	0.23
CuminicAldehyde	97	15.42	19.82	1.715	1255	0.42
(+) Carvone	98	15.46	15.34	1.327	1258	0.32
(-) Alpha CampholenicAcid	98	15.58	7.99	0.69	1266	0.17
Trans Alpha Bergamotene	98	18.05	21.94	1.89	1397	0.47
Trans Beta Farnesene	95	18.68	9.96	0.86	1502	0.21
Beta Selinene	96	18.78	31.45	4.082	1509	1.01
Beta Bisabolene	96	18.93	15.68	2.03	1523	0.5
Calarene	92	19.07	11.02	1.43	1535	0.35
1s Cis Calamenene	92	19.18	14.86	1.92	1545	3.91
Cis Alpha Bisabolene	91	19.32	24.11	3.13	1556	6.25
4,7 Dimethyl-1-Tetralone	92	19.46	5.86	0.76	1568	0.104
Beta Eudesmol	94	20.71	7.29	0.94	1678	0.23
14-Norcadin-5-En-4-One Isomer B	93	21.16	5.44	0.707	1707	0.17

Rt retention time; KI, Kovats indices; QI, Quality index of identification by comparison with the spectra library; C_x, Concentration of each compound in samples.

30 and 1000°C under N_2 atmosphere (Figure 3).

The surface areas and the pore volumes of the samples were determined by micrometrics ASAP 2000 volumetric adsorption-desorption apparatus, using nitrogen as adsorbent (Zaitan et al., 2008). In this method, a mass of 1 kg of raw clay was dispersed in 5 L of distilled water with a solid/liquid ratio: 1/5. The mixture was stirred for an hour, until the homogenization full suspension, followed by treatment with HCl (0.5 M) to remove carbonate. The resulting mixture was washed by H_2O_2 (10%) to oxidize organic matter.

The resultant product was then washed extensively (six times) with NaCl 1 M and centrifuged to give saturated clays. The dark grey residue in the centrifuge tube was eliminated because it contained the fraction enriched in impurity (quartz, cristobalite, feldspar …).

The samples were then washed and dialyzed against distilled water until the conductivity in the dialysis bath was less than 2 µS/cm. The granular fraction size ≤ 2 µm were then obtained as bay accurate sedimentation. The air dried clays were gently grounded to give a powder.

Adsorption studies

Adsorption of essential oil by the different bentonite fractions was carried out in batch. Increasing amounts of clay fractions (0.03, 0.067, 0.093, 0.121, 0.159 and 0.206 g) were dispersed in 2 ml oil solution (0.754 mg of oil in 2 ml of solution) and equilibrated in an

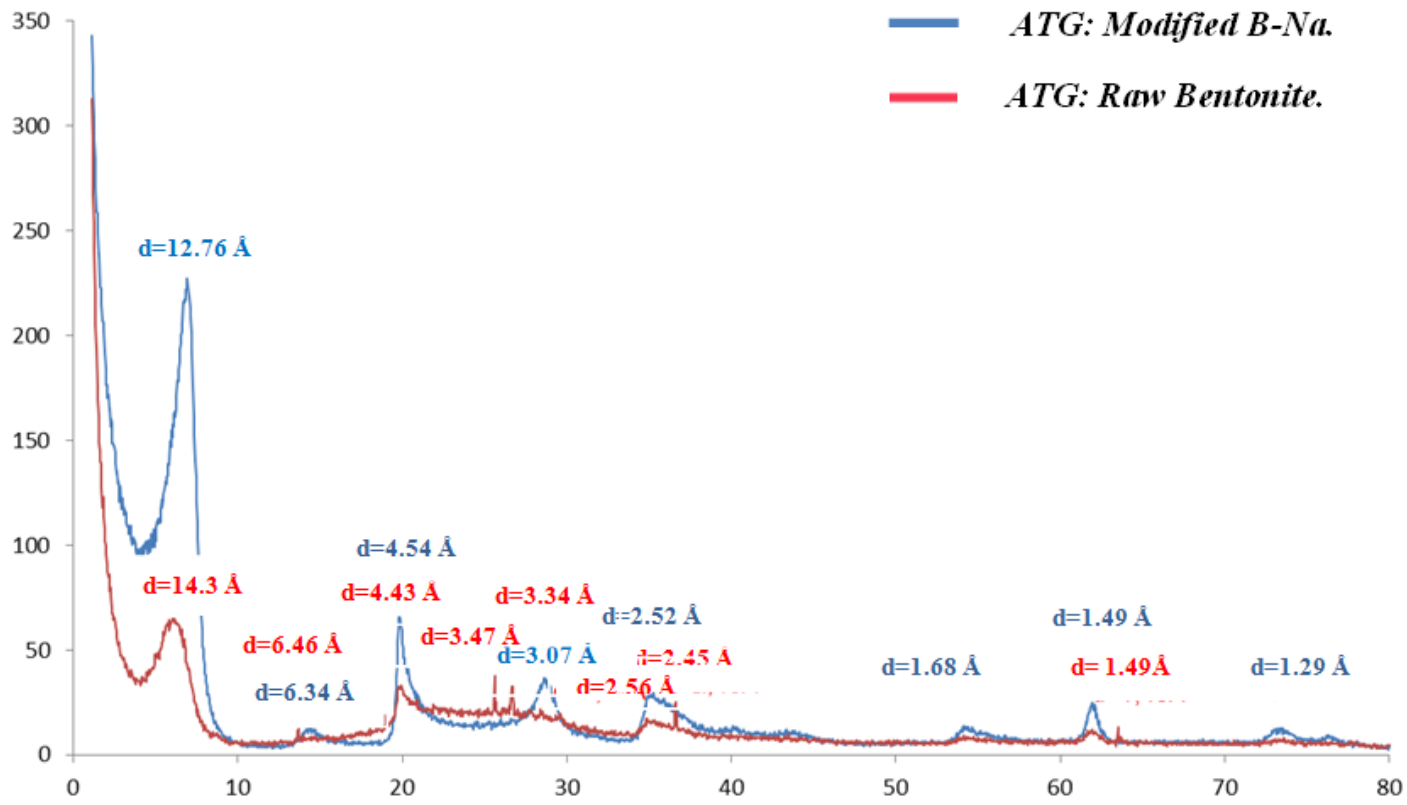

Figure 1. Diffractograms of the fine fraction powder of raw and sodium modified bentonite.

overhead shaker at room temperature (19°C) for 3 h. The particles were allowed to settle and were separated by centrifugation. The essential oil concentration in the supernatant was determined by GC-FID.

Adsorption isotherm

Adsorption isotherms were determined using the peak area of each component of the essential oils (Nguemtchouin et al., 2009). The adsorbed percentage was calculated as:

$$\% \ adsorbed = \frac{100(A0-Ax)}{A0} \quad (1)$$

Where, A_0 is the peak area of each oil component in the initial solution; A_x is the peak area of each component in the supernatant.

The mass concentration of each compound in the initial essential oil has been determined by depending on the peak area of the internal calibrated (BHT).

$$C(\mu g/ml) = \frac{A0 \times Ae}{me} \quad (2)$$

Where, A_0 is the peak area of each oil component in the initial solution; A_e is the peak area of internal calibrates in the initial solution; m_e is mass of the internal calibrated (in 2 ml of initial solution of essential oil).

The amount of each compound adsorbed by clay fractions is:

$$Qn(\mu g/g) = \frac{(ci-cf)\times V}{mc} \quad (3)$$

The percentage of each oil component in the initial solution was calculated as:

$$\%C = \frac{Cx}{Ceo} \times 100 \quad (4)$$

Where, C_i is the concentration of each component in the initial solution and C_{eo} is the concentration of the essential oil in solution. The equilibrium concentration was calculated as:

$$Ce(\mu g/ml) = \frac{Ax}{A0} \times \frac{meo}{Veo} \times \%C \quad (5)$$

Where, V_{eo} is the volume of solution (ml).

RESULTS AND DISCUSSION

Identification of the compounds

The identification of the compounds was made through a comparison of retention time (Rt) and Kovats indices with results obtained by GC-FID. Chromatographic analysis showed that lavender essential oil contains more than 50

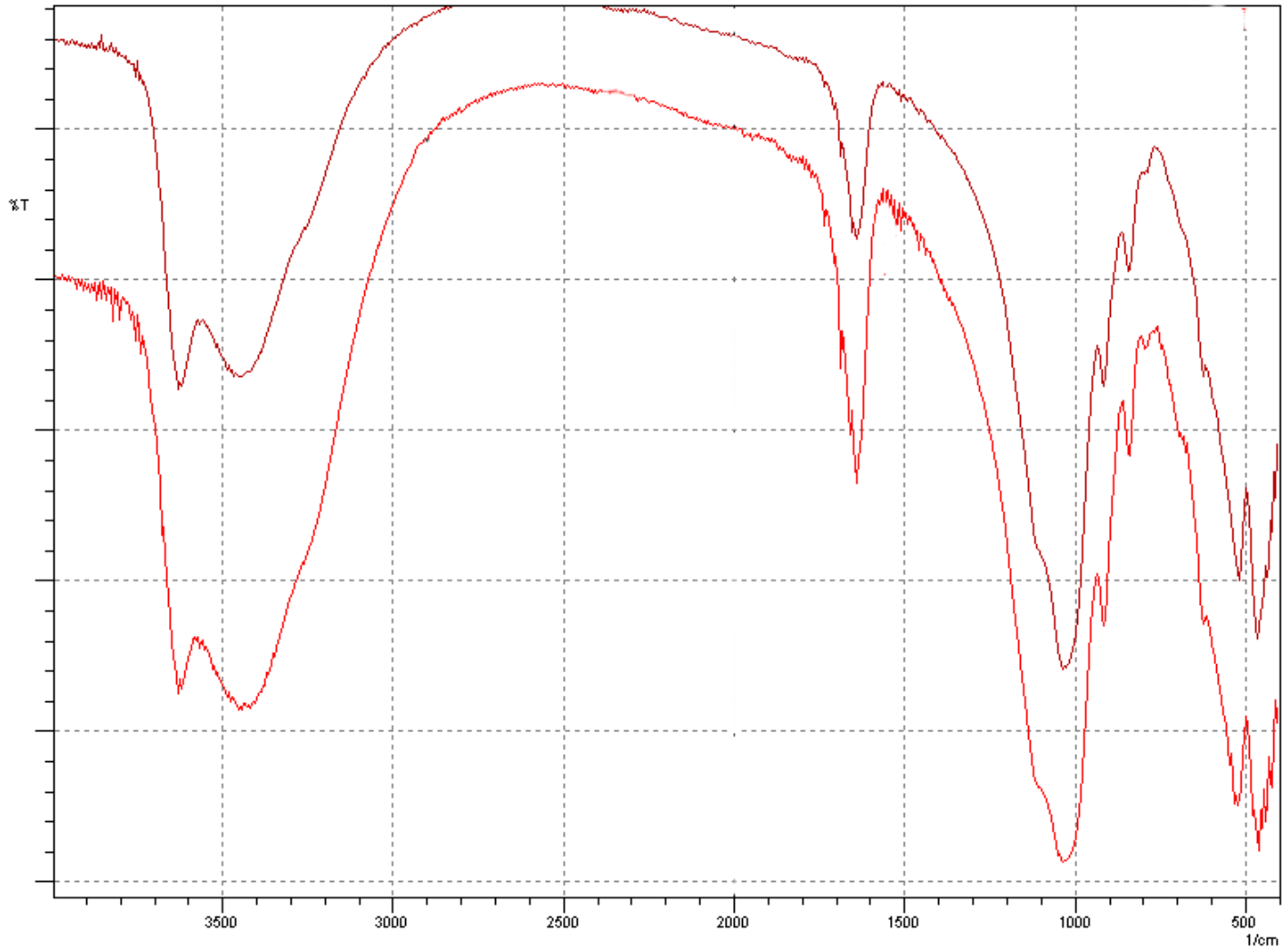

Figure 2. Infra-red of raw and sodium modified bentonite.

components, 35 major compounds of lavender essential oil were selected (the most major components: 1,8-cineole 23.42% and 2-Beta Pinene 19.81%) mono terpene hydrocarbons, MH (α-thujene, α-pinene, sabinene, β-pinene, limonene …), oxygenated mono terpenes OM (Beta Eudesmol, Cis Linalol oxide, 1,8-cineole ……), sesquiterpene hydrocarbon ST, ((+) Carvone, Calarene, Cryptone, Verbenene ……).

Characterization of the bentonite

The major element composition of the investigated clay mineral is presented in Table 2 as % oxides. The main components are SiO_2 (61.17%) and Al_2O_3 (15.13%), with the exception of hectorite, which contains ~ 6% MgO, 4% CaO, Fe_2O_3 (3.25%) and other elements present in minor amounts (K_2O, SO_3, CuO, TiO_2 and ZnO). A small percentage of organic matter (MO = 1.08%) and a percentage of water was estimated to ~ 10.56%.

The fine fraction (≤ 2 µm) was purified and sodium exchanged. The surface areas and the pore volumes of the samples: specific surface S_{BET} = 83.5 m^2g^{-1}, total pore volume V_t = 0.213 cm^3g^{-1}, External specific surface S_{ext} = 81.024 m^2g^{-1}. Its cation exchange capacity, determined by adsorption of a copper ethylene di-amine complex (Amman, et al., 2005; Bergaya and Vayer, 1997), is 107 meq/100 g (ignited) clay. Chemical analyses of the samples are given in Table 1.

The samples of clays were characterized by X ray diffraction (XRD), differential thermal analysis and thermo gravimetric analysis (DTA-TGA) and infrared (I.R). XRD of the purified bentonite powder showed that the latter is of the same family of smectites with reflection (001) located at 12A. The presence of the line (06.33) at d = 1.49 Å showed that it consists of montmorillonite. The

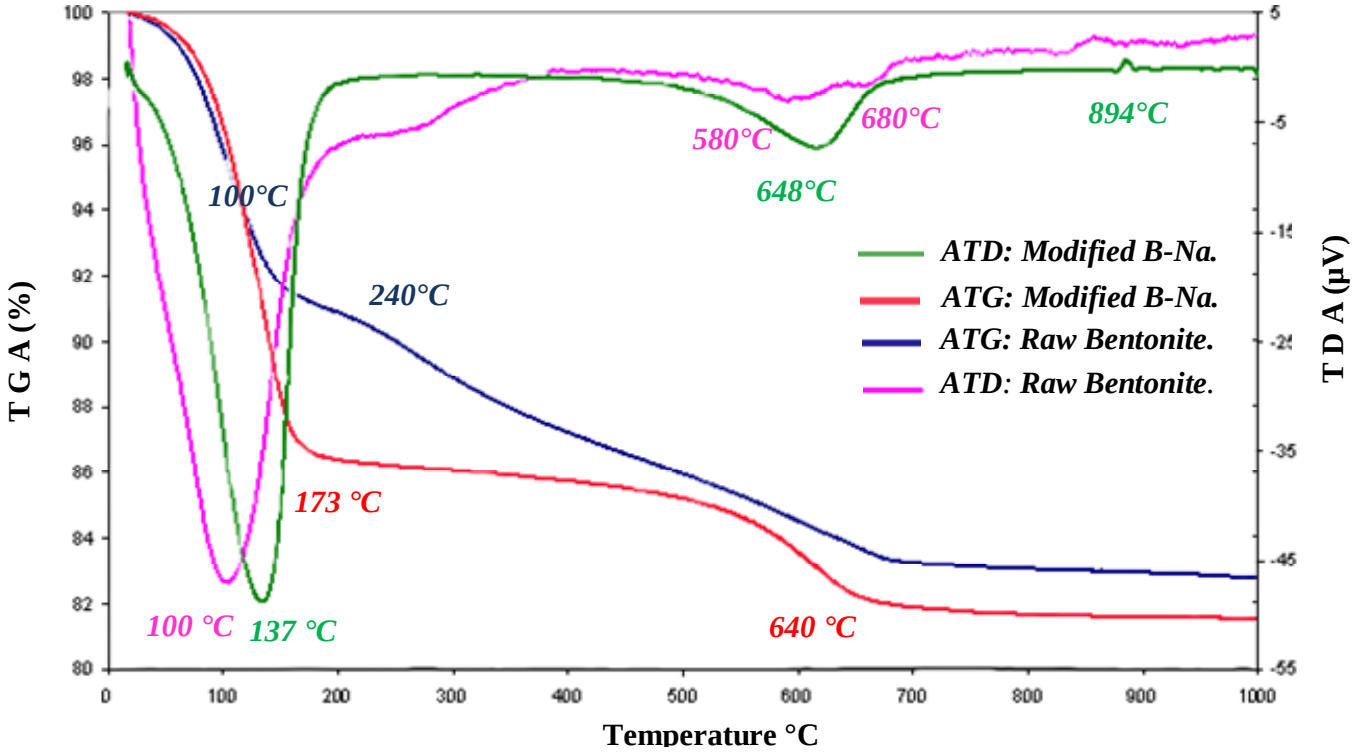

Figure 3. TDA and TGA of sodium modified bentonite.

Table 2. Chemical composition (wt %) of sodium modified and raw bentonite.

Oxide	SiO_2	Al_2O_3	CaO	MgO	Fe_2O_3	Na_2O_2	K_2O	SO_3	CuO	TiO_2	ZnO
Na-B	61.17	15.13	4.00	6.00	3.25	1.1	0.52	0.38	0.13	0.12	0.1
Raw-B	64.05	16.33	4.13	6.69	3.44	1.12	0.65	0.37	0.09	0.1	0.05

presence of crystalline phases in the form of impurities Quartz (Q) d = 3.34 Å was also noted.

XRD of Brute and purified bentonite powder shows that bentonite is of the same smectite family with reflection (001) at 14a. This shows that natural bentonite is a calcium form. The presence of the line (06.33) at d = 1.49 Å shows that it consists of montmorillonite. It is also noted that there is presence of crystalline phases in the form of impurities Quartz (Q) d = 3.34 Å. Examination of the infrared absorption spectra of the crude and purified samples of bentonite shows absorption bands that are presented as follows (Farmer, 1979; Salerno et al, 2001).

The spectra show two absorption bands between 3200 and 3800 cm^{-1} and between 1600 and 1700 cm^{-1}. The tape that lies between 1600 and 1700 cm^{-1} is attributed to stretching vibrations of the OH group constitution water plus the vibration binding adsorbed water. The band in the range 3200-3800 cm^{-1} with a strong peak at the shoulders 3435 and 3621 cm^{-1} characterize the montmorillonite and correspond to stretching vibrations of the OH groups of the octahedral layer is coordinated with Al + Mg (3640 cm^{-1}) or Al 2 (3600 cm^{-1}).

The deformation vibrations of H_2O molecules are characterized by the band 3400 cm^{-1}. The band, centered around 1630 cm^{-1}, is assigned to the deformation vibrations of H_2O molecules adsorbed between the sheets.

The intense band situated between 900 and 1200 cm^{-1} and centered around 1040 cm^{-1} corresponds to stretching vibrations of Si-O bond. In the purified clay (Na-montm), it is situated around 1030 cm^{-1} between 1115 and 1020 cm^{-1}. The bands situated at 425, 525 and 468 cm^{-1} are assigned respectively to the deformation vibration of Si-O- Al bonds, Si-O and Si-Mg-Fe-O.

Examination of the thermal analysis curve of the purified sodium bentonite, shows, in the field of low temperatures, the existence of a 137°C intense endothermic phenomenon, this phenomenon is linked to the starting zeolite and the hygroscopic water of bentonites. Mass loss that accompanied these thermal accidents is

very important; it is ~13.54% of the initial mass. Another endothermic phenomenon of low intensity occurs at a temperature of 640°C. It corresponds to the departure of the structural water. The mass loss associated with this phenomenon is ~3.62% of weight. The differential thermal analysis (DTA) curve also exhibits an exothermic accident to 894.25°C due to the crystallization of the bentonite.

The DTA curve relating to the Brute bentonite presents two endothermic phenomena at 100 and 240°C. This duplication is due to the presence of two types of water molecules, these are respectively hygroscopic and zeolitic water. Two other endothermic phenomena of low intensity occur in the area of average temperature 580 and 680°C correspond respectively to the strongly retained water and water of constitution. The DTA curve also shows a broad exothermic accident in the temperature range of 820 and 930°C.

Adsorption isotherms

Adsorption isotherms of *L. angustifolia* components are shown in Figure 4, Adsorption decreased in the order:

2-beta pinene > alpha thujon > camphor > L- linalool > fenchol > (Z E) alpha farnesene > alpha pinene > Cis linalool oxide > Trans alpha bergamotene > camphene > pirille alcohol > 1-Cis calamenene > beta eudesmol > Trans beta farnesene > 4-7 dimethyl 1 tetra lone.

The other compounds are: sabinene, (+) carvone, 1-methyl adamantine, cryptone, 1-alpha terpineol, alpha campholene aldehyde, 1-4 terpineol, verbinone, cuminic aldehyde, (-) alpha campholenic acide, beta selinene, 1-4 norcadin-5-ene-4-one isomer B show a total adsorption of sodium on bentonite.

The adsorption isotherms also show the existence of an over saturation for 2-beta pinene and 1-8 Cineol which have the highest concentrations. The same phenomenon is observed for pirille alchool, 4-7 dimethyl tetra-lone and Beta eudesmol, over saturation of the last three is due to the saturation of all active sites by other most concentrated components as the 2-bêta pinene, 1-8 Cineol… The rest of the components as: verbenene, Limonene, M-cymene, beta bisabolene, calarene and Cis alpha bisabolene, have no affinity for the bentonite; thus, their adsorption is very low.

This adsorption amount of terpenics and the other components could be a result of many factors. The selectivity was affected by the abundance of each component in the crude essential oil: 2-beta pinene, alpha thujon, camphor, L-linalool, fenchol (Z E) alpha farnesene; these were the most adsorbed compounds as they were the most abundant ones.

The selectivity of adsorption was affected by the polarity of terpenic components: 2-beta pinene 1-8 cineol and alpha thujon were adsorbed in larger amounts than some others mono-terpene hydrocarbons (Figure 4).

Langmuir and Freundlich models

Under ideal saturated conditions, the solid liquid ratio should not influence the amount of organic or inorganic molecules adsorbed per unit of adsorbent. However, some interested studies have (Puls, et al., 1991) shown that both organic and inorganic contaminant adsorption is dependent on solid-liquid ratio to some degree and the competition system of mixture.

In order to optimize the design of an adsorption system and to optimize the use of capsules in various formulations, it is important to establish the most appropriate correlation for the equilibrium curves (Allen and Mckay, 1987).

In this respect, the equilibrium experimental data of the adsorption of each component in the crude essential oil on clays were studied using Freundlich and Langmuir models. The Freundlich model (Van Bemmelen, 1888) and (Freundlich, 1909) is an empirical equation employed to describe heterogeneous systems; characterized by the heterogeneity factor nf, describes reversible adsorption, and is not restricted to the formation of the monolayer (Ho and Mackay, 1998).

The Langmuir equation model assumes that the solid adsorbent has a limited adsorption capacity (q_m), all the active sites are identical, they are only a complex of solute-molecule (monolayer adsorption) and that there is no interaction between the adsorbed molecules.

Freundlich:

$$q_e = K_F C_e^{1/n} \quad (6)$$

$$Log\ qe = Log\ KF + n\ Log\ Ce \quad (7)$$

Another use of the results by the Freundlich isotherm is to draw logarithmic scale variations in the distribution coefficient K_d according to q_e

$$Log\ Kd = \left(\frac{1}{n}\right) Log\ KF + \left[\frac{(n-1)}{n}\right] Log\ qe \quad (8)$$

The Langmuir model has two linear forms:
Form I:

$$\frac{Ce}{qe} = \frac{1}{KL\,qm} + \left(\frac{1}{qm}\right) Ce \quad (9)$$

Form II:

$$\frac{1}{qe} = \frac{1}{qm} + \frac{1}{qm*KL*Ce} \quad (10)$$

(a) Total adsorption

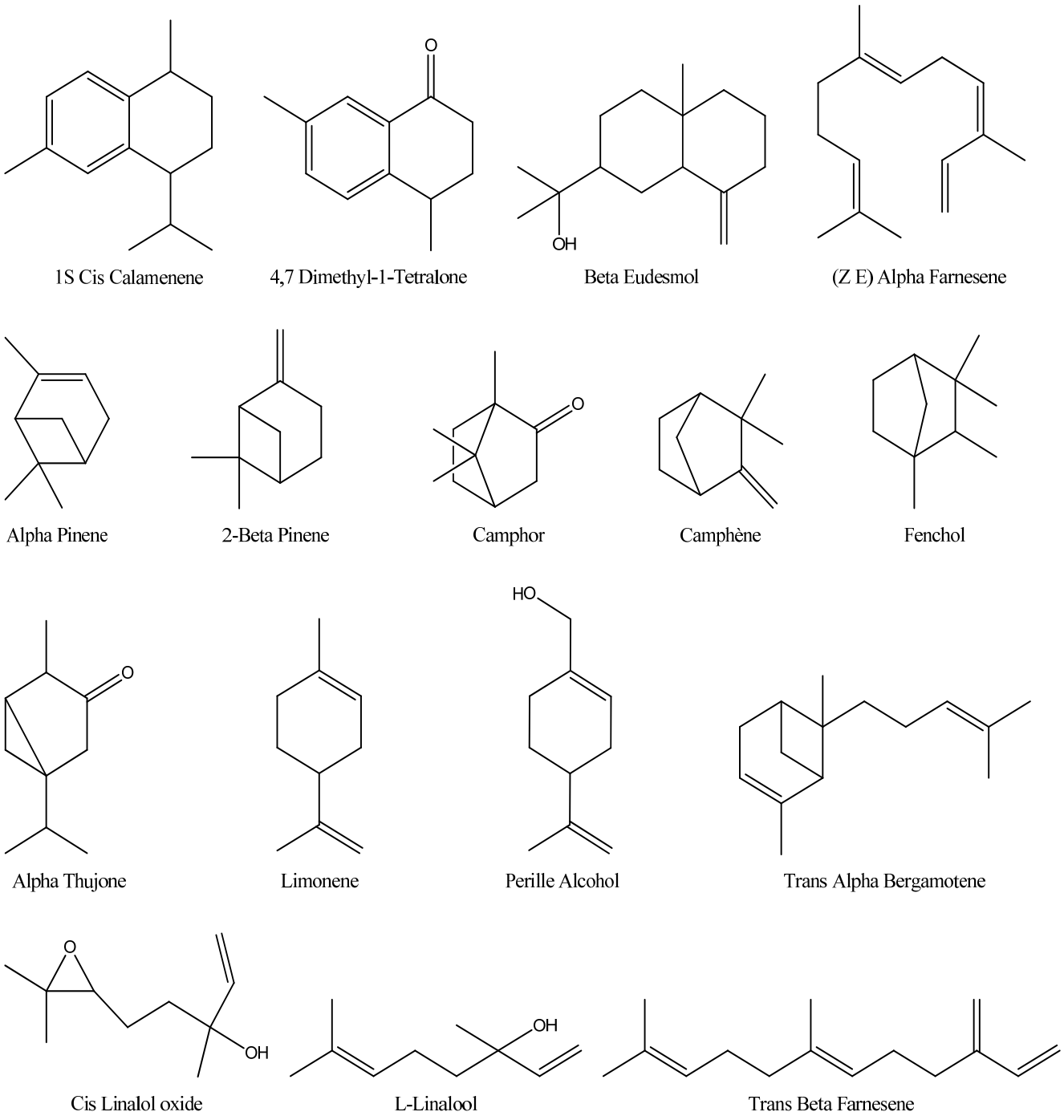

Figure 4. (a) Major components in *Lavandula angustifolia* essential oil with adsorption isotherms. **(b)** Major components in *Lavandula angustifolia* essential oil with total adsorption.

C_e and qe are the equilibrium concentration and amount adsorbed, K_L is a direct measure for the intensity of the adsorption process or related to the heat of adsorption (dm^3 mg^{-1} or $L.mg^{-1}$), and q_m is a constant related to the

(b) Adsorption isotherms

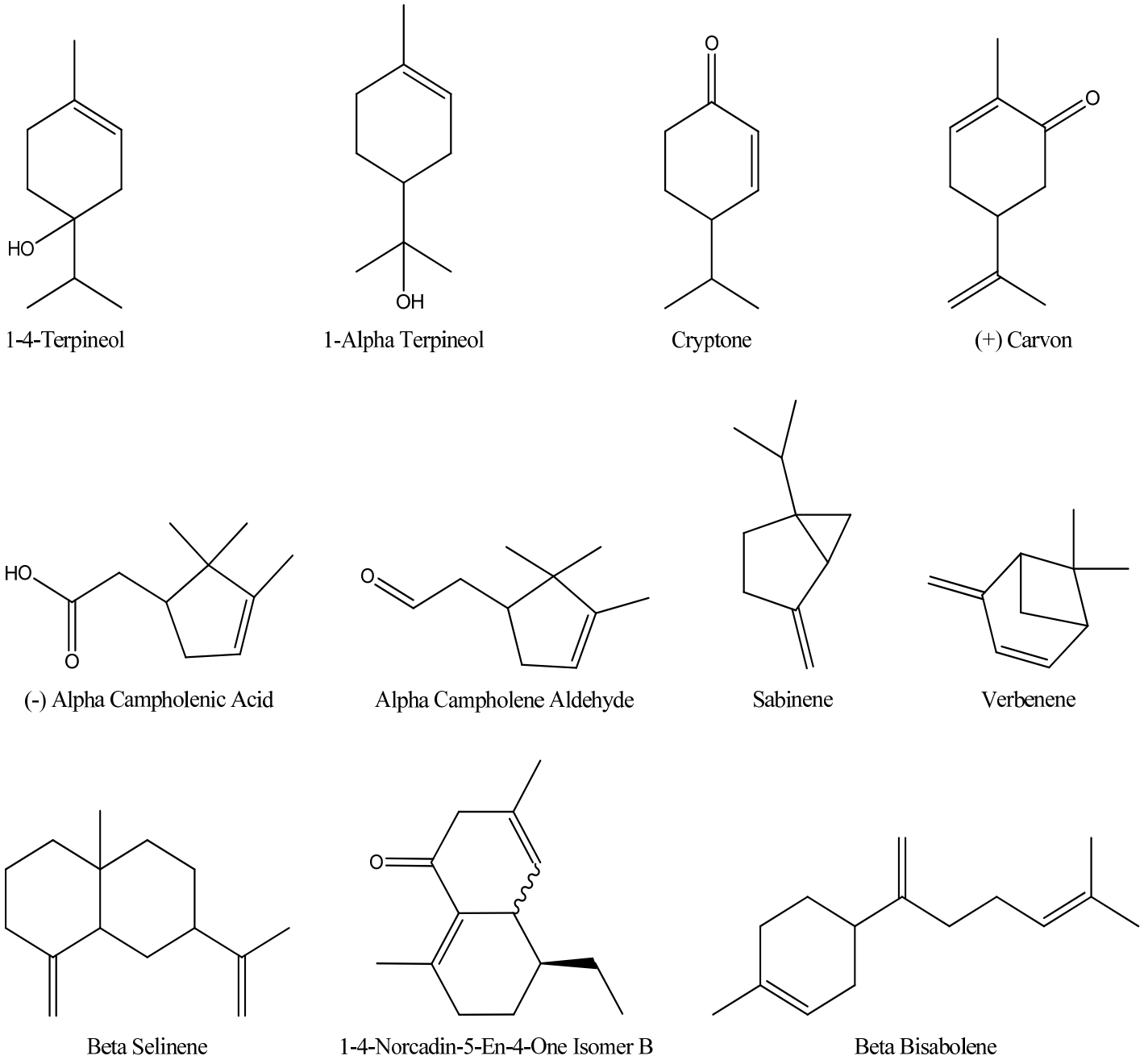

Figure 4 Contd.

area occupied by a monolayer of absorbate, reflecting the limiting adsorption capacity (mg g^{-1}). A plot of C_e/q_e vs C_e, q_m and K_L can be determined from the slope and intercept. K_F is a constant for the system, related to the bonding energy.

K_F can be defined as adsorption or distribution coefficient and represents the quantity of each compound adsorbed onto adsorbents for a unit equilibrium concentration (dm^3 $mg^{-1})^{1/n}$ or (mg g^{-1}) In accordance with (Hasley, 1952), the relationship between K_F and q_m is:

$$K_F = q_m / C_0^n \quad (11)$$

(qm) is the maximum adsorption capacity. The slope 1/n, ranging between 0 and 1, is a measure for the adsorption intensity or surface heterogeneity (Haghseresht, 1998). A

Table 3. Langmuir and Freundlich adsorption constants of *Lavandula angustifolia* oil on sodium modified bentonite.

Compound	Model						
	Freundlich			Langmuir			
	n	K_F	R^2	K_L	$q_{m\ (theo)}$	$q_{m\ (exp)}$	R^2
1 Cis Calamenene	0.255	17.939	0.7032	139.314	12.225	12.24	0.98562
1-8 Cineol	4.051	1.445	0.83265	0.541	1207.318	1235.48	0.14605
2 -β-pinene	0.513	2090.084	0.63727	3.262	2684.139	1506.143	0.5378
4 7 Dimethyl	6.832	$5.1\ E^{+11}$	0.68509	148.214	11.206	7.154	0.11826
α-Pinene	3.582	12.819	0.99216	4.032	130.548	147.9	0.62173
α-Thujon	0.0744	1102.196	0.69709	313.374	1111.569	1107.82	0.99994
β-eudesmol	1.672	2484.607	0.75252	25.548	23.579	8.5049	0.0528
Camphene	2.838	3518.183	099214	7.279	39.479	31.56	0.05866
Camphor	1.678	$2.1651E^{+5}$	0.93528	42.234	719.424	669.68	0.97415
Cis Linalool Oxide	0.147	85.031	0.7147	175.412	68.966	67.88	0.99687
Fenchol	1.093	4445.555	0.92506	18.930	298.507	185.039	0.43408
Linalool	0.353	795.594	0.94472	333.749	272.480	362.03	0.95582
Pirille alchool	3.047	$1.593E^{+6}$	0.75589	1405.113	25.867	18.21	0.79193
Trans α-Bergamotene	0.449	157.524	0.99268	242.491	39.904	40.269	0.92397
Trans β- farnesene	0.084	9.923	0.62409	1085.549	8.006	7.569	0.99547
Z E α-farnesene	0.04	184.485	0.9988	176.1109	177.620	177.649	0.99989

K_F, Adsorption or distribution coefficient; R^2, Freundlich model and correlation coefficients; K_L, direct measure for the intensity of the adsorption process or related to the heat of adsorption; $q_{m\ (theo)}$ and $q_{m\ (exp)}$, limited adsorption capacity.

value for 1/n below one indicates a normal Langmuir isotherm while 1/n above one is indicative for a cooperative adsorption (Fytianos et al., 2000).

A plot of Lnq_e vs. C_e enables the empirical constants K_F and 1/n to be determined from the intercept and slope of the linear regression. The two common isotherm models have been tested in the present study: Langmuir and Freundlich models. Applicability of the isotherm equations was compared in Table 3 by judging the correlation coefficients, R^2:

The plot of Ln qe vs. Ln Ce according to the Freundlich model and correlation coefficients (R^2) indicates that adsorption isotherm is linear for: 1-8 Cineol, 2-Beta pinene, 4-7 di-methyl-tetralone, Alpha Pinene, Beta eudesmol, camphene, Fenchol and Trans alpha Bergamotene. But the sorption behaviour of others compounds does not conform to this model. The Langmuir model was also fit for describing the sorption behaviour of *L. angustifolia* essential oil. The coefficients (R^2) for Langmuir model shows that the sorption of: 1-Cis Calamenene, alpha Thujon, camphor, Cis Linalool oxide, L-Linalool, Pirille alcohol, Trans beta farnesene and (Z E) alpha farnesene can conform to the Langmuir model.

Considering some individual components, they presented the highest adsorption capacity for 2-beta pinene with qm = 1506.143 ug/g et K_L = 3.262, K_F = 2090.084 and n = 0.513 puis 1-8 Cineol with qm =1235.48 ug/g, K_L = 0.541, K_F = 1.445 and n = 4.051. α-Thujon, with qm = 1107.82 ug/g, K_L = 313.374, K_F = 1102.196 and n = 0.0744.

We also note that the values of $qm_{(exp)}$ are compatible with the values of $qm_{(theo)}$ especially for compounds that follow the Langmuir model as:

1-Cis calamenene (qm_{theo}= 12.225 ug/g and qm_{exp} = 12.24 ug/g), 1-8 Cineol (qm_{theo}= 1207.318 ug/g and qm_{exp} = 1235.48 ug/g), 4-7 dimethyl tetralone (qm_{theo}= 11.206 ug/g and qm_{exp} = 7.154 ug/g), α-Thujon (qm_{theo}= 1111.569 ug/g and qm_{exp}=1107.82 ug/g), Cis linalool oxide (qm_{theo}= 68.966 ug/g and qm_{exp} = 67.88 ug/g), Trans α-Bergamotene (qm_{theo}= 39.904 ug/g and qm_{exp} = 40.269 g/g), Trans β- farnesene (qm_{theo} = 8.006 ug/g and qm_{exp} =7.569 ug/g) (Figures 5, 6, 7 and 8).

Conclusion

The terpenes: 2-beta pinene, alpha thujon, camphor, L-linalool, 1-8 cineol was absorbed by bentonite in higher amounts than others mono-terpenes. The adsorption amount of terpenics and the other components was a result of many factors.

The selectivity was affected by the abundance of each component in the crude essential oil depended on the particle size fractions; the finer fractions adsorbed higher amounts. The selectivity of adsorption was affected by the polarity of terpenic components; 2-beta pinene 1-8 cineol and alpha thujon were adsorbed in larger amounts than some other monoterpene hydrocarbons. The adsorption isotherm of the terpenic compound on

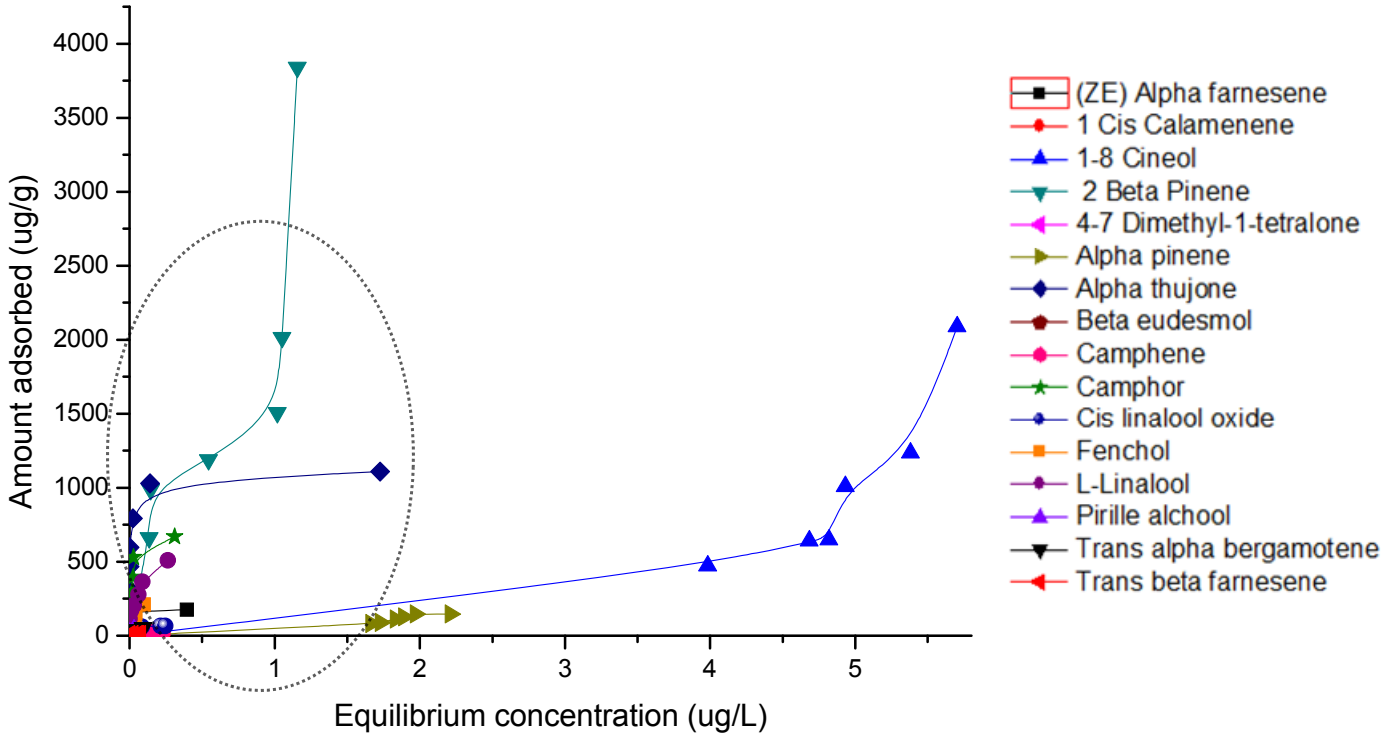

Figure 5. Adsorption isotherms of *Lavandula angustifolia* components on sodium modified bentonite.

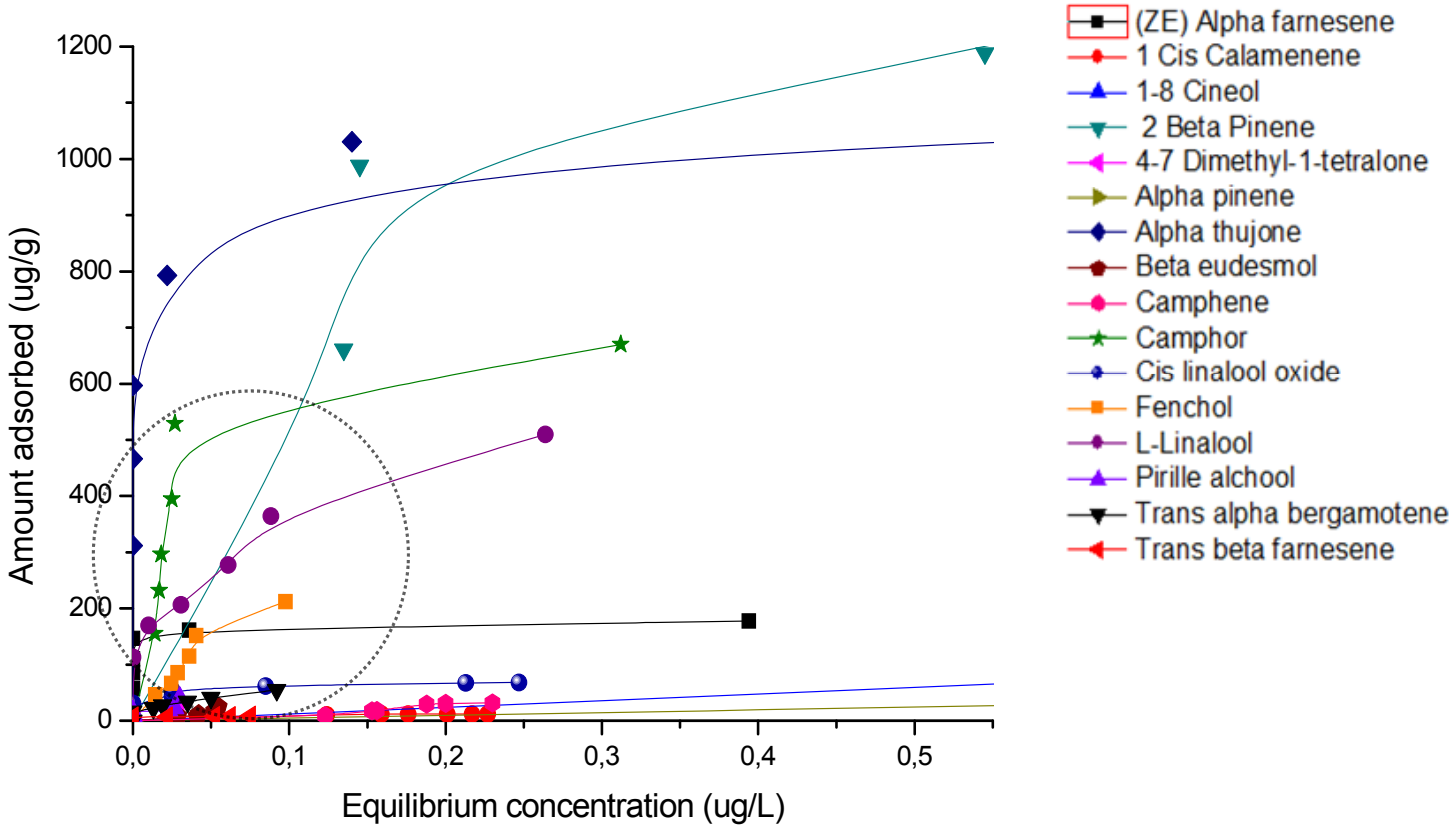

Figure 6. Adsorption isotherms of *Lavandula angustifolia* components on sodium modified bentonite (Zoom 1).

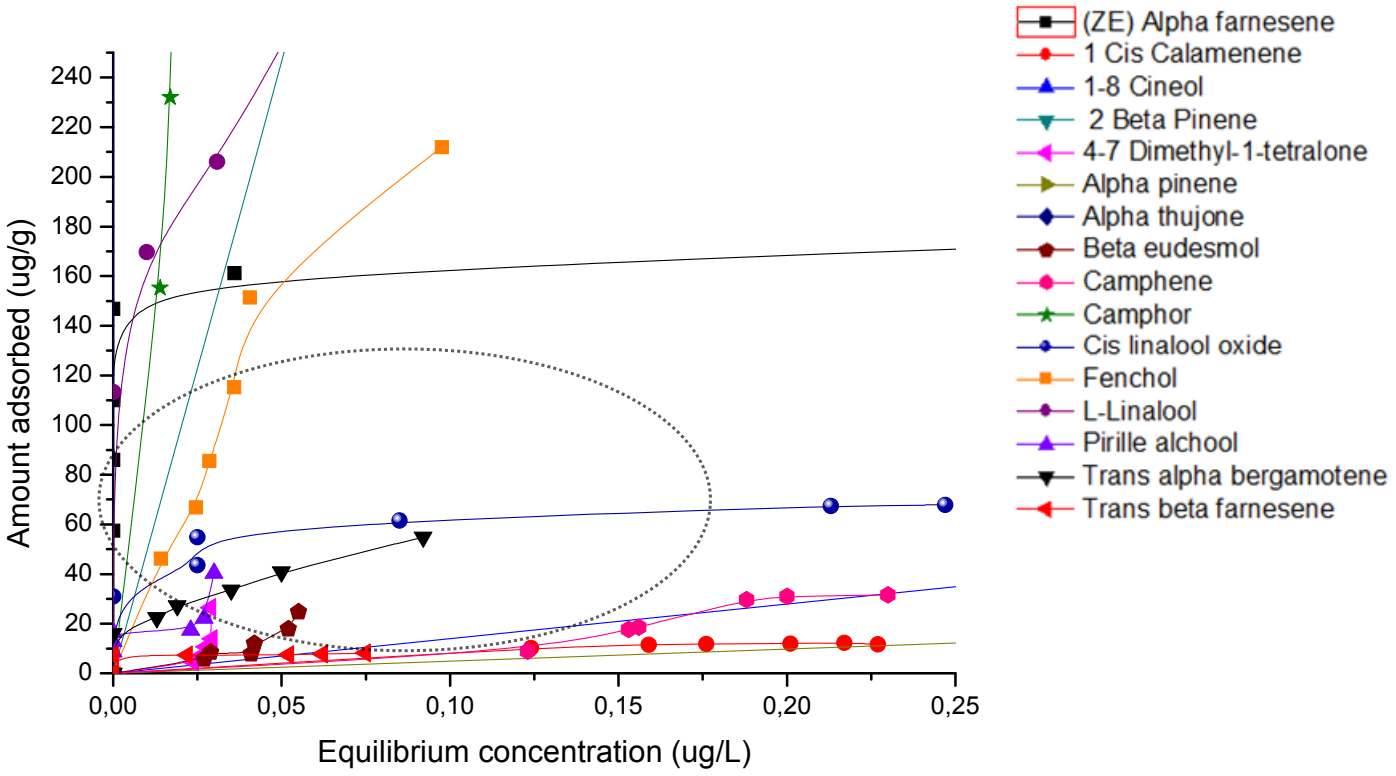

Figure 7. Adsorption isotherms of *Lavandula angustifolia* components on sodium modified bentonite (Zoom 2).

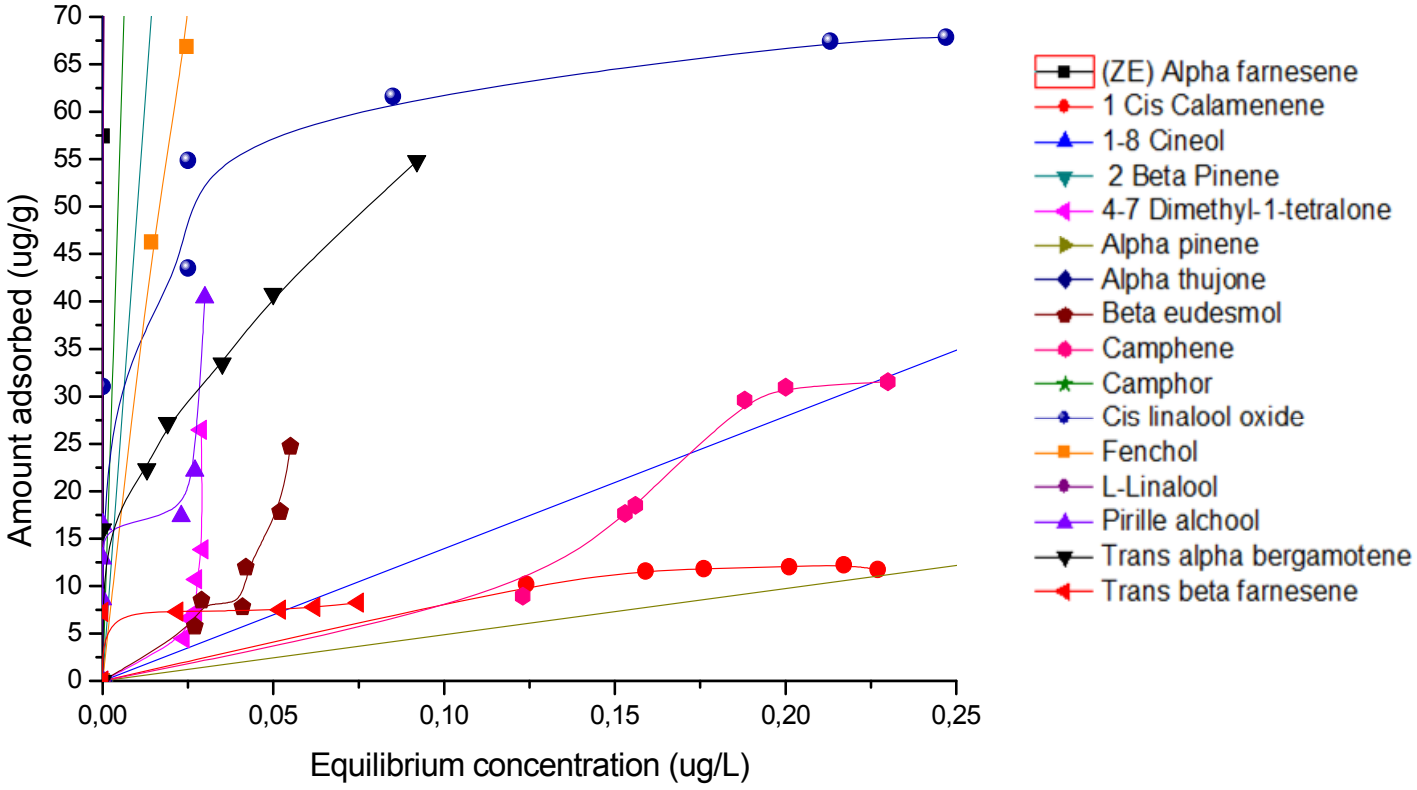

Figure 8. Adsorption isotherms of *Lavandula angustifolia* components on sodium bentonite (Zoom 3).

bentonite was fitted with the Langmuir like: 1 Cis calamenene, alpha thujon, camphor, Cis linalool oxide, linalool, pirille alcohol, trans beta farnesene, (Z E) alpha farnesene) and Freundlich model like: 1-8 Cineol, 2 Beta pinene, 4-7 dimethyltetralone, alpha pinene, beta eudesmol, camphene, Fenchol and Trans alpha bergamotene.

Conflict of Interests

The author(s) have not declared any conflict of interest.

ACKNOWLEDGEMENTS

The authors are sincerely thankful to the CUD (Commission Universitaire pour le Developpement) of Belgium for their financial support for this work through the convention of CUD research project OUJ3 and training in the Laboratory of General Chemistry in Gembloux Faculty. They are also grateful to CNRST - Morocco (PROTARS p23/66) and to LACPREEN for their financial support.

REFERENCES

Amman L, Bergaya F, Lagaly G (2005). Determination of the cation exchange capacity (CEC) of clays with copper complexes. Revisited Clay Minerals 40:441-453.

Allen SJ, McKay G (1987). Diffusion model for the sorption of dyes on peat. J. Sepn. Process Technol. 9:18-25.

Bergaya F, Vayer M (1997). CEC of Clays. Measurement by adsorption of a copper ethylene diamine complex. Appl. Clay Sci. 12: 275-280.

Cavanagh HMA, Wilkinson JM (2005). Lavender essential oil. A review. Austr. Infection Control 10(1):35-37.

Grim RE, Guven N (1978). Bentonites, Geology, Mineralogy, Properties and uses. Developments in sedimentology. Amsterdam Elsevier 24: 217-248.

Halsey GD (1952). The role of surface heterogeneity, Advanced Catalysis 4: 259-269.

Hanamanthagoudaa MS, Kakkalameli S, Naik PM, Nagella P, Seetharamareddy HR, Murthy (2010). Essential oils of Lavandula bipinnata and their antimicrobial activities. J. Food Chem. 118:836-839.

Ho YS, McKay G (1998). Sorption of dye from aqueous solution by peat. J. Chem. Eng. 70:115-124.

Freundlich H (1909). Kapillarchemie. Akademische Verlagsgesellschaft, Leipzig, Germany. 15. M. Baganeet S. Guiza. Ann. Chem. Sci. Mater. 25:650.

Lagaly G (2001). Pesticide-clay interactions and formulations. Applied Clay Sci. 18:205-209.

Lajide L, Escoubas P, Mitzutani J (1995). Termite antifeedant activity in *Xylopia aethiopica*. Phytochemistry 40(4):1105-1112.

Lis-Balchin M, Hart S (1999). Studies on the mode of action of the essential oil of lavender (*Lavandula angustifolia* P. Miller). Phytother. Res. J. 13:540.

Muyima NYO, Zulu G, Bhengu T, Popplewell D (2002). The potential application of some novel essential oils as natural cosmetic preservatives in an aqueous cream formulation. Flavour Fragrance 17(4):258-266.

Ngamo T, Goudoum LS, Ngassoum A, Mapongmetsem MB, Lognay G, Malaisse F, Hance T (2007). Chronic toxicity of essential oils of 3 localaromatic plants towards Sitophilus zeamais Motsch. (Coleoptera: Curculionidae). Afr. J. Agric. Res. 2(4):164-167.

Nguemtchouin MMG, Ngassoum MB, Ngamo LST, Mapongmetsem PM, Sieliechi J, Malaisse F, Lognay GC, Haubruge E, Hance T (2009). Adsorption of essential oil components of Xylopia aethiopica (Annonaceae) by kaolin from Wak. Adamawa province (Cameroon). Appl. Clay Sci. 44:1-6.

Puls RW, Powell RM, Clark D, Eldred CJ (1991). Effects of pH, solid/solution ratio, ionic strength, and organic acids on Pb and Cd sorption on kaolinite. Water, Air Soil Pollut. 57-58(1-4):423

Van Bemmelen JM (1888). Die Adsorption Verbindungen und das Adsorption vermo¨gen der Ackererde. Die Landwirtschaftlichen Versuchs-Stationen. 35:69-136.

Zaitan H, Bianchi D, Achak O, Chafik T (2008). A comparative study of the adsorption and desorption of o-xylene onto bentonite clay and alumina. J. Hazard. Mater.153:852-859.

academicJournals

Vol. 13(33), pp. 3426-3432, 13 August, 2014
DOI: 10.5897/AJB2014.13656
Article Number: 8B167A546626
ISSN 1684-5315

http://www.academicjournals.org/AJB

African Journal of Biotechnology

Full Length Research Paper

Induction and optimization of cellulases using various agro-wastes by *Trichoderma virdii*: Effect of alkali pretreatment

Meenakshi Goyal[1]* and Giridhar Soni[2]

[1]Department of Biochemistry, Punjab Agricultural University, Ludhiana 141001, India.
[2]Department of Plant Breeding and Genetics, Punjab Agricultural University, Ludhiana 141001, India

Received 25 January, 2014; Accepted 28 July, 2014

This study presents optimization of various lignocellulosics and alkali pretreatment for maximum cellulase production by *Trichoderma virdii* sp. Maximum endoglucanase (642 IU/L) and exoglucanase (187IU/L) activity was achieved with maize straw at 5% concentration. Oat hay was the most suitable agro-waste for β - glucosidase (7100 IUL^{-1}) production followed by maize straw (6500 IUL^{-1}). Maize straw was chosen in an effort to enhance cellulase production with 0.1 N NaOH, 0.5 N NaOH and I.0 N NaOH pretreatment. 0.1 N NaOH produced desirable results showing 2.5, 1.6, and 1.7 fold increase in endoglucanase, exoglucanase and β-glucosidase activity. This 0.1 N pretreated straw produced reducing sugars 3.5 times more than untreated straw.

Key words: Lignocellulosics, maize straw, cellulase production, *Trichoderma virdii*, alkali pretreatment

INTRODUCTION

Lignocellulosic biomass is the most abundant organic raw material in the world (Singh et al., 2006). The recent thrust in bioconversion of agriculture waste to chemical feed stock has led to extensive studies on cellulolytic enzymes produced by fungi and bacteria. Low cost of enzyme production improves the economics, as the cost of enzyme constitutes a major part of the total cost of hydrolysis (Baig et al., 2004). Successful utilization of abundantly available lignocellulosics as an alternate carbon source for cellulose production can lower the cost of enzyme production.

India is a land of agriculture. After harvesting and processing of various cereal crops, about 300 million tons of straw is produced annually. These agro- wastes can effectively be utilized for the production of cellulases which can be used in the saccharification of these wastes. The ability of various fungal spp. to produce cellulases on various lignocellulosics has been reported (Baig et al., 2003; Singh et al., 2010).

This study presents a comparison of various lignocellulosic wastes (maize straw, Jowar straw, Bajra straw, wheat straw, oat hay and berseem hay) for efficient on-site production of cellulase by a local soil isolate of *Trichoderma viride* (S 34). A methodology is formulated for maximum cellulase production by manipulating medium components and with alkali pretreatment. The cellulolytic enzymes will be used for saccharification of pretreated straw.

*Corresponding author. E-mail: meenakshigoyal@pau.edu

Table 1. Effect of incubation period on endonuclease activity (IUL^{-1}) by *Trichoderma viride* (S34) at 25°C using various carbon sources at 1% level.

Carbon source	Incubation days				
	7	11	14	17	21
CMC	628	692	607	500	482
Maize straw	26	143	160	197	187
Jowar straw	66	162	106	106	82
Wheat straw	23	28	53	17	10
Bajra straw	44	51	51	106	82
Oat hay	87	99	120	85	73
Barseem hay	13	21	32	32	9

MATERIALS AND METHODS

Substrates

Natural lignocellulosics namely maize straw, Jowar straw, Bajra straw,wheat straw, oat hay and berseem hay were dried in an oven and ground in a Wiley Mill to pass through I mm screen and utilized as substrate for submerged fermentation (SmF). All the lignocellulosics were passed through same mash size to provide equal surface area for fungus to grow and do not differ due to difference in oxygen diffusion, nutrient absorption and assimilation by mycelia.

Liquid state fermentation

T. viride (S34) was inoculated in Erlenmeyer flasks (250 ml) containing sterilized enzyme production medium with 1-5% of different lignocellulosics as sole carbon source. The broth culture was incubated at 25°C up to 21 days. The supernatants, collected after centrifugation of contents, were used for assaying cellulase.

Enzyme assay

Activity of cellulases was assayed by reported methods (Ray et al., 1993). For endoglucanase activity, suitably diluted enzyme solution was incubated with 1% CMC and 0.5 M citrate buffer (pH 4.8) in a total volume of 2 ml at 50°C for 30 min. For exoglucanase activity, 0.1-0.5 ml of enzyme solution was incubated with Whattman filter paper strip (1 x 10 cm) and 0.5 M citrate buffer (pH 4.8) in a total volume of 2 ml at 50°C for 60 min. β-glucosidase activity was measured with 0.05-0.1 ml of enzyme solution in a reaction mixture of 2 ml containing 1 ml of 1% cellobiose and 0.5 M citrate buffer (pH 4.8). The reaction mixture was incubated for 15 min at 50°C. The liberated sugars in the above assays were estimated by Nelson method (Nelson, 1944) and the activity was expressed in International Unit (IU). One unit of cellulose is defined as the amount of enzyme that released one micromole of reducing sugar per minute under the assay conditions (pH 4.8, 50°C).

Optimization of culture condition

Optimum culture conditions including incubation period (7, 14, 17, 21 days), carbon source (maize straw, Jowar straw, wheat straw, oat hay and berseem hay), concentration of lignocellulosics (1, 2, 3, 5%), pH (4 - 6.5), temperature (20, 25, 30 and 35°C) and nitrogen (ammonium chloride, sodium nitrate, ammonium nitrate, ammonium sulphate, urea and peptone; 0.05% w/v) were determined for maximum growth of *T. viride* and cellulase activity was recorded.

Pretreatment of lignocellulosics

Overnight dried lignocellulosics were autoclaved with 10 ml of different concentrations of alkali (0.1, 0.5 and 1.0 N) for 30 min in 150 ml Erlenmeyer flasks. After cooling, the alkalinity was neutralized with acid and stock production media was added to make final volume (30 ml) having desired concentrations of nutrients and pH 4.0. The fermentation was carried out with *T. viride* (S 34) for 14 days at 25°C. The filtrate was used for the estimation of cellulase.

Saccharification of agro wastes

Saccharification experiment was performed with crude enzyme preparation obtained by fermenting 5% alkali treated and untreated Jowar for 14 days using *T. viride* (S34). The enzyme concentration used was 0 (control), 0.5 and 1 ml/g of substrate in the reaction mixture containing 50 mM sodium acetate buffer (pH-5.0) in a total volume of 30 ml and 3% of lignocellulosics in each flask. Each treatment was taken in triplicates. The reaction mixture was incubated at 45°C under shaking conditions at 100 rev min^{-1} up to 72 h and samples were drawn for the determination of reducing sugars by Nelson (1944) method.

RESULTS AND DISCUSSION

Optimization of medium constitutes

The carbon source of the medium was affected considerably in the synthesis of cellulolytic enzymes by *T. viride* (S 34) in liquid cultures. Maize straw, jowar straw, wheat straw, oat hay and berseem hay invariably affected the synthesis of cellulolytic enzymes in the medium. Maximum induction of endoglucanase (Table 1) and exoglucanase (Table 2) activity among agro-wastes was achieved by maize straw at 17th day followed by jowar straw at 11 day incubation period. Oat hay produces maximum β-glucosidase at 14 day incubation period (Table 3). Very low level of induction was seen with berseem hay and wheat straw. The variability in the production as well as incubation period on different lignocellulosics could be attributed to various factors such

Table 2. Effect of incubation period on exonuclease activity (IUL^{-1}) by *Trichoderma viride* (S34) at 25°C using various carbon sources at 1% level.

Carbon source	Incubation days				
	7	11	14	17	21
CMC	53	199	67	50	32
Maize straw	4	5	10	30	21
Jowar straw	11	13	12	6	9
Wheat straw	3	3	7	4	4
Bajra straw	7	5	2	9	3
Oat hay	5	6	14	1	10
Barseem hay	5	6	8	10	2

Table 3. Effect of incubation period on β-glucosidase activity (IUL^{-1}) by *Trichoderma viride* (S34) at 25°C using various carbon sources at 1% level.

Carbon source	Incubation days				
	7	11	14	17	21
CMC	6400	7467	4053	1705	1560
Maize straw	4693	5100	5808	6200	5700
Jowar straw	1599	3541	1400	1386	1251
Wheat straw	1636	1386	2418	355	482
Bajra straw	1209	1920	2453	3840	3203
Oat hay	3200	4551	6187	5227	5183
Barseem hay	1000	1067	1972	2150	1505

as variable cellulose content, heterogeneity of structure and accessibility of cellulose for microbial attack leading to difference in the lag period of growing fungus. A number of reports are available for the use of lignocellulosics by *Trichoderma* spp. (Muthuvelayudham and Viruthagir, 2006; Kubicek et al., 2009). However most of the *Trichoderma* spp. described in the literature are deficient (Duff, 1985) or low (Tiwari et al., 2013) in the production of β-glucosidase. Therefore cellobiose accumulates and represses the enzyme biosynthesis. These rate-limiting steps in the bioconversion of lignocellulosic residues to industrially important products remain one of the most significant hurdles in saccharification and producing economically feasible cellulosic ethanol.

In the present study, *T. viride* (S 34) produces a good amount of β-glucosidase enzyme on all type of lignocellulosics especially on oat hay (7100 UL^{-1}). Higher induction of cellulase with maize straw could be attributed due to more cellulose content compared to other lignocellulosics (Goyal et al., 2008).

Cellulase induction was maximized with CMC as carbon source but the use of purified cellulose as substrate is uneconomical for large scale production of enzymes. High cost of cellulases production hindered use of this enzyme in industry. Therefore efforts were made to optimize cellulase production with cheaply available agricultural lignocellulose waste. Increased concentrations of all lignocellulosics favored higher induction of cellulase complex with differences in the yield of enzyme. Maize straw at 5% level was effectively utilized by fungus to increase the production to 3 times for endoglucanase (Figure 1a) and about 6 times for exoglucanase (Figure 1b) from that at 1% level. Increased production of cellulases by raising lignocellulosic concentration was also observed by Jadhav et al. (2013).Oat hay proved to be maximum β-glucosidase producer at 5% level (Figure 1c).

Alkali pretreatment of lignocellulosics remove acetyl and uronic acid substitution on hemicelluloses increasing accessibility of hemicellulose and cellulose for enzyme attack (Chang and Holtzapple, 2000). Therefore, pretreatment of 5% maize straw with different concentrations of NaOH (0.1 - 1.0 N) and subsequent fermentation was tried. Mild treatment (0.1 N NaOH) showed desirable results with higher production of cellulase than produced with CMC (Figure 2). This induction might be attributed due to changes in the structure of maize biomass with increased solublization of hemicelluloses, reduced crystallinity and increased available surface area and pore volume of substrate (Singh et al., 2010). More severe alkali treatment might have resulted into the production of toxic compounds like furfurals inhibiting microbial metabolism and thus decreasing the

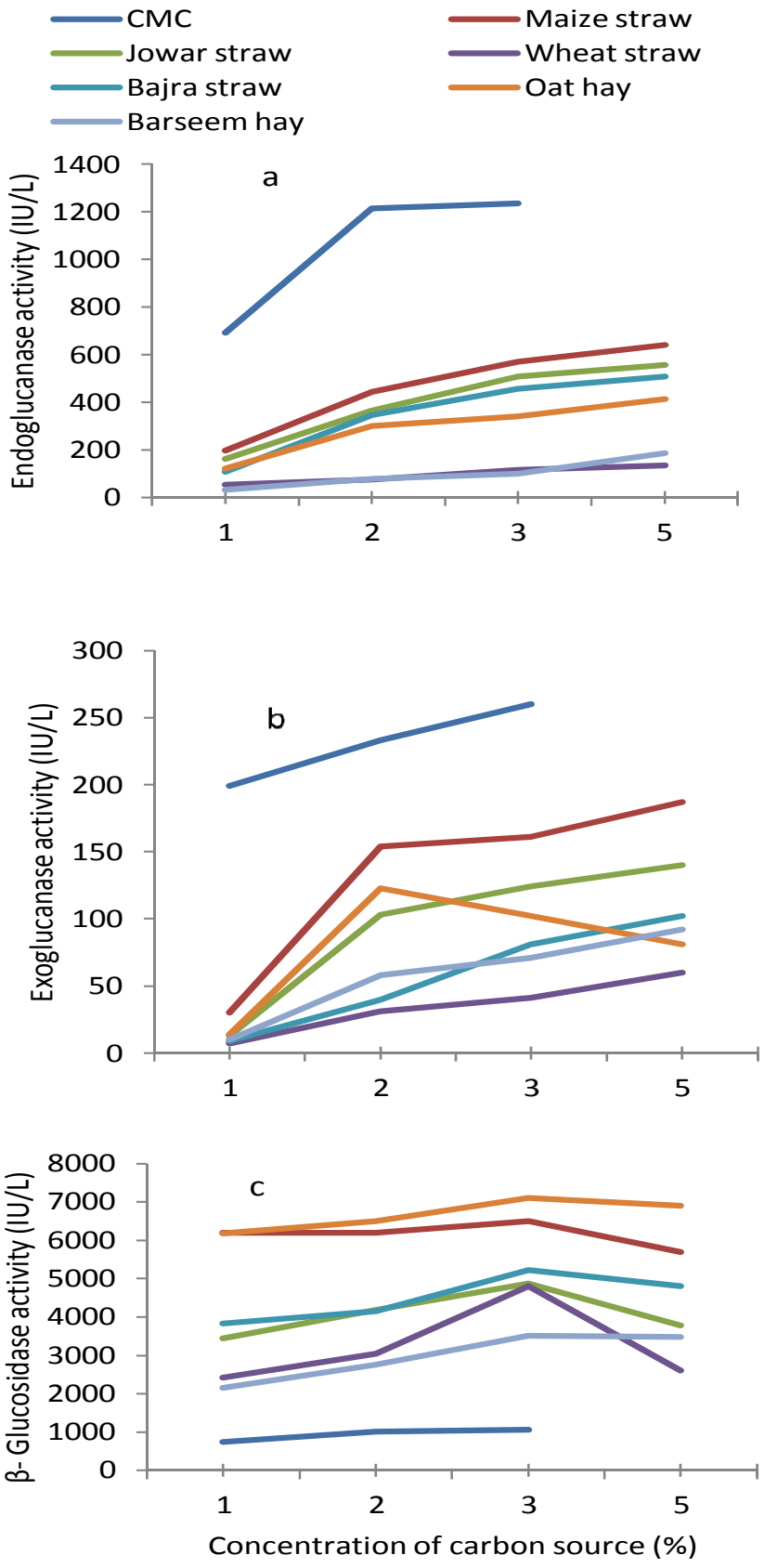

Figure 1. Effect of different carbon source concentration on (a) endoglucanase, (b) exoglucanase and (c) β-glucosidase activity.

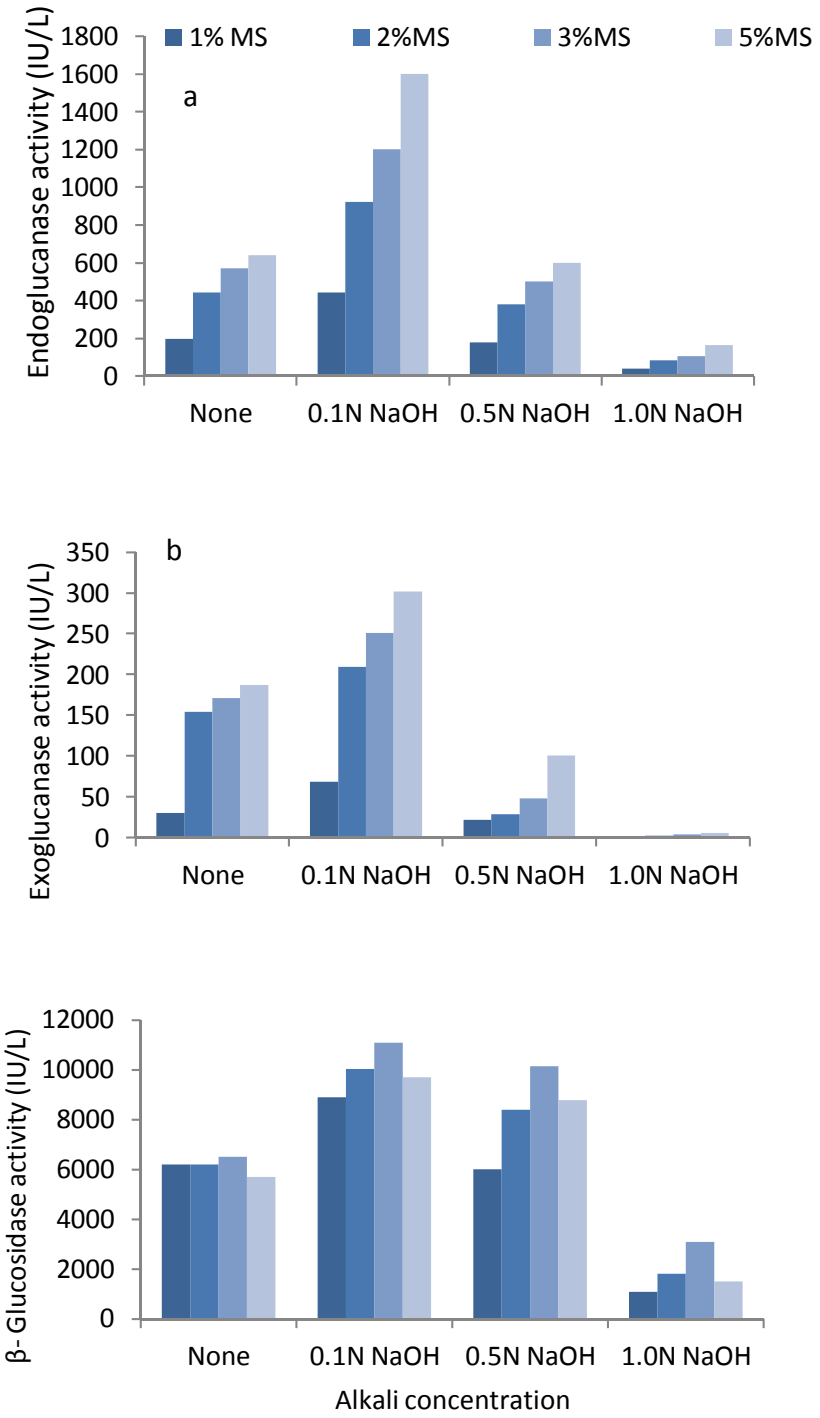

Figure 2. Effect of alkali pre treatment on (a) endoglucanase, (b) exoglucanase and β-glucosidase activity.

production of cellulase to many fold.

Effect of N source, temperature and pH on cellulase production

Enzyme activity got influenced when $NaNO_3$ as sole nitrogen source was used (Table 4). Maximum enzyme activity was recorded at 25°C (Table 4). A *Trichoderma* strain in a recent paper preferred temperature 35°C for maximum growth (Leghlimi et al., 2013).

At pH 4, the fungal strain showed heavy growth and higher cellulase enzyme activity. Similar pH dependency was shown by strain of *Aspergillus* grown on sawdust

Table 4. Effect of nitrogen source, incubation temperature and initial pH on cellulases activity (IUL^{-1}) by *Trichoderma viride* (S34) using carbon source at 1% level.

Nitrogen source	Enzyme activity(IUL^{-1})		
	Endoglucanase	Exoglucanase	β-Glucosidase
0.05% N (w/v)			
NH_4Cl	128.0	10.2	2346.6
$NaNO_3$	165.6	15.0	3540.9
NH_4NO_3	106.6	8.7	2986.6
$(NH_4)_2SO_4$	136.0	11.4	2026.6
NH_2CoNH_2	45.3	4.1	3199.9
Peptone	15.9	3.2	3201.0
Incubation Temperature (°C)			
20	152.5	11.2	3224
25	188.7	16.2	3504.8
30	106.5	7.1	2124.6
35	51.0	2.4	1202.6
Initial pH			
4.0	195.8	1.05	3504.0
4.5	174.2	10.2	1802.0
5.0	124.6	7.6	1002.6
5.5	109.6	5.2	804.6
6.0	50.5	2.1	502.8
6.5	44.8	1.8	214.7

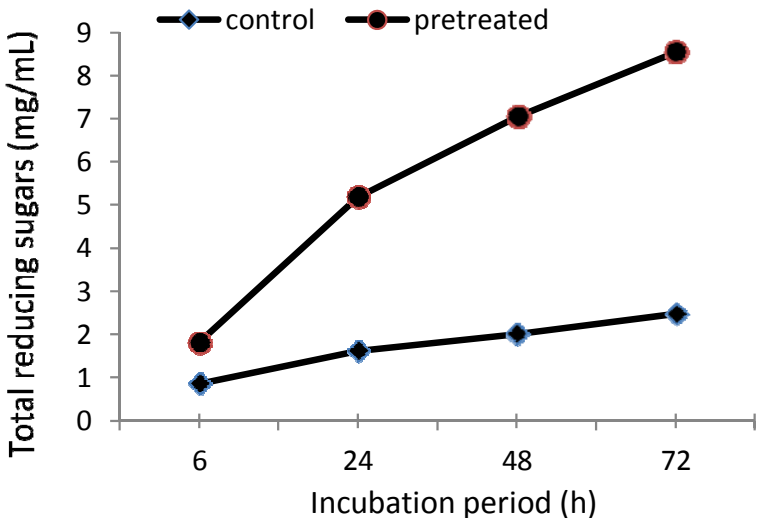

Figure 3. Effect of pretreatment on total reducing sugars.

(Milala et al 2009) and CMC (Oyeleke et al., 2012).

Saccharification of pre-treated maize straw

Cellulases produced from *T. viride* were used for saccharification of maize straw at pH 5.0 and temperature 45°C (Figure 3). The results show highest level of total reducing sugars with the pretreated agro- waste. Release of reducing sugar increased with increase of incubation period.

At the end of 72 h reducing sugars were released 3.5

fold more with alkali treated maize straw than produced with nontreated straw (Milala et al., 2009).

Conclusions

Maize straw could provide an economical advantage as carbon source for production of cellulase enzymes by using *Trichoderma viride* as fungal source. Factors [pH (4), temperature (25°C) and nitrogen source($NaNO_3$)] were optimized for maximum cellulase production. In optimum conditions production of endoglucanase, exoglucanase, β-glucosidase and reducing sugars in hydrolysis process showed best results with mild alkali pretreatment.

Conflict of Interests

The author(s) have not declared any conflict of interests.

ACKNOWLEDGEMENT

Authors acknowledge CSIR, New Delhi for the financial assistance to carry out this study.

REFERENCES

Baig MMV, Baig MLB, Baig MIA, Yasmeen M (2004). Saccharification of banana agro-waste by cellulolytic enzymes. Afr. J. Biotechnol. 3:447-450.

Baig MMV, Mane VP, More DR, Shinde LP, Baig MIA (2003). Utilization of Agricultural Waste of Banana: Production of Cellulases by Soil fungi. J. Environ. Biol. 24:173-176.

Chang VS, Holtzapple MT (2000). Fundamental factors affecting biomass enzymatic reactivity. App.l Biochem. Biotechnol. 84:5-37.

Duff SJB (1985). Cellulase and β- Glucosidase production by mixed cultures of *Trichoderma reesei* Rut 30 and *Aspergillus phoenicis*. Biotech. Lett. 7:185-190.

Goyal M, Kalra KL, Sareen VK, Soni G (2008). Xylanase production with xylan rich lignocellulosic wastes by a local soil isolate of *Trichoderma viride*. Braz. J. Microbiol. 39:535-541.

Jadhav AR, Girde AV, More SM, More SB, Khan S (2013). Cellulase production by utilizing agricultural wastes. Res. J. Agri. For. Sci 7:6-9.

Kubicek CP, Mikus M, Schuster A, Schmoll M, Seiboth B (2009). Metabolic engineering strategies for the improvement of cellulase production by *Hypocreajecorina*. Biotechnol. Biofuels. 2:19-33.

Leghlimi H, Meraihi Z, Boukhalfa-Lezzar H, Copinet E, Duchiron F (2013). Production and characterization of cellulolytic activities produced by *Trichoderma longibrachiatum* (GHL) Afr. J. Biotechnol. 12:265-275.

Milala MA, Shehu BB, Zanna H, Omosioda VA (2009). Degradation of agro wastes by cellulase from *Aspergillus candidus*. Asian. J. Biotechnol. 1:51-56.

Muthuvelayudham R, Viruthagir M (2006). Fermentative production and kinetics of cellulose protein on *Tricoderma reesei* using sugarcane bagasse and rice straw. Afr. J. Biotechnol. 5:1873-1881.

Nelson N (1944). A photometric adaptation of Somogyi method for the determination of glucose. J. Biol. Chem. 153:315-380.

Oyeleke SB, Oyewole OA, Egwim EC, Dauda BEN, Ibeh EN (2012). Cellulase and pectinase production potentials of *Aspergillus niger* isolated from corn cob Bayero. J. Pure. App. Sci. 5(1):78-83.

Ray L, Pal A, Ghosh AK, Chattodhyay P (1993). Cellulase and β -glucosidase from *Aspergillus niger* and saccharification of some cellulosic wastes. J. Microbiol. Biotechnol. 8:85-94.

Singh A, Singh N, Bishnoi NR (2010). Enzymatic hydrolysis of chemically pretreated rice straw by two indigenous fungal strains: a comparative study. JSIR 69:232-237.

Singh R, Singh N, Parkash A, Poonia S (2006). Saccharification studies by a thermophilic fungus *Sporotricum thermophile* isolated from agriculture waste of Bhopal. Indian J. Environ. Ecoplann. 12:97-104.

Tiwari P, Mishra BN, Sangwan SN (2013). β-Glucosidases from the fungus *Trichoderma*: An Efficient Cellulase Machinery in Biotechnological Applications. Biomed. Res. Internat. pp. 1-10.

academicJournals

Vol. 13(33), pp. 3433-3442, 13 August, 2014
DOI: 10.5897/AJB2014.13679
Article Number: 3FACC8B46627
ISSN 1684-5315

http://www.academicjournals.org/AJB

African Journal of Biotechnology

Full Length Research Paper

Early gonad development in zebrafish (*Danio rerio*)

Grace Emily Okuthe[1]*, Shirley Hanrahan[2] and Barry Collins Fabian[3]

[1]Department of Zoology, Walter Sisulu University, P/BX1 Mthatha, 5117, Mthatha, South Africa.
[2]School of Animal Plant and Environmental Sciences, University of the Witwatersrand, P/BX3 Wits 2050, Johannesburg, South Africa.
[3]School of Molecular and Cell Biology, University of the Witwatersrand, P/BX3 Wits 2050, Johannesburg, South Africa.

Received 31 January, 2014; Accepted 4 July, 2014

Gonadogenesis in zebrafish goes through an initial ovarian phase then subsequently into either ovarian or testicular phases. How germ cells choose to commit to an oogenic fate and enter meiosis or alternatively not enter meiosis and commit to a spermatogenetic fate remains a key question. This study investigated events of early gonadogenesis in zebrafish with the aim of unraveling the events surrounding the mitotic/meiotic transition in juvenile ovaries. Primordial germ cells were identified at eight days post fertilization (dpf). Mitotic divisions were apparent at 15 dpf, and meiosis initiated in some gonads after 22 dpf. After 40 dpf, female gonads contained various germ cells including oogonia, post-pachytene and early pre-vitellogenic oocytes, whereas in some gonads, degenerative post-pachytene oocytes and proliferating germ were observed. The occurrence degenerating oocytes as well as a relatively larger proportion of proliferating "gonial" germ cells in the latter gonads was considered the first indication of spermatogenic activity, marking the onset of secondary (testicular) gonadogenesis. It could not be determined here whether primordial germ cells were involved in secondary gonadogenesis. While the mechanisms of this phenomenon in zebrafish ovaries are not well addressed, here it can be seen in the context of an apoptotic regulation.

Key words: *Danio rerio*, gonad, mitotic/meiotic transition, development, sex inversion.

INTRODUCTION

Zebrafish (*Danio rerio*) is a member of the family *Cyprinid*, and can grow up to about 3 to 5 cm total length in adulthood, although females are a little larger. This fish has become a popular tool in studying development and can be easily stimulated to produce throughout the year (Hisaoka and Firlit, 1962). A single female can spawn up to 400 eggs and fertilization success is generally over 70-80% (Eaton and Farley, 1974). It has a very short generation time and reaches sexual maturity within three months.

Many aspects of zebrafish development have been described in the literature, including early embryonic patterning (Kimmel, 1993), early development of the nervous system (Kimmel et al., 1994), and aspects of cell fate and lineage determination (Kimmel and Law, 1985; Kimmel and Warga, 1987). Embryonic development and biology of zebrafish have also been described(Streisinger et al., 1981; Warga and Kimmel, 1990; Westerfield,

*Corresponding author. E-mail: ageokuthe@gmail.com. Tel: +27 47 5022823. Fax: + 27 47 5022725.

1993). Other aspects of zebrafish oocyte growth, egg formation including gene expression patterns, have been reported fairly extensively in the literature (Hisaoka and Firlit, 1962; Takahashi, 1977; Selman et al., 1993; Howley and Ho, 2000; Pelegri, 2003; Lessman, 2009). Although methods used to classify stages of oocyte growth by these early authors differ from those of Selman et al. (1993), all of the above studies have proved useful in understanding morphological events of oocyte growth in zebrafish.

Previous studies undertaken on early differentiation of zebrafish germ cells are those reported by Takahashi (1977), which described events of juvenile inter-sexuality. In this study, stages of oocyte growth in juvenile gonads are not described in detail. Hisaoka and Firlit (1962) described stages of oocyte development in immature and mature zebrafish gonads based on morphological observation with respect to the staining pattern of nuclear structures with nucleic acid stains. In this study, transitional stages of gonad development in juvenile fish are not described in detail. Selman et al. (1993) used a modified class scheme to describe stages of oocyte growth in an adult ovary based on physiological, biochemical and morphological observations. Consequently, the transformation of oogonia into primary (meiotic) oocytes is not described. Staging series of zebrafish oocytes presented by Hisaoka and Firlit (1962) precedes that of Selman et al. (1993) by 31 years. Although, all of the above studies have proved useful in understanding morphological events of oocyte development in zebrafish, overall, pictorial or graphic representations of these previous reports on the reproductive characteristics of early zebrafish gonads are scattered. Oogenesis is typically studied in adult ovary. Consequently, these studies do not help a reader to follow in detail the transitional events occurring during early ontogeny.

Since a comprehensive study on oocyte development in the adult zebrafish ovary had been described by Selman et al. (1993) and partially by Hisaoka and Firlit (1962), it was the aim of this study to follow germ cell differentiation in carefully staged phases of gonad ontogeny, prior to those covered by these previous workers. While the present study takes into account the events surrounding the mitotic/meiotic transformation during early gonadogenesis, it was important to follow the process of oogenesis through the mitotic/meiotic transition and beyond.

MATERIALS AND METHODS

Sample collection and processing

Six fish at each developmental stage were selected from hatchery tanks at hatch [4 days post fertilization (dpf)], every three days from 8 to 31 dpf and weekly thereafter up to 55 dpf. Larvae and juvenile fish were killed by anaesthetizing with MS222 (4.2 ml tricaine stock solution in 100 ml tank water) as described by Westerfield (1993). They were individually measured for total length, and the trunk region of bigger fish being cut out before fixation and smaller fish processed whole. Tissue samples were fixed in Bouin's solution overnight (Humason, 1979), dehydrated through alcohol series, cleared in methyl benzoate (Sigma–Aldrich, St. Louis, MO, USA) and embedded in Paraplast® (Merck, Darmstadt, Germany). Gonadal regions were also fixed in 2% paraformaldehyde and 2.5% glutaraldehyde (Karnovsky, 1969) in 0.1 M phosphate buffer, (0.1 M NaH_2PO4, 25 ml; 0.1 M Na_2HPO4, 81 ml; dH_2O, 250 ml; adjusted to pH 7.4 and topped up to 500 ml with dH_2O) for 6 h at room temperature and then washed in phosphate buffer overnight at room temperature, and post-fixed for 1 h in 1% osmium tetroxide in phosphate buffer and embedded in araldite. Tissue section (5–7 µm thick) of the trunk region of each fish were cut and mounted on slides coated with 3-amino-propyl-triethoxy saline (Sigma–Aldrich, St. Louis, MO, USA), and stained with Mayer's modified haematoxylin and eosin.

Semi-thick sections (1-2 µm) of araldite embedded tissues were cut with a glass knife on a Reichert Ultracut S and stained on a 90°C hot plate with toluidine blue and thereafter examined and photographed under a Leica DM750 microscope attached to a DFX 310 FX digital camera. Images were possessed using LAS imaging software Version 3.5. To measure oocyte sizes, slides were examined under low power. Gonads of juvenile fish were sexed on the basis of tissue configuration and germ cell composition into different developmental stages. Gonads of inverting individuals were categorized according to the extent of degeneration of female germinal cells.

Experimental protocols for the study were approved by the Animal Ethics Screening Committee (No. 2000/98/1), University of the Witwatersrand.

RESULTS

Gonads of larval zebrafish

At hatch, no distinct primordial germ cells (PGCs) were found in sections due to distortion of the larvae due to tissue processing. At 8 days post fertilization (dpf), the yolk sac was present but smaller in size. In some individuals' yolk, globules were assimilated and disappeared with the transition of larvae to active feeding. Primordial germ cells (PGCs) were attached to the dorsal walls of the coelomic cavity on both sides of the mesentery (Figure 1a) often in isolation or in pairs. A group of PGCs were observed at the intestinal level. The PGCs were large (4-5 µm) in diameter, ovoid or rounded shaped.

Their large irregular shaped nuclei contained loose network of thin chromatin threads and did not contain a nucleolus. There were no signs of mitotic activity at this stage of development.

At 13 days post fertilization (dpf), the number of germ cells had increased from two to six per cross section; signs of mitotic activity of the PGCs were evident in some gonads (Figure 1b). Germ cells were attached to the wall of the ceolomic wall by a narrow band of peritoneal cells, in the region of the posterior half of the swim bladder. The nucleoli of the germ cells observed at this stage of development were solitary, intensively stained with haematoxilyn and eosin (H&E) and occupied a central

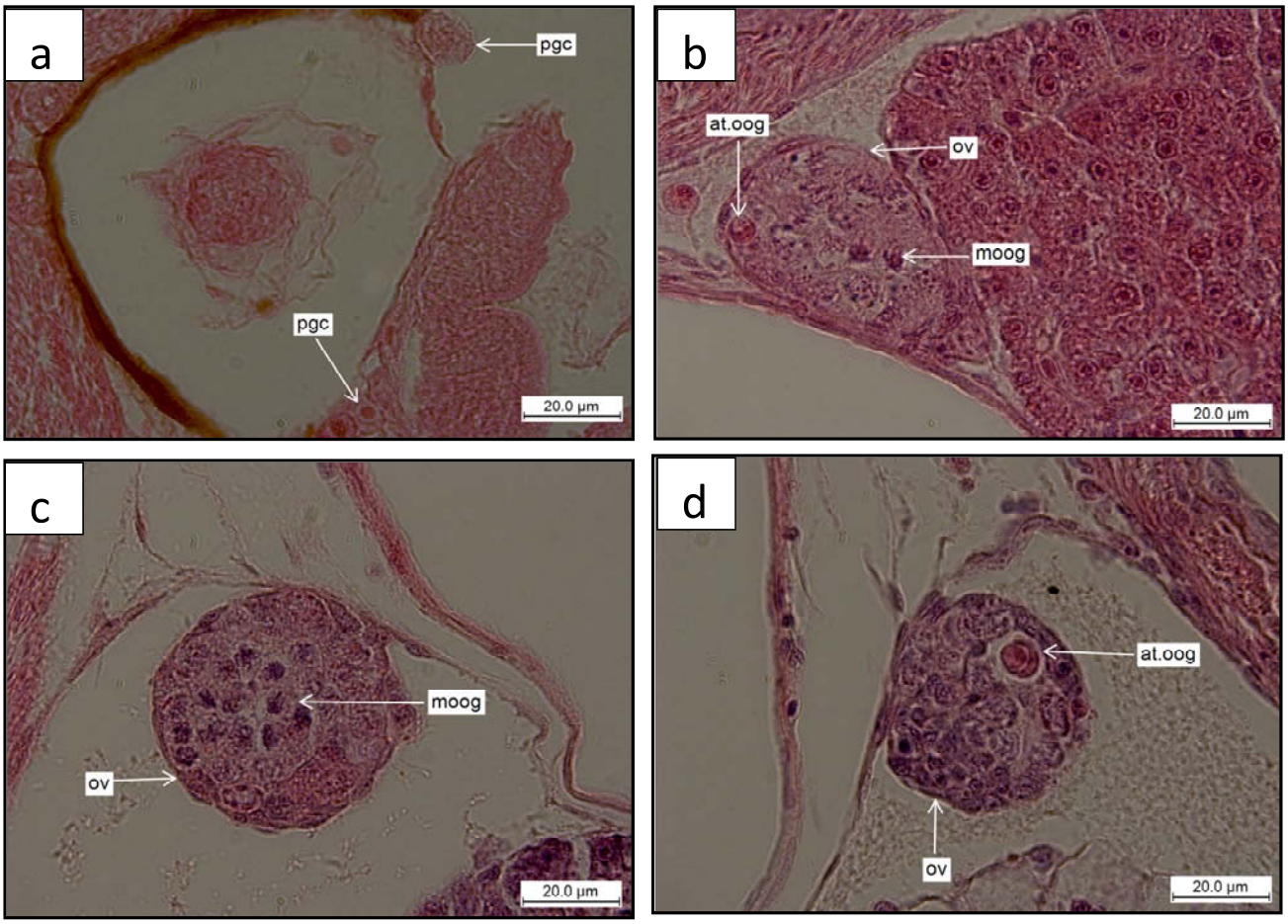

Figure 1. Selected histological sections of larval zebrafish gonads stained with H & E. **a**, Primordial| germ cells (pgc) attached to the body wall on both sides of the mesentery (Scale bar = 20.0 µm). **b,** Gonads of fish at 13 dpf. **c** and **d**, Mitotic activity evident in sections of juvenile fish at 16 dpf. pgc, primordial germ cell; oog, oogonia; moog, mitotic oogonia; at.oog, atretic oogonia. n.oog, nest of oogonia.

position. The scant cytoplasm of the germ cells stained weakly with H&E. Germ cells observed at this stage of development had morphological characteristics of either oogonia or spermatogonia and measured 4-10 µm in diameter. Although germ cells had morphological characteristics of oogonia or spermatogonia, implying onset of morphological sex differentiation, sex differences could not be distinguished with certainty. Therefore, gonads were interpreted as of the indifferent type.

By 16 dpf, gonads were larger in size but still showed a simple anatomical organization. Germ cell mitotic activity had intensified (Figure 1c). Although the total number of germ cells was unknown, germ cells had increased in number compared with the previous stage of development. Gonads of fish at 16 dpf were considered to be at the initial stage of germ cell proliferation.

Gonads of Juvenile zebrafish

Mitotic germ cells had increased in number in gonads of fish by 19 dpf. Gonads of some fish contained large numbers of proliferating germ cells (Figure 2a and b). At three weeks, a prominent cavity had formed (Figure 2b) in some gonads. At this developmental period, an increase in number of proliferating germ cells was observed. Between days 22 and 35 dpf, gonads were composed of “transforming oogonia” (oogonia that were no longer dividing), early meiotic prophase and post-pachytene oocytes (Figure 2c).

"Transforming" oogonia were morphologically similar to those germ cells observed at 16 dpf, but were larger in size (7-10 µm) and showed an increased cytoplasmic-nuclear ratio. It was not possible to detect any changes in the nature of chromatin in "transforming" oogonia in Paraplast embedded sections but in 1 µm sections (Figure 2c) fine sparse chromatin granules were seen scattered throughout the nucleoplasm. The centrally located nucleolus was still present in these germ cells. The nuclei of these germ cells stained only lightly with H&E and toluidine blue

Early meiotic oocytes were round and had become

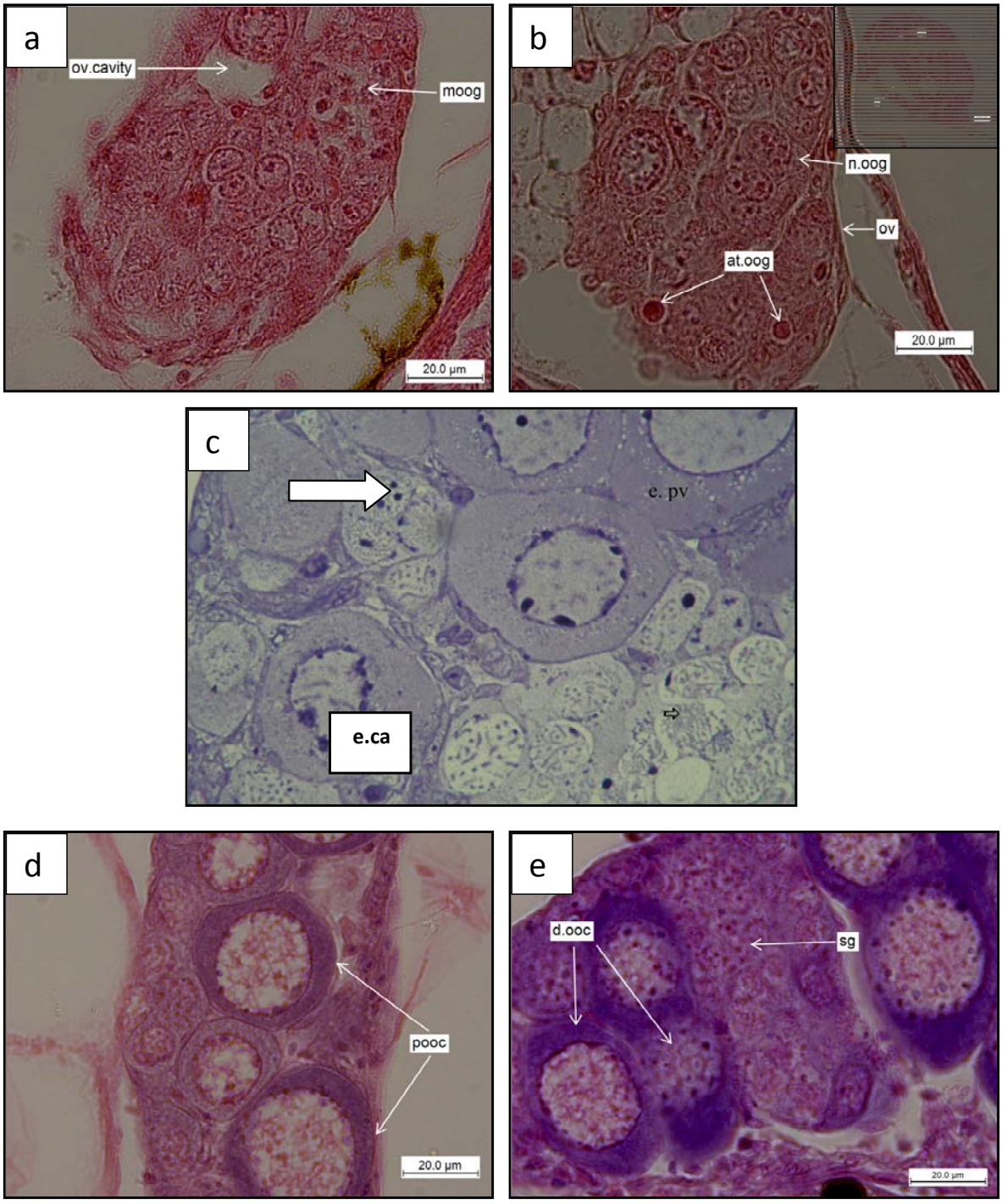

Figure 2. Selected histological sections of Juvenile zebrafish gonads stained with H&E. **a** and **b**, shows mitotic oogonia, atretic oogonia, and an ovarian cavity at days 19 and 22 post fertilization. **c**, shows transforming oogonia (long thick arrow) and early meiotic oocytes (short thick arrows). d and e, shows gonads in early stages of sex inversion at 45-49 dpf. m.oog, mitotic oogonia; at.oog, atretic oogonia; d.ooc, degenerating post pachytene oocytes; sg, spermatogonial proliferation; e.ca, early cortical alveoli stage oocytes; ov, ovary; ov. cavity, ovarian cavity; ca, cortical alveoli; pooc, post pachytene oocytes.

increasingly larger (10-19 µm) and their nuclei, which were also relatively large and filling the majority of the cell, stained only lightly with H&E (Figure 2c). These oocytes were distinguished from "transforming" oogonia because of the changes in chromosome structure. The most distinctive difference among the various stages of

early meiotic stages was the pattern of chromatin condensation. In the leptotene stages of the meiotic prophase, chromosomes had thickened and could be recognized in sections.

The zygotene oocytes were approximately the same size as the leptotene oocytes, but characterized by a more clearly defined and localized chromatin. A distinguishing feature of the zygotene oocytes being the increase in size and density of chromatin strands. Oocytes of the zygotene stage had prominent nucleoli on the opposite side of the conspicuous chromatin within the nuclei.

Post-pachytene oocytes were surrounded by a monolayer of somatic (granulosa) cells, indicating the onset of ovarian follicle organization (Figure 2d). These oocytes had increased cytoplasmic volume, were larger than early meiotic oocytes (30 - 117 μm) with their nuclei being central and contained two to four relatively large basophilic nucleoli. Cytoplasmic RNA in post-pachytene oocytes was basophilic when stained with haematoxylin, and deep blue when stained with toluidine blue (Figure 2c), while a less basophilic cytoplasm and an increased number of nucleoli in the nucleus characterized late post-pachytene oocytes. Accumulation of cytoplasmic RNA was coincident with the formation of multiple nucleoli in the oocyte nucleus.

Gonads with altered morphology (inverting gonads)

At 45 to 49 dpf, two types of gonads were identified. Typical gonads were common and exhibited asynchronous oocyte development similar to those observed in the previous stage of development. The other type of gonads contained only post-pachytene oocytes, (Figure 2d and e) and mitotically dividing "gonial" germ cells (Figure 2f). Oocytes with unusual shapes showed morphological features similar to degenerating cells and lacked the clear structure of a normal growing oocyte. It appeared that many of these oocytes begun to degenerate accompanied by various degrees of abnormalities.

The most prominent feature observed in degenerating oocytes was a marked distortion in the overall appearance of the oocytes accompanied by the disintegration of cytoplasm. An interesting feature observed in some gonads at 45 days of development was the occurrence of empty follicles (spaces) in histological sections. The area around the empty follicles or degenerating oocytes was characterized by the presence of densely packed stromal (epithelial) cells believed to be either blood cells or phagocytes. Post pachytene oocytes in inverting gonads had unusual shapes and their cytoplasm stained intensively with Haematoxylin.

In contrast to the appearance of degenerating oocytes in these gonads, numerous small "islets" of quiescent and clusters of proliferating “gonial" germ cells were seen in parts of the gonads in some fish at 49 dpf. Quiescent and proliferating germ cells were seen along the slit-like openings (ovarian lamellae) within gonad sections (Figure 2e). The formation of these slits was a characteristic feature of these gonads at this developmental stage. The number of mitotically dividing germ cells observed at this stage of development outnumbered those observed during the initial ovarian differentiation stages of development.

At 49 dpf, typical ovaries exhibited asynchronous oocyte development wherein ovaries possessed oocytes in the post-pachytene and pre-vitelogenic stages of development. Inverting gonads remained smaller in size possessing "gonial" germ cells and fewer growing oocytes.

Gonads of immature zebrafish

In the subsequent stages of development (55 to 60 dpf), normal ovaries showed typical patterns of sexual development for asynchronously spawning fish (Tyler and Sumpter, 1996), where gonads contained oocytes at various stages of development. From 55 dpf onwards, male and female gonads could be distinguished clearly as maturing testes or ovaries. In Immature testis the number of germ cells, now termed spermatogonia, spermatocytes and spermatids had increased in number. In some individuals, large cysts of spermatocytes at the various stages of the meiotic prophase could be recognized in sections as well as spermatids (Figure 3c and d). In addition, testicular tissues were arranged almost completely in lobules.

Ovaries contained numerous large post-pachytene and a few early pre-vitellogenic oocytes (Figure 3a and b). An increase in the number of cortical alveoli was noted in pre-vitellogenic oocytes. The nuclei of the later oocytes contained numerous small nucleoli. Cortical alveoli were in a thin ring between the germinal vesicle or seen all over the cytoplasm of the pre-vitellogenic oocytes. There were no signs of testicular tissues in all gonads.

Maturing ovaries were formed of rows of post-pachytene, early as well as late pre-vitellogenic and early and late vitellogenic oocytes. Late pre-vitellogenic oocytes were similar to early pre-vitellogenic oocytes but were larger measuring 98 - 264 μm in diameter with multiple cortical alveoli situated in a thick ring between the germinal vesicle and the vitelline membrane or filling the whole cytoplasm. The nuclei of the later germ cells were lobed and contained numerous nucleoli. Early vitellogenic oocytes were large (117-314 μm).

Late vitellogenic oocytes were very large (151 - 361 μm) with yolk granules distributed homogeneously in the cytoplasm. The nuclei of oocytes in the advanced stages of vitellogenic stages of development were slightly displaced from the center to the oocyte membrane. A thin, but distinguishable granulosa and thecal layers

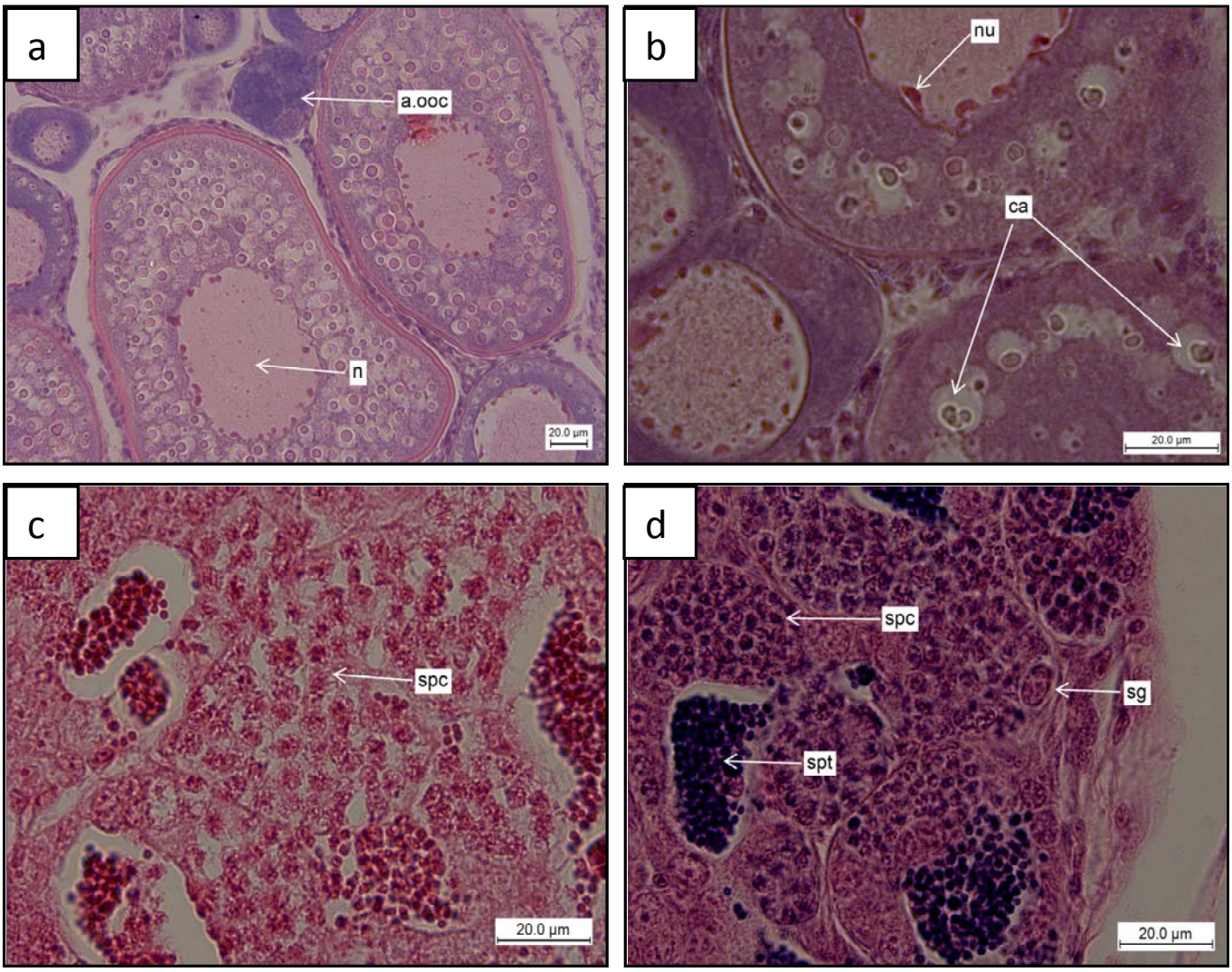

Figure 3. Selected histological sections of maturing zebrafish gonads stained with H & E. **a** and **b,** shows oocytes at the cortical alveoli stage of growth at 55 dpf. **c** and **d,** shows maturing testis in fish at 55 and 60 dpf. a.ooc, atretic oocyte; n, nucleus; nu, nucleoli; ca, cortical alveoli; spc, spermatocyte; sg, spermatogonia; spt, spermatids.

surrounded these oocytes. Vitellogenic oocytes were the most advanced stage of oocyte development observed therefore no mature stage oocytes has been described here.

DISCUSSION

This study, examined the sequence of events leading to the formation of oocytes including secondary gonado-genesis (testicular differentiation) in zebrafish. It has been confirmed here that gonad development follows the general pattern described by Takahashi, (1977), but there are other aspects that differ, specifically the timing of events.

It is believed that differences are related to rearing conditions, and differences in studied strains rather than differences in gonad development. Primordial germ cells (PGCs) were identified with certainty at 8 dpf. Although not labeled with lineage markers, the PGCs were identified by their common morphological characteristics: Irregular outlines, a high nucleus to cytoplasm ratio, a relatively large cell in relation to surrounding somatic cells, by their location and age of fish. The appearance of some germ cells at the intestinal level in the present study led to the assumption that the PGCs in zebrafish settle first at the gut (intestinal) level before spreading out to other parts of the gonadal anlage. Some investigators consider PGCs segregation at the sub-intestinal yolk part as their initial site of colonization of the genital ridge prior to their settlement to other parts of gonadal anlage (Mezhnin, 1978). PGCs observed at the intestinal level in the present study, were possibly still in the process of migration to the dorsal mesentery. In teleost fish studied

to date, primordial germ cells migrate to the genital ridges before hatching (Satoh and Egami, 1972; Hamaguchi, 1982; Parmentier and Timmermans, 1985). In the present study, and at 13 days post fertilization, the initial development of gonadal anlage had commenced, suggesting that the PGCs in zebrafish migrated to the gonadal ridges prior to its formation. This would be in accordance with the findings of Parmentier and Timmermans (1985) and Timmermans and Taverne (1987) in other cyprinid fish. In contrast, in other vertebrates, PGCs migrate to the previously formed genital ridges (Nieuwkoop and Sutasurya, 1979).

In most teleosts fish, the number of PGCs at hatching is small. The average number in carp for example, is 23 per larvae (Parmentier and Timmermans, 1985). The number remains low for six weeks after which a rapid proliferation occurs, resulting in a mean number of 130 at seven weeks and 250 at nine weeks. Proliferating germ cells were seen for the first time in the present study at 16 dpf. Initially the germ cell numbers remained low for up to two weeks, after which a rapid increase in the number of germ cells was noticed. However, their exact number was not known and no information was found in the literature about their exact number at this stage in development.

The increase in the proliferative activity of germ cells at 19 dpf signified the transition from gonadal primordia to differentiating gonads. The beginning of this developmental period corresponds with the transition from larval to juvenile life stages in the zebrafish (Brown, 1997). Day 19, therefore, marked the end of the indifferent period of gonad development.

At three weeks of age, a cavity was recognized and identified as the future ovarian cavity in females. In some teleosts, the development of associated somatic cells, such as the ovarian cavity is helpful in the following ovarian differentiation besides the morphology of the cells. The proliferative activity of germ cells at 19 dpf appears to be the strongest indicator of ovarian differentiation in zebrafish followed by the presence of an ovarian cavity at 22 dpf. Based on this finding from this stage onwards, gonads were called ovaries and the period marked the end of the indifferent period of gonad development and the onset of morphological sex differentiation.

Ovarian differentiation (transformation of an oogonium into an oocyte) and the commencement of meiosis in zebrafish as in other teleost fish are characterized by changes of nuclear structure. One of the ultrastructural characteristics of oocytes at the early meiotic prophase is the formation of synaptonemal complexes, which appear in meiotic germ cells of animals and plants generally. These structures have been identified in oocytes at zygotene and pachytene stages ovarian development in the medaka (Hamaguchi, 1982), the amago salmon (Nakamura and Nagahama, 1993) and in the channel catfish (Patino et al., 1996). According to Selman and Wallace (1989), oogenesis commences when oogonia transform into leptotene oocytes at the initiation of meiosis. The process is preceded by DNA replication and begins with the pairing and condensation of homologous chromosomes in the first meiotic division (leptotene-zygotene). At pachytene, the homologous condensing chromosomes form synaptonemal complexes. Sooner or later, oocytes arrest in the lamp brush (diplotene) stage of growth. According to Takahashi (1977) oogenesis is said to begin when cysts of germ cells originating from the mitoses of pre-existing PGCs appear to be in initial phases of the meiotic prophase as evidenced by the formation of "auxocytes" (Stage IB oocytes). In the work by Takahashi (1977) no mention is made of the criteria used in identifying the various stages of germ cell development making comparisons difficult.

Examination of the zebrafish larval gonads during the mitotic/meiotic transition in the present study led to the identification of four cell types. "Transforming" oogonia being the smallest germ cells (7 - 10 µm), which give rise to primary oocytes, which eventually pass through the leptotene, zygotene, pachytene and the diplotene stages of the meiotic prophase, diplotene oocytes being the largest germ cells (30-117 µm). The most distinctive difference among the first three stages of the primary oocyte is the pattern of chromatin condensation. mitotic/meiotic transition is a gradual process and is distinguished by active gene transcription that results in the production of vast amounts of RNA species. Accumulation of cytoplasmic RNA is coincident with the formation of multiple nucleoli in the oocyte nucleus or germinal vesicle. In the current study, cytoplasmic RNA in post-pachytene oocytes was basophilic when stained with haematoxylin, and deep blue when stained with toluidine blue.

The presence of synaptonemal complexes, which represents the condensed, homologous chromosomes in synapses, identifies oocytes in the pachytene stage of the first meiotic prophase (Grier, 2000). This implies that during this developmental period, germ cells were in the meiotic phase of development and that germ cells identified in some gonads prior to this stage of development were definitely oogonia. Thus ovarian differentiation in some zebrafish had begun. Initially, clusters of early meiotic oocytes formed a smaller proportion of germ cell composition in gonads.

By 31 to 35 dpf, clusters occupied extended areas of the gonads still enveloped by follicle cell processes. In adult ovaries (Selman et al., 1993), the number of oogonia and early meiotic oocytes appear to be relatively low compared to those observed in juveniles in the present study; moreover, transformation of oogonia into meiotic oocytes is rare event in adult ovarian sections (Selman et al., 1993). The low number of early meiotic oocytes, in adult ovarian sections implies a fast development from oogonia via oocytes in chromatin nucleolus stage to oocytes in early post-pachytene phase

in adult females. In most teleosts, oogenesis (Bromage and Cumaranatunga, 1982) appear to occur cyclically with an accelerated development just after spawning making it difficult to observe oogonia and early meiotic oocytes in adult ovarian sections.

As oocytes of the early meiotic prophase continue to develop, they become completely enveloped by pre-follicle cells disrupting the organization of the cells nests. The mechanisms leading to the separation of germ cells from the "nests" could not be established from the observations of the present study. However, it has been suggested elsewhere that the thin cytoplasmic digitations that stromal cells develop around the clustered oocytes play a role in this process (Andreucceti, et al., 1990). The newly formed oocytes continue to differentiate independently and asynchronously, enveloped by a monolayer of squamous follicle cells and eventually transform themselves into growing post-pachytene (diplotene) oocytes.

This is the last stage at which the last events of meiotic prophase are completed, after which the oocyte enters the diplotene stage.

In the current study, post-pachytene oocytes were seen for the first time between days 31 and 35 post fertilization. In the study of Takahashi (1977) oocytes of the first phase of growth or auxocytes were observed by 14 days post hatch (dph). In this study, characteristic features of germ cells were not provided making comparisons difficult. The present view is that germ cells labeled as auxocytes by Takahashi (1977) at 14 dph may have been oogonia. Consequently, his previous report of occurrence of meiotic oocytes at 10 dph is doubtful. Oogonia may have been erroneously described as stage I ocytes, since there are strong similarities between oogonia and oocytes when they first enter diplotene especially before the onset of cytoplasmic RNA accumulation so that basophilic cytoplasm would confer unequivocal similarity.

According to the findings of the current study, gonads of nearly all fish examined between days 45 to 49 post fertilization contained degenerating or atretic oocytes. This may have been indicative of impending sex reversal. In various mammalian (Byskov, 1978) as well as fish species (Coward and Bromage, 1998), atresia (resorption) is a common phenomenon. Atresia can be found throughout the reproductive cycle in fish, but has only been clearly shown to affect vitellogenic oocytes at the post-spawning periods. According to Takahashi (1977), "the atretic disintegration of auxocytes is the most general and legible feature representing the initiation of sex inversion in gonads. Histological observations of sex inversion of zebrafish juveniles in the present study reveal that sex inversion from ovaries to testes begins with a degeneration of oocytes as stated above. Here, the presence of slit like openings (ovarian lamellae) was one of the features associated with the onset of oocyte degeneration and eventual sex inversion. "Islets" of "gonial" germ cells seen along gonad periphery and along slits within the gonad wall were considered to be spermatogonia although it was not possible to distinguish resting oogonia from spermatogonia, as both are of similar size and appearance.

The occurrence of numerous degenerating oocytes as well as a relatively larger proportion of "islets" of proliferating "gonial" germ cells was considered the first outstanding indication of spermatogenic activity in these ovaries. The formation of the future testis was thought to start from these peripheral “male nests", when the first indications of ovarian degeneration appeared. Gonads with numerous "islets" of "gonial", degenerating as well as mitotic germ cells, were termed inverting gonads (presumptive testes).

The process of oocyte degeneration and resorption in juvenile zebrafish ovaries appear to depend on the size, differentiation level and specific features of the individual germ cells. Lysis of the post-pachytene oocytes is preceded by an intensification of cytoplasmic staining and change in shape of the oocytes probably indicating degeneration (Kobayashi and Hishida, 1985). The resorption of larger pre-vitellogenic oocytes that have cortical alveoli is preceded by active participation of cells of the follicular epithelium.

The invasion of the shrunken degenerating oocytes by aggregations of phagocytes or blood cells as observed in the present study may indicate phagocytic mechanisms, which could lead to the removal of the nuclear and ooplasmic contents with the phagocytes being probably derived from the follicle cells. Whether the migrating cells absorbed residual degenerating cells phagocytically or not could not be determined with certainty. Interestingly, disintegration of cytoplasm of germ cells and follicular atresia also occurs in normal adult female fish (Guraya, 1986).

The first indication of the sex inversion as observed in the present study was the degeneration of female germ cells (post-pachytene oocytes). As degeneration of female germ cells proceeded, stromal somatic cells invade the gonad. Sooner or later, spermatogonial proliferation ensued. The presence of spermatogonia was the first indication of spermatogenic activity in the gonad, whether PGCs were involved in spermatogonial proliferation or not could not be detected in histological preparations. Shortly afterwards, the gonads became testes; female germ cells having disappeared.

It can be said here that the strongest indicators of pre-maturational sex change in juvenile zebrafish was the presence of transitional individuals whose gonads contain degenerative ovarian tissues and developing testicular tissues. The presence of degenerating ovarian tissues simultaneously with a large number of developing spermatogonia in the same gonad strongly supports protandrous hermphroditism in juvenile zebrafish. Juvenile inter-sexuality has also been reported in male and female yellow eels of *Anguilla anguilla* by Kuhlmann

(1957), cited in Colombo and Grandi (1995). The coexistence of both germinal tissues in zebrafish juveniles is probably exclusive to the juvenile period, since functional female germ cells were not seen in active male gonads confirming previous indications of protogyn in juvenile zebrafish (Takahashi, 1977).

The duration of sex change in zebrafish juveniles could not be determined definitely from the results of the present study, but in specimen examined, sex change occurred in fish at 16 to 22 mm total length (TL), a quite different size range from the 12 to 26 mm (TL) range reported by Takahashi (1977). This difference could be attributed to differences in growth rate of individuals or other social and/or genetic variation among individuals (Wang et al., 2007). Molecular factors initiating and regulating the processes of oocyte degeneration or atresia and sex inversion in zebrafish could not be determined in the present study. While mechanisms of this phenomenon in normal ovaries are also not well addressed (Guraya, 1986), here, it can be seen in the context of an apoptotic regulation.

In conclusion, the present work presents a description of the morphology of early gonad differentiation in zebrafish. The exhaustive stage analysis conducted in this study has integrated and interconnected the findings of Selman et al. (1993) for the adult ovary and has also extended the study of Takahashi (1977). From results presented in this study, the possible involvement of primordial germ cells in secondary gonadogenesis (male testicular differentiation) could not be determined. The mitotic/meiotic transition was a gradual process. This work was necessary for other works to follow.

Conflict of Interests

The author(s) have not declared any conflict of interests.

ACKNOWLEDGEMENTS

This study was supported by National Research Foundation grant-holders (B.C. Fabian), bursary to Grace Emily Okuthe, grants to Professor B.C. Fabian from the National Research Foundation and the Developmental Biology Research Program of the University of the Witwatersrand, South Africa.

REFERENCES

Andreucceti P, Motta C, Filosa S (1990). Regulation of oocyte numbers during oocyte differentiation in the lizard (*Podarcis sicula*). Cell Differ. Dev. 29:129-134.

Bromage N, Cumaranatunga R (1982). Egg production in the rainbow trout, In: Recent Advances in Aquaculture. (Muir JF, Roberts RJ (Eds.). 62-38. London: Croom Helm.

Brown DD (1997). The role of thyroid hormone in zebrafish and axolotl development. P. Natl. Acad. Sci. USA. 94:13011-13016.

Byskov AG (1978). Follicular atresia, In: Jones, R.E. (Ed), The Vertebrate Ovary. Plenum, New York. pp. 533-562.

Colombo G, Grandi G (1995). Sex differentiation in the European eel: Histological analysis of the effects of sex steroids on the gonad. J. Fish Biol. 47:394-413.

Coward K, Bromage NR (1998). Histological classification of oocyte growth and the dynamics of ovarian recrudescence in *Tilapia zillii*. J. Fish Biol. (53):285-302.

Eaton RC, Farley RD (1974). Spawning cycle and egg production of zebrafish, *Brachydanio rerio,* in the laboratory. Copeia 1974:195-204.

Grier H (2000). Ovarian germinal epithelium and folliculogenesis in the common snook, *Centropomus undecimalis* (Teleostei: Centorpomide, J. Morphol. 243:249-321.

Guraya SS (1986). The cell and molecular biology of fish oogenesis, In: Monographs of Developmental Biology, Karger, Basel. 18:1-223.

Hamaguchi S (1982). A light and electron-microscopic study on the migration of primordial germ cells in the teleost, *Oryzias latipes.* Cell Tissue Res. 227:139-151.

Hisaoka KK, Firlit CF (1962). The localization of nucleic acids during oogenesis in the zebrafish. Am. J. Anat. 110:203-216.

Howley C, Ho RK (2000). mRNA localization patterns in zebrafish oocytes. Mech. Dev. 92:305-309.

Humason GL (1979). Animal tissue techniques, W.H. Freman, San Fransisco. p. 661.

Karnovsky MJ (1969). A formaldehyde-gluteraldehyde fixative of high osmolality, for use in electron microscopy. J. Cell Biol. 276:137-138.

Kimmel CB (1993). Patterning the brain of the zebrafish embryo. Annu. Rev. Neurosci. 16:707-732.

Kimmel CB, Law RD (1985). Cell lineage of zebrafish blastomeres. I. Cleavage pattern and cytoplasmic bridges between cells. Dev. Biol.108:78-85.

Kimmel CB, Warga RM (1987a). Cell lineages generating axial muscle in the zebrafish embryo. Nature. 327:234-237.

Kimmel CB, Warga RM (1987b). Intermediate cell lineage of the zebrafish embryo. Dev. Biol. 124:269-280.

Kimmel CB, Warga RM, Law DA (1994). Cell cycles, clone strings, and the origin of the zebrafish central nervous system. Development. 120:265-276.

Kobayashi MK, Hishida T (1985). Morphological observation on reversal processes of sex-differentiation in the female gonad of the medaka, *Oryzias latipes*, by androgen. Medaka 3:25-37.

Lessman CA (2009). Oocyte maturation: converting the zebrafish oocyte to the fertilizable egg. Gen. Comp. Endocrinol. 161:53-7.

Mezhnin, N I (1978). Development of the gonads in the early ontogeny of the common perch Perca fluviatilis L. Vopr. Ikhfiol. 18 (1): 84-101.

Nakamura M, Nagahama Y (1993). Ultrastructural study on the differentiation in the Amago salmon (*Oncorhynchus rhodurus*). Aquaculture 112:237-251.

Nieuwkoop BP, Sutasurya LA (1979). Primordial germ cells in the chordates: *Embryogenesis and phylogenesis*, Cambrige University Press, London.

Parmentier HK, Timmermans LPM (1985). The differentiation of germ cells and gonads during development of carp (*Cyprinus carpio*): a study with anti-carp sperm monoclonal antibodies. J. Embryol. Exp. Morph. 90:13-32.

Patino R, Davis KB, Scheoore JE, Urguz C, Parker NC, Simco BA, Goudie CA (1996). Sex differentiation of channel catfish gonads: normal development and effects of temperature. J. Exp. Zool. 276: 209-218.

Pelegri F (2003). Maternal factors in zebrafish development. Dev. Dyn. 2003:535-54.

Sato N, Egami N (1972). Sex differentiation of germ cells in the teleost, *Oryzias latipes*, during normal embryonic development. J. Exp. Morph. 28:385-395.

Selman K, Wallace RA (1989). Cellular aspects of oocytes growth in teleosts. Zool. Sc. 6:211-231.

Selman K, Wallace RA, Saarka A, Qi X (1993). Stages of oocyte development in the zebrafish, *Brachydanio rerio.* J. Morphol. 218:203-224.

Streisinger G, Walker C, Dower N, Knauber D, Singer F (1981). Production of clones of homozygous diploid zebrafish (*Brachydanio rerio*). Nature 291:293-296.

Takahashi H (1977). Juvenile hermaphroditism in the zebrafish

Brachydanio rerio. Bull. Fac. Fish Hokkaido Univ. 28:57-65.
Timmermans LPM, Taverne N (1987). Origin and differentiation of primordial germ cells in the rosy barb, *Barbus conchonius* (Cyprinidae, Teleostei). Acta Morphol. Neer. Sci. 21:182.
Tyler CR, Sumpter JP (1996). Oocyte growth and development in teleosts. Rev. Fish. Biol. Fish. 6:285-318.
Wang XG, Bartfai R, Sleptsova-Freidrich I, Orban L (2007). The timing and extent of 'Juvenile ovary' phase are highly variable during zebrafish testis differentiation. J. Fish. Biol. 70:33-44.
Warga RM, Kimmel CB (1990). Cell movements during epiboly and gastrulation in zebrafish. Development. 108:569-580.
Westerfield M (1993). The zebrafish book: Guide for laboratory use of zebrafish. (*Brachydanio rerio*), Eugene: Oregon Press.

academicJournals

Vol. 13(33), pp. 3443-3449, 13 August, 2014
DOI: 10.5897/AJB2014.13944
Article Number: 61E3A8C46628
ISSN 1684-5315

http://www.academicjournals.org/AJB

African Journal of Biotechnology

Full Length Research Paper

Pequi pulp (*Caryocar brasiliense* Cambess): Drying kinetics and thermodynamic properties

Silva, R. M.[1], Placido, G. R.[2]*, Oliveira, D. E. C.[3], Silva, M. A. P.[2] and Caliari, M.[4]

[1]Federal Institute of Goiano - Rio Verde Campus, CP 66, 75901-970, Rio Verde, Goiás, Brazil.
[2]Faculty of the Graduate Program in Animal Science, Federal Institute Goiano - Rio Verde Campus, CP 66, 75901-970, Rio Verde, Goiás, Brazil.
[3]Agronomy, Federal Institute of Goiano - Rio Verde Campus, CP 66, 75901-970, Rio Verde, Goiás, Brazil.
[4]Food Science and Technology, Federal University of Goiás, CP 131, 74690-900, Goiânia - GO, Brazil.

Received 26 May, 2014; Accepted 4 August, 2014

The objective of this study was to evaluate the drying kinetics of Pequi pulp (*Caryocar brasiliense* Cambess) at temperatures of 40, 50 and 60°C, and the thermodynamic properties for this process. Eleven mathematical models commonly used to represent the drying process of agricultural products were fitted to experimental data. The Fick's second law was used to determine the diffusion coefficients of Pequi fruits through the drying kinetics. The model of Midilli best represented the drying process of Pequi pulp. The calculated effective diffusivity was 4.69988 × 10^{-14}, 5.277436 × 10^{-14} and 5.609491 × 10^{-14} (m^2s^{-1}) for temperatures of 40, 50 and 60°C, respectively, and the energy activation for the process was 7694.94 J mol^{-1}. The enthalpy decreased with increasing temperature, with values of 5091.41, 5008.27 and 4925.13 ($Jmol^{-1}$) for temperatures of 40, 50 and 60°C, respectively. The entropy values found were -251.01, -250.38 and -250.05 ($J.Mol^{-1}K^{-1}$) for the same temperatures. The values obtained from the Gibbs free energy for the drying of Pequi pulp increased with increasing temperature. The obtained data were consistent to the drying process, and the mathematical equations were effective to explain the migration of water within the product.

Key words: Effective diffusivity, drying models, enthalpy, entropy, Gibbs free energy.

INTRODUCTION

Pequi (*Caryocar brasiliense* Cambess., Caryocaraceae) is a typical fruit from the savannah ecosystem (“Cerrado”) with high nutritional value, being economically exploited by the regional population in the fresh form or in the preparation of juices, ice creams, liqueurs, jams and traditional dishes; however, the fruit is not widespread throughout Brazil due to its high perishability (Machado et al., 2013).

Pequi fruits give a sharp and distinctive flavor of regional cuisine, leading to customer acceptance and satisfaction (Geöcze et al., 2013). Pequi pulp is rich in lipids (33.4 g.100 g^{-1}) and is an important source of dietary fiber (10.02 g.100 g^{-1}), has protein content of 3 g.100 g^{-1} and provides about 358 Kcal.100 g^{-1} of material, which correspond to 18 g.100 g^{-1} the caloric needs of an adult on a diet of 2,000 kcal. In addition, there is a predominance of unsaturated fatty acids in the pulp lipids, with oleic acid showing the highest occurrence.

*Corresponding author. Email: geovanarochaplacido@yahoo.com.br, marcotonyrv@yahoo.com.br.

Table 1. Mathematical models applied to drying curves.

Model	Model description
Approximation	$RX = a \cdot \exp(-k \cdot t) + (1 - a) \cdot \exp(-k \cdot b \cdot t)$
Two-term	$RX = a \cdot \exp(-k_0 \cdot t) + b \cdot \exp(-k_1 \cdot t)$
Two- term exponential	$RX = a \cdot \exp(-k \cdot t) + (1 - a) \cdot \exp(-k \cdot a \cdot t)$
Handerson & Pabis	$RX = a \cdot \exp(-k \cdot t)$
Logarítmo	$RX = a \cdot \exp(-k \cdot t) + c$
Midilli	$RX = a \cdot \exp(-k \cdot t^n) + b \cdot t$
Newton	$RX = \exp(-k \cdot t)$
Page	$RX = \exp(-k \cdot t^n)$
Thompson	$RX = \exp((-a - (a^2 + 4 \cdot b \cdot t)^{0,5})/2 \cdot b)$
Verma	$RX = a \cdot \exp(-k \cdot t) + (1 - a) \cdot \exp(-k_1 \cdot t)$
Wang & Singh	$RX = 1 + a \cdot t + b \cdot t^2$

Where, t: drying time, h; k, k_o, k_1: drying constants h^{-1}, and a, b, c, n: model coefficients.

To meet Pequi market during the offseason, the conservation of Pequi pulp is basically by freezing and in the form of acidified canned products. The use of other conservation techniques such as dehydration/drying can provide other ways of use and application, preserving the pulp and increasing the life of the product, in addition to promoting the development of differentiated products (Lewicki, 2006).

Dried fruits and vegetables have gained commercial importance and its growth on a commercial scale has become an important sector of the agricultural industry. The lack of adequate treatment causes considerable damage and waste of seasonal fruits in many countries, which is estimated at 30-40% in developing countries. It is necessary to remove the moisture content of the fruit to a certain level after harvest to prevent the growth of mold and bacterial action (Azharul Karim and Hawlader, 2005).

Oven drying is an inexpensive process, but often leads to degradation of labile compounds and/or oxidizable substrates such as carotenoids and lipids. To overcome these limitations, drying is generally carried out at moderate temperature (40-60°C) (Durante et al., 2014).

The drying process consists of the removal of most of the moisture content of a product, causing unfavorable conditions for the continuity of metabolic activity and growth of microorganisms (Martinazzo et al., 2007). The study on the required parameters of drying kinetics is important in order to improve the drying process and obtain a quality product that meets consumer demands (Cano-Chauca et al., 2004).

The use of mathematical models for the representation of the drying process is crucial, considering that the information generated is of great value for designing, development and improvement of processes and equipment, as well as for the prediction of drying times.

MATERIALS AND METHODS

Pequi fruits were purchased from local market of Rio Verde, Goiás State, Brazil, and transported to the Laboratory of Fruits and Vegetables - Federal Institute Goiás - Rio Verde Campus, Goiás, Brazil. In the laboratory, they were received and sanitized in 150 ppm chlorine solution for 15 min and subsequently dried. Then, Pequi fruits were sliced with an average thickness of 2.33 mm, vacuum packaged, and stored in low-density polyethylene bags until time of drying in oven.

Drying the Pequi pulp

Pequi samples were dried in a Marconi oven model MA 035 - Piracicaba - Brazil, with forced air ventilation and air flow rate of 7.728 $kg.(m^2s)^{-1}$ at three temperature conditions: 40, 50 and 60°C. During drying in perforated trays, samples were weighed from 20 to 20 min up to obtaining water content of 0.111 (decimal, db), determined at 105 ± 1°C for 24 h (AOAC, 2000). The entire drying process was carried out in three replicates.

Temperature and relative humidity of the environment external to the drying chamber were monitored using a thermohygrometer, and the internal temperature was monitored by a thermometer placed inside the drying chamber. The relative humidity inside the drying chamber was obtained by means of the basic psychrometric principles, using the GRAPSI software.

Drying kinetics

The following expression was used to determine the moisture content in the Pequi pulp during drying:

$$RX = \frac{X - X_e}{X_i - X_e}$$

Where, RX is the humidity ratio, dimensionless; X is the moisture content at time t, decimal dry basis (kg water, kg^{-1} dry matter); X_e is the equilibrium water content of the product, decimal dry basis (kg water, kg^{-1} dry matter); and X_i is the initial moisture content, decimal dry basis (kg water, kg^{-1} dry matter).

The modeling is intended to adjust one or more models throughout the studied range of this variable (Corrêa et al., 2010). The experimental drying data of Pequi pulp were fitted to mathematical models often used to represent the drying of agricultural products, as presented in Table 1.

The liquid diffusion model for flat plate geometry with known thickness (Fick's law and eight-term approximation equation) was

fitted to experimental Pequi pulp drying data in accordance with the following expression:

$$RX = \frac{X - X_e}{X_i - X_e} = \frac{8}{\pi^2} \sum_{N_t=0}^{\infty} \frac{1}{(2N_t+1)} \exp\left[-(2N_t+1)^2 \pi^2 D \frac{t}{4L^2} \right]$$

Where, N is the number of terms; D_{eff} is the liquid diffusion coefficient, m^2s^{-1}, and L is the half the sample thickness, m.

The relationship between the effective diffusion coefficient and the increase in the drying air temperature was described by the Arrhenius equation.

$$D_{eff} = D_0 \exp\left(-\frac{E_a}{RT}\right)$$

Where, Do is the pre-exponential factor; Ea is the activation energy, $kJ.mol^{-1}$; R is the universal gas constant, 8.134 $kJ.kmol^{-1}.K^{-1}$, and T is the absolute temperature, K.

Thermodynamic properties

The thermodynamic properties of Pequi pulp drying process were obtained by the method described by Jideani and Mpotokwana (2009).

$$\Delta H = E_a - RT$$

$$\Delta S = R\left(\ln A_0 - \ln\left(\frac{k_B}{h_P}\right) - \ln T\right)$$

$$\Delta G = \Delta H - T\Delta S$$

Where, ΔH = enthalpy, J mol^{-1}; ΔS = entropy, J mol^{-1}; ΔG = Gibbs free energy, J mol^{-1}; kB = Boltzmann constant, 1.38 x 10-23 J K^{-1}, and hp = Planck's constant, 6.626 x 10-34 J s^{-1}.

Statistical analysis

Mathematical models were fitted using nonlinear regression by the Gauss-Newton method using a statistical program. Determination of the investigated components was carried out in three replicates. The models were selected considering the magnitude of the determination coefficient (R^2), relative mean error (P) and estimated mean error (SE). Relative mean error values lower than 10% were considered as a criterion for the selection of models, according to Mohapatra and Rao (2005).

$$SE = \sqrt{\frac{\sum (Y - \hat{Y})^2}{GLR}}$$

$$P = \frac{100}{N} \sum \frac{|Y - \hat{Y}|}{Y}$$

Where, Y is the value experimentally observed; $\hat{Y}$ is the value estimated by the model; N is the number of experimental observations; GLR is the degrees of freedom of the model (number of experimental observations minus the number of coefficients of the model).

RESULTS AND DISCUSSION

Drying kinetics

Pequi pulp showed initial water content of 1.25 dry basis (decimal db) when submitted to the three drying temperatures that promoted relative humidities of 25.96; 15.30 and 9.80%, respectively. Table 2 shows the R^2, SE and P values for each model considered in this study for different drying temperatures.

The determination coefficient R^2 is one of the main criteria for choosing the model that best fits the drying process; however, besides R^2, parameters SE and P are used for determining the adjustment quality (Doymaz, 2012). The choice of the most appropriate model was given by R^2 > 98 %, SE < 10 % values (decimal) and lower P values.

It was observed that for all temperatures, the models were satisfactory to describe the drying process, except for the model of Wang and Singh. At 60°C, the model of Midilli ($RX = a \exp(-k t^n) + b t$) showed satisfactory R^2, SE and P values, so, based on the results obtained for other temperatures, this model was chosen to represent the drying process of Pequi pulp.

Radunz et al. (2011), in his work with carqueja, found that the model of Midilli et al. presented adequate fit to the experimental data for the entire temperature range studied (40-90°C). Lima et al. (2007) dried facheiro pulp and concluded that among the models fitted to the drying kinetics data, the equation of Midilli showed the highest determination coefficient and the lowest mean squared deviation values, corroborating this work. Resende et al. (2010) recommends the model of Midilli for drying processes for presenting simple mathematical operations.

Figure 1 shows the moisture content *versus* Pequi pulp drying time curves studied at different temperatures (40, 50 and 60°C) in oven drier with air circulating.

The longest drying time was at temperature of 40°C, about 5.67 h, while for temperature of 50°C, the drying time was around 5.33 h and at 60°C, it was 4.67 h. The drying curves were well-defined, that is, without floating point throughout the process, indicating homogeneity in the dryer.

It was observed that increased temperatures decrease the drying time of Pequi pulp, since it results in rapid evaporation of water present in the solid. Silva et al. (2009) reported that the increase in temperature causes an increase of the drying rate, which suggests the moisture diffusion from within the product to its surface as the physical mechanism predominant throughout the drying process, with no periods of constant drying rate. Silva et al. (2014) concluded that the drying of whole bananas also occurred exclusively during the period of decreasing rate for all temperatures evaluated. Togrul and Pehlivan (2004) found no periods of constant rate throughout the drying process of apricots, grapes, figs,

Table 2. Values of the determination coefficient (R^2), estimated mean error (SE), relative mean error (P) for mathematical models used in the drying of Pequi pulp (*Caryocar brasiliense* Cambess) at 40, 50 and 60°C.

Model description	R^2 (%)	SE (decimal)	P (%)
40°C			
Approximation	99.96	0.0062	2.3054
Two-term	99.96	0.0064	2.3154
Two- term exponential	99.94	0.0070	2.5640
Handerson & Pabis	99.90	0.0092	3.0179
Logarithmic	99.93	0.0076	2.5614
Midilli	99.96	0.0062	2.3031
Newton	99.84	0.0110	3.9719
Page	99.96	0.0059	2.3253
Thompson	99.94	0.0069	2.4894
Verna	99.96	0.0062	2.3054
Wang & Singh	98.31	0.0371	14.23
50°C			
Approximation	99.97	0.005092	1.3392
Two-term	99.98	0.004905	1.2547
Two- term exponential	99.95	0.006570	2.4539
Handerson & Pabis	99.88	0.010360	5.6170
Logarithmic	99.98	0.004828	1.0532
Midilli	99.98	0.004393	1.5906
Newton	99.87	0.010176	5.8201
Page	99.91	0.008733	3.9863
Thompson	99.95	0.006792	2.5855
Verna	99.97	0.005092	1.3393
Wang & Singh	98.54	0.035443	16.267
60°C			
Approximation	98.78	0.0321	7.8128
Two-term	99.91	0.0092	3.3070
Two- term exponential	99.86	0.0103	3.4578
Handerson & Pabis	99.30	0.0234	4.7387
Logarithmic	99.42	0.0221	5.7471
Midilli	99.93	0.0080	2.3108
Newton	98.78	0.0297	7.8126
Page	99.76	0.0138	5.1096
Thompson	99.52	0.0193	6.6302
Verna	99.91	0.0088	3.3069
Wang & Singh	96.31	0.0537	17.911

peaches and plums, confirming the drying curve obtained in this work.

To maintain the microbiological safety level of the product, that is, to reduce the risk of contaminants, it is desirable to dry the product to obtain moisture ratio less than 0.15 (decimal db) (Krokida and Philippopoulos, 2005).

Figure 1 shows that constant k of the model of Midilli increases in absolute values with increasing temperature, since higher temperatures lead to higher drying rates; however, the other coefficients of the model of Midilli (*a, n* and *b*) did not show a clear trend as a function of drying temperatures. Reis et al. (2012) also reported increased k constant with increasing temperature when drying basil leaves.

The use of kinetic models is a way to predict the drying process at different temperatures, making mathematical models an interesting tool to be used during the kinetic

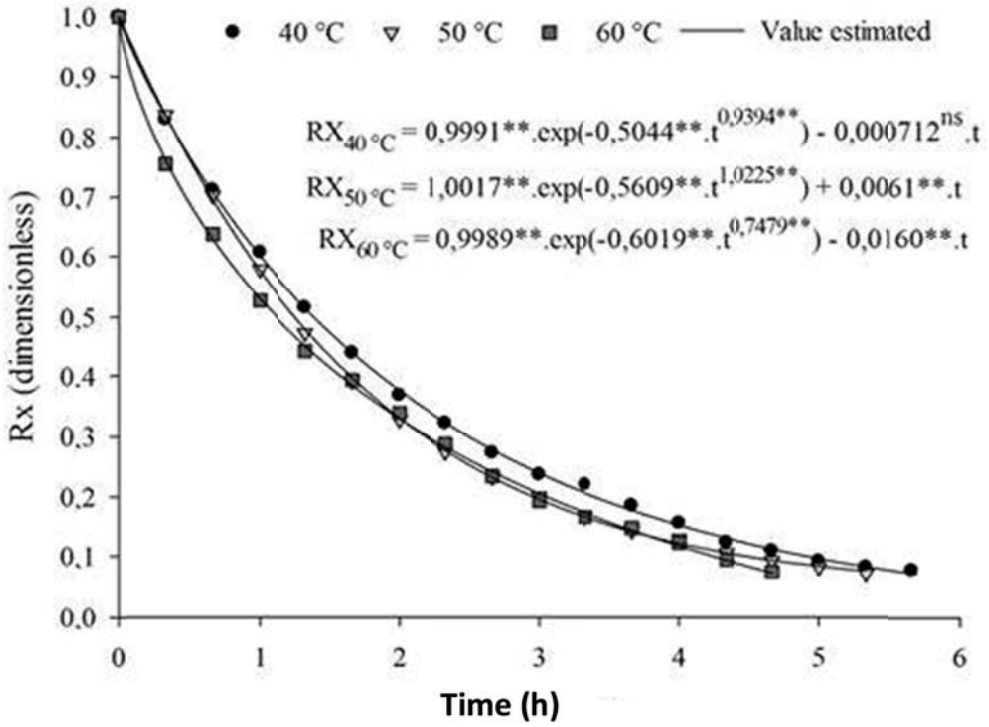

Figure 1. Experimental moisture content values and values estimated by the model of Midilli for drying of Pequi pulp (*Caryocar brasiliense* Cambess) at different temperature conditions.

Table 3. Effective diffusivity and activation energy values for the drying process of Pequi pulp (*Caryocar brasiliense* Cambess) at temperatures of 40, 50 and 60°C.

Property	Temperature		
	40°C	50°C	60°C
Effective diffusivity ($m^2.s^{-1}$)	$4.6990x10^{-14}$	$5.2774\ x10^{-14}$	$5.6095\ x10^{-14}$
Activation energy ($J.mol^{-1}$)		7694.94	

evaluation of a drying process within the temperature range evaluated. Table 3 shows the effective diffusivity results for the different drying temperatures.

It was observed that the effective diffusivity values increase with increasing temperature. This increase is due to increased vapor pressure within the solid, which facilitates the migration of water to the surface of the product. Chen et al. (2012) observed a gradual increase in the effective diffusivity values with increasing temperature during the drying process of biomass.

It is known that the effective diffusivity of different biomaterials varies according to their structure, temperature, and moisture content (Perea-Flores et al., 2012). Madamba et al. (1996) reported that the effective diffusivity coefficients for agricultural products are in the order of 10^{-9} to 10^{-11}, thus differing from the present work in more than 1000 times, which is possibly due to the biological structure of Pequi pulp, since it is rich in lipids and can interfere with the connections of water with the pulp. Oliveira et al. (2012) found low diffusivity coefficients in the drying of corn grains cultivar AG 7088 (from 1.54×10^{13} to 4.85×10^{13}), explaining that these values are due to the chemical composition of the product, and evidencing that to dry an agricultural product, the water must pass through layers of different cell tissues and depending on the chemical composition of these layers, the product presents different characteristics with the environment.

Janjai et al. (2010) obtained similar values for effective diffusivity in drying of lychee, which are on the order of 1.479×10^{-13} and 1.542×10^{-13} at temperatures of 50 and 60°C respectively, explaining that these values vary according to the biological structure of the fruit.

It was observed that the activation energy for the drying of the Pequi pulp was 7.69 kJ mol^{-1} for temperature ranging from 40 to 60°C. For Zogzas et al. (1996), the

Table 4. Values of the enthalpy and entropy variation and the Gibbs free energy for the drying process of Pequi pulp (*Caryocar brasiliense* Cambess) at temperatures of 40, 50 and 60°C.

Thermodynamic properties	Temperature (°C)		
	40	50	60
Enthalpy ($J.mol^{-1}$)	5091.41	5008.27	4925.13
Entropy ($J.mol^{-1}.K^{-1}$)	-251.01	-250.38	-250.05
Gibbs free energy ($J.mol^{-1}$)	83693.70	85919.44	88229.35

activation energy for agricultural products ranged from 12.7 to 110 kJ mol^{-1}. In the present work, the activation energy value found was lower; however, it was higher than that reported by Faria et al. (2012), for the drying of crambe (4.97 kJ mol^{-1}).

Thermodynamically, activation energy is defined as how easy water molecules overcome the energy barrier during migration within the product (Corrêa et al., 2007). It is noteworthy that for drying processes, the lower the activation energy, the higher the water diffusivity within the product (Faria et al., 2012), indicating a facilitated drying process.

Thermodynamic characteristics

Table 4 shows the values of the enthalpy and entropy variation and the Gibbs free energy. The calculation of these energies is relevant, since entropy and enthalpy result in Gibbs free energy, which is a thermodynamic state function representing the maximum amount of energy released in a process occurring at constant temperature and pressure that is free to perform the useful work (Ascheri et al., 2009).

This study shows lower enthalpy values for higher temperatures during the drying process, indicating a smaller amount of energy required for the drying to occur at higher temperatures, that is, enthalpy decreases with increasing temperature. Oliveira et al. (2010) explained that lower enthalpy values indicate lower energy required by the drying process to remove water within the product.

In absolute scale, entropy decreased with increasing temperature. Reduced entropy values can be explained by the fact that when the product is being dehydrated, there is a reduction in the moisture content and the movement of water molecules in the product becomes more difficult (Corrêa et al., 2011). Moreira et al. (2008) explained that negative entropy values are assigned to the existence of chemical adsorption and / or structural modifications of the adsorbent.

Positive values for the Gibbs free energy mean that the drying phenomenon is not a spontaneous process, that is, it requires an energy source for the process to occur. This was expected, since the samples were in an environment with higher humidity (harvest), being subsequently submitted to a process to reduce the humidity values. Corrêa et al. (2011) dried corn cobs and obtained the same trend of increased Gibbs free energy values with increasing process temperature, also observed in this study, which indicates a greater amount of energy with increasing temperature.

Conclusion

Based on experimental data, it was concluded that the removal of water from Pequi pulp occurred during periods of decreasing rate for all temperatures. Among the models investigated in this study, the model of Midilli showed satisfactory data to explain the drying process of Pequi pulp. The constant k of the model of Midilli increases with increasing temperature, as also observed for the diffusion coefficient.

In the drying of Pequi pulp, enthalpy decreases with increasing temperature. The entropy was negative for the entire temperature range studied. The Gibbs free energy was positive for all temperatures, and increased with increasing temperature.

Conflict of Interests

The author(s) have not declared any conflict of interests.

ACKNOWLEDGMENTS

The Foundation for Research Support of the State of Goiás (FAPEG) for the financial support for this project and Coordination of Improvement of Higher Education Personnel (CAPES) for granting Post-doctoral scholarship to the second and fourth authors are acknowledged.

REFERENCES

AOAC (Association of Official Analitical Chemistry) (2000). Official methods of analysis of the association of official analytical chemistry, no. 925.09.

Ascheri DPR, Moura WS, Ascheri JLR, Freitas Junior EA (2009). Propriedades termodinâmicas de adsorção de água do amido de rizomas do lírio-do-brejo (Hedychium coronarium). Ciência e Tecnologia de Alimentos 29.

Azharul Karim MD, Hawlader MNA (2005). Mathematical modelling and experimental investigation of tropical fruits drying. Int. J. Heat Mass Transf. 48:4914-4925.
Cano-Chauca M, Ramos AM, Stringheta PC, Marques JA, Silva PI (2004). Curvas de secagem e avaliação da atividade de água da banana-passa. Boletim Centro de Pesquisa de Processamento de Alimentos 22:121-132.
Chen D, Zheng Y, Zhu X (2012). Determination of effective moisture diffusivity and drying kinetics for poplar sawdust by thermogravimetric analysis under isothermal condition. Bioresour. Technol. 107:451-455.
Corrêa PC, Botelho FM, Oliveira GHH, Goneli ALD, Resende O, Campos SC (2011). Mathematical modeling of the drying process of corn ears. Acta Sci. Agron. 33:575-581.
Corrêa PC, Oliveira GHH, Botelho FM, Goneli ALD, Carvalho FM (2010). Modelagem matemática e determinação das propriedades termodinâmicas do café (*Coffea arábica L.*). durante o processo de secagem. Rev. Ceres 57:595-601.
Corrêa PC, Resende O, Martinazzo AP, Goneli ALD, Botelho FM (2007). Modelagem matemática para a descrição do processo de secagem do feijão (Phaseolus vulgaris L.) em camadas delgadas. Eng. Agríc. 27:2.
Doymaz I (2012). Evaluation of some thin-layer drying models of persimmon slices (diospyros kaki L.). J. Energy Convers. Manag. 56:199-205.
Durante M, Lenucci MS, D'Amico L, Piro G, Mita G (2014). Effect of drying and co-matrix addition on the yield and quality of supercritical CO_2 extracted pumpkin (Cucurbita moschata Duch.) oil. Food Chem. 148:314-320.
Faria RQ, Teixeira IR, Devilla IA, Ascheri DPR, Resende O (2012). Cinética de secagem de sementes de crambe. Rev. Bras. Eng. Agríc. Ambient. 16:573-583.
Geöcze KC, Barbosa LCA, Fidêncio PH, Silvério FO, Lima CF, Barbosa MCA, Ismail FMD (2013). Essential oils from pequi fruits from the Brazilian Cerrado ecosystem. Food Res. Int. 54:1-8.
Janjai S, Mahayothee B, Lambert N, Bala BK, Precoppe M, Nagle M, Muller J (2010). Diffusivity, shrinkage and simulated drying of litchi fruit (Litchi Chinensis Sonn.). J. Food Eng. 96:214-221.
Jideani VA, Mpotokwana SM (2009). Modeling of water absorption of botswana bambara varieties using Peleg's equation. J. Food Eng. 92: 182-188.
Krokida MK, Philippopoulos C (2005). Rehydration of dehydrated foods. Drying Technol. 23:799-830.
Lewicki PP (2006). Design of hot air drying for better foods. Trends Food Sci. Technol. 17:153-163.
Lima EE, Figueirêdo RMF, Queiroz AJM (2007). Cinética de secagem de polpa de facheiro. Revista Brasileira de Produtos Agroindustriais 9:17-28.
Machado MTC, Mello BCBS, Hubinger MD (2013). Study of alcoholic and aqueous extraction of pequi (Caryocar brasiliense Camb.) natural antioxidants and extracts concentration by nanofiltration. J. Food Eng. 117:450-457.
Madamba PS, Driscoll RH, Buckle KA (1996). The thin-layer drying characteristics of garlic slices. J. Food Eng. 29:75-97.
Martinazzo AP, Corrêa PC, Melo EC, Barbosa FF (2007). Difusividade efetiva em folhas de Cymbopogon citratus (DC.) Stapf submetidas à secagem com diferentes comprimentos de corte e temperaturas do ar. Rev. Bras. Plant Med. 9:68-72.
Mohapatra D, Rao PS (2005). A thin layer drying model of parboiled wheat. J. Food Eng. 66:513-518.
Moreira R, Chenlo F, Torres MD, Vallejo N (2008). Thermodynamic analysis of experimental sorption isotherms of loquat and quince fruits. J. Food Eng. 88:514-521.
Oliveira DEC, Resende O, Smaniotto TAS, Campos RC, Chaves TH (2012). Cinética de secagem dos grãos de milho. Revista Brasileira de Milho e Sorgo 11:190-201.
Oliveira GHH, Corrêa PC, Araújo EF, Valente DSM, Botelho FM (2010). Desorption isotherms and thermodynamic properties of sweet corn cultivars (*Zea mays* L.). Int. J. Food Sci. Technol. 45:546-554.
Perea-Flores MJ, Garibay-Febles V, Chanona-Pérez JJ, Calderón-Domínguez G, Méndez-Méndez JV, Palacios González E, Gutiérrez-Lopez GF (2012). Mathematical modelling of castor oil seeds (Ricinus communis) drying kinetics in fluidized bed at high temperatures. Ind. Crops Prod. 38:64-71.
Radunz LL, Amaral AS, Mossi AJ, Melo EC, Rocha RP (2011). Avaliação da cinética de secagem de carqueja. Eng. Agric. 19.
Reis RC, Devilla IA, Ascheri DPR, Servulo ACO, Souza ABM (2012). Cinética de secagem de folhas de manjericão (Ocimun basilicum L.) via infravermelho. Rev. Bras. Eng. Agríc. Ambient. 16:1346-1352.
Resende O, Ferreira LU, Almeida DP (2010). Modelagem matemática para descrição da cinética de secagem do feijão adzuki (Vigna angularis). Revista Brasileira de Produtos Agroindustriais 12:171-178.
Silva AS, Melo KS, Alves NMC, Fernandes TKS, Farias PA (2009). Cinética de secagem em camada fina da banana maçã em secador de leito fixo. Revista Brasileira de Produtos Agroindustriais 11:129-136.
Silva WP, Silva CMDPS, Gama FJA, Gomes JP (2014). Mathematical models to describe thin-layer drying and to determine drying rate of whole bananas. J. Saudi Soc. Agric. Sci. 13:67-74.
Togrul IT, Pehlivan D (2004). Modelling of thin layer drying kinetics of some fruits under open-air sun drying process. J. Food Eng. 65:413-425.
Zogzas NP, Maroulis ZB, Marinos-Kouris D (1996). Moisture diffusivity data compilation in foodstuffs. Drying Technol. 14:2225-2253.

African Journal of Biotechnology

Related Journals Published by Academic Journals

- *Biotechnology and Molecular Biology Reviews*
- *African Journal of Microbiology Research*
- *African Journal of Biochemistry Research*
- *African Journal of Environmental Science and Technology*
- *African Journal of Food Science*
- *African Journal of Plant Science*
- *Journal of Bioinformatics and Sequence Analysis*
- *International Journal of Biodiversity and Conservation*

academicJournals